



HAL
open science

Radical Mediated C-H and Si-H Functionalization to Construct C-C/C-N/C-Si Bonds

Shuai Liu

► **To cite this version:**

Shuai Liu. Radical Mediated C-H and Si-H Functionalization to Construct C-C/C-N/C-Si Bonds. Organic chemistry. Université de Bordeaux, 2023. English. NNT : 2023BORD0197 . tel-04198559

HAL Id: tel-04198559

<https://theses.hal.science/tel-04198559>

Submitted on 7 Sep 2023

HAL is a multi-disciplinary open access archive for the deposit and dissemination of scientific research documents, whether they are published or not. The documents may come from teaching and research institutions in France or abroad, or from public or private research centers.

L'archive ouverte pluridisciplinaire **HAL**, est destinée au dépôt et à la diffusion de documents scientifiques de niveau recherche, publiés ou non, émanant des établissements d'enseignement et de recherche français ou étrangers, des laboratoires publics ou privés.

THÈSE PRÉSENTÉE
POUR OBTENIR LE GRADE DE

**DOCTEUR DE
L'UNIVERSITÉ DE BORDEAUX**

ÉCOLE DOCTORALE DES SCIENCES CHIMIQUES
SPÉCIALITÉ : CHIMIE ORGANIQUE

Par SHUAI LIU

**Fonctionnalisation des liaisons C-H et Si-H médiée par des radicaux pour la
construction de liaisons C-C/C-N/C-Si**

Sous la direction de : Prof. Dr. Yannick LANDAIS

Co-directeur : Dr. Frédéric ROBERT

Soutenue le 19 Juillet 2023

Membres du jury :

Prof. Brigitte BIBAL	Université de Bordeaux	Président du jury
Dr. Emmanuel MAGNIER	Université Versailles St-Quentin-en-Yvelines	Rapporteur
Dr. Morgan DONNARD	Université de Strasbourg	Rapporteur
Prof. Isabelle GILLAIZEAU	Université d'Orléans-Pôle de chimie	Examinatrice
Prof. Yannick LANDAIS	Université de Bordeaux	Directeur de thèse
Dr. Frédéric ROBERT	Université de Bordeaux	Co-directeur de thèse

Fonctionnalisation des liaisons C-H et Si-H médiée par des radicaux pour la construction de liaisons C-C/C-N/C-Si

Résumé: Ce mémoire de doctorat décrit principalement les quatre travaux suivants : 1) Une nouvelle stratégie efficace pour accéder aux carbamates benzyliques par activation de la liaison C-H a été rapportée. L'utilisation d'une quantité catalytique d'un complexe Cu(I)/diimine en combinaison avec un oxydant (tel que le NFSI ((PhSO₂)₂NF) par exemple) et H₂NCO₂R en tant que source d'amine a conduit directement à la formation de la liaison C-N en position benzylique. Les conditions de réaction douces et la large variété de substrats font de cette transformation une méthode utile pour l'incorporation, en fin de synthèse, d'un fragment carbamate sur des alcanes. 2) Une arylation de la liaison δ-C(sp³)-H intramoléculaire sélective a été développée, médiée par des trifluorométhanesulfonamides aliphatiques grâce à la lumière visible. La réaction consiste en une cascade radicalaire démarrant par la génération d'un radical sulfonamidyle lequel déclenche un transfert d'atome d'hydrogène-1,5 pour donner un radical centré sur le carbone δ. Ce radical va pouvoir cycliser sur un groupe thiopolyfluoroaryle voisin pour donner une gamme de thiochromanes synthétiquement utiles. Le processus de cyclisation se produit selon deux voies distinctes selon la nature des substituants en position ortho de la liaison C-S du produit de départ. 3) Nous avons découvert une catalyse duale Ir[d(CF₃ppy)₂dtbbpy]PF₆ / NiBr₂ médiée par la lumière visible pour la construction de la liaison C-Si, par couplage entre d'hydrosilanes bon marché et facilement disponibles avec des bromures aliphatiques et aryliques. Cette voie peut s'avérer une approche précieuse pour incorporer du silicium dans les molécules bioactives en fin de synthèse, car elle peut être appliquée non seulement aux bromures d'aryle et d'hétéroaryle, mais aussi aux bromures d'alkyle primaires. 4) Nous avons enfin décrit une réaction de silylation d'oléfines électrodéficientes catalysée par CuCl₂ en présence d'hydrosilanes, sans aucun autre additif. Le catalyseur CuCl₂ devient actif par transfert de charge ligand-métal (LMCT), facilitant la création d'un radical chloré, lequel agit comme un agent de transfert d'atome d'hydrogène puissant, capable d'abstraire les hydrogènes d'une liaison Si-H. Cette réaction simple et pratique a le potentiel pour une application large en chimie médicinale.

Mots-clés : carbamates, catalyse au cuivre, activation de la liaison C-H, radical sulfonamidyle, 1,5-HAT, thiochromanes, hydrosilanes, borure de nickel, chlorure de cuivre, alcènes.

Radical Mediated C-H and Si-H Functionalization to Construct C–C/C–N/C–Si Bonds

Abstract: This Ph.D. thesis mainly describes the following four different studies: 1) A new efficient strategy to access benzylic carbamates through C-H activation was reported. The use of a catalytic amount of a Cu(I)/diimine ligand in combination with NFSI ((PhSO₂)₂NF) or F-TEDAPF₆ as oxidants and H₂NCO₂R as an amine source directly leads to the C–N bond formation at the benzylic position. The mild reaction conditions and the broad substrate scope make this transformation a useful method for the late-stage incorporation of the ubiquitous carbamate fragment onto hydrocarbons. 2) Visible light-mediated intramolecular site-selective δ -C(sp³)–H bond arylation of aliphatic trifluoromethanesulfonamides was developed. The reaction proceeds through a radical cascade including the generation of a sulfonamidyl radical, which triggers a 1,5-hydrogen atom transfer, affording a δ -C-centered radical, which finally cyclized onto a neighboring thiopolyfluoroaryl moiety to deliver a range of synthetically useful thiochromanes. The cyclization process occurs through two distinct pathways depending on the nature of the substituent X, ortho to the native C–S bond. 3) We discovered a visible-light mediated dual Ir[d(CF₃ppy)₂dtbbpy]PF₆ / NiBr₂ catalysis for the construction of C–Si bond, through coupling between inexpensive and readily available hydrosilanes as the silicon source and aliphatic and aromatic bromides. This pathway is a valuable technique for incorporating silicon into drug molecules at the later-stage, as it can be applied not only to aryl bromides and heteroaryl bromides but also to primary alkyl bromides. 4) We described CuCl₂-catalyzed silylation of electron-deficient olefins in the presence of hydrosilanes, without any other additives. The CuCl₂ catalyst becomes active through ligand-to-metal charge transfer (LMCT), facilitating the creation of a chlorine radical that functions as a potent hydrogen atom transfer agent, capable of abstracting hydrogens from Si–H bonds. This simple and practical reaction has the potential for wide application in medicinal chemistry.

Keywords: carbamates, copper catalysis, C–H activation, sulfonamidyl radical, 1,5-HAT, thiochromanes, hydrosilanes, nickel boride, copper chloride, alkenes.

Acknowledgments

First, I would like to express my sincere gratitude for the financial support from the China Scholarship Council (CSC).

I would like to thank the members of my thesis committee for their insightful comments and feedback, which considerably improved the quality of my research.

I would also like to thank my supervisor, Professor Yannick Landais, for his guidance, encouragement, and support throughout my Ph.D. studies. His insight and critical suggestions were invaluable in developing my research and assisting me in achieving my goals.

I am grateful to Dr. Frédéric Robert, my co-supervisor, for assisting me in analyzing complex NMR spectra, strange unexpected products, and discussing mechanisms, techniques, and providing significant computational studies.

My sincere appreciation goes to the staff and faculty of ISM for making all the paperwork and weekend access go smoothly, which helped me to obtain my Ph.D. more easily. I am very grateful for the analytical platform CESAMO! Thank you for patiently facilitating my analyses, even when they were not obvious or easy.

Furthermore, I would like to express my gratitude to Jonathan for always caring to provide all the needed materials and reagents and driving me to play badminton every Wednesday. And also, thanks to other members of the laboratory: Damien, Dickson, Margaux, Jiwang Fang, Lucile, Louis, Mohamed, Nivesh, Martin, Gulbin, Iman... And I am really appreciated to have many wonderful Chinese friends in Bordeaux: Jian Zhang, Jiabao Lin, Jiaming Huang, Xiangzhuo Liu, Zhenwei Li, Xuewen Zhou, Hanyu Ye, Xinrui Li, Shuning Han, Naixin Kang, Wenjuan Wang, Yue Liu, Tiejun Li... Thank you for being a part of my life in Bordeaux.

Last but not least, I am deeply grateful to my family and my girlfriend, Tong Shen, for their unwavering love, encouragement, and support, which have sustained me throughout my academic pursuits.

Thank you for being a part of this journey and contributing to making my Ph.D. dream a reality.

Table of Contents

Résumé de Recherche	1
List of Abbreviations, Acronyms, and Symbols	9
Chapter 1: Radical-Mediated C–H Bond Activation.....	13
1.1 Introduction	13
1.2 The reactivity of the C–H bond	13
1.3 Pioneering studies and selected examples	14
1.3.1 Nitrogen-centered radical promoted C–H functionalization	14
1.3.2 Oxygen-centered radical promoted C–H functionalization	16
1.3.3 Halogen radical promoted C–H functionalization	18
Chapter 2 Copper-catalyzed oxidative benzylic C(sp ³)–H amination: Direct synthesis of benzylic carbamates	21
2.1 Introduction	21
2.1.1 Intermolecular allylic C–H amination.....	21
2.1.2 Intermolecular benzylic C–H amination	22
2.1.3 Intermolecular alkane C–H amination	24
2.1.4 Intramolecular C-H amination and remote C–H amination	26
2.2 Results and discussion	28
2.2.1 Development of carbamates synthesis	28
2.2.2 Optimization of the C-H amination.....	30
2.2.3 Scope of the C–H amination	32
2.2.4 Mechanistic studies	34
2.2.5 Proposed reaction mechanism.....	37
2.3 Conclusion	38
2.4 Experimental part.....	39
2.4.1 General Information.....	39
2.4.2 General Procedure.....	39
2.4.3 Synthesis of Starting Materials	40
2.4.4 Characterization Data.....	45
Chapter 3 Thiochromane Formation via Visible-Light Mediated Intramolecular δ -C(sp ³)–H Bond Arylation of Sulfonamides.....	55

3.1 Introduction	55
3.1.1 N-Leaving-Group (N-halogen, N-O, N-S, N-N) bond cleavage.....	55
3.1.2 N-H bond cleavage.....	59
3.2 Results and discussion	62
3.2.1 Optimization of intramolecular δ -C(sp ³)-H arylation.....	64
3.2.2 Substrate scope.....	65
3.2.3 Mechanistic studies.....	71
3.2.4 Side-products formation.....	71
3.2.5 Computational studies.....	72
3.2.6 Proposed mechanisms.....	76
3.2.7 Conclusion	77
3.3 Experimental part.....	78
3.3.1 General information	78
3.3.2 Synthesis of the starting Materials	79
3.3.3 General Procedure C for photoredox reactions	91
3.3.4 Characterization Data.....	91
3.3.5 Crystallographic data	99
Chapter 4 Copper Catalyzed Silylation of Alkenes by Photoinduced	105
Ligand-to-Metal Charge Transfer.....	105
4.1 Structure and stability of silyl radicals	105
4.2 General mechanism	106
4.3 Visible-light-mediated silylation of alkene.....	107
4.4 Visible-light-mediated silylation of arene and heteroarene	112
4.5 Results and discussion	115
4.5.1 Optimization of silylation of ethyl acrylate	117
4.5.2 Substrate scope.....	118
4.5.3 Proposed mechanism.....	119
4.6 Conclusion	120
4.7 Experimental part.....	121
4.7.1 General information	121
4.7.2 Synthesis of the starting Materials	121
4.7.3 General Procedure B for photoredox reactions	123

4.7.4 Characterization Data.....	123
Chapter 5 Visible-light mediated silylation of aryl/ heteroaryl/alkyl bromides using hydrosilanes.....	127
5.1 Introduction	127
5.2 Results and discussion	128
5.2.1 Optimization of silylation of methyl 4-bromobenzoate	128
5.2.2 Substrate scope.....	130
5.2.3 Mechanistic studies.....	132
5.2.4 Proposed mechanism.....	133
5.3 Conclusion	134
5.4 Experimental part.....	134
5.4.1 General information	134
5.4.2 Synthesis of the starting Materials	135
5.4.3 General Procedure C for photoredox reactions	137
5.4.4 Characterization Data.....	137
Chapter 6 Cu-Catalyzed Remote C(sp ³)–H silylation of Alcohol	145
6.1 Introduction	145
6.2 Optimization of the reaction conditions.....	148
6.3 Conclusion	152
6.4 Experimental part.....	152
6.4.1 General information	152
6.4.2 Synthesis of the starting Materials	152
Conclusions and Perspectives.....	157
1. Conclusions	157
2 Perspectives	159
References	161

Résumé de Recherche

Titre : Fonctionnalisation des liaisons C-H et Si-H médiée par des radicaux pour la construction de liaisons C-C/C-N/C-Si

Mots-clés : carbamates, catalyse au cuivre, activation de la liaison C-H, radical sulfonamidyle, 1,5-HAT, thiochromanes, hydrosilanes, borure de nickel, chlorure de cuivre, alcènes.

Les uréthanes (ou carbamates) constituent une famille importante de composés azotés largement répandus en raison de leurs activités biologiques, mais aussi en tant qu'unité répétitive dans les polyuréthanes, la sixième classe de polymères de commodité. De plus, les uréthanes jouent un rôle prépondérant en tant que groupes protecteurs pour les amines et les acides aminés. Cependant, malgré les nombreuses avancées récentes, l'accès à la liaison uréthane reste un domaine émergent. Les protocoles traditionnels pour l'installation du groupe carbamate comprennent l'addition d'alcools à des isocyanates cancérogènes, disponibles à partir d'intermédiaires acylazides ou de dérivés du phosgène toxiques. Inspirés par la réaction de Kharasch-Sosnovsky, nous avons décrit une amination directe de la liaison C-H d'une variété de substrats benzyliques catalysée par le cuivre, conduisant à des carbamates avec des rendements satisfaisants. La combinaison entre des oxydants forts, c'est-à-dire le NFSI ou le F-TEDA-PF₆ et le système catalytique Cu(I)/diimine s'est avérée être très efficace pour accéder à des carbamates comprenant des dérivés N-Cbz et N-Troc.

Une variété de systèmes benzyliques cycliques et acycliques ont été ainsi examinés, et les carbamates correspondants ont été obtenus avec des rendements modérés à bons, comme résumé dans le Schéma 1. Le milieu réactionnel présente également une excellente tolérance vis-à-vis des groupements fonctionnels et d'une large gamme de substrats. La gêne stérique autour du centre réactionnel est apparue comme un facteur limitant, comme le montre la formation de **105d** et **105l** avec un rendement modéré ou en comparant les biphényles ortho- et para-substitués **105n** et **105o**. Certains hétérocycles (**105v** and **105w**) peuvent également réagir facilement pour obtenir les produits souhaités. Dans certains cas, il a été démontré que le NFSI fournissait une conversion plus faible, étant remplacé avec succès par le F-TEDA-PF₆.

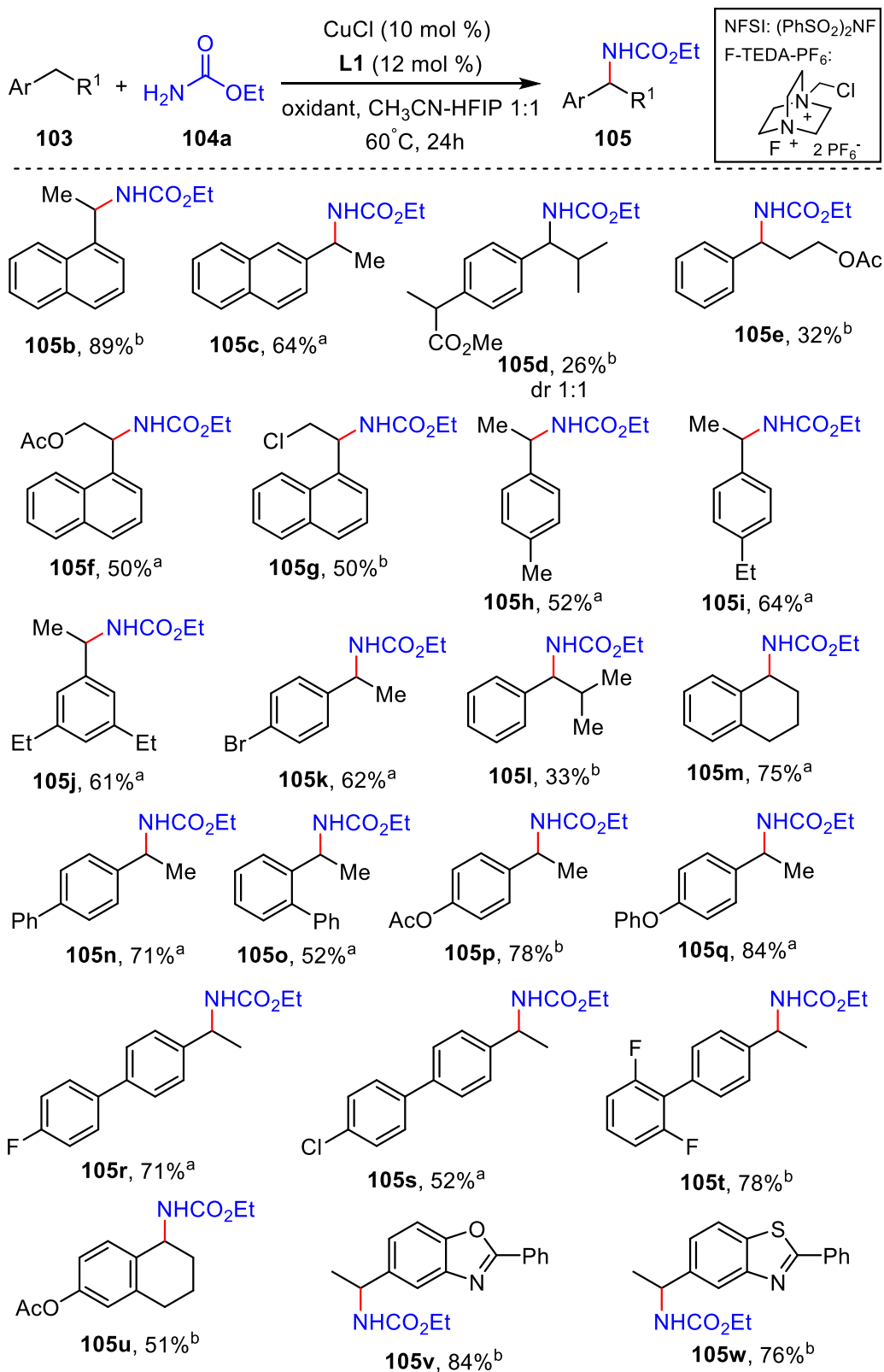


Schéma I Champ d'application de l'amination C–H de substrats benzyliques avec le carbamate

104a. ^a NFSI est utilisé comme oxydant. ^b F-TEDA- PF_6^- est utilisé comme oxydant.

Ensuite, pour élargir la variété d'uréthanes accessibles par cette approche, nous avons varié la

À travers une série d'études mécanistiques, nous avons identifié la génération de radicaux et de carbocations benzyliques dans ce système. Par conséquent, le mécanisme réactionnel peut emprunter deux voies. L'une est une voie radicalaire organométallique. L'autre est un processus croisé radical-polaire.

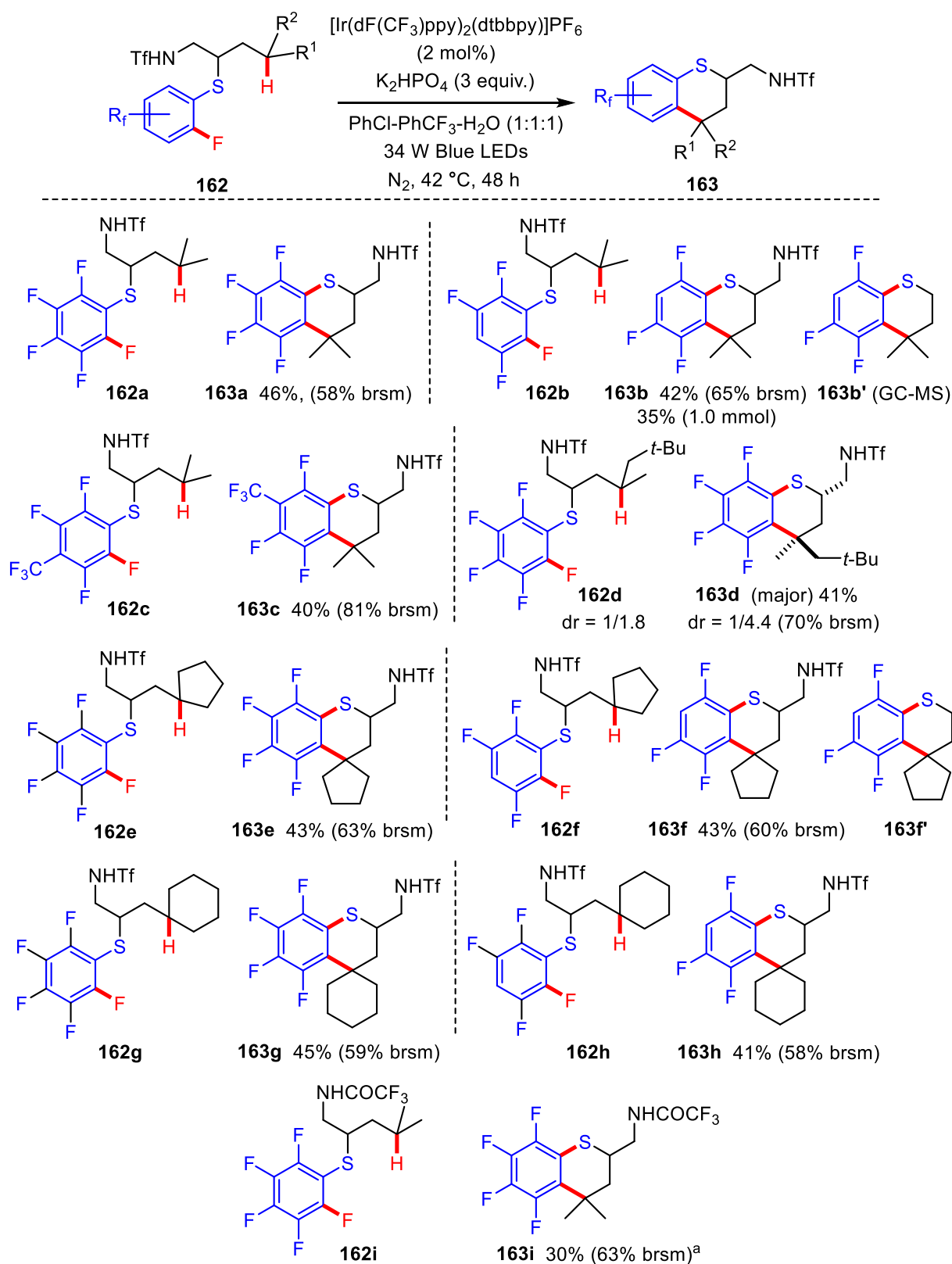
Nous avons également mis en place une nouvelle arylation distale photocatalysée d'alkylsulfonamides. La méthodologie offre une voie d'accès à une gamme de thiochromanes polyfluorés par le biais d'un processus comprenant la génération d'un radical sulfonamidyle à partir d'une sulfonamide simple, suivie d'un processus de transfert d'hydrogène-1,5. Le radical centré ainsi généré sur le carbone δ cyclise alors sur le fragment thioaryle voisin par le biais de deux voies différentes pour donner les thiochromanes correspondants.

Pour les composés ne contenant que du fluor en position *ortho* par rapport au soufre, comme dans **162a-i**, la substitution homolytique du fluor a conduit au produit de cyclisation correspondant (Schéma III). De manière intéressante, lorsque la réaction a été étendue au précurseur tétrafluoré symétrique **162b**, le produit cyclisé **163b** a été obtenu, comme le montrent de manière non équivoque des études de diffraction des rayons X, suggérant une migration de soufre à travers un réarrangement radicalaire de type Truce-Smiles C-S, plutôt qu'une substitution homolytique directe du fluor. Un comportement similaire a été observé pour **162c**, lequel conduit au thiochromane **163c**, dont la structure a également été prouvée par DRX.

Pour les composés ne contenant que des hydrogènes en position *ortho* par rapport au soufre, comme dans **162j-k**, la substitution de l'hydrogène a eu lieu avec une efficacité relative, comme illustré par la formation de **163j-k** (Schéma IV). La structure de **163j** et **163l** a été attribuée de manière non équivoque par DRX, suggérant ici une substitution aromatique homolytique directe (HAS). Des problèmes de régiosélectivité ont été remarqués lorsque les atomes d'hydrogène et de fluor étaient en compétition comme dans le composé **162n**, ce qui a conduit à la formation d'un mélange de **163na** et **163nb**, dans lequel la substitution d'hydrogène est favorisée. Les substituants aryle riches en électrons, comme dans le composé **162o-p**, ont tendance à migrer de manière efficace du soufre vers l'azote en raison d'une bonne complémentarité en termes de polarité entre le radical électrophile centré sur l'azote et l'arène riche en électron, l'attaque *ipso* prévalant sur le processus [1,5]-HAT.

Des études mécanistiques détaillées et des calculs DFT ont révélé qu'il existe deux mécanismes de réaction différents en fonction de la nature des substrats. La première voie implique une cyclisation 6-*exo* du radical C-centré sur l'arène, favorisée pour les substrats non fluorés, tandis que

la seconde privilégie un réarrangement radicalaire de type Truce-Smiles et se produit de préférence avec des substrats ayant une liaison C_{sp2}-F *ortho* par rapport à la liaison C-S native.



^a K₃PO₄ was used as a base and PhCF₃ as a solvent

Schéma III Arylation photocatalysée δ-(Csp³-H) de sulfonamide **162a-i**. Substitution homolytique de fluor.

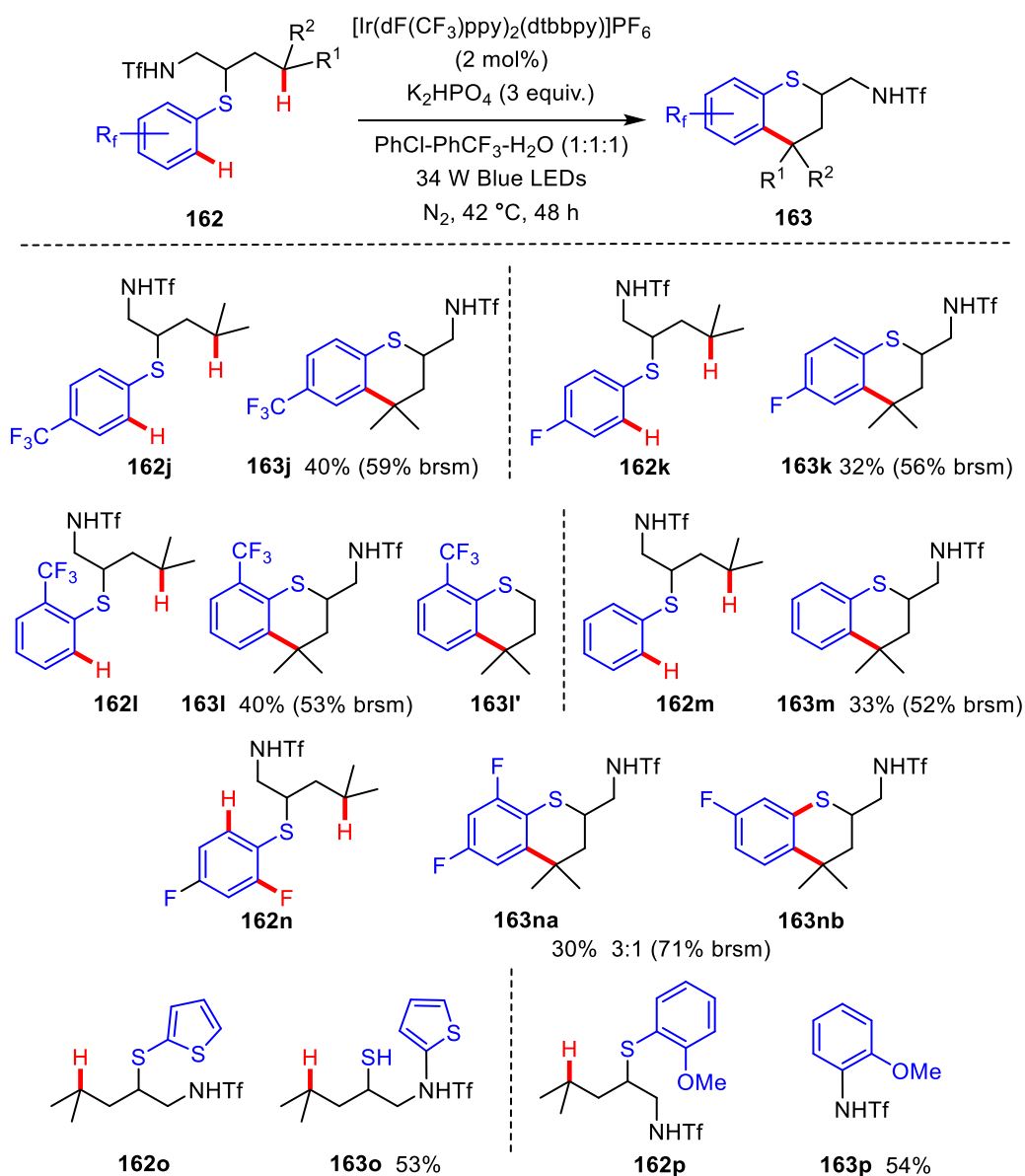


Schéma IV Arylation photocatalysée-(Csp³-H) de la sulfonamide **162j-p**. Substitution homolytique de l'hydrogène.

Les composés contenant du silicium ont suscité une attention croissante de la part de la communauté des chimistes de synthèse en raison de leur large gamme d'applications dans la fabrication de matériaux optoélectroniques organiques et dans le secteur pharmaceutique. Ainsi, nous avons présenté un protocole simple et efficace pour la silylation des alcènes, qui implique l'utilisation de CuCl_2 catalytique en tant que réactif de transfert d'atome d'hydrogène (HAT) permettant l'abstraction d'un atome d'hydrogène des hydrosilanes de manière économique en termes d'atomes (Schéma V). Tout d'abord, différents arylsilanes (**215a-c**) ont été testés et les produits correspondants ont été obtenus avec de bons rendements. $(\text{TMS})_3\text{Si-H}$ (**215d**) et l'alkylsilane (**215e**) sont également compatibles avec les conditions de réaction. De plus, cette réaction a été testée avec un large éventail

d'alcènes pauvres en électrons, y compris des acrylates d'alkyle, du (éthène-1,1-diylbisulfonyl)dibenzène, du (vinylsulfonyl)benzène, de l'éthyl 2-((phénylesulfonyl)méthyl)acrylate et du but-3-én-2-one. Ce sont des partenaires d'alcène viables.

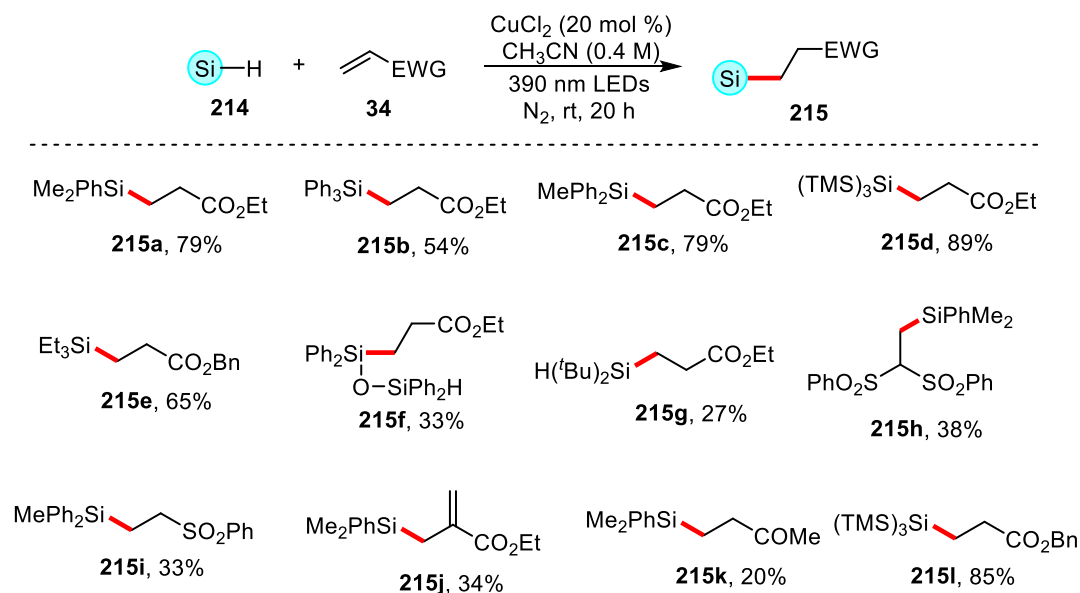


Schéma V Silylation catalysée par CuCl₂ d'alcènes déficients en électrons.

Enfin, nous avons développé une méthode catalytique puissante pour la synthèse de divers composés organosiliciés. L'utilisation du complexe [Ir(dF(CF₃)ppy)₂(dtbbpy)]PF₆ en combinaison avec le système catalytique NiBr₂/dtbpy s'est révélée être un protocole remarquablement efficace pour la synthèse de silanes aryle/hétéroaryle/alkyle en utilisant des hydrosilanes disponibles dans le commerce comme source de silicium (Schéma VI). Indépendamment de la présence d'un groupe électro-déficient ou électro-donneur sur le cycle benzénique, celui-ci peut réagir facilement pour produire les produits correspondants. Cependant, les substrats déficients en électrons réagissent mieux, probablement parce que les substrats riches en électrons peuvent être oxydés par les photocatalyseurs à l'état excité. Il est intéressant de noter que les dérivés de certains produits naturels (**217p-s**) réagissent également efficacement, fournissant le produit désiré avec des rendements modérés à bons. À notre satisfaction, nous avons constaté que les bromures d'hétéroaryles (**217t-v**) et les bromoalcane primaires (**217w-y**) étaient des substrats appropriés pour ces conditions de réaction, malgré les faibles rendements obtenus.

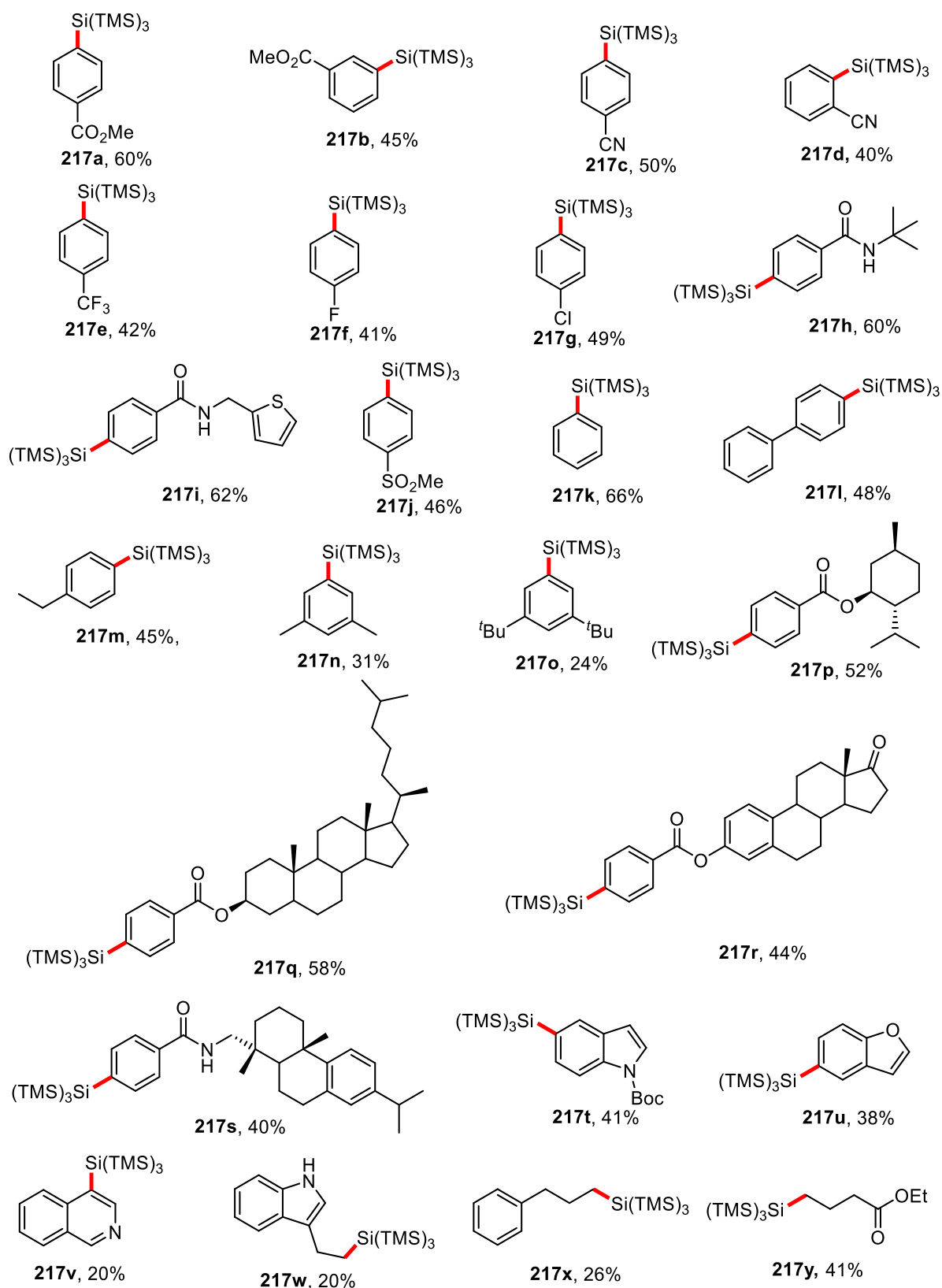
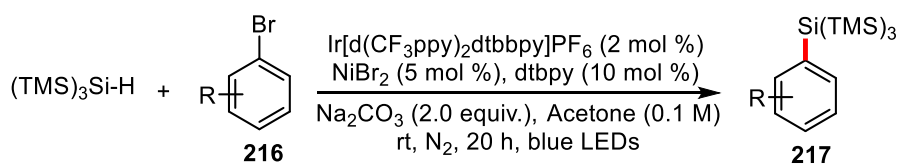


Schéma VI Portée du bromure

List of Abbreviations, Acronyms, and Symbols

Ac	acetyl group
AIBN	azobis(isobutyronitrile)
aq.	Aqueous
Ar	aryl group, mono or polysubstituted
Atm	atmospheric pressure
BDE	Bond Dissociation Energy
Bn	benzyl group
Boc	tert-butyloxycarbonyl group
b.p.	boiling point
Brsm	based on recovered starting material
Bipy	Bipyridine
<i>t</i>-BuOK	potassium <i>tert</i> -butoxide
Bz	benzoyl group
°C	degree Celsius
cat.	catalytic quantity/catalyst
Cbz	carboxybenzyl group
CCDC	Cambridge Crystallographic Data Centre
CFL	Compact Fluorescent Lamp
CI	Chemical Ionization
<i>m</i>-CPBA	<i>meta</i> -chloro perbenzoic acid
Δ	chemical shift
ΔG	Gibbs free energy
DBU	1,8-diazabicyclo[5.4.0]undec-7-ene
DCE	1,2-dichloroethane
DFT	Density Functional Theory
DG	Directing group
DIC	<i>N,N'</i> -diisopropylcarbodiimide
DIPA	Diisopropylamine
DIPEA	<i>N,N'</i> -diisopropylethylamine
DMA	Dimethylacetamide
DMAP	4-dimethylaminopyridine
DME	Dimethoxyethane
DMF	Dimethylformamide
DMSO	Dimethylsulfoxide
Dr	Diastereomeric ratio
Dtbpv	4,4'-Di- <i>tert</i> -butyl-2,2'-bipyridine
E⁰	Standard reduction potential
E_{ox}	Oxidation potential
E_{red}	Reduction potential
EDG	Electron Donating Group
Ee	Enantiomeric excess
Eq.	Equation

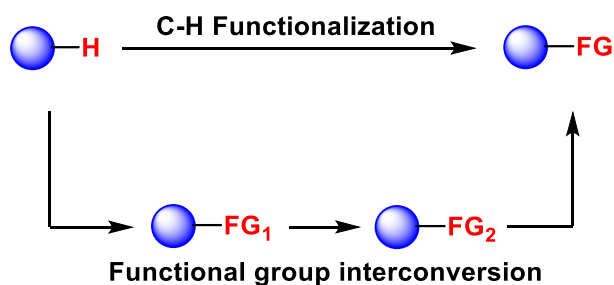
equiv.	Equivalent
Er	Enantiomeric ratio
ESI	ElectroSpray Ionization
eV	Electron volt
EWG	Electron Withdrawing Group
<i>fac</i>-Ir	<i>facial</i> -Iridium
FD	Field Desorption
FI	Field Ionization
Γ	Gamma
GC-MS	Gas Chromatography-Mass Spectrometry
HAT	Hydrogen Atom Transfer
HFIP	1,1,1,3,3,3-hexafluoroisopropanol
HOMO	Highest Occupied Molecular Orbital
HPLC	High-Performance Liquid Chromatography
HRMS	High Resolution Mass Spectrometry
hν	Photochemical activation
Hz	Hertz
IR	Infrared Spectroscopy
<i>J</i>	Coupling constant
J	Joule
K	rate constant
Kcal	Kilocalorie
KHMDS	potassium bis(trimethylsilyl)amide
kJ	Kilojoule
λ	Lambda/wavelength
L	Ligand
LA	Lewis acid
LAH	Lithium aluminium hydride
LED	Light-Emitting Diode
LMCT	Ligand-to-Metal Charge Transfer
LRMS	Low Resolution Mass Spectrometry
LUMO	Lowest Unoccupied Molecular Orbital
<i>M</i>	<i>meta</i> position
M	Concentration (mole per liter)
MHz	Megahertz
Mmol	Millimole
Mol	Mole
mol%	Molar percentage
m. p.	Melting point
Ms	Mesylate group
MS	Molecular sieves
MsCl	Methanesulfonyl chloride
MW	Molecular weight
N	Wavenumber
N	Molar number

NCS	<i>N</i> -chlorosuccinimide
Nd	Not determined
NHPI	<i>N</i> -Hydroxyphthalimide
Nm	Nanometer (10 ⁻⁹ meter)
NOESY	Nuclear Overhauser Effect Spectroscopy
NR	No reaction
Nu	Undefined nucleophile
<i>O</i>	<i>Ortho</i> position
[O]	Oxidation
<i>P</i>	<i>Para</i> position
PC	Photocatalyst
PE	Petroleum ether
PET	Photoinduced Electron Transfer
PG	Protecting group
pH	Potential of Hydrogen
PIDA	(Diacetoxyiodo)benzene
PIFA	(bis(trifluoroacetoxy)iodo)benzene
<i>pKa</i>	-log ₁₀ (<i>K</i> _a)
Ppm	Parts per million
R, R_n, R'	Undefined alkyl group
R_f	Retention factor
Rt	Room temperature (20-25 °C)
sat.	Saturated
SET	Single Electron Transfer
S_N2	Bimolecular nucleophilic substitution
SOMO	Singly Occupied Molecular Orbital
<i>t/tert</i>	<i>Tertio</i>
TBACl/TBAF	Tetrabutylammonium chloride/fluoride
TBDMS/TBS	<i>Tert</i> -butyldimethylsilyl group
TBDMSCl/TBSCl	<i>Tert</i> -butyldimethylsilyl chloride
TEMPO	2,2,6,6-tetramethylpiperidine- <i>N</i> -oxy radical
Tf	Triflate group
TFA	Trifluoroacetic acid
TFAA	Trifluoroacetic anhydride
Tf₂O	triflic anhydride
THF	Tetrahydrofuran
TLC	Thin Layer Chromatography
TMS	Trimethylsilyl group
<i>p</i>-Tol	<i>Para</i> -tolyl group
Ts	Tosyl group
TTMS	Tris(trimethylsilyl)silane
UV	Ultraviolet irradiation
wt. %	Weight percent
X	Undefined halogen

Chapter 1: Radical-Mediated C–H Bond Activation

1.1 Introduction

During the last decades, the field of C–H activation in organic chemistry has grown dramatically.¹⁻⁴ The direct conversion of C–H bonds into desired functional groups, late-stage modification of complex polyfunctional molecules and direct functionalization of oil or natural gas have always been the ultimate goals of synthetic chemists. The traditional model involves a multi-step interconversion of functional groups to transform the initial C–H bond into the target functional group or C–C bond skeleton (Scheme 1).⁵ This approach has the drawback of being wasteful and unfriendly to the environment. Thus, *in situ* C–H functionalization can reduce wastes by turning a multi-step synthesis into a one-step synthesis. The biggest challenge is the control of site selectivity in this chemistry.⁶ In fact, most organic compounds feature multiple types of C–H bonds, which have very little difference in reactivity, leading to a chemoselectivity issue.



Scheme 1 Traditional method for C–H functionalization

1.2 The reactivity of the C–H bond

C–H bonds have very low reactivity due to extremely low acidity, little polarization, and high bond dissociation energy (BDE). The BDE and *pK_a* of several types of C–H bonds are shown in Scheme 2.^{5,7} BDE decreased with increasing *pK_a* except for allylic C–H. Hybridization also affects BDE; the more *s* character is present on the C–H bond, the stronger is the BDE of the C–H bond. BDE can also be reduced by the effects of conjugation and hyperconjugation. For example, with the increase of substituents on carbon, BDE would be weakened, as with the presence of conjugated substituents. These properties are exactly the opposite of the stability of free radicals.

Structure	$\text{H}-\text{C}\equiv\text{C}-\text{H}$		$\text{H}_2\text{C}=\text{C}-\text{H}$	$\text{H}_3\text{C}-\overset{\text{H}}{\underset{\text{H}}{\text{C}}}-\text{H}$	$\text{H}_3\text{C}-\overset{\text{CH}_3}{\underset{\text{H}}{\text{C}}}-\text{H}$	$\text{H}_3\text{C}-\overset{\text{CH}_3}{\underset{\text{CH}_3}{\text{C}}}-\text{H}$	
BDE (kJ/mol)	552.2	473.0	460.3	410.8	397.9	389.9	361.1
PKa	~ 25	43	44	~ 50	~ 50	~ 50	43
Hybridization	C(sp)	C(sp ²) _{arom}	C(sp ²) _{vinyl}	C(sp ³) _{1°}	C(sp ³) _{2°}	C(sp ³) _{3°}	C(sp ³) _{allylic}

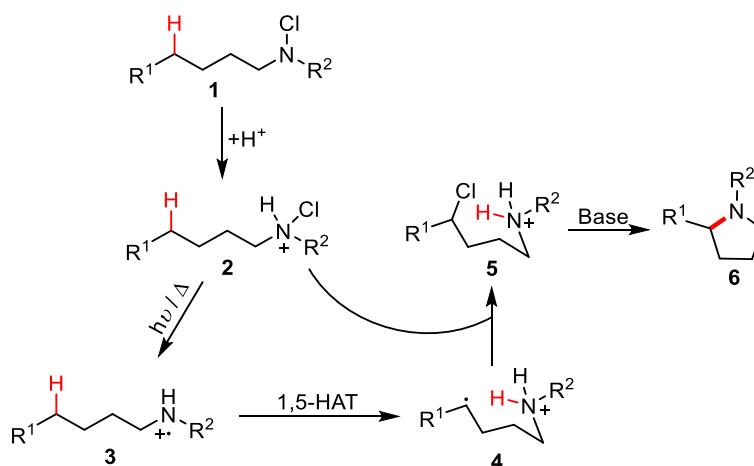
Scheme 2 BDE and *p*Ka of several types of C–H bonds

1.3 Pioneering works and selected examples

Halogen-, nitrogen-, oxygen-, and methyl-based radicals are widely known to be highly effective hydrogen-abstracting species. Their high reactivity is due to high bond dissociation energies of newly formed bonds after hydrogen abstraction. Recent research has shown that heteroatom-centered radicals can be used to enable site-specific intermolecular functionalizations of inert aliphatic C–H bonds.⁸⁻¹³

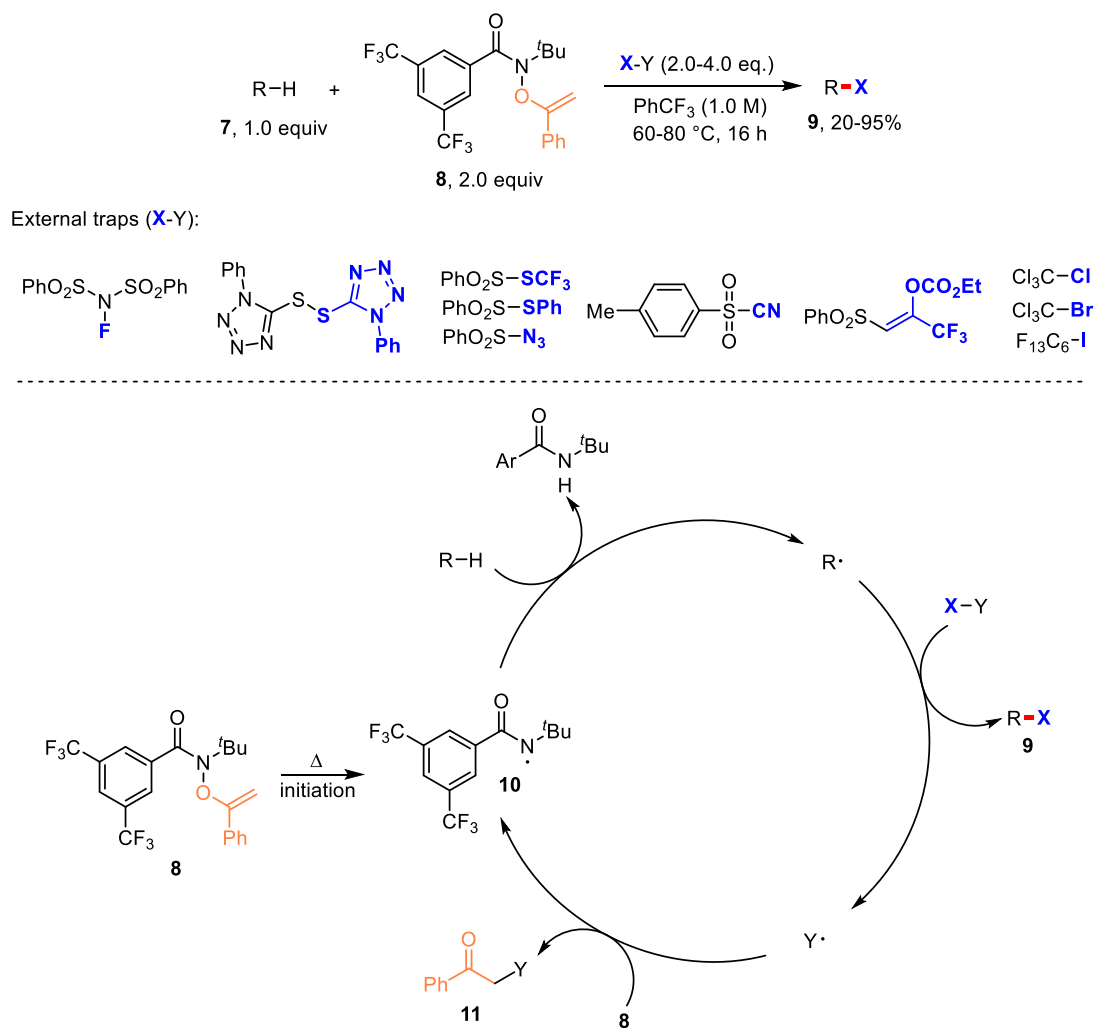
1.3.1 Nitrogen-centered radical promoted C–H functionalization

A. W. Hoffman reported his pioneering work on direct functionalization of alkyl C–H bonds to access pyrrolidines from *N*-chloroamines in 1883 (Scheme 3).¹⁴ *N*-chloroamine **1** is first protonated under strongly acidic conditions, and then the N–Cl bond is homolytically cleaved under heating or light to generate a nitrogen-centered radical cation species **3**, which undergoes 1,5-hydrogen atom transfer to provide carbon-centered radical intermediate **4**. The alkyl radical **4** abstracts a chlorine from another *N*-chloroamine to complete the radical chain. The newly formed chloride **5** finally performs intramolecular nucleophilic substitution under basic conditions to obtain the targeted product **6**.



Scheme 3 Hofmann-Löffler-Freytag (HLF) reaction

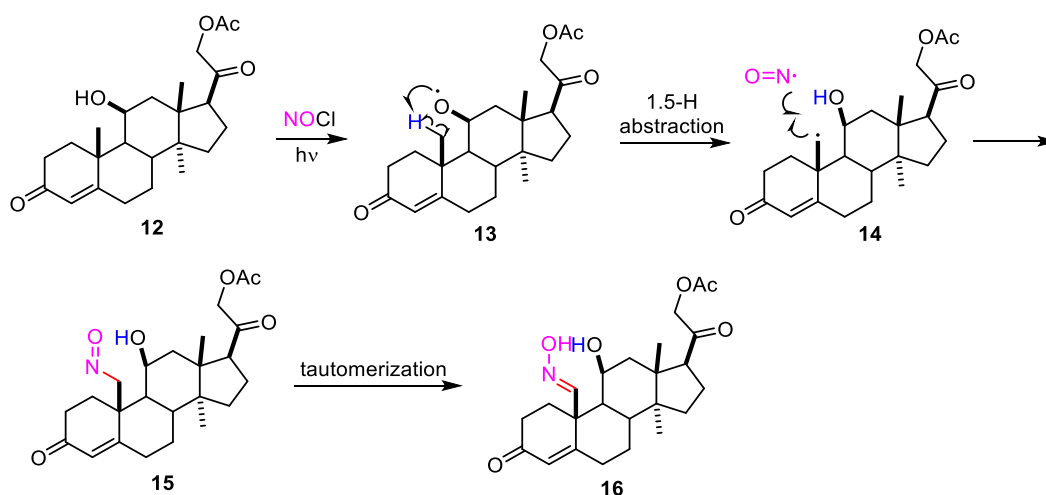
After that, a series of highly effective nitrogen-centered radical precursor reagents, such as NFSI, or Selectfluor,[®] having weak N-F bonds, and others were developed and are now widely employed in the modification of organic molecules and medicinally relevant targets. Recently, Alexanian¹⁵ and co-workers developed a universal strategy for the diversification of aliphatic C–H bonds in small molecules and polyolefins using an *O*-alkenylhydroxamate **8** as an optimal reagent capable of creating reactive nitrogen-centered radical (Scheme 4). The reaction mechanism is a free radical chain process. Under heating conditions, homolytic cleavage of *O*-alkenylhydroxamate **8** affords the amidyl radical **10**, which snatches a hydrogen atom from aliphatic alkanes or polyolefins to form the corresponding alkyl radicals or macroradicals respectively. The desired product **9** would be formed in good yield by the reaction of alkyl radicals with diverse trapping reagents. The radical **Y** generated at the same time interacts with the substrate **8** to regenerate the amidyl radical **10** and ketone **11**, completing the cycle.



Scheme 4 Amidyl radicals in aliphatic C–H bond functionalization of small molecules and polyolefins.

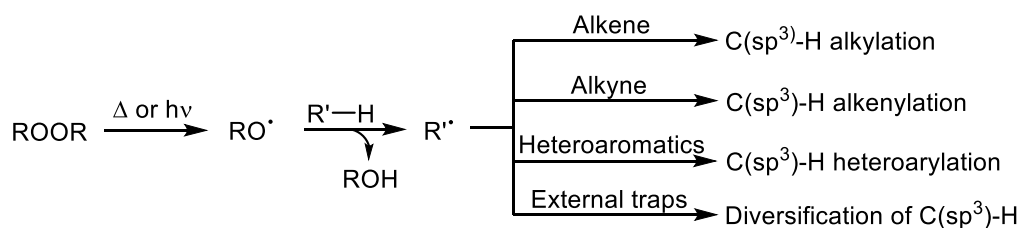
1.3.2 Oxygen-centered radical promoted C–H functionalization

The Barton nitrite-ester reaction is a well-known example of site-selective C–H bond functionalization, with a mechanism similar to that of the Hofmann-Löffler-Freytag reaction. The process, initiated with a homolytic RO–NO cleavage, subsequently proceeds with a δ -hydrogen atom abstraction, free radical recombination (with the persistent radical NO) and tautomerization to yield an oxime **16** (Scheme 5)¹⁶. In rigid structures, such as steroid skeletons, the reaction performs efficiently. This technique has recently regained interest in a number of research teams and has created fruitful results.¹⁷ For example, Zhu¹⁸⁻²⁰, Chen²¹, Zuo²², Liu²³ *et al.* achieved oxygen-centered radical mediated intramolecular functional group migration processes as well as intermolecular distant C–H arylation, alkylation and amination.



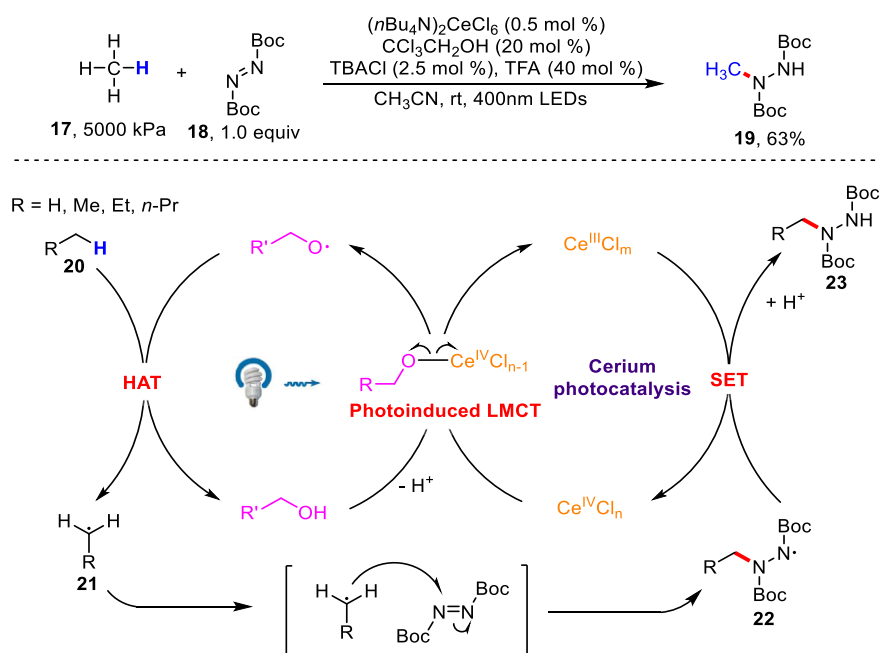
Scheme 5 Barton Nitrite Ester Reaction

Peroxides, exhibiting weak O–O bonds (e.g. *t*-BuO–O*t*-Bu, BDE = 25-50 kcal/mol), are prone to homolysis by increasing the temperature (thermolysis) or under light (photolysis) to generate oxygen-centered radicals.^{24,25} Additionally, some of them, such as *tert*-butyl peroxide and benzoyl peroxide, can undergo further fragmentation to generate alkyl and aryl radicals respectively. The majority of them are commercially available and stable at room temperature, degrading at only slightly higher temperatures, making them the most popular radical initiators. Peroxides are commonly employed in the field of unsaturated C–H bond functionalization owing to these characteristics.⁴ The general mechanism is shown in Scheme 6. Peroxides homolysis first generates oxygen-centered radicals, which then abstract a hydrogen atom from aliphatic alkanes to give alkyl radicals, which are eventually added to alkenes, alkynes, heteroaromatics, or trapped by external scavengers to yield the desired product.



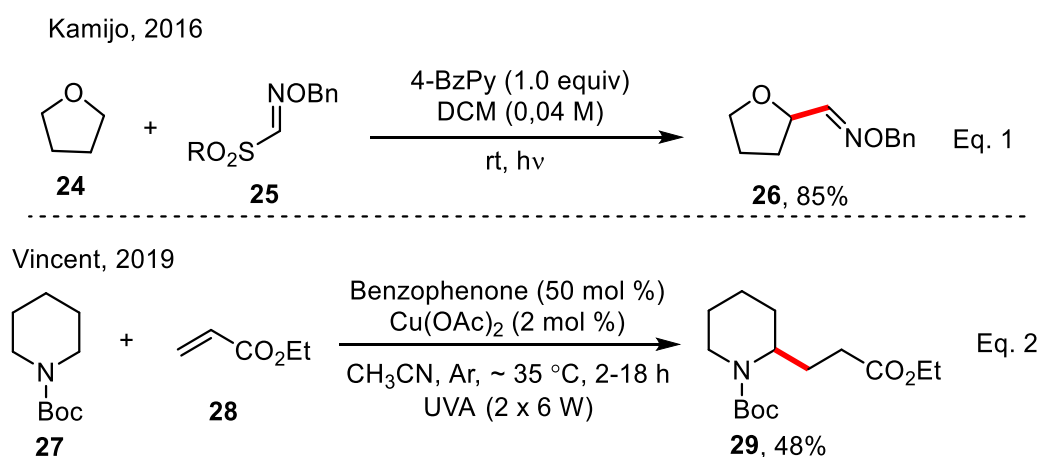
Scheme 6 Peroxide-initiated C–H Functionalization

In 2018, Zuo²⁶ and co-workers describe the process of photocatalytic C–H amination, alkylation, or arylation of methane and light alkanes in the presence of visible light at room temperature, using abundant and inexpensive cerium salts as photocatalysts and simple alcohols as hydrogen atom transfer agents (Scheme 7). Interestingly, different regioselectivities can be obtained by using different alcohols as hydrogen atom transfer catalysts. Mechanistic investigations showed that the Ce(IV)-alkoxy complex is first created by the coordination of an alcohol with the Ce(IV) salt, and then undergoes a photoinduced ligand-to-metal charge transfer (LMCT) to produce a highly active alkoxy radical and a reduced Ce(III) species. After that, the alkoxy radical abstracts a hydrogen atom from the alkyl substrate **20** to generate an alkyl radical **21**, which then undergoes radical addition with di-*tert*-butyl azodicarboxylate (DBAD) to construct a new C–N bond and forms a nitrogen-centered radical intermediate **22**. A single electron transfer from the Ce(III) salt to radical intermediate **22** would regenerate the active Ce(IV) catalyst and provide the target product **23** after protonation.



Scheme 7 Ce-mediated alkoxy radical generation for the selective functionalization of light alkanes.

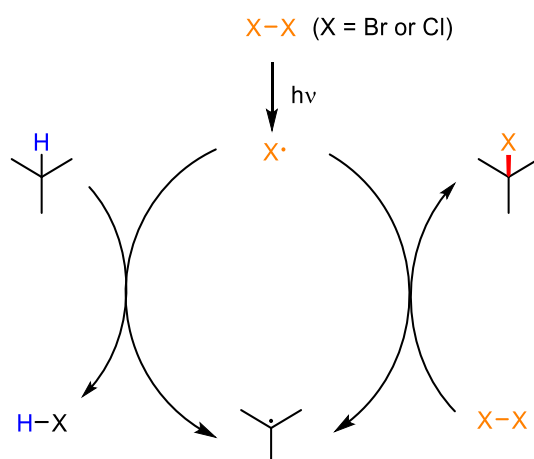
N-Hydroxyphthalimide (NHPI) is a powerful oxygen-centered radical precursor usually applied in the oxidation of alkyl C–H bonds to yield alcohols, ketones, aldehydes, or acids.²⁷ Recently, Kamijo²⁸ and Vincent²⁹ *et al.* developed the aldoximation and alkylation of unreactive C(sp³)–H bonds using arylketones as hydrogen atom transfer photocatalysts (Scheme 8). This strategy mainly relies on the photoactivation of the C=O double bond of arylketones under UV light to generate a diradical species. The resulting oxygen-centered radicals have high electrophilicity and can successfully abstract a hydrogen atom in hydrocarbons to generate alkyl radicals, which are finally coupled with radical acceptors to afford the desired products.



Scheme 8 Arylketones catalyzed C–H functionalization.

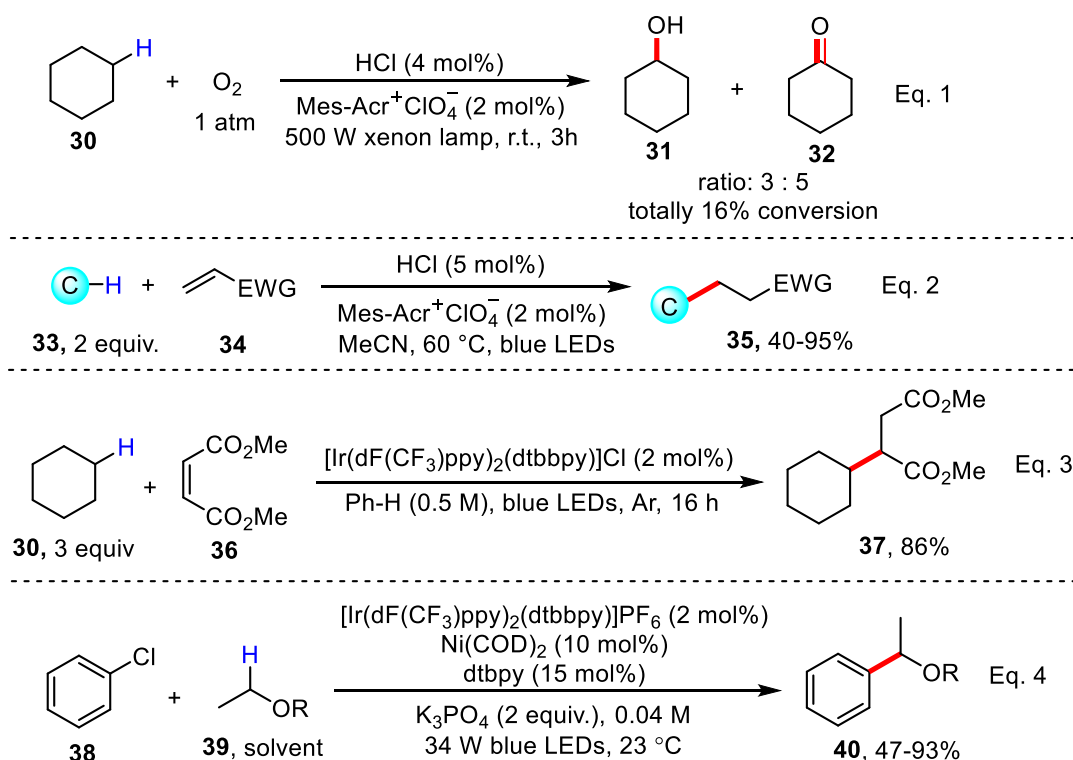
1.3.3 Halogen radical promoted C–H functionalization

Alkanes can be chlorinated or brominated by chlorine or bromine under irradiation with visible or UV-light (Scheme 9). Halogen radicals, generated with the assistance of light irradiation, can abstract a hydrogen atom from an alkane to form a carbon-centered radical. The latter can then react with a dihalogen to provide a halogenated product and regenerate the halogen-centered radical.^{30,31} Although this reaction is adaptable to alkyl chains with different functional groups, it is typically not employed in synthesis due to poor selectivity, which results in the production of a mixture of monohalogen, dihalogen, and polyhalogenates. The tertiary carbon atoms are preferentially attacked in alkanes without functional groups, followed by the secondary carbon atoms. The primary carbon positions are the most difficult to activate, which may be related to the stability of radicals. But benzylic carbons are halogenated faster than tertiary carbons.³² Electron-withdrawing groups, such as carbonyl and cyano, rarely undergo halogenation at the α -position. On the contrary, the halogenation reaction easily occurs at the α -position of ether, which is related to the polarity matching between free radicals.³³



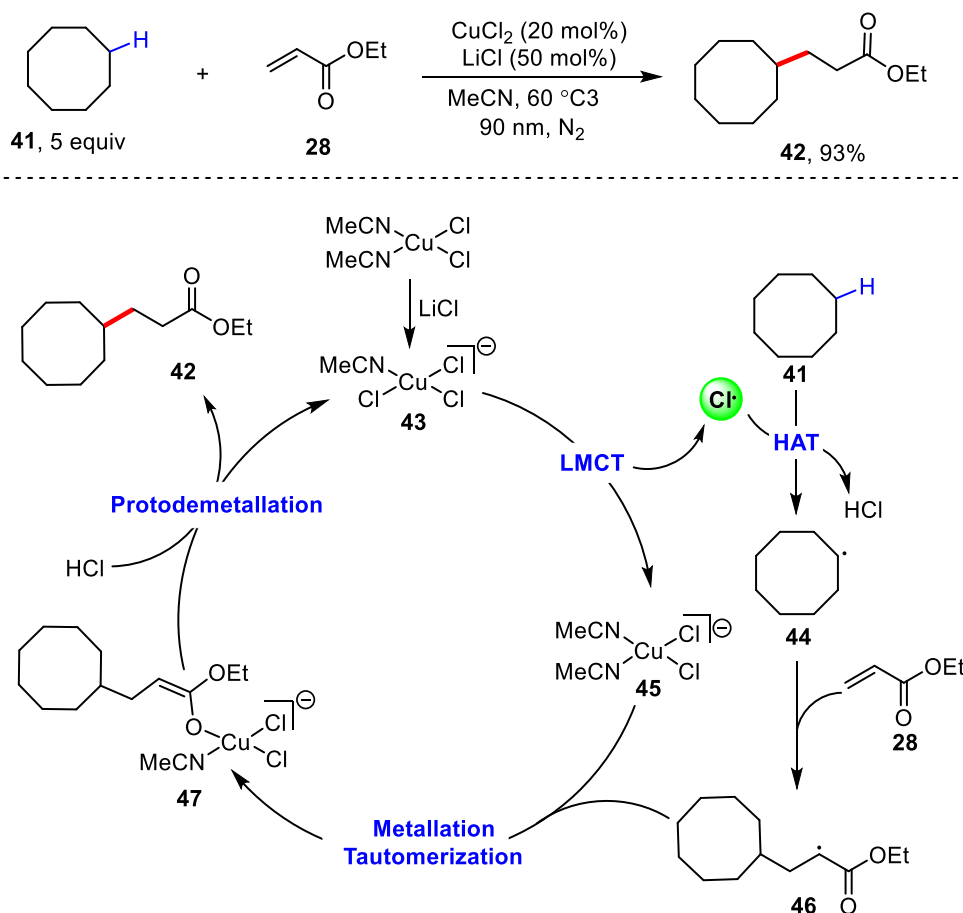
Scheme 9 Radical Halogenation

In the presence of the photocatalyst 9-mesityl-10-methylacridinium, Fukuzumi^{34,35} employed HCl as a hydrogen atom transfer catalyst to achieve the oxidation of simple alkanes C–H and benzylic C-H (Scheme 10, Eq. 1). Similar conditions were used by Wu³⁶ to accomplish a series of C-H alkylations of simple alkanes (Scheme 10, Eq. 2). Barriault³⁷ *et al.* discovered that the photocatalyst [Ir(dF(CF₃)ppy)₂(dtbbpy)]Cl would produce chlorine radicals when exposed to blue light, enabling a variety of hydrogen atom transfer reactions to be achieved (Scheme 10, Eq. 3). Doyle³⁸ and co-workers developed an efficient strategy relying on nickel and photoredox catalysis to generate chlorine radical, using aryl chlorides as both cross-coupling partners and the chlorine radical source to access the α -oxy C(sp³)–H arylation products (Scheme 10, Eq. 4).



Scheme 10 Chlorine radical mediated alkanes C–H functionalization.

Recently, Rovis³⁹ and co-workers described Cu-catalyzed C(sp³)-H bond alkylation via the coupling of unactivated C(sp³)-H bonds with electron-deficient olefins (Scheme 11). This group proposed that the reaction involves a ligand-to-metal charge transfer mechanism. CuCl₂ can first coordinate with the solvent acetonitrile before interacting with LiCl to generate the photoactive CuCl₃⁻ species **43**. A reactive chlorine radical is then generated by photoinduced ligand-to-metal charge transfer (LMCT). The chlorine radical abstracts a hydrogen atom from the alkane nucleophile **41** to afford HCl and a reactive alkyl radical **44**, which undergoes a radical addition reaction with olefin **28** to provide a more stable radical α to an ester **46**. The Cu-complex **47** would be formed after metalation and tautomerization. Protodemetalation with HCl yields the target product and regenerates the photoactive CuCl₃⁻.



Scheme 11 CuCl₂ catalyzed C(sp³)-H bond alkylation via photoinduced LMCT.

Chapter 2 Copper-catalyzed oxidative benzylic C(sp³)-H amination:

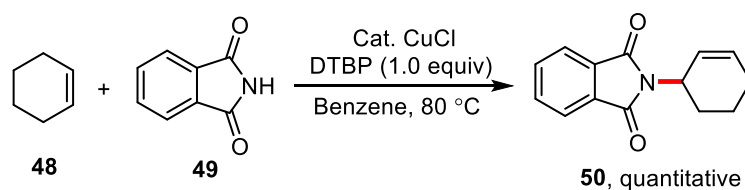
Direct synthesis of benzylic carbamates

2.1 Introduction

The direct building of C–N bonds from the functionalization of C–H bonds is still a very active field of research, as nitrogen-containing structures are abundant in natural products, synthetic intermediates, molecules of pharmaceutical interest, and functional materials.⁴⁰⁻⁴³ Transition metal-catalyzed transformation of prevalent C–H bonds into valuable C–N bonds provides an effective synthetic strategy for manufacturing N-functionalized compounds.^{44,45} Particularly, Kharasch-Sosnovsky type reactions relying on a Cu-catalyzed oxidative amination and amidation of hydrocarbons have currently renewed interest among chemists, allowing an access to a wide range of nitrogen derivatives.

2.1.1 Intermolecular allylic C–H amination

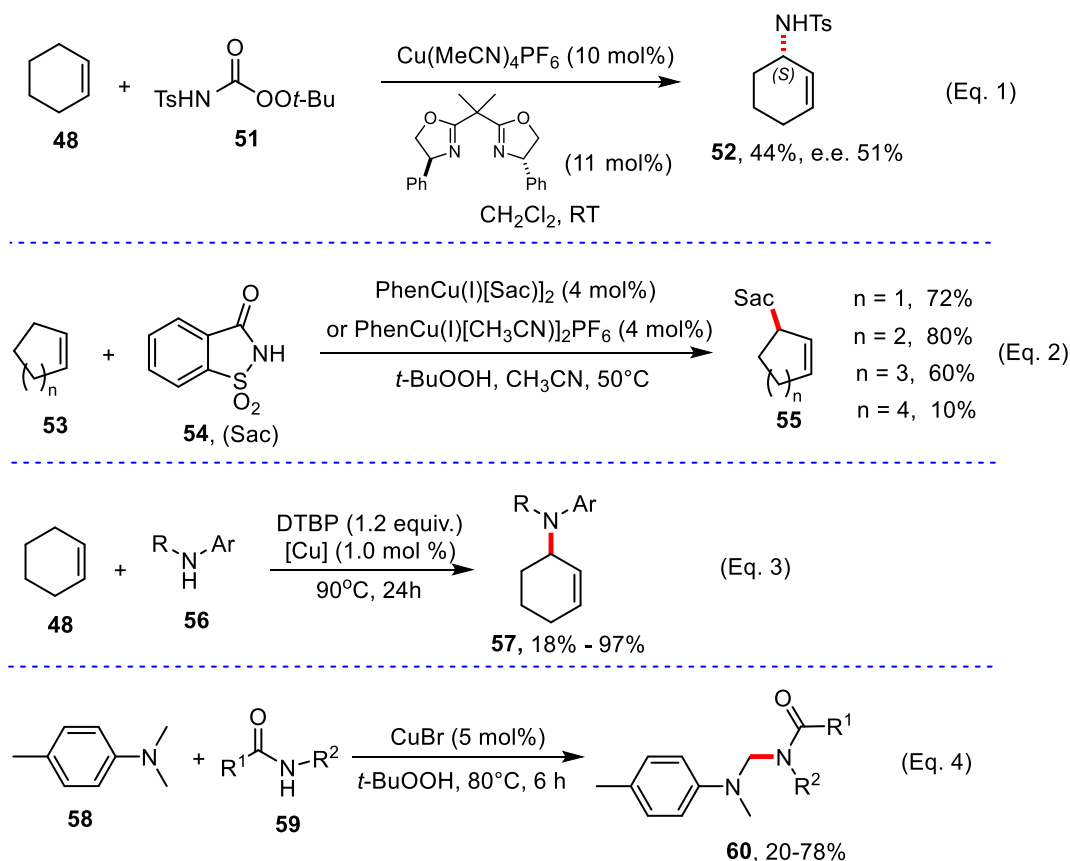
The Kharasch-Sosnovsky reaction, first described in the 1950s by Kharasch and Sosnovsky, demonstrated one of the most efficient techniques for the synthesis of valuable allylic amines or esters via allylic C–H oxidation of alkenes in the presence of Cu(I) and peroxides (Scheme 12).^{46,47} Other oxidizing agents, such as *N*-bromo and *N*-chlorosuccinimide, also react smoothly in replacement of peroxides.⁴⁸



Scheme 12. Kharasch-Sosnovsky reaction (first discovered in 1958).

Inspired by the Kharasch-Sosnovsky reaction, Clark⁴⁹ and co-workers developed a copper-catalyzed asymmetric allylic amination reaction of cyclohexene **48** and peroxy-carbamate **51** at room temperature (Scheme 13, Eq. 1). Single electron transfer (SET) from the Cu complex to the peroxy-carbamate **51** resulted in the production of copper-carbamate species, which could then evolve through decarboxylation to form the Cu-sulfonamide species. Finally, the amino group could be installed onto the hydrocarbon substrate by reductive elimination. It is worth noting that peroxy-carbamates bearing an arylamino instead of a sulfonamide group led to an allylic ester, as the

decarboxylation was slower in this case. In the same year, similar conditions were employed by Slough⁵⁰ to perform the coupling of saccharin **54** to cycloalkenes **53** (Scheme 13, Eq. 2). Cyclic olefins of various sizes react smoothly. Subsequently, Warren⁵¹ and co-workers disclosed copper-catalyzed allylic C–H amination in the presence of DTBP to afford the corresponding product in good yields (Scheme 13, Eq. 3). Fu⁵² *et al.* developed a novel approach shown below for the copper-catalyzed amination of a C–H bond α to nitrogen (Scheme 13, Eq. 4). A wide variety of amides, both primary and secondary, gave the desired products in good yields.

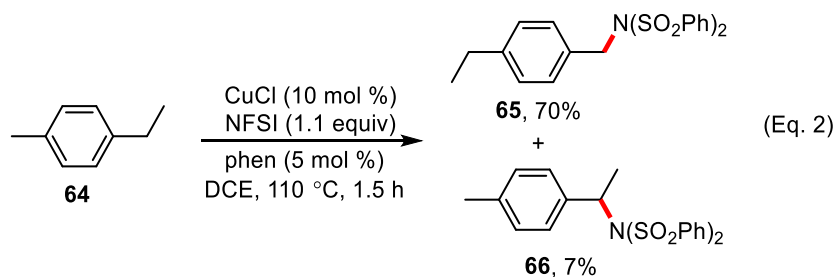
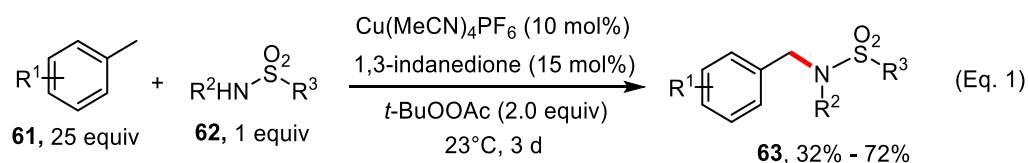


Scheme 13. Allylic C-H and C–H bonds α to nitrogen oxidation and amination.

2.1.2 Intermolecular benzylic C–H amination

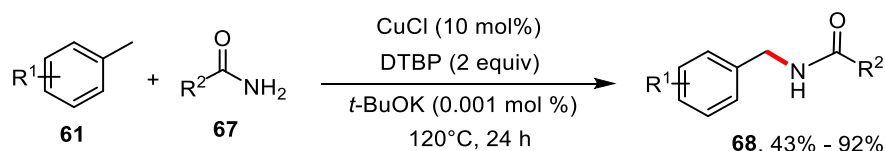
Benzylic hydrocarbons have also proved to be a suitable class of substrates, which could be aminated under similar conditions to the Kharasch-Sosnovsky reaction. Fan⁵³ *et al.* developed an efficient sulfonamidation reaction of benzylic substrates **61** using commercially available $\text{Cu}(\text{MeCN})_4\text{PF}_6$ as the catalyst and inexpensive *t*-BuOOAc as the oxidizing agent, leading to the target products in moderate to good yield (Scheme 14, Eq. 1). Liu⁵⁴ and colleagues demonstrated the benzylic C–H sulfonamidation by using *N*-Fluorobenzenesulfonimide (NFSI) instead of the conventional oxidant peroxide (Scheme 14, Eq. 2). *N*-Fluorobenzenesulfonimide serves as both

oxidant and the nitrogen source. Contrary to previously reported, the data unexpectedly showed a clear preference for primary C–H bonds over secondary C–H bonds in the sulfamidation reaction.



Scheme 14 Benzylic C–H oxidation sulfamidation.

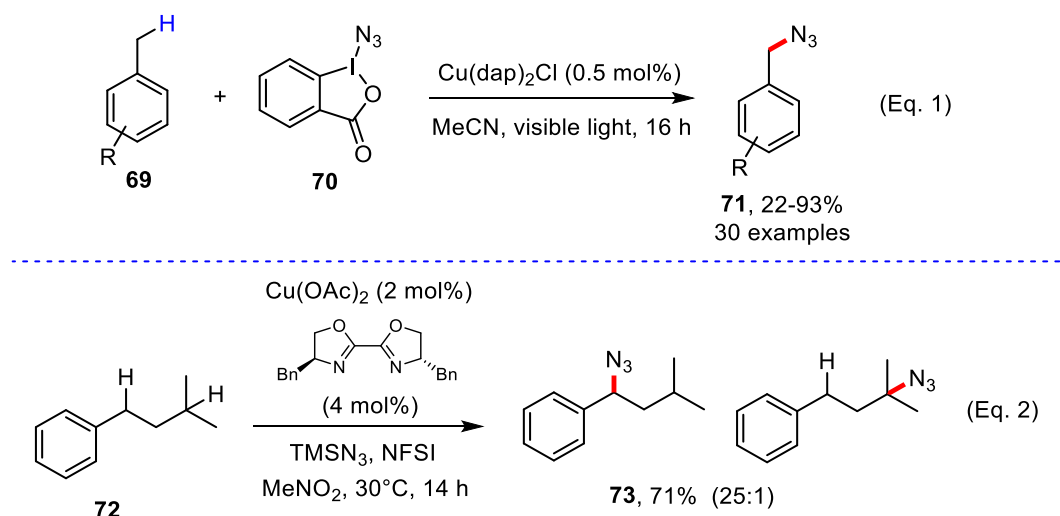
An efficient copper-catalyzed C–N bond construction protocol via C–H/N–H cross-coupling of amides with primary benzylic hydrocarbons was reported by Huang (Scheme 15).⁵⁵ Unlike other approaches, in this one the metal does not need a ligand, but trace amounts of potassium *tert*-butoxide are required.



Scheme 15 Benzylic C–H oxidation amidation.

Greaney⁵⁶ and co-workers described a benzylic C–H azidation using Zhdankin's reagent **70** as an azide source and Cu(dap)₂Cl (dap = 2,9-bis(*p*-anisyl)-1,10-phenanthroline) as a photocatalyst under visible light (Scheme 16, Eq. 1). The group proposed that the reaction involves radical chain mechanism through single electron transfer from the photo-excited Cu-catalyst to the Zhdankin reagent, providing a N₃ radical, which can then abstract a benzylic hydrogen atom from substrate **69** to form benzylic radical. The reaction is then propagated through the benzylic radical, which interacts with the Zhdankin reagent to give the final product **71**. More recently, Stahl⁵⁷ group reported a practical method for the synthesis of azides relying on Cu-catalyzed oxidative azidation of benzylic systems in the presence of TMS-N₃ and *N*-Fluorobenzenesulfonimide (NFSI) (Scheme 16, Eq. 2). This strategy exhibits good benzylic site selectivity and broad functional group tolerance. A radical-

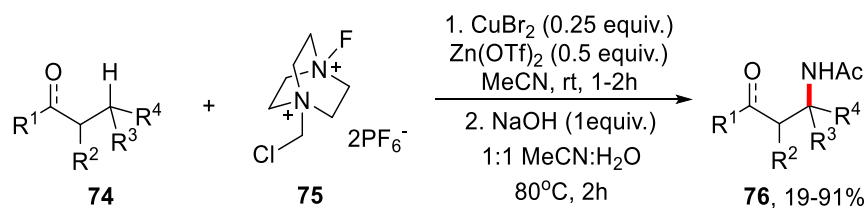
polar cross-over mechanism involving a benzylic cation is supported by experimental and computational data.



Scheme 16 Benzylic C–H oxidative azidation.

2.1.3 Intermolecular alkane C–H amination

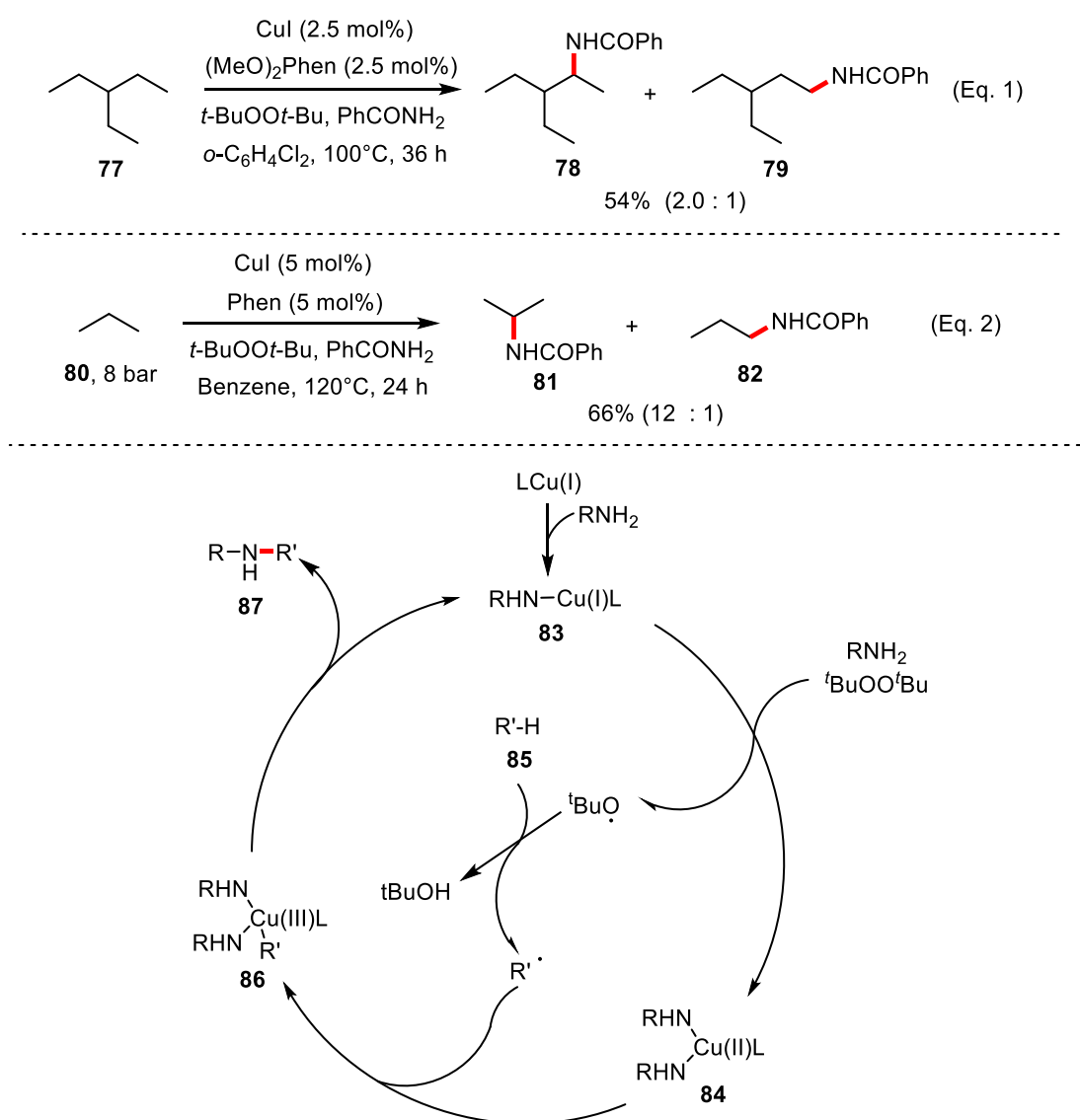
Allylic and benzylic C–H bond aminations are well established due to the relatively weak BDE of their respective C–H bonds. Recent studies have focused on the C–H amination of simple alkanes including light alkanes and even methane. In 2012, Baran⁵⁸ developed a mild intermolecular Ritter-type C–H amination system with inexpensive acetonitrile as a nitrogen source, CuBr₂ as a catalyst, and F-TEDA-PF₆ as a HAT reagent (Scheme 17). A broad scope of substrates can be aminated, using this strategy, showing excellent functional group tolerance.



Scheme 17 Copper mediated Ritter-Type C–H amination.

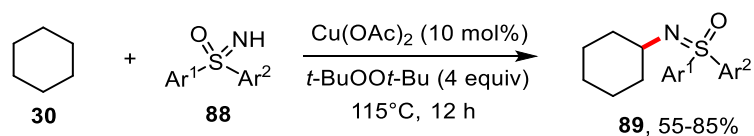
Subsequently, Hartwig⁵⁹ described a novel method to achieve intermolecular unactivated C(sp³)-H amidation between aliphatic alkanes and various amides (Scheme 18, Eq. 1). Interestingly, this reaction occurs preferentially at secondary sites over tertiary sites and even in some cases primary sites, the least reactive relative to tertiary ones due to steric reasons. The group then performed the C–H amidation of several light alkanes such as ethane, propane, and *iso*-butane, under very similar conditions (scheme 18, Eq. 2).⁶⁰ It is worth mentioning that when high-pressure carbon dioxide is utilized as the reaction medium, the reaction proceeds smoothly and the product is delivered in a

moderate yield. In contrast to heavier alkanes, selectivities in light alkanes matched the rate of H abstraction by the *t*-BuO radical, albeit with a lower product ratio. The following mechanism was proposed based on the isolation and characterization of the reaction intermediate Cu-amine complex. Firstly, Cu(I)-amine complex **83** would be formed after Cu(I) reaction with amine. One-electron could transfer from complex **83** to DTBP, generating a *tert*-butoxy radical and a potential intermediate [LCu(II)(amine)((*O*'Bu)], which would react rapidly with another amine to afford a bis-amino-copper species **84**. The *tert*-butoxy radical abstracts a hydrogen atom from alkane **85** to form alkyl radical, which coordinate to Cu(II)-complex **84** to produce a Cu(III)-complex **86**. The final product **87** would be generated after rapid reductive elimination with the regeneration of active Cu(I)-complex **83**.



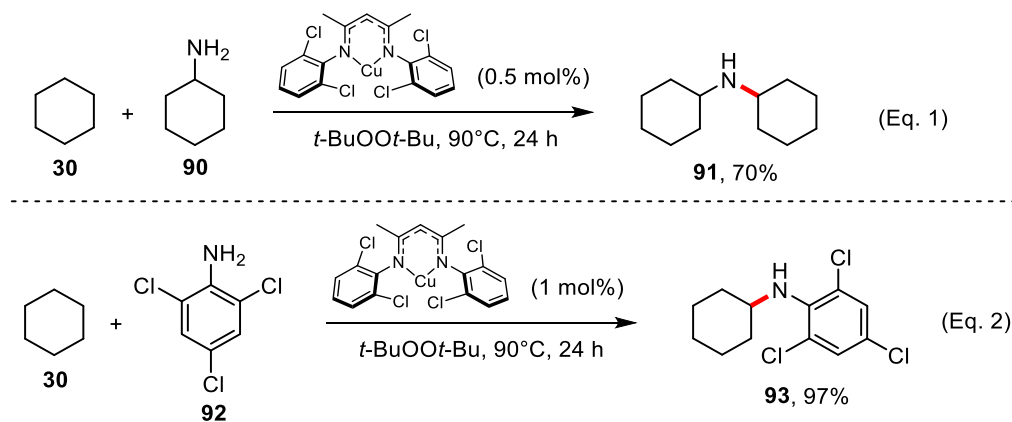
Cheng⁶¹ discovered a copper-catalyzed oxidative C(sp³)-H/N-H coupling of sulfoximines with

simple alkanes. This strategy involved the construction of C(sp³)-N bonds via a radical pathway and tolerated a variety of functional groups on the phenyl rings, including halogen, methyl, and aryl.



Scheme 19 Copper mediated alkyl C–H sulfoximation.

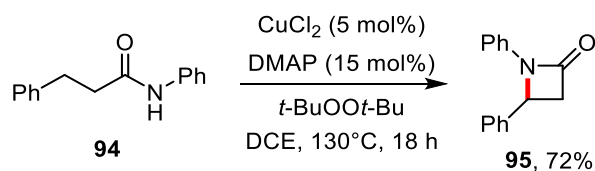
Warren⁶² and coworkers described an efficient β -diketiminato-copper complex catalyzed amination reaction of benzylic and unactivated cyclic hydrocarbons with unactivated amines, employing *t*-BuO-*O*-*t*-Bu as an oxidant (Scheme 20, Eq. 1). The use of X-ray, electron-paramagnetic resonance (EPR), and *in situ* UV-visible spectroscopy to characterize Cu complexes has allowed for a better understanding of the role of the metal catalyst in the reactions involved. A radical process is supported by calculations and kinetic studies. The reaction mechanism proposed in this paper is consistent with that described previously (Scheme 18). Shortly afterward, they developed a catalytic C-H amination with aromatic amines under the same conditions and discovered that arylamines with electron-withdrawing groups on the arene preferred the C–H amination (Scheme 20, Eq. 2).⁶³



Scheme 20 Copper-mediated alkyl C–H amination.

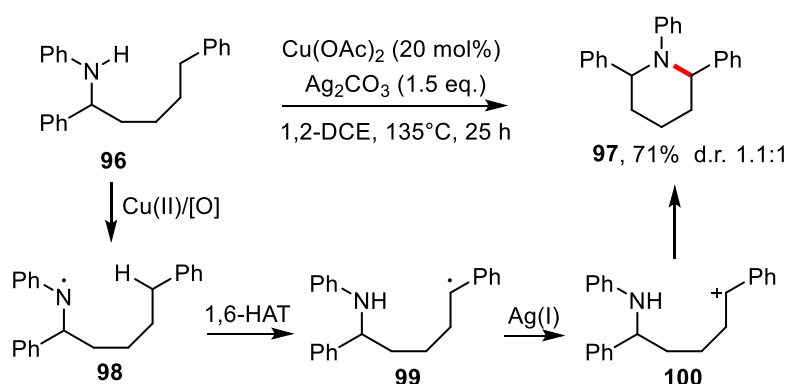
2.1.4 Intramolecular C-H amination and remote C–H amination

By employing quinoline as the directing group (DG), Ge⁶⁴ and coworkers and Kanai⁶⁵ and coworkers described the first copper-catalyzed intramolecular C(sp³)-H oxidative amidation to access diverse β -lactams in good yields. Kondo's⁶⁶ group recently developed an intramolecular Kharasch–Sosnovsky-type C(sp³)-H amidation protocol that does not require pre-functionalization and DG installation (Scheme 21).



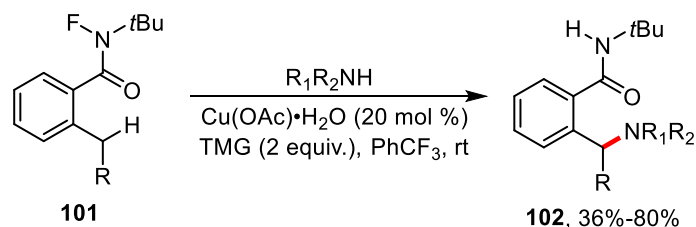
Scheme 21 Copper mediated intramolecular C–H amidation.

In 2021, Wang⁶⁷ *et al.* reported an efficient approach for the synthesis of nitrogen-containing heterocycle skeletons, using Ag_2CO_3 as oxidant and $\text{Cu}(\text{OAc})_2$ as catalyst. Nitrogen-centered radical **98** would be first formed in the presence of copper catalyst and Ag(I) salt. Then benzylic radical **99** would be generated after 1,6-hydrogen atom transfer. It undergoes a second oxidation to generate *in situ* carbocation **100** followed by a facile intramolecular amination.



Scheme 22 Copper-mediated intramolecular C–H amination.

In 2020, Liu⁶⁸ developed an efficient strategy for selective amination of remote saturated C–H bonds, starting from a *N*-fluoroamide, using various primary, secondary, and aromatic amines, to produce the remote aminated product (Scheme 23). The reaction experienced a highly ordered single electron transfer, 1,5-hydrogen atom migration, and C–N coupling process, exhibiting excellent chemical selectivity and functional group compatibility.

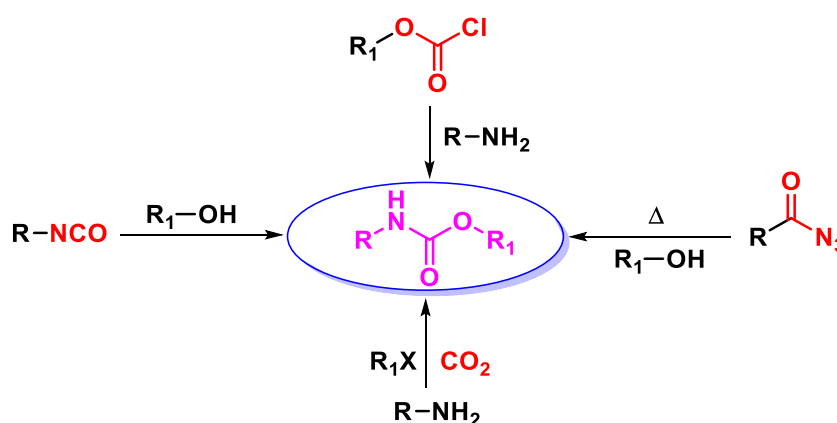


Scheme 23 Copper-mediated remote C–H amination.

2.2 Result and discussion

2.2.1 Development of carbamates synthesis

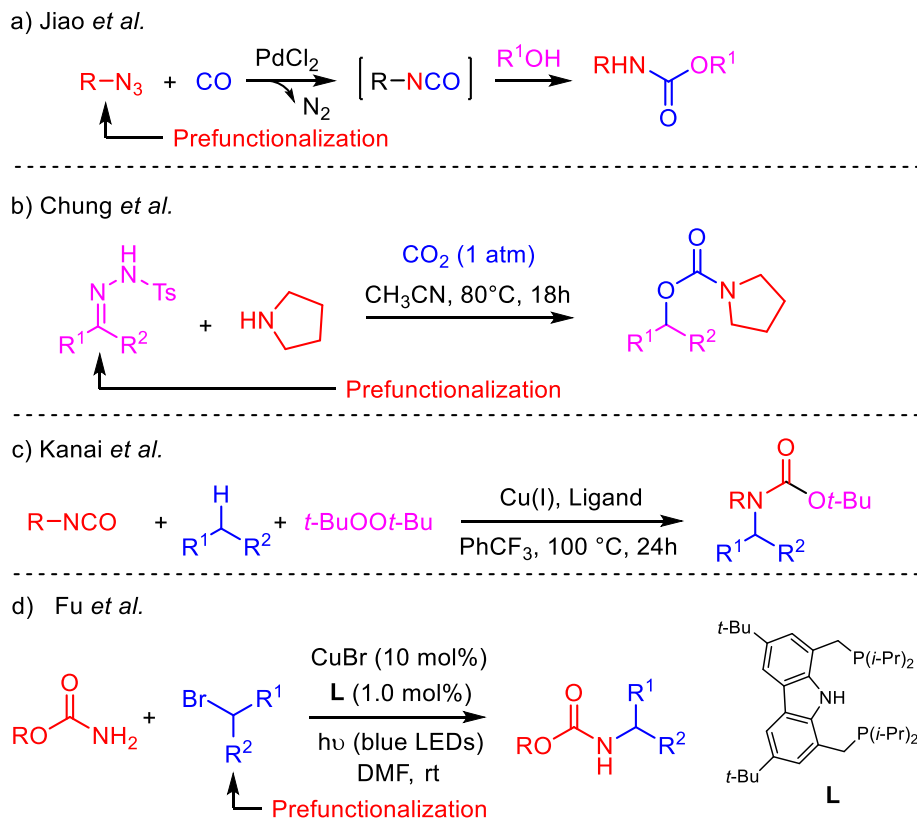
Urethanes (carbamates) are an important family of nitrogen compounds that are widespread due to their biological activities,⁶⁹⁻⁷² but also as a repeating unit in polyurethanes, the 6th class of commodity polymers.⁷³ In addition, urethanes also play a prominent role as protecting groups for amines and amino acids.⁷⁴ However, in spite of the many recent developments, access to the urethane linkage still remains a burgeoning field. Traditional protocols for installing the carbamate group include the addition of alcohols to carcinogenic isocyanates, available from acyl azide intermediates or toxic phosgene (Scheme 24).⁷⁵ Carbon dioxide was also shown to be an attractive alternative to phosgene, as it is nontoxic and widely available.⁷⁶⁻⁷⁸



Scheme 24 Traditional methods to access carbamates.

Several advancements have been made recently to efficiently construct urethanes. Jiao et al. described a straightforward and easily accessible method for the synthesis of carbamates through a three-component process involving azides, CO, and alcohols (Scheme 25a).⁷⁹ The approach involves the *in-situ* generation and application of isocyanate. In addition, this method allows for convenient modification of bioactive molecules and the construction of macrocycles. The mechanism indicates that the substrate azide initially reacts with the Pd catalyst to generate a palladium nitrene species with the release of N₂. Subsequently, a CO insertion and reductive elimination process result in the formation of an isocyanate. Finally, nucleophilic attack of the alcohol on the resulting isocyanate leads to desired product carbamate. In a similar vein, Jiang's group developed an alkali metal promoted coupling of CO₂, amines and *N*-tosylhydrazones, which led to a variety of carbamates in a single step.⁸⁰ The reaction is proposed to proceed by forming a carbo-cation intermediate, which is then trapped by a carbamate anion generated from the amine reaction with CO₂. Similar but greener

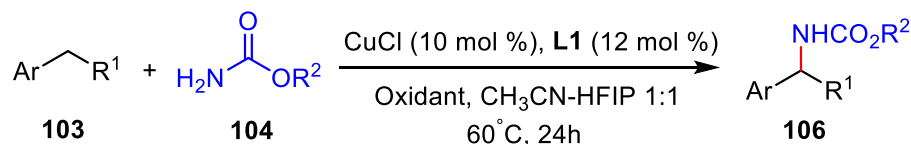
conditions were later proposed by Chung's group (Scheme 25b).⁸¹ Compared to Jiang's reaction conditions, this method does not require the addition of stoichiometric amounts of base as a promoter. It also operates at lower CO₂ pressure and reaction temperatures. Interestingly, Kanai *et al.* devised an original access to *N*-Boc carbamates through C–H activation in the presence of peroxide and isocyanates (Scheme 25c).⁸² This novel protocol enables the direct conversion of various unactivated hydrocarbon feedstocks into *N*-alkyl-*N*-aryl and *N,N*-dialkyl carbamates without the need for pre-functionalization or installation of a directing group. The reaction exhibits a wide range of substrate scope, with a site selectivity preference of 3° > 2° > 1°. Finally, Fu and co-workers described visible-light Cu(I)-catalyzed access to urethanes (Scheme 25d).⁸³ They achieved this by designing and synthesizing a new copper-based photoredox catalyst that incorporates a tridentate carbazole/bisphosphine ligand. Under blue light irradiation, the catalyst is capable of reducing alkyl bromides into alkyl radicals and generating Cu(II) intermediates. The latter would oxidize a Cu(I)-nucleophile species to a Cu(II)-nucleophile complex, which then couples with the alkyl radical to deliver the final product. These strategies have their own merits but also limitations, such as expensive catalysts, the use of carcinogenic isocyanates or hazardous peroxides, the need for prefunctionalized substrates, and harsh reaction conditions.



Scheme 25 Reported protocol for urethane synthesis.

As mentioned above, the direct functionalization of the C(sp³)-H bond represents one of the most efficient, atom and step economic strategies to introduce functional groups on a carbon skeleton. We thus describe here an alternative strategy relying on a Cu(I)-catalyzed oxidative amination of hydrocarbons at the benzylic C(sp³)-H position, which affords regioselective access to simple carbamates under mild conditions (Scheme 26).

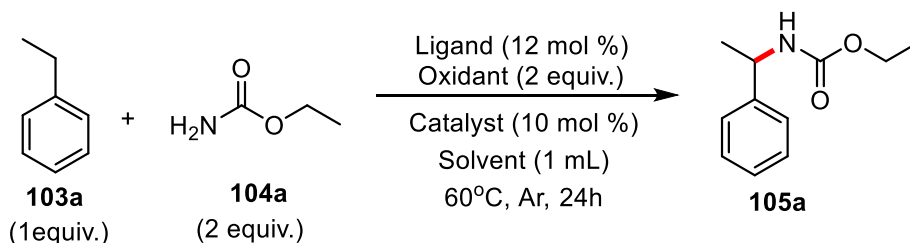
This work



Scheme 26 Copper-catalyzed oxidative benzylic C(sp³)-H amination.

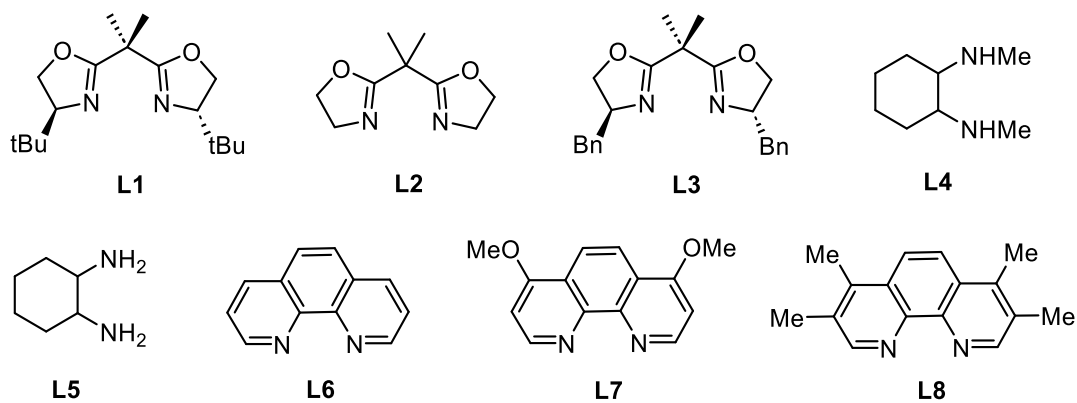
2.2.2 Optimization of the C-H amination

First, ethylbenzene **103a** and ethyl carbamate **104a** were used as the model substrates to optimize the reaction conditions (Table 1). The desired product **105a** was obtained in 72% isolated yield when using CuCl (10 mol%), ligand **L1** (12 mol%), NFSI (2.0 eq.) as the oxidant in a binary 1:1 MeCN-HFIP solvent system (Table 1, entry 1).⁸⁴ Cu catalyst proved to be essential in this reaction, as the target product was not obtained without Cu catalyst (Table 1, entry 6). Changing CuCl for CuOAc (Entry 4) did not improve the process, and iron catalyst proved to be totally inefficient in this context (entry 5).⁸⁵ Several oxidants were also tried, including Selectfluor and F-TEDA-PF₆. The former led to disappointing conversion (entry 2), while the latter led to **105a** in 53% yield (entry 3). It was later found that NFSI and F-TEDA-PF₆ were both efficient for this transformation depending on the nature of the substrate (vide infra). A mixture of MeCN and HFIP in various ratio were tested (Table 1 entries 14-22), and a 1:1 ratio was finally found to afford an optimal conversion (Table 1 entry 21). A large number of commonly used ligands were also screened with **L1** giving the best yields (Table 1, entry 1, 7-13). However, the selectivity was not obtained using the chiral ligand **L1**. This could be attributed to the formation of carbocation intermediates during the reaction process (vide infra). Photochemical activation of the deep green solution of NFSI-CuCl and **L1** using red LEDs ($\lambda_{\text{max}} = 628 \text{ nm}$) was also tested, leading to **105a** in 43% yield at 25°C (entry 23). When the reaction was performed in the dark at 25°C, only 6% of **105a** was isolated (entry 24), indicating the importance of light. Our efforts to increase yields further using a photochemical activation, however, remained unsuccessful. The optimal thermal conditions in entry 1 were finally retained to extend the substrate scope.

Table 1 Optimization of the C–H amination of **105a** with carbamate **104a**

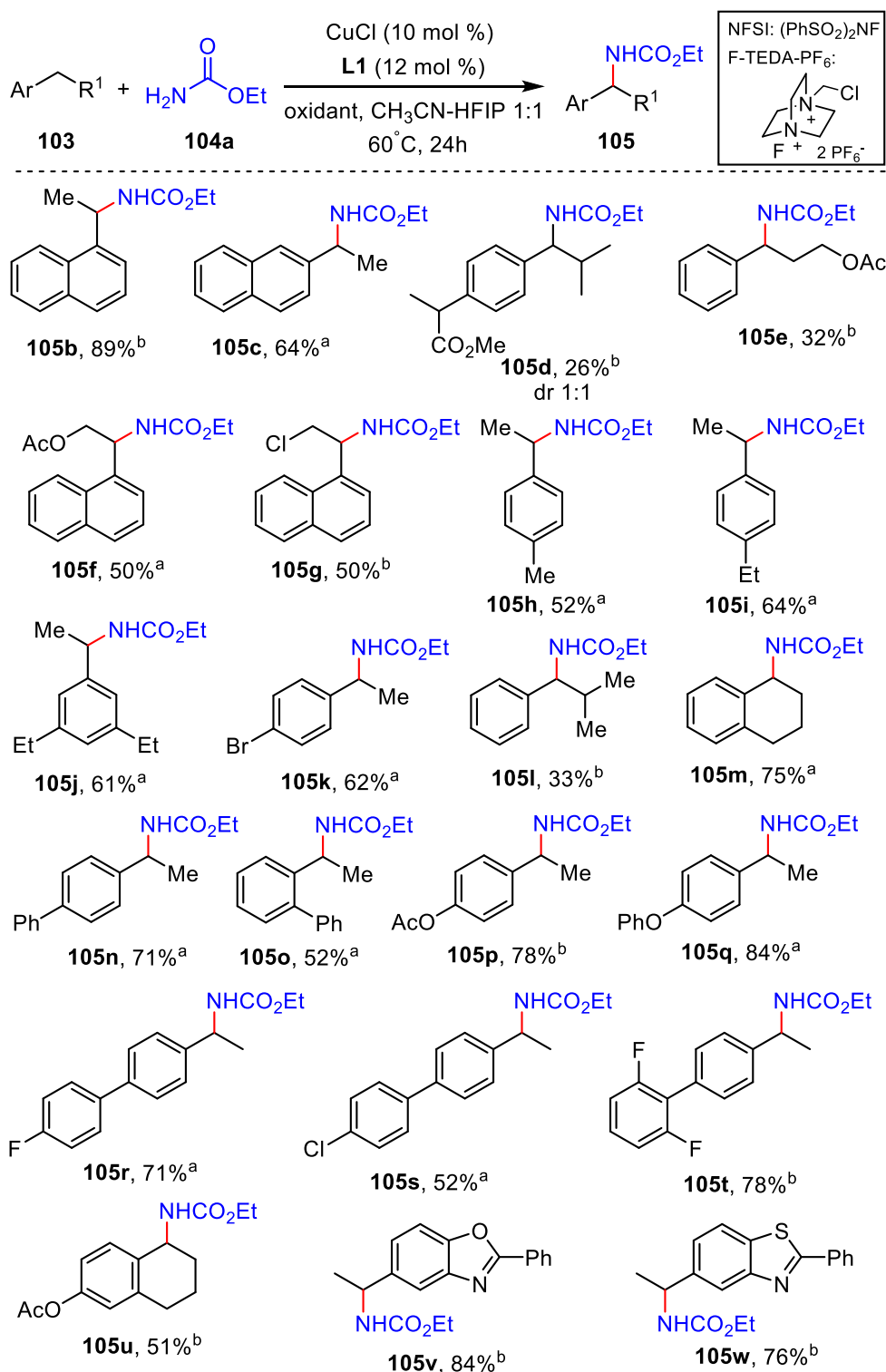
Entry ^a	Substrate	Oxidant	Catalyst	Ligand	Solvent	Yield ^b
1	0.25 mmol	NFSI	CuCl	L1	HFIP/CH₃CN (1:1)	72%
2	0.25 mmol	Selectfluor	CuCl	L1	HFIP/CH ₃ CN (1:1)	5%
3	0.25 mmol	F-TEDA-PF ₆	CuCl	L1	HFIP/CH ₃ CN (1:1)	53%
4	0.25 mmol	NFSI	Cu(OAc)	L1	HFIP/CH ₃ CN (1:1)	68%
5	0.25 mmol	NFSI	Fe(OAc) ₂	L1	HFIP/CH ₃ CN (1:1)	ND
6	0.25 mmol	NFSI	-	L1	HFIP/CH ₃ CN (1:1)	ND
7	0.25 mmol	NFSI	CuCl	L2	HFIP/CH ₃ CN (1:1)	ND
8	0.25 mmol	NFSI	CuCl	L3	HFIP/CH ₃ CN (1:1)	ND
9	0.25 mmol	NFSI	CuCl	L4	HFIP/CH ₃ CN (1:1)	ND
10	0.25 mmol	NFSI	CuCl	L5	HFIP/CH ₃ CN (1:1)	ND
11	0.25 mmol	NFSI	CuCl	L6	HFIP/CH ₃ CN (1:1)	ND
12	0.25 mmol	NFSI	CuCl	L7	HFIP/CH ₃ CN (1:1)	ND
13	0.25 mmol	NFSI	CuCl	L8	HFIP/CH ₃ CN (1:1)	ND
14	0.25 mmol	NFSI	CuCl	L1	MeCN	33%
15	0.25 mmol	NFSI	CuCl	L1	MeCN/HFIP (99 :1)	37%
16	0.25 mmol	NFSI	CuCl	L1	MeCN/HFIP (98 :2)	40%
17	0.25 mmol	NFSI	CuCl	L1	MeCN/HFIP (95 :5)	27%
18	0.25 mmol	NFSI	CuCl	L1	MeCN/HFIP (9 :1)	27%
19	0.25 mmol	NFSI	CuCl	L1	MeCN/HFIP (7 :3)	54%
20	0.25 mmol	NFSI	CuCl	L1	MeCN/HFIP (6 :4)	56%
21	0.25 mmol	NFSI	CuCl	L1	MeCN/HFIP (1 :1)	72%
22	0.25 mmol	NFSI	CuCl	L1	HFIP	8%
23 ^c	0.25 mmol	NFSI	CuCl	L1	HFIP/CH ₃ CN (1:1)	43%
24 ^d	0.25 mmol	NFSI	CuCl	L1	HFIP/CH ₃ CN (1:1)	6%

^a Reaction conditions: **103a** (0.25 mmol), Carbamate (0.5 mmol), NFSI (0.5 mmol), CuCl (0.025 mmol), Ligand (0.03 mmol) in a 1:1 MeCN/HFIP (1.0 mL) at 60°C for 24 h. ^b Isolated yield. ^c Reaction performed at 25°C under red-LEDs irradiation. ^d In the dark at 25°C.



2.2.3 Scope of the C–H amination

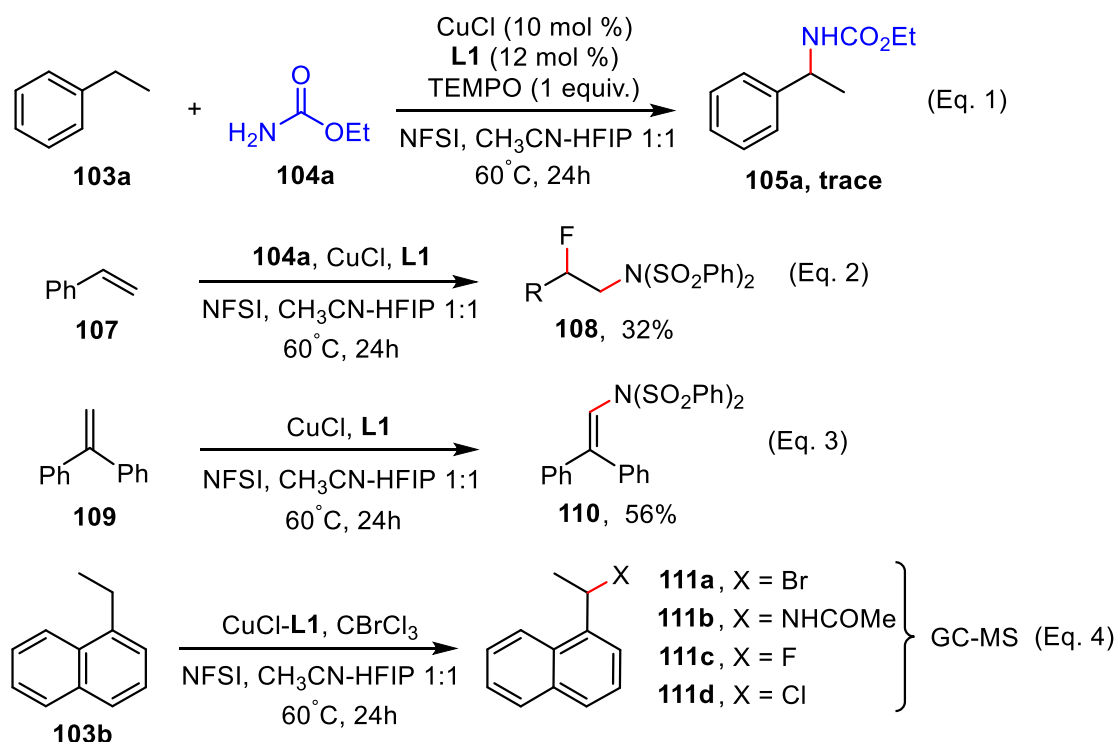
A variety of cyclic and acyclic benzylic systems was thus screened, and the corresponding carbamates obtained in moderate to good yields as summarized in Scheme 27. Functional groups including esters (in **105d**, **105f**, **105p**, **105u**) ether (**105q**), or halogens (Cl, Br, F) in **105g**, **105k**, **105r-t** are compatible with reaction conditions. Steric hindrance around the reacting center appears as a limiting factor as shown with the formation of **105d** and **105l** in moderate yield or comparing *ortho*- and *para*-substituted biphenyls **105n** and **105o**. Heterocycles are compatible with the C–H amination conditions as shown by the access to **105v-w** in good yields. In some cases, NFSI was shown to provide lower conversion, being successfully replaced with F-TEDA-PF₆, which led to cleaner reactions and proved also to be easier to discard from the crude reaction mixture by chromatography.



Scheme 27 Scope of the C–H amination of benzylic substrates with carbamate **2a**. ^a NFSI used as oxidant. ^b F-TEDA-PF₆ used as oxidant.

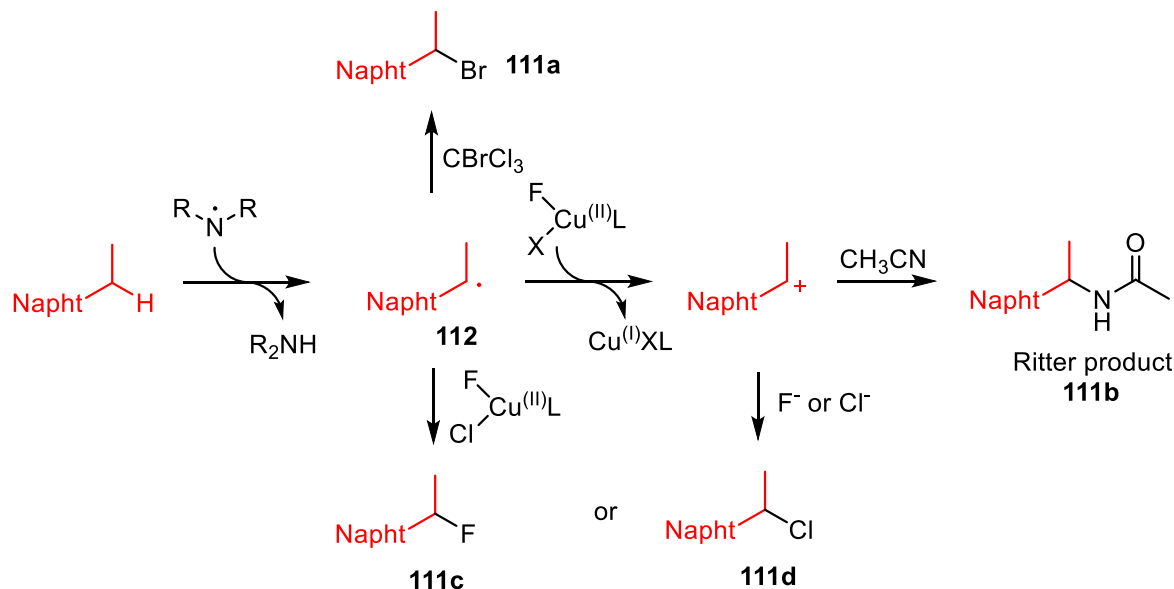
Next, to broaden the variety of urethanes accessible through this approach, we varied the nature of the substituents on the carbamate, in order to access for instance to *N*-Cbz or *N*-Troc groups, typical amine protecting groups.⁷⁴ Results summarized in Scheme 28, clearly show, as mentioned before, that yields decreased with the increasing steric hindrance of the carbamate moiety, the *N*-Boc

used as radical traps. For instance, styrene **107** was submitted to the above conditions, affording the fluorosulfonylamide addition product **108** in modest yield (Scheme 29, Eq. 2).⁸⁶ Interestingly, when the reaction was performed without **104a**, **108** was isolated in a similar yield. 1,1-Diphenylethylene **109**, under standard conditions, without **104a**, led to trisubstituted olefin **110** (Scheme 29, Eq. 3). These experiments suggest that the electrophilic $(\text{PhSO}_2)_2\text{N}$ radical is generated upon oxidation of NFSI by the Cu(I) salt,^{68d,84,87} the addition of which onto unactivated olefins **107** and **109** being favored on polar grounds.⁸⁷ Attempts to trap a putative benzylic radical by adding CBrCl_3 , using **103b** under standard conditions, failed to produce benzyl bromide **111a**, and led instead to **105b** in high yield (80-90%). When the reaction was repeated in the absence of **104a**, **111a** was detected through GC-MS, along with the corresponding amide **111b**, fluoride **111c**, chloride **111d** and several other unidentified products (Scheme 29, Eq. 4). While **111a** is indicative of the presence of a benzylic radical, formation of **111b** may be assigned to a Ritter reaction between the corresponding benzylic cation and CH_3CN . **111c-d** may in turn be issued either from a radical or from a cationic pathway.⁸⁷



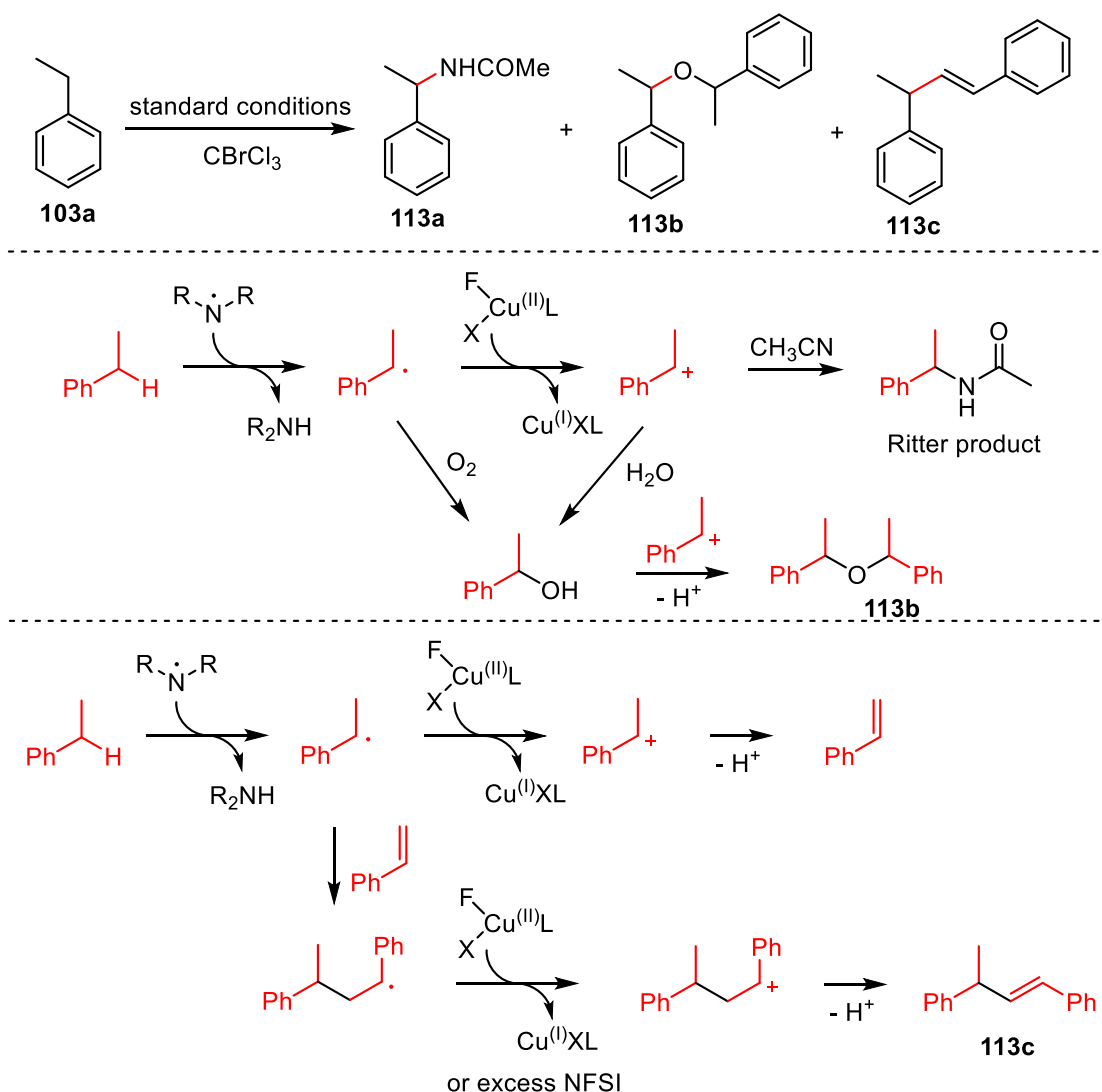
The presence of the Ritter product **111b** as well as bromide **111a**, fluoride **111c**, and chloride **111d** may be explained as shown below (Scheme 30). Hydrogen abstraction by the sulfonamidyl radical provides a benzylic radical **112**, which may be oxidized further into a cation. The latter reacts with the solvent (CH_3CN) to provide the corresponding amide **111b**. Bromide **111a** is generated

through reaction of the benzylic radical **112** with CBrCl_3 . Fluoride **111c**, and chloride **111d** may be formed through two different pathway: (1) through reaction of the benzylic radical **112** with Cu(II)FCl or the fluorosulfonylamide; (2) through reaction of the benzylic cation with fluoride or chloride anions present in the medium.



Scheme 30 Possible mechanism for product **111a**, **111b**, **111c**, and **111d**.

Similar results were obtained during reaction of ethylbenzene **103a** with CBrCl_3 , under standard conditions, leading to a Ritter product **113a** and by-products suggesting the presence of both radical and cationic species (Scheme 31). The presence of the Ritter product **113a** and that of the ether **113b** may be explained as shown below. Hydrogen abstraction by the sulfonamidyl radical provides a benzylic radical, which may be oxidized further into a cation. The latter reacts with the solvent (CH_3CN) to provide the corresponding amide **113a**. The benzylic alcohol may be formed through reaction of the benzyl radical with oxygen traces or through reaction of the benzylic cation with traces of water. Ether **113b** is then generated through the reaction of the benzyl alcohol with the benzylic cation. The dimeric product **113c** is postulated to be generated as shown below. The benzylic cation formed as explained before loses a proton to form styrene. The benzylic radical may then add onto styrene to provide a stabilized benzylic radical that is oxidized into the corresponding cation (by Cu(II) or excess NFSI) affording the dimeric product **113c** with structure as shown.

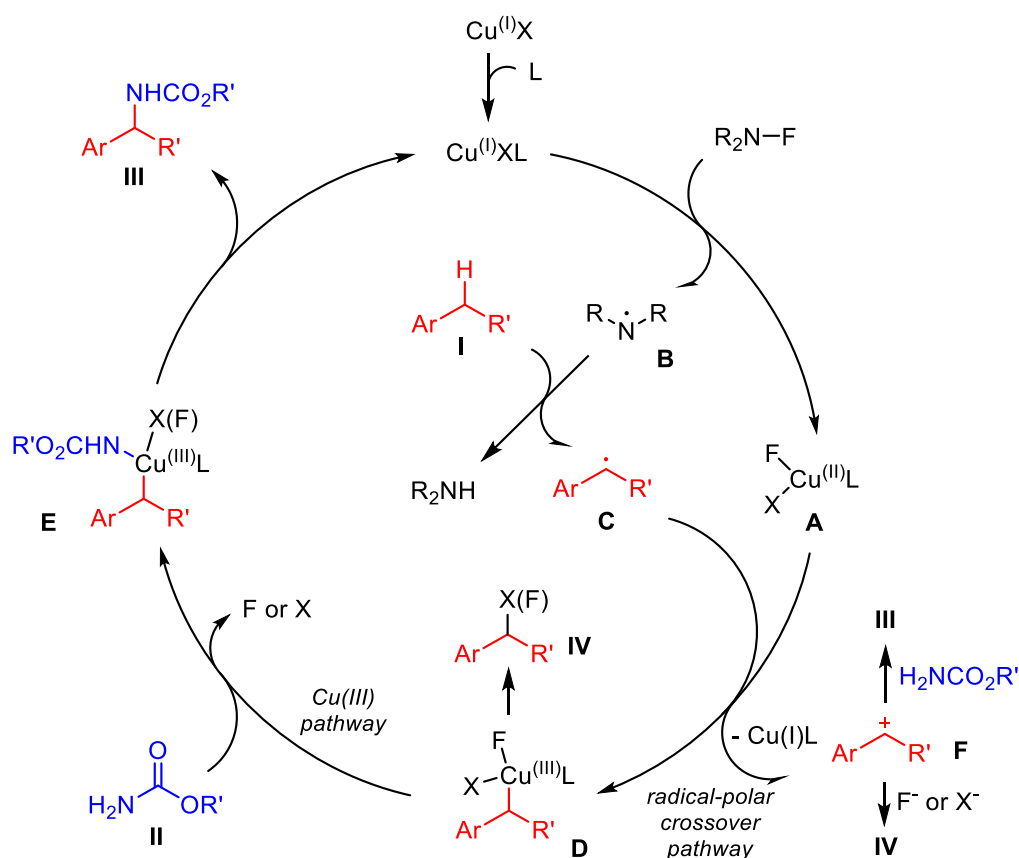


Scheme 31 Possible mechanism for product **113a**, **113b**, and **113c**.

2.2.5 Proposed reaction mechanism

Based on the above experimental evidence and previous literature reports,^{68d,84,87-89} a tentative mechanism for the benzylic C–H amination is finally proposed as depicted in Scheme 32. We first anticipated a single-electron transfer from the Cu(I)–L complex to NFSI (or F-TEDA-PF₆), which would provide a Cu(II)–complex **A** along with a nitrogen-centered radical **B**. The latter would subsequently abstract the benzylic hydrogen of substrate **I** to generate a benzylic radical **C**. This may then evolve following two possible pathways, e.g. (1) through a combination with Cu-complex **A** to afford Cu(III) species **D**,⁹⁰ which could lead to intermediate **E** after ligand exchange with carbamate **II**, providing urethane **III** upon reductive elimination or benzyl halides **IV** in the absence of **II**. A radical-polar crossover process (2) should also be invoked through oxidation of **C** by Cu(II) species **A** into benzylic cation **F**.^{84b} The absence of enantioselectivity using chiral ligand **L1** in our

experiments and the formation of Ritter product **111b** points toward the formation of such a cation. Finally, a similar reasoning should apply to addition products **108** and **110**. The radical resulting from the addition of $(\text{PhSO}_2)_2\text{N}$ onto **107** and **109** may be oxidized into a cation such as **F**, which would then evolve toward **110** though proton elimination or trapped by a fluoride anion leading to **108**. The absence of carbamate addition in the last case may be explained by the steric hindrance of the $(\text{PhSO}_2)_2\text{N}$ group preventing the approach of **104a**, as observed above for hindered benzylic substrates (i.e. **105d**, **105l**). A Cu(II) complex such as **D** may also explain the formation of **108**.⁸⁸ Additional mechanistic studies will however be required to firmly distinguish between these pathways, studies that are currently ongoing.



Scheme 32 Proposed reaction mechanism for the benzylic C–H amination.

2.3 Conclusion

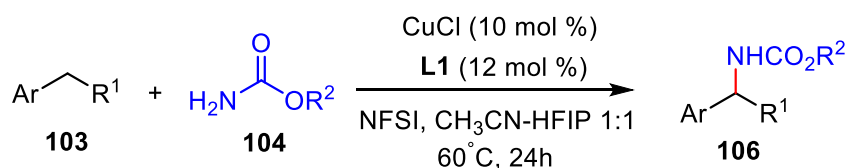
In summary, we reported a direct Cu-catalyzed C–H amination of a variety of benzylic substrates, leading to carbamates in satisfying yields. The combination between strong oxidants, *i.e.* NFSI or F-TEDA-PF₆ and Cu(I)-catalyst/diimine system was found to be highly efficient to access carbamates including N-Cbz and N-Troc derivatives. This methodology avoiding carcinogenic isocyanates and unsafe peroxides should be useful for late-stage functionalization of hydrocarbons in medicinal chemistry where urethanes are widespread.

2.4 Experimental part

2.4.1 General Information

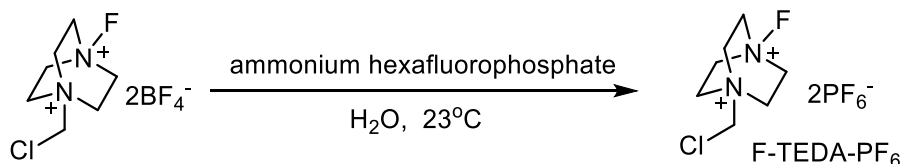
All reactions were carried out under an argon atmosphere. Solvents were dried over activated alumina columns on a M-BRAUN Solvent Purification System (SPS-800) unless otherwise noted. The calculated experimental yields refer to chromatographically and spectroscopically ($^1\text{H-NMR}$) homogeneous materials unless otherwise stated. All reagent-grade chemicals were obtained from commercial suppliers and were used as received unless otherwise stated. ^1H NMR and ^{13}C NMR were recorded at room temperature on various spectrometers: a Bruker Avance 300 (^1H : 300 MHz, ^{13}C : 75 MHz) and a Bruker Avance 600 (^1H : 600 MHz, ^{13}C : 150 MHz) using CDCl_3 as internal reference unless otherwise indicated. The chemical shifts (δ) and coupling constants (J) are expressed in ppm and Hz respectively. The following abbreviations were used to explain the multiplicities: br = broad, s = singlet, d = doublet, t = triplet, q = quartet, dd = doublet of doublets, m = multiplet, quint = quintuplet, hex = hexuplet, hept = heptuplet. Compounds were described as mixtures when it was not possible, in our hands, to separate both compounds. FTIR spectra were recorded on a Perkin-Elmer Spectrum 100 using a KBr pellet. High-resolution mass spectra (HRMS) were recorded with a Waters Q-TOF 2 spectrometer in the electrospray ionization (ESI) mode unless otherwise noted. Melting points were not corrected and determined by using a Stuart Scientific SMP3 apparatus. Analytical thin layer chromatography was performed using silica gel 60 F254 pre-coated plates (Merck) with visualization by ultraviolet light. Flash chromatography was performed on silica gel (0.043-0.063 mm) with ethyl acetate (EtOAc) and Petroleum ether (PE) as eluents unless otherwise indicated.

2.4.2 General Procedure



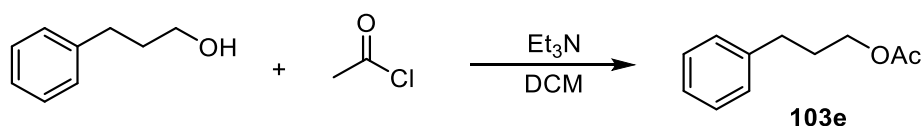
Synthesis of urethanes from benzylic hydrogens: In a glovebox under an argon atmosphere, the ligand L1 (0.03 mmol, 12 mol%), the CuCl (0.025 mmol, 10 mol%) in a 1:1 MeCN/HFIP mixture (1 mL) were placed in a dried sealed tube (10 mL). The resulting mixture was stirred at room temperature for 20 minutes. Then, NFSI (157 mg, 0.5 mmol, 2 equiv.), the carbamate (0.5 mmol, 2 equiv.) and the substrate (0.25 mmol, 1 equiv.) were added. The tube was sealed and the mixture was heated at 60°C for 24h. The mixture was then solubilized in DCM and evaporated under reduced pressure. The crude mixture was purified by column chromatography to afford the product.

2.4.3 Synthesis of Starting Materials

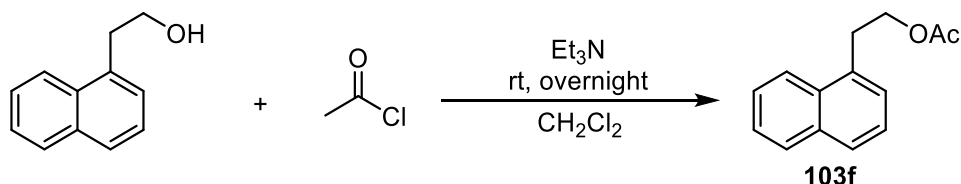


F-TEDA-PF₆: (Compound above have been prepared following methods of a literature reference 1.) The ammonium hexafluorophosphate (2.93 g, 18 mmol, 6 equiv.) was added to Selectfluor (1.06 g, 3.0 mmol, 1 equiv.) in water (9.0 mL) at 23°C. The resulting mixture was stirred for 1 h, and then the suspension was filtered off and washed with water (5×5 mL) and Et₂O (10 mL). The solid was dried under vacuum at 40°C for 48h and the expected salt obtained as a white solid (1.14 g, 81%) used in the next step without further purification. ¹H NMR (300 MHz, CD₃CN) δ 5.29 (s, 2H), 4.71 (q, *J* = 7.4 Hz, 6H), 4.34 – 4.19 (m, 6H). ¹³C NMR (76 MHz, CD₃CN) δ 69.67 (d, *J* = 2.7 Hz), 57.78 (d, *J* = 15.2 Hz), 54.26 (dt, *J* = 5.9, 2.6 Hz).

NMR spectroscopic data were identical to those previously reported.⁹¹



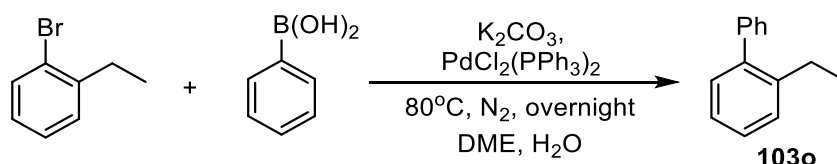
Benzenepropanol, 1-acetate (103e): A solution of 3-phenylpropan-1-ol (0.68 mg, 5.0 mmol, 1 equiv.) in DCM (20 mL) was added triethylamine (0.84 mL, 6 mmol, 1.2 equiv.), followed by the dropwise addition of acetyl chloride (0.43 mL, 6 mmol, 1.2 equiv.). The resulting mixture was stirred overnight at room temperature, then diluted with DCM (20 mL) and quenched with water (20 mL). After extraction with CH₂Cl₂ (3×25 mL), the solvent was dried over magnesium sulfate and removed in vacuo. The crude residue was purified by flash column chromatography on silica gel (PE/EA = 20:1) to afford the target compound **1e** (0.76 g, 76%) as colorless oil. ¹H NMR (300 MHz, CDCl₃) δ 7.36 – 7.27 (m, 2H), 7.25 – 7.17 (m, 3H), 4.11 (t, *J* = 6.6 Hz, 2H), 2.71 (dd, *J* = 8.7, 6.7 Hz, 2H), 2.07 (s, 3H), 2.04 – 1.92 (m, 2H). ¹³C NMR (76 MHz, CDCl₃) δ 171.0, 141.2, 128.4, 128.4, 126.0, 63.8, 32.2, 30.2, 20.9. NMR spectroscopic data were identical to those previously reported.⁹²



1-Naphthaleneethanol, 1-acetate (103f): A solution of 2-(1-naphthyl)ethanol (1.00 g, 6.32 mmol, 1 equiv.) in CH₂Cl₂ (20 mL) was placed under inert atmosphere and at 0°C in an ice water bath. Triethylamine (1.06 mL, 7.59 mmol, 1.2 equiv.) was added at 0°C, followed by the dropwise addition of acetyl chloride (0.54 mL, 7.59 mmol, 1.2 equiv.). The resulting mixture was stirred overnight at room temperature, then diluted with dichloromethane (20 mL) and quenched with water (40 mL). The organic phase was separated and phases were washed with brine (2×20 mL) and eventually dried over magnesium sulfate. Solvent was removed in vacuo. The crude residue was

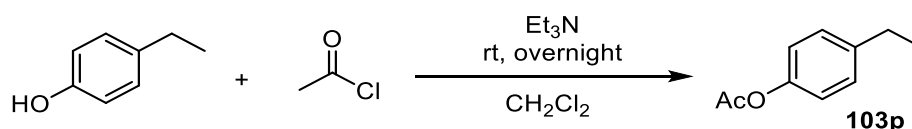
purified by flash column chromatography on silica gel (PE/EA-10:1) to afford the target compound (1.10 g, 81%) as colorless oil. ¹H NMR (300 MHz, CDCl₃) δ 8.12 (d, *J* = 8.2 Hz, 1H), 7.95 – 7.86 (m, 1H), 7.79 (d, *J* = 7.9 Hz, 1H), 7.61 – 7.35 (m, 4H), 4.44 (t, *J* = 7.4 Hz, 2H), 3.44 (t, *J* = 7.4 Hz, 2H), 2.08 (s, 3H). ¹³C NMR (76 MHz, CDCl₃) δ 171.2, 134.0, 133.8, 132.2, 128.9, 127.6, 127.1, 126.3, 125.8, 125.6, 123.71 64.6, 32.4, 21.2.

NMR spectroscopic data were identical to those previously reported.⁹³



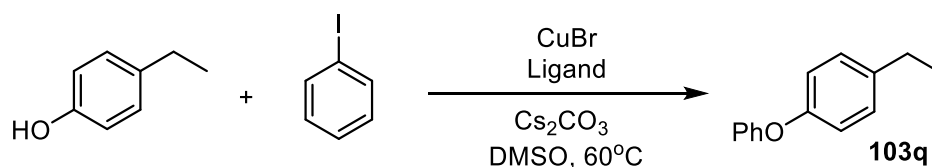
2-Ethyl-1,1'-biphenyl (103o): In a 50 mL two-neck round bottom flask, 1-bromo-2-ethylbenzene (1 equiv. 5 mmol, 920 mg), phenylboronic acid (1.2 equiv. 6 mmol, 732 mg), K₂CO₃ aqueous solution (2M, 12 mL) and DME were added under N₂ atmosphere. The mixture was then stirred at room temperature for 30 minutes. Then, the PdCl₂(PPh₃)₂ (2 mol %, 0.1 mmol, 70 mg) was added and the reaction mixture was stirred at 80°C overnight under N₂ atmosphere. The mixture was extracted with EtOAc (3×20 mL), dried over Na₂SO₄. Solvent was removed in vacuo. The crude residue was purified by flash column chromatography on silica gel (PE/EA = 50:1) to afford the target compound (874 mg, 96%) as colorless oil. ¹H NMR (300 MHz, CDCl₃) δ 7.53 – 7.25 (m, 9H), 2.69 (q, *J* = 7.5 Hz, 2H), 1.18 (td, *J* = 7.5, 0.8 Hz, 3H). ¹³C NMR (76 MHz, CDCl₃) δ 142.1, 141.7, 130.1, 129.3, 128.7, 128.1, 127.6, 126.9, 125.7, 26.3, 15.8.

NMR spectroscopic data were identical to those previously reported.⁹⁴



4-Ethylphenyl acetate (103p): The product was obtained following the same procedure as **1f**. Colorless oil (0.77g, 94%). ¹H NMR (300 MHz, CDCl₃) δ 7.24 – 7.16 (m, 2H), 6.99 (dd, *J* = 8.5, 2.2 Hz, 2H), 2.65 (q, *J* = 7.6 Hz, 2H), 2.29 (s, 3H), 1.24 (td, *J* = 7.6, 2.0 Hz, 3H). ¹³C NMR (76 MHz, CDCl₃) δ 169.8, 148.7, 141.9, 128.9, 121.4, 28.4, 21.3, 15.7.

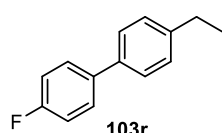
NMR spectroscopic data were identical to those previously reported.⁹⁵



1-Ethyl-4-phenoxybenzene (103q): In a three-necked reaction vessel equipped with a magnetic stirring bar, CuBr (144 mg, 1 mmol, 0.1 equiv.), Cs₂CO₃ (6.84 g, 21 mmol, 2.1 equiv.) and ethyl 2-oxocyclohexanecarboxylate (340 mg, 2 mmol, 0.2 equiv.) were dissolved in DMSO (10 mL) under a N₂ atmosphere. Then iodobenzene (2.04 g, 10 mmol, 1 equiv.) and 3-ethylphenol (1.47 g, 12 mmol, 1.2 equiv.) were added, and the mixture was heated to 60°C. After the reaction was completed,

the crude solution was filtered through a pad of silica gel. The filtrate was washed with brine, dried over MgSO₄ and concentrated under vacuum. The crude residue was purified by flash column chromatography on silica gel (PE/EtOAc-50:1) to afford the target compound (1.7 g, 86%) as colorless oil. ¹H NMR (300 MHz, CDCl₃) δ 7.42 – 7.31 (m, 2H), 7.24 – 7.17 (m, 2H), 7.15 – 7.08 (m, 1H), 7.07 – 6.94 (m, 4H), 2.68 (q, *J* = 7.6 Hz, 2H), 1.29 (t, *J* = 7.6 Hz, 3H). ¹³C NMR (76 MHz, CDCl₃) δ 157.9, 155.0, 139.4, 130.0, 129.8, 129.8, 129.1, 122.9, 119.2, 118.5, 28.3, 15.9. NMR spectroscopic data were identical to those previously reported.⁹⁶

4-Ethyl-4'-fluoro-1,1'-biphenyl (103r): The product was obtained following the same procedure as



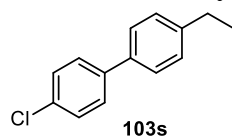
10. White solid (950 mg, 95%).

¹H NMR (400 MHz, CDCl₃) δ 7.60 – 7.53 (m, 2H), 7.52 – 7.47 (m, 2H), 7.30 (d, *J* = 8.0 Hz, 2H), 7.18 – 7.11 (m, 2H), 2.73 (q, *J* = 7.6 Hz, 2H), 1.31 (t, *J* = 7.6 Hz, 3H). ¹³C NMR (76 MHz, CDCl₃) δ 162.4 (d, *J* = 245.8 Hz), 143.5, 137.8, 137.4

(d, *J* = 3.3 Hz), 128.6 (d, *J* = 8.0 Hz), 128.5, 127.1, 115.7 (d, *J* = 21.4 Hz), 28.6, 15.7.

NMR spectroscopic data were identical to those previously reported.⁹⁷

4-Chloro-4'-ethyl-1,1'-biphenyl (103s): The product was obtained following the same procedure as

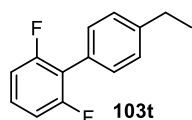


10. White solid (946 mg, 88%).

¹H NMR (400 MHz, CDCl₃) δ 7.54 – 7.47 (m, 4H), 7.43 – 7.37 (m, 2H), 7.32 – 7.27 (m, 2H), 2.71 (q, *J* = 7.6 Hz, 2H), 1.29 (t, *J* = 7.6 Hz, 3H). ¹³C NMR (76

MHz, CDCl₃) δ 143.9, 139.7, 137.5, 133.2, 129.0, 128.5, 128.3, 127.0, 28.7, 15.7.

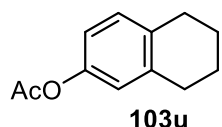
4'-Ethyl-2,6-difluoro-1,1'-biphenyl (103t): The product was obtained following the same procedure as **10.** White solid (1.0 g, 93%).



¹H NMR (400 MHz, CDCl₃) δ 7.51 – 7.42 (m, 2H), 7.39 – 7.26 (m, 3H), 7.09 – 6.95 (m, 2H), 2.77 (q, *J* = 7.6 Hz, 2H), 1.35 (t, *J* = 7.6 Hz, 3H). ¹³C NMR (76 MHz,

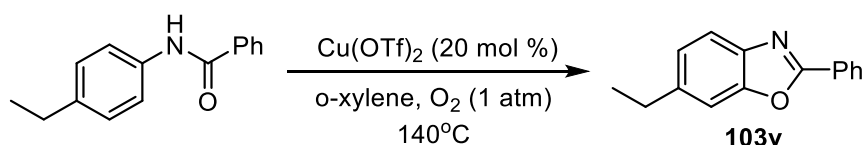
CDCl₃) δ 160.3 (dd, *J* = 248.2, 7.2 Hz), 144.4, 130.3 (t, *J* = 1.8 Hz), 128.7 (t, *J* = 10.4 Hz), 127.9, 126.5, 118.6 (t, *J* = 18.7 Hz), 113.9 – 108.3 (m), 28.8, 15.5.

5,6,7,8-Tetrahydronaphthalen-2-yl acetate (103u): The product was obtained following the same procedure as **1p.** Colorless oil (1.56 g, 82%).



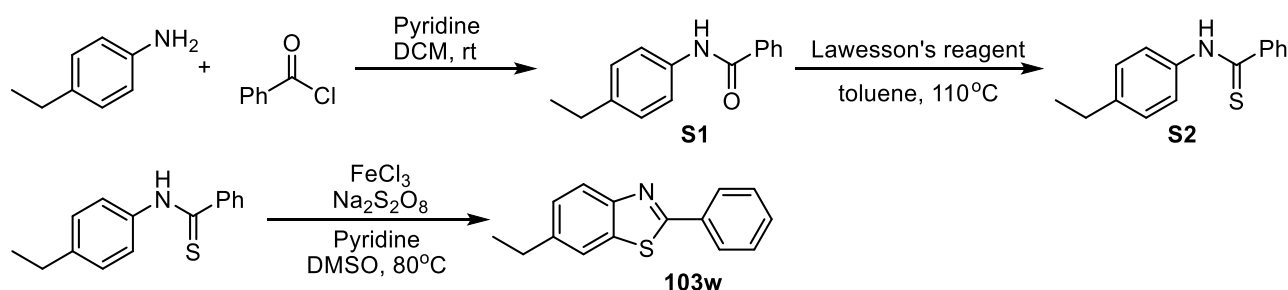
¹H NMR (300 MHz, CDCl₃) δ 7.16 – 7.04 (m, 1H), 6.90 – 6.77 (m, 2H), 2.91 – 2.72 (m, 4H), 2.31 (s, 3H), 1.84 (h, *J* = 3.4, 2.9 Hz, 4H). ¹³C NMR (76 MHz, CDCl₃) δ 169.6, 148.2, 138.3, 134.6, 129.8, 121.6, 118.5, 29.4, 28.8, 23.1, 22.8,

21.0. NMR spectroscopic data were identical to those previously reported.⁹⁸



6-Ethyl-2-phenylbenzo[d]oxazole (103v): (Compound above has been prepared following a reported method¹¹). To a dried Schlenk tube was added the *N*-(4-ethylphenyl)benzamide (1.13 g, 5 mmol, 1 equiv.) and Cu(OTf)₂ (362 mg, 1 mmol, 0.2 equiv.). The tube and its contents were then purged under oxygen and *o*-xylene (10 ml) was added via syringe. The reaction mixture was then heated with stirring at 140°C for 48h under oxygen (balloon) atmosphere. The mixture was then concentrated under reduced pressure. The residue was diluted with EtOAc and water, the combined organic phase washed with brine, dried (MgSO₄) and concentrated in vacuum. The residue was purified by silica gel chromatography to afford the target compound **1v** (360 mg, 32%) as yellow solid. ¹H NMR (300 MHz, CDCl₃) δ 8.33 – 8.17 (m, 2H), 7.67 (dd, *J* = 8.1, 0.6 Hz, 1H), 7.52 (ddd, *J* = 3.5, 2.4, 1.3 Hz, 3H), 7.41 (dd, *J* = 1.6, 0.8 Hz, 1H), 7.20 (dd, *J* = 8.1, 1.6 Hz, 1H), 2.80 (q, *J* = 7.6 Hz, 2H), 1.31 (t, *J* = 7.6 Hz, 3H). ¹³C NMR (76 MHz, CDCl₃) δ 162.8, 151.2, 142.3, 140.2, 131.4, 129.0, 127.6, 127.5, 124.9, 119.6, 109.7, 29.3, 16.1.

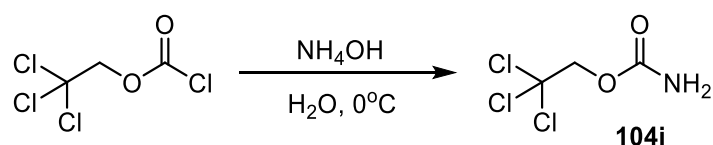
NMR spectroscopic data were identical to those previously reported.⁹⁹



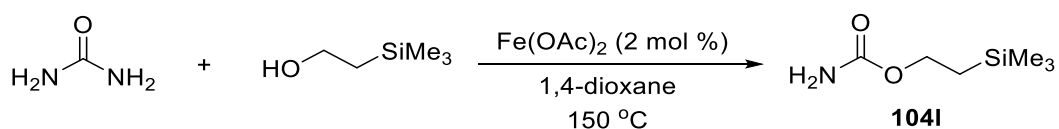
***N*-(E-ethylphenyl)benzamide (S1):** To a solution of 3-ethylaniline (2.42 g, 20 mmol, 1 equiv.) and pyridine (2.3 mL, 28 mmol, 1.4 equiv.) in DCM (40 mL) at 0 °C, benzoyl chloride (3.10 g, 22 mmol, 1.1 equiv.) was added dropwise. The reaction was gradually warmed to room temperature and stirred overnight. After being quenched with water, the mixture was extracted with DCM. The organic phase was washed with HCl(aq) (1M) and brine, dried over MgSO₄. The solvent was removed under reduced pressure, and the crude residue was recrystallized with PE/EtOAc to afford **S4** (4.3 g, 95%) as a white solid. ¹H NMR (300 MHz, CDCl₃) δ 8.12 – 8.03 (m, 1H), 7.89 – 7.79 (m, 2H), 7.61 – 7.47 (m, 3H), 7.47 – 7.37 (m, 2H), 7.22 – 7.12 (m, 2H), 2.64 (q, *J* = 7.6 Hz, 2H), 1.24 (t, *J* = 7.6 Hz, 3H). ¹³C NMR (76 MHz, CDCl₃) δ 166.0, 140.7, 135.7, 135.1, 131.7, 128.7, 128.4, 127.2, 120.7, 28.4, 15.8.

***N*-(4-Ethylphenyl)benzothioamide (S2):** To a three-necked vessel (50 mL) equipped with a stir bar, **S4** (2.25 g, 10 mmol, 1 equiv.) and Lawesson's reagent (2.12 g, 5.25 mmol, 0.52 equiv.) were dissolved in anhydrous toluene (15 mL) under a N₂ atmosphere. The resulting mixture was stirred at 110°C for 3 h. After cooling to room temperature, the organic solvent was removed, and the residue purified by flash column chromatography on silica gel (PE/EtOAc-10:1) to afford **S5** (723 mg, 30%) as a yellow solid. ¹H NMR (300 MHz, CDCl₃) δ 8.97 (s, 1H), 7.94 – 7.80 (m, 2H), 7.67 (d, *J* = 8.0 Hz, 2H), 7.46 (dt, *J* = 14.7, 7.1 Hz, 3H), 7.29 (s, 1H), 2.68 (q, *J* = 7.6 Hz, 2H), 1.26 (t, *J* = 7.6 Hz, 3H). ¹³C NMR (76 MHz, CDCl₃) δ 198.4, 143.4, 136.8, 131.4, 128.80, 128.6, 126.8, 123.9, 28.7, 15.5.

6-Ethyl-2-phenylbenzo[d]thiazole (103w): (Compound above has been prepared following a reported methods¹²). To a three-necked vessel (50 mL) equipped with a stir bar, FeCl₃ (10 mg, 0.06 mmol, 0.1 equiv.), **S5** (145 mg, 0.6 mmol, 1 equiv.) and Na₂S₂O₈ (286 mg, 1.2 mmol, 2 equiv.) were dissolved in a solution of pyridine (95 mg, 1.2 mmol, 2 equiv.) in DMSO (2 mL) under a N₂ atmosphere. The mixture was stirred at 80°C for 3h. After cooling to room temperature, the reaction mixture was quenched with water and extracted with EtOAc (2×5 mL). The organic layers were combined, dried over MgSO₄, concentrated under reduced pressure, and purified by silica gel chromatography (PE/EtOAc-20:1) to yield the product (100 mg, 70%). ¹H NMR (300 MHz, CDCl₃) δ 8.16 – 8.05 (m, 2H), 8.04 – 7.95 (m, 1H), 7.70 (dq, *J* = 1.4, 0.7 Hz, 1H), 7.52 – 7.43 (m, 3H), 7.34 (dt, *J* = 8.5, 1.1 Hz, 1H), 2.79 (q, *J* = 7.6 Hz, 2H), 1.32 (t, *J* = 7.6 Hz, 3H). ¹³C NMR (76 MHz, CDCl₃) δ 167.2, 152.5, 141.9, 135.4, 133.9, 130.8, 129.1, 127.5, 126.9, 122.9, 120.3, 29.1, 15.9. NMR spectroscopic data were identical to those previously reported.¹⁰⁰



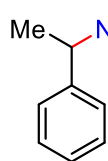
2,2,2-Trichloroethyl carbamate (104i): (Compound above has been prepared following a reported methods¹⁰¹). Commercially available 2,2,2-trichloroethyl chloroformate was added dropwise to an excess of ammonium hydroxide with vigorous stirring at 0°C. The white precipitated product was dissolved in methylene chloride, washed with water and brine, dried over MgSO₄, filtered, and the solvent removed. The product was isolated as a white solid in near quantitative yield. ¹H NMR (300 MHz, CDCl₃) δ 5.16 (s, 2H), 4.72 (s, 2H). ¹³C NMR (76 MHz, CDCl₃) δ 155.2, 95.4, 74.8. NMR spectroscopic data were identical to those previously reported.¹⁰¹



2-(Trimethylsilyl)ethyl carbamate (104I): (Compound above has been prepared following a reported methods¹⁰²). In a glass pressure tube (25 mL) under an Ar atmosphere, Fe(OAc)₂ (17.4 mg, 0.1 mmol, 0.02 equiv.), urea (301 mg, 5 mmol, 1 equiv.) and alcohol (887 mg, 7.5 mmol, 1.5 equiv.) were dissolved in 1,4-dioxane (10 mL). Next, the tube was closed and the resulting mixture stirred at 150°C in an oil bath for 6h. After cooling down to room temperature, the crude mixture was directly purified by flash chromatography on silica gel to afford the corresponding product (115 mg, 14%). ¹H NMR (300 MHz, CDCl₃) δ 4.62 (s, 2H), 4.23 – 4.08 (m, 2H), 1.08 – 0.80 (m, 2H), 0.04 (s, 9H).

2.4.4 Characterization Data

Ethyl (1-phenylethyl)carbamate (105a)



R_f = 0.25-0.3 (PE : EA = 5:1).

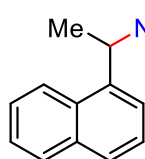
FT-IR ν_{max} (cm⁻¹) = 3324, 2979, 1699, 1538, 1532, 1247, 1064, 700.

¹H NMR (300 MHz, CDCl₃) δ 7.37 – 7.22 (m, 5H), 5.08 – 4.70 (m, 2H), 4.10 (qd, J = 7.1, 1.7 Hz, 2H), 1.48 (d, J = 6.8 Hz, 3H), 1.22 (t, J = 7.1 Hz, 3H).

¹³C NMR (76 MHz, CDCl₃) δ 155.9, 143.8, 128.7, 127.4, 126.0, 60.9, 50.7, 22.64 14.7.

HRMS (ESI): [M+Na]⁺ C₁₁H₁₅O₂NNa⁺: calcd. 216.09950 found 216.09873.

Ethyl (1-(naphthalen-1-yl)ethyl)carbamate (105b)



R_f = 0.25-0.3 (PE : EA = 10:1).

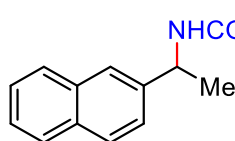
m.p. = 98-101°C

FT-IR ν_{max} (cm⁻¹) = 3324, 2978, 1694, 1704, 1531, 1513, 1245, 1064, 777.

¹H NMR (300 MHz, CDCl₃) δ 8.14 (d, J = 8.3 Hz, 1H), 7.92 – 7.73 (m, 2H), 7.60 – 7.40 (m, 4H), 5.65 (d, J = 7.3 Hz, 1H), 4.99 (s, 1H), 4.13 (qd, J = 7.1, 0.9 Hz, 2H), 1.65 (d, J = 6.8 Hz, 3H), 1.22 (t, J = 7.0 Hz, 3H). ¹³C NMR (76 MHz, CDCl₃) δ 155.9, 139.1, 134.1, 131.0, 129.0, 128.3, 126.5, 125.9, 125.4, 123.4, 122.3, 61.0, 46.7, 21.9, 14.7.

HRMS (ESI): [M+Na]⁺ C₁₅H₁₇O₂NNa⁺: calcd. 266.11515 found 266.11470.

Ethyl (1-(naphthalen-2-yl)ethyl)carbamate (105c)



R_f = 0.25-0.3 (PE : EA = 10:1).

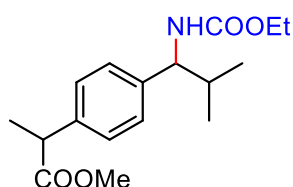
m.p. = 66-68°C

FT-IR ν_{max} (cm⁻¹) = 3323, 2977, 1699, 1527, 1246, 1064.

¹H NMR (300 MHz, CDCl₃) δ 7.93 – 7.69 (m, 4H), 7.55 – 7.38 (m, 3H), 5.03 (s, 2H), 4.12 (qd, J = 7.1, 1.9 Hz, 2H), 1.57 (d, J = 6.4 Hz, 3H), 1.23 (t, J = 7.1 Hz, 3H). ¹³C NMR (76 MHz, CDCl₃) δ 156.0, 141.2, 133.5, 132.8, 128.6, 128.0, 127.7, 126.3, 125.9, 124.6, 124.4, 61.0, 50.8, 22.6, 14.7.

HRMS (ESI): [M+Na]⁺ C₁₅H₁₇O₂NNa⁺: calcd. 266.11515, found 266.11465.

Methyl 2-(4-(1-((ethoxycarbonyl)amino)-2-methylpropyl)phenyl)propanoate (105d)



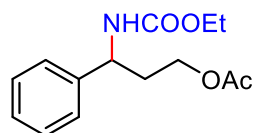
R_f = 0.25-0.3 (PE : EA = 5:1).

FT-IR ν_{max} (cm⁻¹) = 3337, 2975, 2959, 1736, 1720, 1529, 1515, 1238, 1212, 1168, 1036.

¹H NMR (300 MHz, CDCl₃) δ 7.26 – 7.20 (m, 2H), 7.16 (d, J = 8.2 Hz, 2H), 4.99 (d, J = 9.1 Hz, 1H), 4.43 (d, J = 8.7 Hz, 1H), 4.07 (qd, J = 7.1, 3.2 Hz, 2H), 3.75 – 3.67 (m, 1H), 3.65 (s, 3H), 1.98 (h, J = 6.8 Hz, 1H), 1.53 – 1.41 (m, 3H), 1.20 (d, J = 7.3 Hz, 3H), 0.93 (d, J = 6.7 Hz, 3H), 0.84 (d, J = 6.7 Hz, 3H). ¹³C NMR (76 MHz, CDCl₃) δ 175.2, 175.1, 156.3, 141.0, 139.3, 127.6, 127.1, 61.0, 60.7, 52.2, 45.2, 33.8, 19.9, 18.7, 18.7, 18.6, 14.7.

HRMS (ESI): [M+Na]⁺ C₁₇H₂₅O₄NNa⁺: calcd. 330.16758 found 330.16681.

3-((Ethoxycarbonyl)amino)-3-phenylpropyl acetate (105e)



R_f = 0.25-0.3 (PE : EA = 5:1).

m.p. = 83-85°C

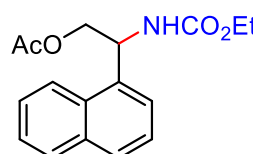
FT-IR ν_{max} (cm⁻¹) = 3330, 2975, 1739, 1719, 1699, 1530, 1368, 1245, 1046, 701.

¹H NMR (300 MHz, CDCl₃) δ 7.37 – 7.23 (m, 5H), 5.06 (d, *J* = 8.3 Hz, 1H), 4.83 (d, *J* = 8.4 Hz, 1H), 4.13 – 4.02 (m, 4H), 2.13 (td, *J* = 6.5, 4.2 Hz, 2H), 2.03 (s, 3H), 1.24 – 1.15 (m, 3H).

¹³C NMR (76 MHz, CDCl₃) δ 171.1, 156.0, 141.8, 128.9, 127.7, 126.4, 61.5, 61.1, 52.7, 35.4, 21.0, 14.7.

HRMS (ESI): [M+Na]⁺ C₁₄H₁₉O₄NNa⁺: calcd. 288.12063 found 288.12035.

2-((Ethoxycarbonyl)amino)-2-(naphthalen-1-yl)ethyl acetate (105f)



R_f = 0.2 (PE : EA = 5:1).

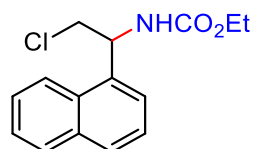
m.p. = 95-97°C

FT-IR ν_{max} (cm⁻¹) = 3332, 2981, 1739, 1715, 1531, 1237, 1061, 1040, 778.

¹H NMR (300 MHz, CDCl₃) δ 8.18 (d, *J* = 8.4 Hz, 1H), 7.85 (ddd, *J* = 19.2, 7.1, 2.4 Hz, 2H), 7.62 – 7.43 (m, 4H), 5.87 (s, 1H), 5.38 (d, *J* = 8.3 Hz, 1H), 4.56 – 4.32 (m, 2H), 4.12 (dt, *J* = 8.5, 6.5 Hz, 2H), 2.07 (s, 3H), 1.24 (d, *J* = 10.6 Hz, 3H). ¹³C NMR (76 MHz, CDCl₃) δ 171.2, 156.1, 134.4, 134.0, 130.9, 129.1, 128.8, 126.9, 126.1, 125.3, 123.4, 122.9, 66.1, 61.3, 50.4, 21.0, 14.7.

HRMS (ESI): [M+Na]⁺ C₁₇H₁₉O₄NNa⁺: calcd. 324.12063 found 324.12085.

Ethyl (2-chloro-1-(naphthalen-1-yl)ethyl)carbamate (105g)



R_f = 0.3-0.4 (PE : EA = 5:1).

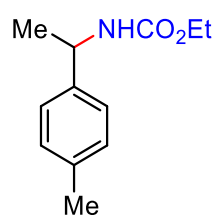
m.p. = 115-117°C

FT-IR ν_{max} (cm⁻¹) = 3319, 3057, 2980, 1695, 1532, 1514, 1253, 1058, 779.

¹H NMR (300 MHz, CDCl₃) δ 8.07 (d, *J* = 8.3 Hz, 1H), 7.86 (ddd, *J* = 18.2, 7.7, 1.8 Hz, 2H), 7.63 – 7.43 (m, 4H), 5.89 (d, *J* = 7.8 Hz, 1H), 5.39 (d, *J* = 8.0 Hz, 1H), 4.15 (q, *J* = 7.1 Hz, 2H), 4.04 (dd, *J* = 11.3, 5.4 Hz, 1H), 3.91 (dd, *J* = 10.9, 5.9 Hz, 1H), 1.26 (d, *J* = 7.0 Hz, 3H). ¹³C NMR (76 MHz, CDCl₃) δ 156.0, 134.3, 134.1, 130.8, 129.3, 129.0, 126.9, 126.1, 125.3, 123.7, 122.5, 61.5, 51.9, 47.2, 14.7.

HRMS (ESI): [M+Na]⁺ C₁₅H₁₆O₂NCINa⁺: calcd. 300.07618 found 300.07637.

Ethyl (1-(p-tolyl)ethyl)carbamate (105h)



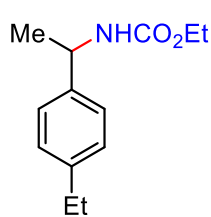
R_f = 0.25-0.3 (PE : EA = 5:1).

FT-IR ν_{max} (cm⁻¹) = 3325, 2977, 2930, 1699, 1529, 1515, 1245, 1064.

¹H NMR (300 MHz, CDCl₃) δ 7.25 – 7.09 (m, 4H), 5.10 – 4.59 (m, 2H), 4.10 (qd, *J* = 7.1, 1.4 Hz, 2H), 2.33 (s, 3H), 1.46 (d, *J* = 6.6 Hz, 3H), 1.22 (t, *J* = 7.1 Hz, 3H). ¹³C NMR (76 MHz, CDCl₃) δ 156.0, 140.8, 137.0, 129.4, 126.0, 60.9, 50.4, 31.1, 21.2, 14.7.

HRMS (ESI): [M+Na]⁺ C₁₂H₁₇O₂NNa⁺: calcd. 230.11515, found 230.11481.

Ethyl (1-(4-ethylphenyl)ethyl)carbamate (105i)



R_f = 0.25-0.3 (PE : EA = 10:1).

m.p. = 44-46°C

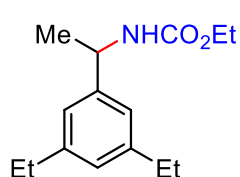
FT-IR ν_{max} (cm⁻¹) = 3325, 3053, 2970, 2932, 2873, 1704, 1525.

¹H NMR (300 MHz, CDCl₃) δ 7.26 – 7.11 (m, 4H), 4.83 (dd, *J* = 15.5, 9.0 Hz, 2H), 4.10 (qd, *J* = 7.1, 1.3 Hz, 2H), 2.63 (q, *J* = 7.6 Hz, 2H), 1.47 (d, *J* = 6.6 Hz, 3H),

1.22 (td, *J* = 7.4, 2.3 Hz, 6H). ¹³C NMR (76 MHz, CDCl₃) δ 156.0, 143.4, 141.0, 128.2, 126.1, 60.9, 50.5, 28.6, 22.6, 15.6, 14.7.

HRMS (ESI): [M+Na]⁺ C₁₃H₁₉O₂NNa⁺: calcd. 244.13080 found 244.13049.

Ethyl (1-(3,5-diethylphenyl)ethyl)carbamate (105j)



R_f = 0.25-0.3 (PE : EA = 10:1).

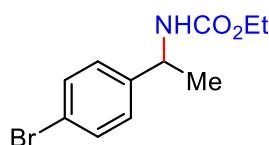
m.p. = 60-63°C

FT-IR ν_{max} (cm⁻¹) = 3325, 2967, 2933, 1700, 1532, 1246, 1062.

¹H NMR (300 MHz, CDCl₃) δ 6.95 (s, 3H), 4.86 (d, *J* = 34.5 Hz, 2H), 4.11 (qd, *J* = 7.1, 1.2 Hz, 2H), 2.72 – 2.54 (m, 4H), 1.48 (d, *J* = 6.8 Hz, 3H), 1.23 (td, *J* = 7.4, 1.6 Hz, 9H). ¹³C NMR (76 MHz, CDCl₃) δ 155.9, 144.7, 143.7, 126.6, 123.0, 60.9, 50.8, 29.0, 22.8, 15.7, 14.7.

HRMS (ESI): [M+Na]⁺ C₁₅H₂₃O₂NNa⁺: calcd. 272.16210, found 272.16149.

Ethyl (1-(4-bromophenyl)ethyl)carbamate (105k)



R_f = 0.25 (PE : EA = 10:1).

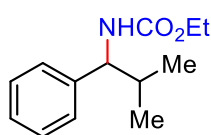
m.p. = 57-59°C

FT-IR ν_{max} (cm⁻¹) = 3319, 2978, 1695, 1529, 1247, 1064.

¹H NMR (300 MHz, CDCl₃) δ 7.52 – 7.40 (m, 2H), 7.24 – 7.11 (m, 2H), 5.03 – 4.62 (m, 2H), 4.09 (qd, *J* = 7.1, 2.0 Hz, 2H), 1.44 (d, *J* = 6.9 Hz, 3H), 1.21 (t, *J* = 7.1 Hz, 3H). ¹³C NMR (76 MHz, CDCl₃) δ 155.9, 143.0, 131.8, 127.8, 121.1, 61.1, 50.2, 22.6, 14.7.

HRMS (ESI): [M+Na]⁺ C₁₁H₁₄O₂NBrNa⁺: calcd. 294.01001 found 294.01014.

Ethyl (2-methyl-1-phenylpropyl)carbamate (105l)



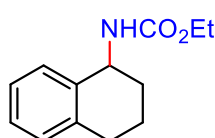
R_f = 0.25-0.3 (PE : EA = 10:1).

FT-IR ν_{max} (cm⁻¹) = 3323, 2959, 1694, 1533, 1239, 1035, 701.

¹H NMR (300 MHz, CDCl₃) δ 7.38 – 7.30 (m, 2H), 7.28 – 7.19 (m, 3H), 5.02 (s, 1H), 4.47 (s, 1H), 4.10 (qd, *J* = 6.9, 2.7 Hz, 2H), 2.00 (dq, *J* = 13.0, 6.5 Hz, 1H), 1.23 (q, *J* = 7.6 Hz, 3H), 0.97 (d, *J* = 6.7 Hz, 3H), 0.86 (d, *J* = 6.8 Hz, 3H). ¹³C NMR (76 MHz, CDCl₃) δ 156.4, 142.1, 128.5, 127.2, 126.9, 61.1, 61.0, 33.9, 19.9, 18.7, 14.7.

HRMS (ESI): [M+Na]⁺ C₁₃H₁₉O₂NNa⁺: calcd. 244.13080, found 244.13045.

Ethyl (1,2,3,4-tetrahydronaphthalen-1-yl)carbamate (105m)



R_f = 0.25-0.3 (PE : EA = 10:1).

m.p. = 65-68°C

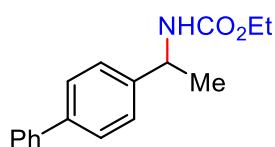
FT-IR ν_{max} (cm⁻¹) = 3313, 3060, 3019, 2978, 2933, 2863, 1694, 1528.

¹H NMR (300 MHz, CDCl₃) δ 7.38 – 7.29 (m, 1H), 7.21 – 7.13 (m, 2H), 7.13 – 7.04 (m, 1H), 4.89 (s, 2H), 4.16 (q, *J* = 7.1 Hz, 2H), 2.77 (q, *J* = 6.8 Hz, 2H), 2.05 (td, *J* = 9.6, 6.5

Hz, 1H), 1.94 – 1.73 (m, 3H), 1.26 (t, $J = 7.1$ Hz, 3H). ^{13}C NMR (76 MHz, CDCl_3) δ 156.3, 137.6, 137.0, 129.2, 128.8, 127.4, 126.3, 60.9, 49.2, 30.6, 29.3, 20.0, 14.8.

HRMS (ESI): $[\text{M}+\text{Na}]^+$ $\text{C}_{13}\text{H}_{17}\text{O}_2\text{NNa}^+$: calcd. 242.11515 found 242.11484.

Ethyl (1-((1,1'-biphenyl)-4-yl)ethyl)carbamate (105n)



m.p. = 125-128°C

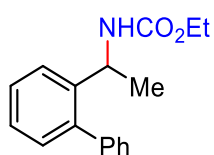
R_f = 0.25-0.3 (PE : EA = 10:1).

FT-IR ν_{max} (cm^{-1}) = 3304, 2980, 1689, 1542, 1254, 1066.

^1H NMR (300 MHz, CDCl_3) δ 7.67 – 7.51 (m, 4H), 7.50 – 7.30 (m, 5H), 5.20 – 4.66 (m, 2H), 4.14 (qd, $J = 7.1, 1.9$ Hz, 2H), 1.52 (d, $J = 6.8$ Hz, 3H), 1.25 (t, $J = 7.1$ Hz, 3H). ^{13}C NMR (76 MHz, CDCl_3) δ 156.0, 142.9, 140.9, 140.3, 128.8, 127.4, 127.3, 127.2, 126.5, 60.9, 50.4, 22.6, 14.7.

HRMS (ESI): $[\text{M}+\text{Na}]^+$ $\text{C}_{17}\text{H}_{19}\text{O}_2\text{NNa}^+$: calcd. 292.13080, found 292.13088.

Ethyl (1-((1,1'-biphenyl)-2-yl)ethyl)carbamate (105o)



R_f = 0.25-0.3 (PE : EA = 10:1)

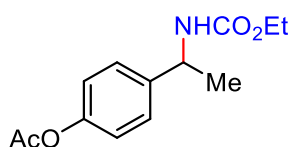
m.p. = 125-129°C

FT-IR ν_{max} (cm^{-1}) = 3332, 2975, 1704, 1520, 1250, 1066.

^1H NMR (300 MHz, CDCl_3) δ 7.48 – 7.26 (m, 8H), 7.20 (dd, $J = 7.6, 1.4$ Hz, 1H), 4.93 (s, 2H), 4.04 (q, $J = 7.1$ Hz, 2H), 1.32 – 1.04 (m, 6H). ^{13}C NMR (76 MHz, CDCl_3) δ 155.58, 141.90, 141.05, 130.47, 129.40, 128.33, 128.04, 127.23, 126.97, 124.84, 60.82, 47.72, 23.40, 14.75.

HRMS (ESI): $[\text{M}+\text{Na}]^+$ $\text{C}_{17}\text{H}_{19}\text{O}_2\text{NNa}^+$: calcd. 292.13080 found 292.13115.

4-((ethoxycarbonyl)amino)ethylphenyl acetate (105p)



R_f = 0.25-0.3 (PE : EA = 5:1).

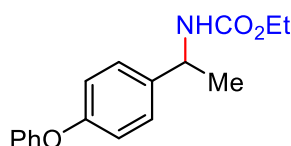
m.p. = 107-109°C

FT-IR ν_{max} (cm^{-1}) = 3328, 2979, 1761, 1702, 1526, 1508, 1370, 1218, 1064.

^1H NMR (300 MHz, CDCl_3) δ 7.35 – 7.27 (m, 2H), 7.11 – 6.97 (m, 2H), 4.89 (d, $J = 33.7$ Hz, 2H), 4.09 (qd, $J = 7.1, 1.5$ Hz, 2H), 2.28 (s, 3H), 1.46 (d, $J = 6.8$ Hz, 3H), 1.21 (t, $J = 7.1$ Hz, 3H). ^{13}C NMR (76 MHz, CDCl_3) δ 169.6, 155.9, 149.8, 141.4, 127.2, 121.7, 77.6, 77.2, 76.7, 61.0, 50.1, 22.5, 21.2, 14.7.

HRMS (ESI): $[\text{M}+\text{Na}]^+$ $\text{C}_{13}\text{H}_{17}\text{O}_4\text{NNa}^+$: calcd. 274.10498 found 274.10521.

Ethyl (1-(4-phenoxyphenyl)ethyl)carbamate (105q)



R_f = 0.25-0.3 (PE : EA = 10:1)

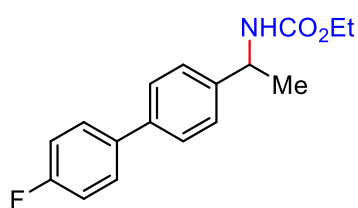
m.p. = 50-52°C

FT-IR ν_{max} (cm^{-1}) = 3324, 2978, 1700, 1590, 1506, 1489, 1238, 1064.

^1H NMR (300 MHz, CDCl_3) δ 7.39 – 7.22 (m, 4H), 7.14 – 7.06 (m, 1H), 7.05 – 6.90 (m, 4H), 5.13 – 4.61 (m, 2H), 4.11 (qd, $J = 7.1, 2.2$ Hz, 2H), 1.48 (d, $J = 6.8$ Hz, 3H), 1.23 (t, $J = 7.1$ Hz, 3H). ^{13}C NMR (76 MHz, CDCl_3) δ 157.3, 156.5, 155.9, 138.7, 130.1, 129.9, 129.8, 127.4, 123.4, 119.0, 60.9, 50.1, 22.6, 14.7.

HRMS (ESI): $[\text{M}+\text{Na}]^+$ $\text{C}_{17}\text{H}_{19}\text{O}_3\text{NNa}^+$: calcd. 308.12571 found 308.12619.

Ethyl (1-(4'-fluoro-[1,1'-biphenyl]-4-yl)ethyl)carbamate (105r)



R_f = 0.25 (PE : EA = 10:1).

m.p. = 155-158°C

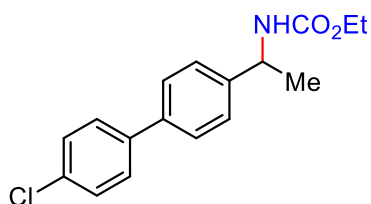
FT-IR ν_{max} (cm⁻¹) = 3292, 2987, 1686, 1547, 1255, 1065, 822, 520.

¹H NMR (300 MHz, CDCl₃) δ 7.59 – 7.45 (m, 4H), 7.38 (d, *J* = 8.3 Hz, 2H), 7.21 – 7.02 (m, 2H), 4.90 (dd, *J* = 20.1, 13.0 Hz, 2H), 4.12 (qd, *J*

= 7.1, 1.8 Hz, 2H), 1.51 (d, *J* = 6.7 Hz, 3H), 1.24 (t, *J* = 7.1 Hz, 3H). ¹³C NMR (76 MHz, CDCl₃) δ 162.6 (d, *J* = 246.3 Hz), 156.0, 143.0, 139.4, 137.1 (d, *J* = 3.2 Hz), 128.7 (d, *J* = 8.0 Hz), 127.4, 126.5, 115.7 (d, *J* = 21.4 Hz), 61.0, 50.4, 22.7, 14.7.

HRMS (ESI): [M+Na]⁺ C₁₇H₁₈O₂NFNa⁺: calcd. 310.12138 found 310.12014.

Ethyl (1-(4'-chloro-[1,1'-biphenyl]-4-yl)ethyl)carbamate (105s)



R_f = 0.25 (PE : EA = 10:1).

m.p. = 154-157°C

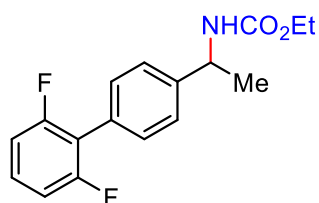
FT-IR ν_{max} (cm⁻¹) = 3289, 2982, 1686, 1542, 1251, 1062, 817, 513.

¹H NMR (300 MHz, CDCl₃) δ 7.50 (tt, *J* = 7.7, 2.2 Hz, 4H), 7.43 – 7.34 (m, 4H), 5.10 – 4.77 (m, 2H), 4.12 (qd, *J* = 7.1, 1.9 Hz, 2H), 1.51

(d, *J* = 6.8 Hz, 3H), 1.24 (t, *J* = 7.1 Hz, 3H). ¹³C NMR (76 MHz, CDCl₃) δ 156.0, 143.4, 139.4, 139.1, 133.5, 129.0, 128.4, 127.3, 126.6, 61.0, 50.4, 22.7, 14.7.

HRMS (ESI): [M+Na]⁺ C₁₇H₁₈O₂NCINa⁺: calcd. 326.09183 found 326.09073.

Ethyl (1-(2',6'-difluoro-[1,1'-biphenyl]-4-yl)ethyl)carbamate (105t)



R_f = 0.25 (PE : EA = 10:1).

m.p. = 135-137°C

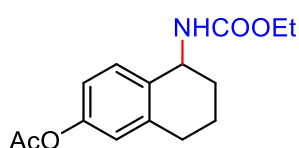
FT-IR ν_{max} (cm⁻¹) = 3354, 2981, 1688, 1521, 1464, 1249, 1230, 1067, 997, 834, 784.

¹H NMR (300 MHz, CDCl₃) δ 7.49 – 7.35 (m, 4H), 7.33 – 7.21 (m, 1H), 7.06

– 6.89 (m, 2H), 4.93 (s, 2H), 4.12 (qd, *J* = 7.1, 1.4 Hz, 2H), 1.52 (d, *J* = 6.5 Hz, 3H), 1.24 (t, *J* = 7.1 Hz, 3H). ¹³C NMR (76 MHz, CDCl₃) δ 160.3 (dd, *J* = 248.6, 7.2 Hz), 156.0, 143.8, 130.7 (t, *J* = 2.0 Hz), 129.0 (t, *J* = 10.4 Hz), 128.3, 126.0, 118.3 (t, *J* = 18.6 Hz), 113.0 – 110.9 (m), 61.0, 50.5, 22.6, 14.7.

HRMS (ESI): [M+Na]⁺ C₁₇H₁₇O₂NF₂Na⁺: calcd. 328.11196 found 328.11069.

5-((ethoxycarbonyl)amino)-5,6,7,8-tetrahydronaphthalen-2-yl acetate (105u)



R_f = 0.25-0.3 (PE : EA = 5:1).

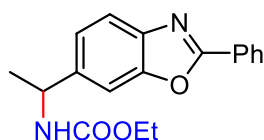
FT-IR ν_{max} (cm⁻¹) = 3323, 2936, 1761, 1703, 1523, 1495, 1209, 1067.

¹H NMR (300 MHz, CDCl₃) δ 7.34 (d, *J* = 8.4 Hz, 1H), 6.94 – 6.74 (m, 2H), 4.87 (s, 2H), 4.15 (q, *J* = 7.1 Hz, 2H), 2.76 (q, *J* = 6.8 Hz, 2H), 2.27

(s, 3H), 2.10 – 1.97 (m, 1H), 1.88 – 1.75 (m, 3H), 1.26 (t, *J* = 7.2 Hz, 3H). ¹³C NMR (76 MHz, CDCl₃) δ 169.7, 156.2, 149.7, 139.1, 134.7, 130.0, 121.8, 119.7, 77.6, 77.2, 76.7, 61.0, 48.8, 30.5, 29.4, 21.2, 19.8, 14.8.

HRMS (ESI): [M+Na]⁺ C₁₅H₁₉O₄NNa⁺: calcd. 300.12063 found 300.12021.

Ethyl (1-(2-phenylbenzo[d]oxazol-6-yl)ethyl)carbamate (105v)



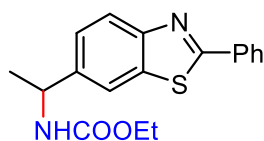
Rf = 0.35 (PE : EA = 5:1).

m.p. = 119-121°C

FT-IR ν_{max} (cm⁻¹) = 3321, 2978, 1702, 1529, 1246, 1062.

¹H NMR (300 MHz, CDCl₃) δ 8.29 – 8.13 (m, 2H), 7.70 (d, *J* = 8.2 Hz, 1H), 7.51 (tt, *J* = 5.5, 2.7 Hz, 4H), 7.31 (dd, *J* = 8.2, 1.7 Hz, 1H), 5.31 – 4.79 (m, 2H), 4.10 (qd, *J* = 7.1, 2.2 Hz, 2H), 1.53 (d, *J* = 6.9 Hz, 3H), 1.22 (t, *J* = 7.2 Hz, 3H). ¹³C NMR (76 MHz, CDCl₃) δ 163.4, 155.9, 151.1, 141.9, 141.4, 131.6, 129.0, 127.7, 127.2, 122.8, 112.0, 108.2, 61.0, 50.8, 22.9, 14.7.
HRMS (ESI): [M+H]⁺ [C₁₈H₁₉O₃N₂]⁺: calcd. 311.13902 found 311.13849.

Ethyl (1-(2-phenylbenzo[d]thiazol-6-yl)ethyl)carbamate (105w)



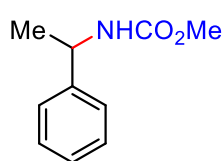
Rf = 0.3 (PE : EA = 5:1).

m.p. = 113-115°C

FT-IR ν_{max} (cm⁻¹) = 3319, 2976, 1700, 1524, 1244, 1068, 764, 689.

¹H NMR (300 MHz, CDCl₃) δ 8.12 – 7.96 (m, 3H), 7.83 (d, *J* = 1.8 Hz, 1H), 7.52 – 7.37 (m, 4H), 5.06 (dd, *J* = 46.1, 7.9 Hz, 2H), 4.11 (qd, *J* = 7.1, 3.1 Hz, 2H), 1.53 (d, *J* = 6.9 Hz, 3H), 1.22 (t, *J* = 7.2 Hz, 3H). ¹³C NMR (76 MHz, CDCl₃) δ 168.2, 155.9, 153.5, 141.4, 135.5, 133.7, 131.1, 129.1, 127.6, 124.7, 123.3, 118.9, 61.0, 50.7, 22.8, 14.7.
HRMS (ESI): [M+H]⁺ C₁₈H₁₉O₂N₂SN⁺: calcd. 327.11618 found 327.11582.

Methyl (1-phenylethyl)carbamate (106a)



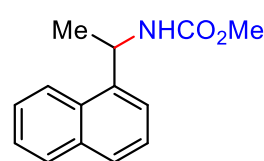
Rf = 0.25 (PE : EA = 10:1).

FT-IR ν_{max} (cm⁻¹) = 3324, 2975, 1704, 1532, 1452, 1251, 1070, 700.

¹H NMR (300 MHz, CDCl₃) δ 7.39 – 7.21 (m, 5H), 5.01 (s, 1H), 4.84 (s, 1H), 3.65 (s, 3H), 1.48 (d, *J* = 6.9 Hz, 3H). ¹³C NMR (101 MHz, CDCl₃) δ 156.3, 143.7, 128.7, 127.4, 126.0, 52.2, 50.7, 22.5.

HRMS (ESI): [M+Na]⁺ C₁₀H₁₃O₂NNa⁺: calcd. 202.08385 found 202.08364.

Methyl (1-(naphthalen-1-yl)ethyl)carbamate (106b)



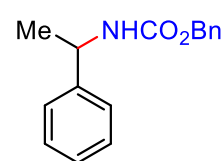
Rf = 0.2 (PE : EA = 10:1).

FT-IR ν_{max} (cm⁻¹) = 3325, 2977, 1713, 1695, 1532, 1249, 1067, 778.

¹H NMR (300 MHz, CDCl₃) δ 8.20 – 8.07 (m, 1H), 7.87 (dd, *J* = 7.7, 1.7 Hz, 1H), 7.79 (dt, *J* = 7.9, 1.2 Hz, 1H), 7.65 – 7.37 (m, 4H), 5.86 – 5.40 (m, 1H), 5.07 (d, *J* = 8.4 Hz, 1H), 3.68 (s, 3H), 1.65 (d, *J* = 6.8 Hz, 3H). ¹³C NMR (76 MHz, CDCl₃) δ 156.3, 138.9, 134.1, 131.0, 129.0, 128.3, 126.5, 125.9, 125.4, 123.3, 122.3, 52.3, 46.8, 21.8.

HRMS (ESI): [M+Na]⁺ C₁₄H₁₅O₂NNa⁺: calcd. 252.09950 found 252.09896.

Benzyl (1-phenylethyl)carbamate (106c)



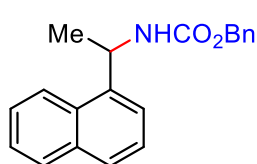
Rf = 0.3 (PE : EA = 10:1).

FT-IR ν_{max} (cm⁻¹) = 3324, 2974, 1702, 1530, 1243, 1056, 697.

¹H NMR (400 MHz, CDCl₃) δ 7.44 – 7.23 (m, 10H), 5.18 – 4.98 (m, 3H), 4.93 – 4.81 (m, 1H), 1.49 (d, *J* = 6.9 Hz, 3H). ¹³C NMR (101 MHz, CDCl₃) δ 155.6, 143.6, 136.6, 128.8, 128.6, 128.3, 127.5, 126.1, 66.9, 50.8, 22.6.

HRMS (ESI): [M+Na]⁺ C₁₆H₁₇O₂NNa⁺: calcd. 278.11515 found 278.11477.

Benzyl (1-(naphthalen-1-yl)ethyl)carbamate (106d)



R_f = 0.3 (PE : EA = 10:1).

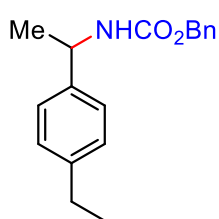
m.p. = 85-88°C

FT-IR ν_{max} (cm⁻¹) = 3326, 2975, 1703, 1518, 1241, 1058, 777.

¹H NMR (300 MHz, CDCl₃) δ 8.20 – 8.09 (m, 1H), 7.92 – 7.84 (m, 1H), 7.79 (dt, *J* = 7.9, 1.2 Hz, 1H), 7.57 – 7.41 (m, 4H), 7.41 – 7.27 (m, 5H), 5.77 – 5.59 (m, 1H), 5.19 – 5.07 (m, 3H), 1.66 (d, *J* = 6.7 Hz, 3H). ¹³C NMR (101 MHz, CDCl₃) δ 155.6, 138.8, 136.6, 134.0, 130.9, 129.0, 128.62, 128.3, 128.2, 126.6, 125.9, 125.4, 123.4, 122.3, 66.9, 46.8, 21.8.

HRMS (ESI): [M+Na]⁺ C₂₀H₁₉O₂NNa⁺: calcd. 328.13080 found 328.13005.

Benzyl (1-(4-ethylphenyl)ethyl)carbamate (106e)



R_f = 0.35 (PE : EA = 10:1).

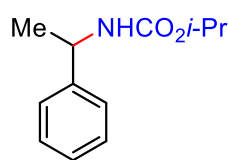
m.p. = 60-63°C

FT-IR ν_{max} (cm⁻¹) = 3324, 2966, 1702, 1513, 1242, 1060, 697.

¹H NMR (400 MHz, CDCl₃) δ 7.51 – 7.08 (m, 9H), 5.19 – 4.92 (m, 3H), 4.91 – 4.75 (m, 1H), 2.64 (q, *J* = 7.6 Hz, 2H), 1.48 (d, *J* = 6.9 Hz, 3H), 1.23 (t, *J* = 7.6 Hz, 3H). ¹³C NMR (101 MHz, CDCl₃) δ 155.6, 143.5, 140.8, 136.6, 128.6, 128.25, 128.1, 126.1, 66.8, 50.6, 28.6, 22.5, 15.7.

HRMS (ESI): [M+Na]⁺ C₁₈H₂₁O₂NNa⁺: calcd. 306.14645 found 306.14618.

Isopropyl (1-phenylethyl)carbamate (106f)



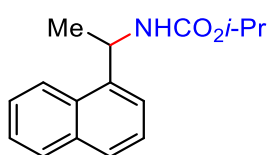
R_f = 0.35-0.4 (PE : EA = 10:1).

FT-IR ν_{max} (cm⁻¹) = 3323, 2979, 1695, 1523, 1249, 1112, 699.

¹H NMR (400 MHz, CDCl₃) δ 7.38 – 7.22 (m, 5H), 4.88 (dq, *J* = 11.8, 5.9 Hz, 3H), 1.47 (d, *J* = 6.7 Hz, 3H), 1.20 (d, *J* = 6.2 Hz, 6H). ¹³C NMR (101 MHz, CDCl₃) δ 155.6, 143.9, 128.7, 127.3, 126.0, 68.2, 50.6, 22.7, 22.3.

HRMS (ESI): [M+Na]⁺ C₁₂H₁₇O₂NNa⁺: calcd. 230.11515 found 230.11495.

Isopropyl (1-(naphthalen-1-yl)ethyl)carbamate (106g)



R_f = 0.25-0.3 (PE : EA = 10:1).

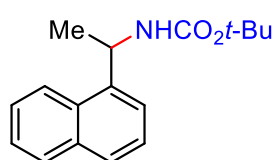
m.p. = 74-76°C

FT-IR ν_{max} (cm⁻¹) = 3326, 2978, 1695, 1529, 1512, 1247, 1111, 1055, 778.

¹H NMR (300 MHz, CDCl₃) δ 8.15 (dd, *J* = 8.0, 2.0 Hz, 1H), 7.87 (dd, *J* = 8.1, 1.5 Hz, 1H), 7.78 (dt, *J* = 7.8, 1.2 Hz, 1H), 7.64 – 7.38 (m, 4H), 5.65 (s, 1H), 4.93 (ddd, *J* = 11.5, 6.8, 5.7 Hz, 2H), 1.64 (d, *J* = 6.9 Hz, 3H), 1.20 (d, *J* = 6.2 Hz, 6H). ¹³C NMR (76 MHz, CDCl₃) δ 155.5, 139.2, 134.1, 131.0, 129.0, 128.2, 126.5, 125.8, 125.4, 123.4, 122.3, 68.3, 46.6, 22.3, 22.0.

HRMS (ESI): [M+Na]⁺ C₁₆H₁₉O₂NNa⁺: calcd. 280.13080 found 280.13016.

Tert-butyl (1-(naphthalen-1-yl)ethyl)carbamate (106h)



R_f = 0.3-0.35 (PE : EA = 10:1).

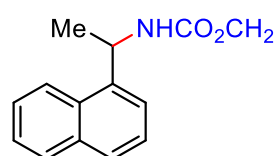
m.p. = 65-67°C

FT-IR ν_{max} (cm⁻¹) = 3342, 2976, 1699, 1506, 1365, 1245, 1169, 1056, 777.

¹H NMR (400 MHz, CDCl₃) δ 8.14 (d, *J* = 8.4 Hz, 1H), 7.87 (dd, *J* = 7.9, 1.6 Hz, 1H), 7.78 (dt, *J* = 8.0, 1.1 Hz, 1H), 7.57 – 7.42 (m, 4H), 5.61 (s, 1H), 4.89 (s, 1H), 1.62 (d, *J* = 10.0 Hz, 3H), 1.44 (s, 9H). ¹³C NMR (101 MHz, CDCl₃) δ 155.1, 139.4, 134.1, 131.0, 128.9, 128.1, 126.4, 125.8, 125.4, 123.5, 122.2, 79.6, 46.3, 28.5, 22.0.

HRMS (ESI): [M+Na]⁺ C₁₇H₂₁O₂NNa⁺: calcd. 294.14645 found 294.14621.

2,2,2-trichloroethyl (1-(naphthalen-1-yl)ethyl)carbamate (106i)



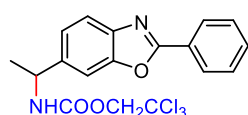
R_f = 0.4 (PE : EA = 10:1).

FT-IR ν_{max} (cm⁻¹) = 3332, 2954, 1724, 1515, 1235, 1115, 777.

¹H NMR (300 MHz, CDCl₃) δ 8.14 – 8.08 (m, 1H), 7.88 (dd, *J* = 7.9, 1.8 Hz, 1H), 7.81 (d, *J* = 8.0 Hz, 1H), 7.59 – 7.41 (m, 4H), 5.70 (p, *J* = 7.0 Hz, 1H), 5.31 (d, *J* = 8.4 Hz, 1H), 4.76 (s, 2H), 1.71 (d, *J* = 6.7 Hz, 3H). ¹³C NMR (76 MHz, CDCl₃) δ 153.7, 137.9, 134.0, 130.9, 128.9, 128.5, 126.6, 125.9, 125.3, 123.1, 122.4, 95.6, 77.5, 77.0, 76.6, 74.5, 47.0, 21.4.

HRMS (ESI): [M+Na]⁺ C₁₅H₁₄O₂NCl₃Na⁺: calcd. 367.99823 found 367.99797.

2,2,2-trichloroethyl (1-(2-phenylbenzo[d]oxazol-6-yl)ethyl)carbamate (106j)



R_f = 0.35 (PE : EA = 5:1).

m.p. = 92-95°C

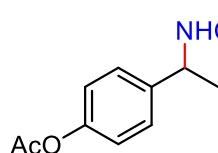
FT-IR ν_{max} (cm⁻¹) = 3325, 2976, 2953, 1738, 1731, 1326, 1244, 1116, 1056,

821, 725.

¹H NMR (300 MHz, CDCl₃) δ 8.32 – 8.12 (m, 2H), 7.71 (d, *J* = 8.2 Hz, 1H), 7.52 (tt, *J* = 6.1, 2.9 Hz, 4H), 7.32 (dd, *J* = 8.2, 1.6 Hz, 1H), 5.56 (d, *J* = 7.7 Hz, 1H), 5.00 (t, *J* = 7.0 Hz, 1H), 4.72 (s, 2H), 1.58 (d, *J* = 6.9 Hz, 3H). ¹³C NMR (76 MHz, CDCl₃) δ 163.6, 153.9, 151.0, 141.6, 140.8, 131.7, 129.0, 127.7, 127.1, 122.8, 120.1, 108.3, 95.6, 74.7, 51.3, 22.7.

HRMS (ESI): [M+H]⁺ [C₁₈H₁₆O₃N₂Cl₃]⁺: calcd. 413.02210 found 413.02147.

4-(1-(((2,2,2-trichloroethoxy)carbonyl)amino)ethyl)phenyl acetate (106k)



R_f = 0.3 (PE : EA = 5:1).

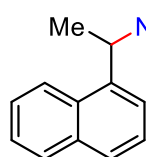
m.p. = 90-92°C

FT-IR ν_{max} (cm⁻¹) = 3342, 2977, 1738, 1733, 1508, 1219, 1199, 728.

¹H NMR (300 MHz, CDCl₃) δ 7.41 – 7.29 (m, 2H), 7.13 – 7.01 (m, 2H), 5.24 (d, *J* = 7.9 Hz, 1H), 4.88 (p, *J* = 7.0 Hz, 1H), 4.78 – 4.63 (m, 2H), 2.29 (s, 3H), 1.52 (d, *J* = 6.9 Hz, 3H). ¹³C NMR (76 MHz, CDCl₃) δ 169.6, 153.8, 150.1, 140.5, 127.3, 122.0, 95.7, 74.7, 50.6, 22.3, 21.3.

HRMS (ESI): [M+Na]⁺ C₁₃H₁₄O₄NCl₃Na⁺: calcd. 375.98806 found 375.98758.

2-(Trimethylsilyl)ethyl (1-(naphthalen-1-yl)ethyl)carbamate (106l)



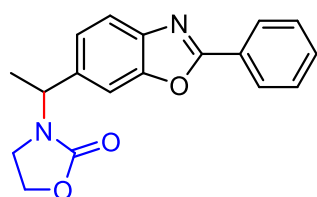
R_f = 0.5 (PE : EA = 10:1).

FT-IR ν_{max} (cm⁻¹) = 3325, 2953, 1697, 1523, 1510, 1248, 1060, 836, 777.

¹H NMR (300 MHz, CDCl₃) δ 8.14 (d, *J* = 7.9 Hz, 1H), 7.87 (dd, *J* = 7.7, 1.7 Hz, 1H), 7.78 (dt, *J* = 7.9, 1.1 Hz, 1H), 7.65 – 7.35 (m, 4H), 5.65 (s, 1H), 4.94 (d, *J* = 9.2 Hz, 1H), 4.17 (td, *J* = 8.0, 2.6 Hz, 2H), 1.65 (d, *J* = 6.7 Hz, 3H), 1.04 – 0.90 (m, 2H), 0.02 (s, 9H).
¹³C NMR (75 MHz, CDCl₃) δ 156.0, 139.1, 134.1, 131.0, 129.0, 128.3, 126.5, 125.9, 125.4, 123.4, 122.3, 63.3, 46.6, 21.9, 17.9, -1.3.

HRMS (ESI): [M+Na]⁺ C₁₈H₂₅O₂NSiNa⁺: calcd. 338.15468 found 338.15416.

3-(1-(2-Phenylbenzo[d]oxazol-6-yl)ethyl)oxazolidin-2-one (106m)



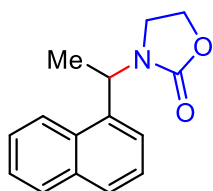
R_f = 0.2 (PE : EA = 2:1).

FT-IR ν_{max} (cm⁻¹) = 3505, 2978, 1745, 1484, 1423, 1249, 1056, 706.

¹H NMR (300 MHz, CDCl₃) δ 8.31 – 8.15 (m, 2H), 7.73 (d, *J* = 8.3 Hz, 1H), 7.59 (dt, *J* = 1.6, 0.7 Hz, 1H), 7.56 – 7.47 (m, 3H), 7.35 (ddd, *J* = 8.3, 1.7, 0.6 Hz, 1H), 5.35 (q, *J* = 7.1 Hz, 1H), 4.27 (dtd, *J* = 23.3, 8.7, 6.8 Hz, 2H), 3.53 (ddd, *J* = 9.3, 8.3, 6.7 Hz, 1H), 3.18 (ddd, *J* = 9.2, 8.3, 6.9 Hz, 1H), 1.65 (d, *J* = 7.2 Hz, 3H).
¹³C NMR (76 MHz, CDCl₃) δ 163.8, 158.0, 151.1, 141.9, 137.3, 131.8, 129.1, 127.7, 127.0, 123.8, 120.0, 109.4, 62.1, 51.7, 40.1, 16.8.

HRMS (ESI): [M+H]⁺ [C₁₈H₁₇O₃N₂]⁺: calcd. 309.12337 found 309.12280.

3-(1-(Naphthalen-1-yl)ethyl)oxazolidin-2-one (106n)



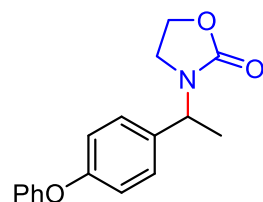
R_f = 0.15-0.2 (PE : EA = 5:1).

FT-IR ν_{max} (cm⁻¹) = 3484, 2979, 1742, 1421, 1252, 781.

¹H NMR (300 MHz, CDCl₃) δ 8.18 (dq, *J* = 8.6, 1.0 Hz, 1H), 7.96 – 7.77 (m, 2H), 7.63 – 7.41 (m, 4H), 5.93 (q, *J* = 6.9 Hz, 1H), 4.24 (ddd, *J* = 9.4, 8.5, 5.8 Hz, 1H), 4.04 (ddd, *J* = 9.3, 8.5, 7.6 Hz, 1H), 3.61 – 3.33 (m, 1H), 2.73 (ddd, *J* = 9.3, 8.4, 5.8 Hz, 1H), 1.73 (d, *J* = 6.9 Hz, 3H).
¹³C NMR (76 MHz, CDCl₃) δ 157.6, 134.8, 134.0, 131.7, 129.2, 128.9, 127.2, 126.3, 124.9, 123.9, 123.6, 62.1, 47.7, 40.1, 16.1.

HRMS (ESI): [M+Na]⁺ C₁₅H₁₅O₂NNa⁺: calcd. 264.09950 found 264.09891.

3-(1-(4-Phenoxyphenyl)ethyl)oxazolidin-2-one (106o)



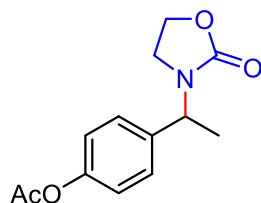
R_f = 0.3 (PE : EA = 5:2).

FT-IR ν_{max} (cm⁻¹) = 3496, 2977, 1745, 1588, 1507, 1489, 1420, 1237.

¹H NMR (300 MHz, CDCl₃) δ 7.40 – 7.27 (m, 4H), 7.15 – 7.08 (m, 1H), 7.05 – 6.93 (m, 4H), 5.21 (q, *J* = 7.1 Hz, 1H), 4.46 – 4.17 (m, 2H), 3.50 (ddd, *J* = 9.1, 8.3, 6.7 Hz, 1H), 3.19 (ddd, *J* = 9.1, 8.3, 7.0 Hz, 1H), 1.57 (d, *J* = 7.1 Hz, 3H).
¹³C NMR (76 MHz, CDCl₃) δ 158.1, 157.1, 157.0, 134.3, 129.9, 128.6, 123.7, 119.2, 118.8, 62.0, 51.10 40.1, 16.7.

HRMS (ESI): [M+Na]⁺ C₁₇H₁₇O₃NNa⁺: calcd. 306.11006 found 306.10963.

4-(1-(2-Oxooxazolidin-3-yl)ethyl)phenyl acetate (106p)



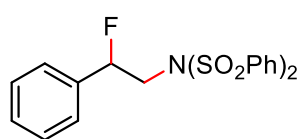
R_f = 0.1 (PE : EA = 5:2).

FT-IR ν_{max} (cm⁻¹) = 3496, 2980, 1747, 1422, 1202.

¹H NMR (300 MHz, CDCl₃) δ 7.48 – 7.30 (m, 2H), 7.12 – 7.02 (m, 2H), 5.21 (q, *J* = 7.1 Hz, 1H), 4.26 (dddd, *J* = 21.9, 9.2, 8.5, 6.8 Hz, 2H), 3.49 (ddd, *J* = 9.2, 8.3, 6.8 Hz, 1H), 3.17 (ddd, *J* = 9.2, 8.3, 6.8 Hz, 1H), 2.29 (s, 3H), 1.57 (d, *J* = 7.1 Hz, 3H). ¹³C NMR (76 MHz, CDCl₃) δ 169.5, 158.0, 150.3, 137.2, 128.3, 121.9, 62.0, 51.0, 40.1, 21.2, 16.5.

HRMS (ESI): [M+Na]⁺ C₁₃H₁₅O₄NNa⁺: calcd. 272.08933 found 272.08872.

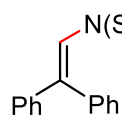
N-(2-fluoro-2-phenylethyl)-N-(phenylsulfonyl)benzenesulfonamide (108)



¹H NMR (400 MHz, CDCl₃) δ 8.15 – 8.07 (m, 1H), 7.90 – 7.82 (m, 3H), 7.67 – 7.37 (m, 11H), 5.40 (t, *J* = 7.3 Hz, 1H), 4.36 – 4.25 (m, 1H), 4.16 – 4.05 (m, 1H). ¹³C NMR (151 MHz, CDCl₃) δ 138.9, 138.0, 134.1, 129.2, 129.1, 129.1, 129.0, 128.9, 128.8, 128.7, 128.3, 125.85 (d, *J* = 6.9 Hz), 60.5, 54.6.

HRMS (ESI): [M+Na]⁺ C₂₀H₁₈O₄FNS₂Na⁺: calcd. 442.05535 found 442.05522.

N-(2,2-diphenylvinyl)-N-(phenylsulfonyl)benzenesulfonamide (110)



¹H NMR (400 MHz, CDCl₃) δ 7.71 (dq, *J* = 7.7, 1.1 Hz, 4H), 7.57 (tt, *J* = 7.2, 1.2 Hz, 2H), 7.40 (tt, *J* = 7.4, 1.0 Hz, 4H), 7.35 – 7.20 (m, 10H), 6.13 (s, 1H). ¹³C NMR (76 MHz, CDCl₃) δ 152.4, 139.9, 138.7, 136.9, 133.9, 130.0, 129.2, 128.9, 128.8, 128.8, 128.5, 128.4, 128.3, 116.4.

HRMS (ESI): [M+Na]⁺ C₂₆H₂₁NO₄S₂Na⁺: calcd. 498.08042 found 498.07968.

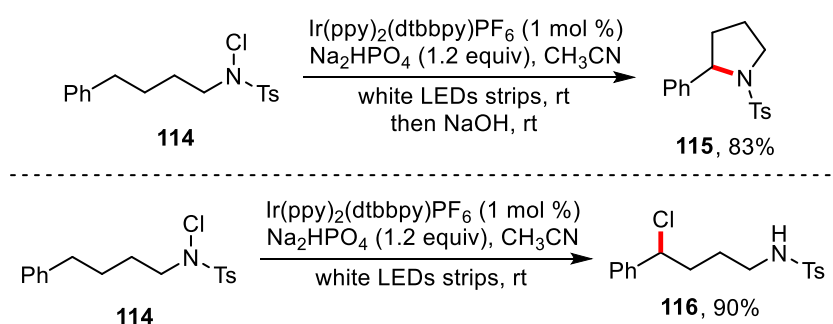
Chapter 3 Thiochromane Formation via Visible-Light Mediated Intramolecular δ -C(sp³)-H Bond Arylation of Sulfonamides.

3.1 Introduction

Abstraction of distal hydrogen atoms by nitrogen-centered radicals is well documented leading to translocated carbon-centered radicals. The Hofmann-Löffler-Freytag (HLF) reaction is a prototype example of this approach, allowing a straightforward access to pyrrolidines via *N*-haloamines.¹⁴ The 1,5-HAT procedure offers a supplementary method for remote C(sp³)-H bond functionalization since its chemoselectivity differs from that of its transition metal-catalyzed counterpart. This powerful strategy has recently been revived, enabling a variety of transformations that were previously difficult to accomplish.¹⁰³

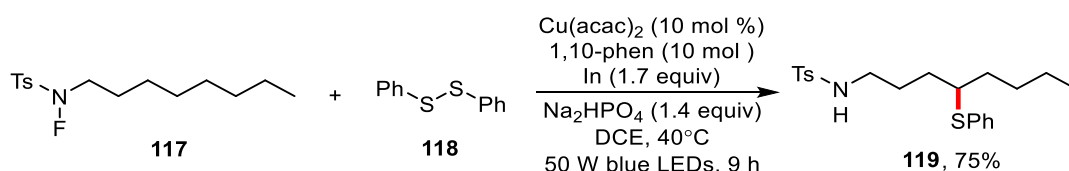
3.1.1 N-Leaving-Group (N-halogen, N-O, N-S, N-N) bond cleavage

In 2015, Yu¹⁰⁴ and co-workers described a visible-light photoredox-catalyzed C(sp³)-H amidation and chlorination reaction of *N*-chlorosulfonamides (Scheme 33). The excited state Ir(III) is oxidatively quenched by substrate **114** to generate Ir(IV) and a nitrogen-centered radical. It undergoes 1,5-hydrogen atom abstraction (HAT) to form a carbon-centered radical, which then is oxidized to carbocation by Ir(IV) with regeneration of Ir(III). The desired chlorinated product **116** would be obtained through radical-polar crossover process.



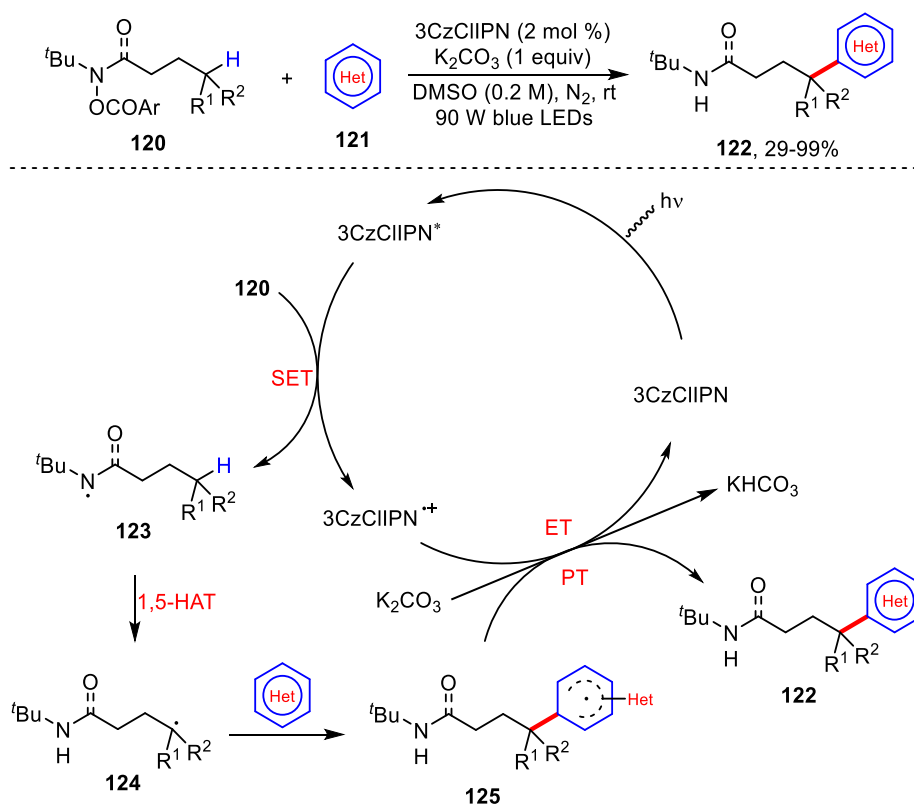
Scheme 33 visible-light-promoted C(sp³)-H amidation and chlorination of *N*-chlorosulfonamides.

A general protocol relying on Cu-catalyzed C-H thiolation of aliphatic amines was reported by Yang¹⁰⁵ (Scheme 34). Primary, secondary, and tertiary C-H bonds are compatible with the system to construct C-S bond in good yields.



Scheme 34 Cu-catalyzed C(sp³)-H thiolation of *N*-fluorosulfonamides.

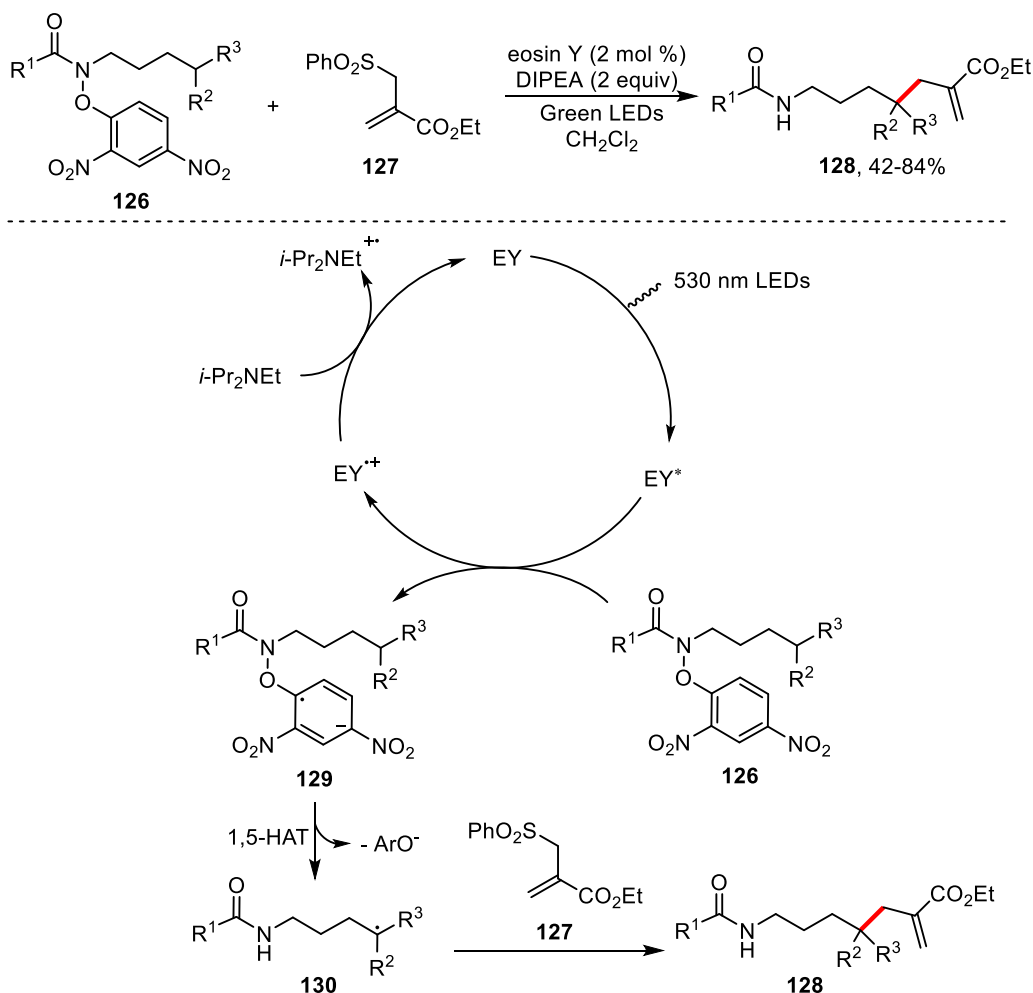
In 2019, Yu¹⁰⁶ *et al.* developed an amidyl radical promoted site-selective remote C(sp³)-H bond heteroarylation in hydroxyamides **120** in the presence of organic photocatalyst and K₂CO₃ via a typical HLF process (Scheme 35). First, single electron transfer from the excited 3CzCIIPN* to substrate **120** generates the amidyl radical **123** and 3CzCIIPN⁺⁺. Then, a 1,5-HAT affords the translocated carbon radical **124**, which is subsequently trapped by the heteroarene to generate a radical intermediate **125**. The target product **122** would finally be obtained through a stepwise electron transfer (ET)/proton transfer (PT) with the assistance of the base and 3CzCIIPN⁺⁺.



Scheme 35 Remote C(sp³)-H bond heteroarylation of hydroxyamides.

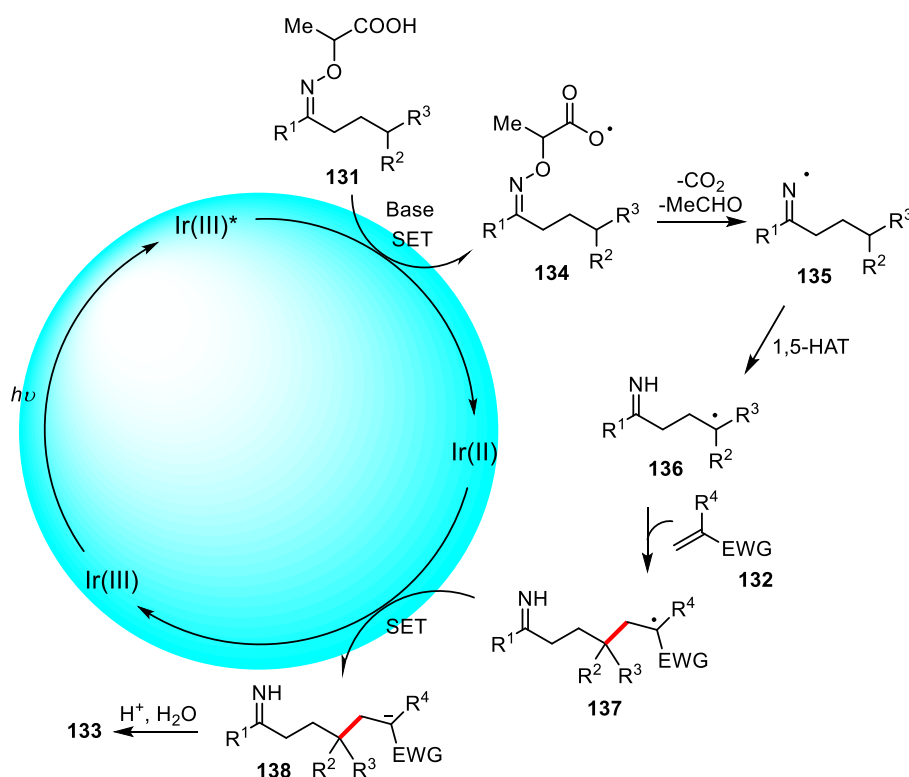
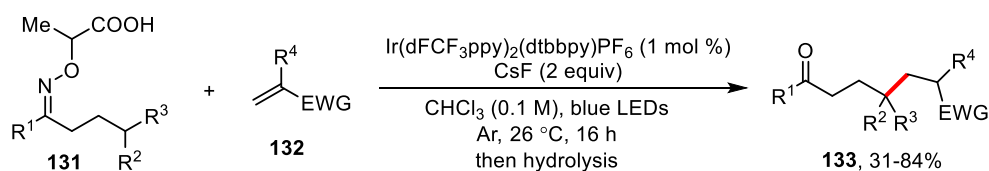
Wang¹⁰⁷ and co-workers reported an organic photoredox catalyzed remote allylation reaction of aryloxy amides **126** with allyl sulfone **127** under green light irradiation (Scheme 36). Both aromatic and aliphatic amide derivatives are capable of producing remote C-H allylation products in good yields. Oxidation of photoexcited catalyst eosin Y by aryloxy amides **126** would provide the radical

anion **129**, which undergoes a fragmentation to generate the amidyl radical. The electrophilic amidyl radical prefers to abstract hydrogen atom at δ position to generate carbon-centered radical **130**. Intermolecular radical addition to allyl sulfone **127** leads to allylation product **128** through displacement of the PhSO₂ radical. The photoactive catalyst eosin Y would be regenerated by oxidizing a molecule of DIPEA.



Scheme 36 Remote C(sp³)-H bond allylation of aryloxy amides.

In 2018, Studer's group developed an efficient approach to achieve intermolecular γ -C(sp³)-H alkylation between aminoxy acids **131** and various electron-deficient olefins **132** (Scheme 37).¹⁰⁸ Firstly, an oxygen-centered radical species **134** is generated through a deprotonation-oxidation process in the presence of an Ir(III) photocatalyst in its excited state. Then, the iminyl radical **135** is formed via the sequential fragmentation of CO₂ and acetaldehyde from **134**. 1,5-HAT then follows to generate the C-centered radical **136** that performs radical addition to electron-deficient olefins **132** to form the radical adduct **137**. The latter is then reduced by Ir(II) into carbanion **138** with regenerated photoactive Ir(III). Protonation and imine hydrolysis of **138** eventually yields product **133**.



Scheme 37 Remote C(sp³)-H bond alkylation of aminoxy-acids.

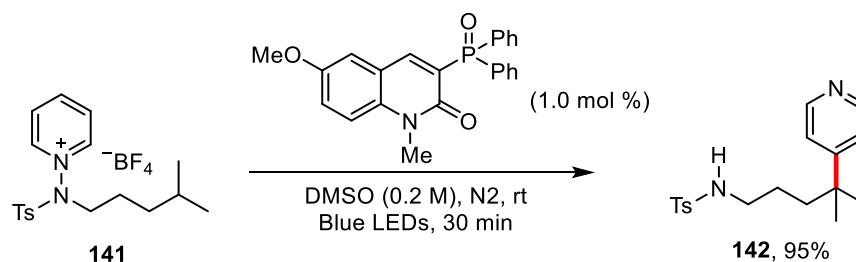
Recently, Alexanian¹⁰⁹ and co-workers described a general method for the functionalization of the remote C(sp³)-H bond of *N*-dithiocarbamates **139** to construct C-S bond under blue-light irradiation (Scheme 38). Primary and secondary C-H sites can both be functionalized in good yield. Under blue light irradiation, the weak N-S bond is easily cleaved homolytically resulting in amidyl radical, which then undergoes 1,5-HAT process to form the distal C-centered radical. It would react with the C=S bond in xanthate **139** to provide desired product **140**.



Scheme 38 Visible-light mediated δ -C-S bond construction.

Visible-light-induced site-selective C(sp³)-H pyridylation of *N*-amidopyridinium salts have been

reported by Hong¹¹⁰ and co-workers (Scheme 39). Single-electron reduction of *N*-amidopyridinium salt **141** yields a sulfonamidyl radical, which can then be converted by 1,5-HAT into an alkyl radical. Ultimately, the radical undergoes a Minisci reaction process to provide the final product **142**.



Scheme 39 Remote C(sp³)-H bond pyridylation of *N*-amidopyridinium salts.

3.1.2 N-H bond cleavage

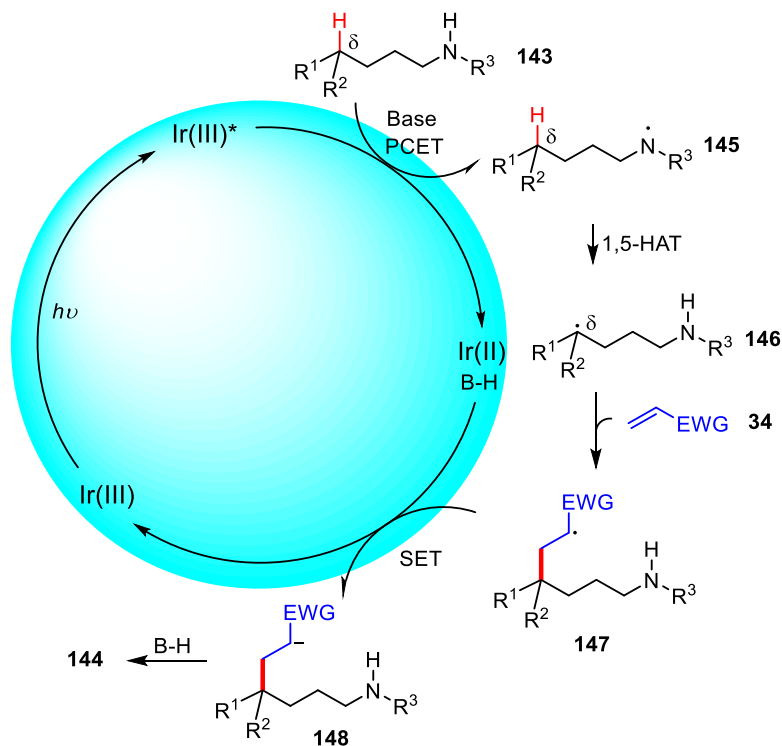
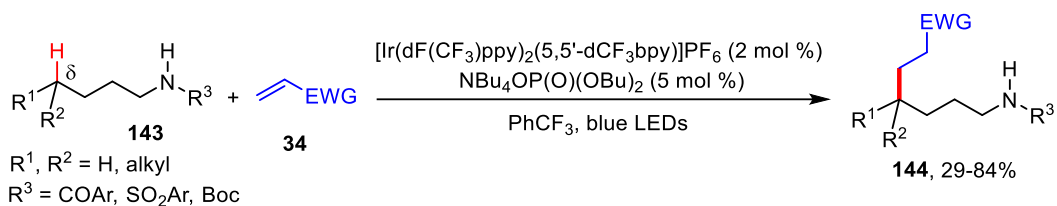
Given the high BDE of the N-H bond in amides, a direct generation of the amidyl radical through homolysis of the N-H bond long remained a difficult goal to attain. Knowles^{111a} and co-workers, however, recently developed a photocatalytic oxidative concerted proton-coupled electron transfer (PCET) (see below for a detailed explanation) approach for catalytic homolysis of amide N-H bonds (Scheme 40a). Mechanistic studies have shown that with the cooperation of the phosphate base and the excited state of Ir(III), the amide N-H bond is homolytically cleaved by the PCET process resulting in amidyl radical **145**, which was followed by a 1,5-HAT process and a Michael addition of the distal C-centered radical **146** to produce the final δ -C(sp³)-H alkylation product **144** after single-electron reduction and protonation.

Proton-coupled electron transfer (PCET) reactions play a crucial role in energy transformation processes in both natural and artificial systems. They have gained significant recognition in areas such as catalysis and synthetic chemistry due to their fundamental importance. These reactions involve a close interplay between proton and electron transfer, leading to a diverse range of mechanistic possibilities, including sequential and concerted mechanisms. This mechanistic complexity contributes to the richness of reactivity observed in PCET reactions.^{111b}

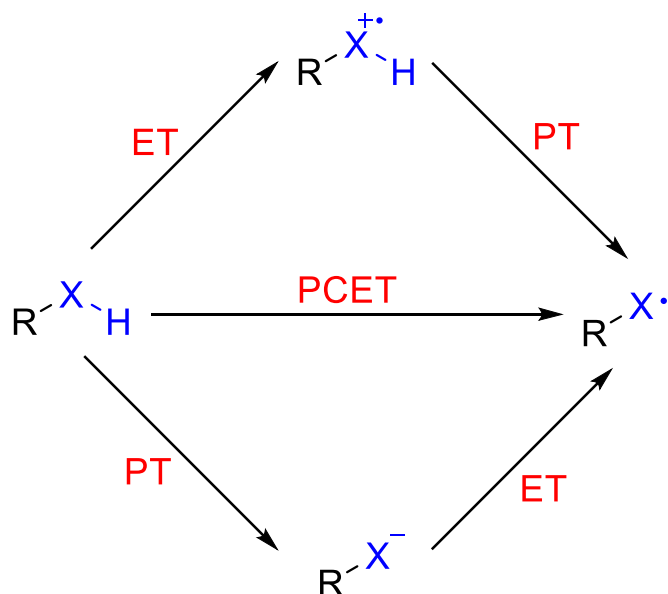
PCET reactions are typically classified into two types based on the order of the electron and proton transfer steps (Scheme 40b):

1. **Concerted PCET:** In this type of PCET, the electron and proton are transferred simultaneously in a concerted manner. The electron and proton transfer steps are strongly coupled and occur in a single step.
2. **Sequential PCET:** In sequential PCET, the electron and proton transfers occur in a

stepwise manner. First, an electron is transferred, followed by the transfer of a proton (or vice versa). The electron and proton transfer steps are decoupled in sequential PCET.

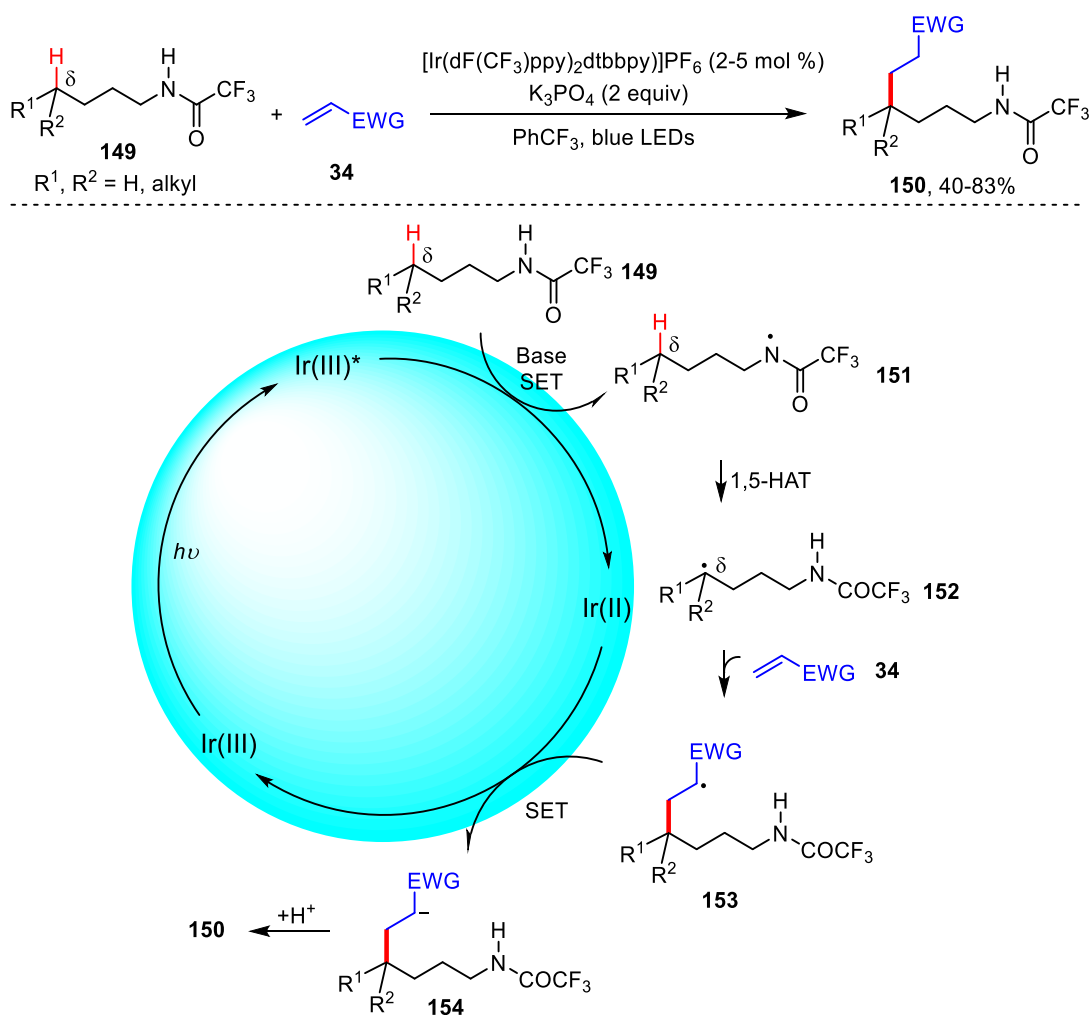


Scheme 40a Amidyl radical-mediated remote C–H alkylation assisted by PCET.



Scheme 40b Concerted PCET and sequential PCET.

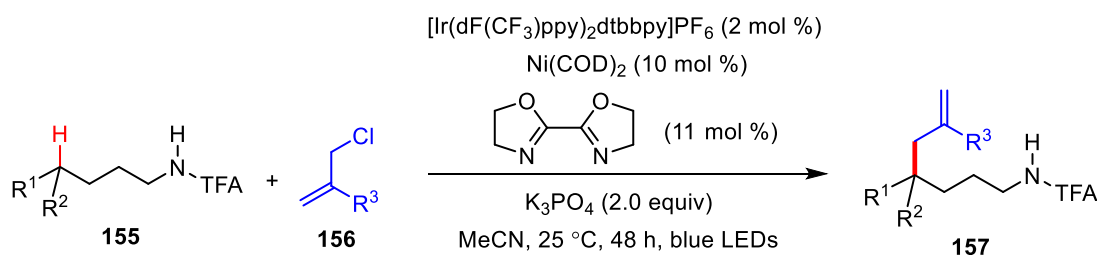
Simultaneously, Rovis *et al.*¹¹² reported a similar process, in which K_3PO_4 was used to abstract the acidic proton from the amide **149** to form an amidyl anion. This anion has a relatively low oxidation potential and can be oxidized by the excited iridium catalyst to generate the key *N*-centered radical species **151** (proton transfer and then electron transfer, stepwise). The amidyl radical **151** launched the subsequent HAT reaction, resulting in translocated carbon radical **152**, which was added to the Michael acceptor **34** to furnish the α -carbonyl radical **153**. The corresponding product **150** would be formed after the reduction of α -carbonyl radical **153** by the *in situ* generated Ir(II) and protonation of the enolate (Scheme 41).



Scheme 41 Visible-light mediated remote C–C bond formation.

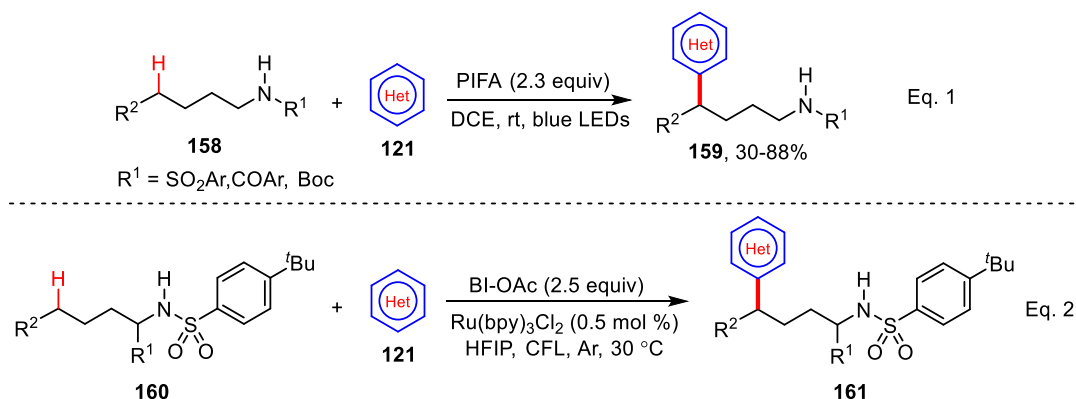
In 2019, Tambar¹¹³ and co-workers developed a direct allylation of secondary amides **155** with allyl chlorides **156** (Scheme 42). This photocatalytic system has good functional group tolerance. Various allyl-substituted amides were obtained in good yields and high δ -selectivities. Interestingly, control experiments show that the presence of Ni(0) complex is not essential for the reaction but

significantly increases the product yield. The Ni(0) species was not involved in their proposed catalytic cycle for product generation.



Scheme 42 Amidyl radical-mediated remote C–H allylation.

Zhu¹¹⁴ *et al.* described a useful protocol for the heteroarylation of amides **158** through a PIFA *in situ* activation of the N–H bond, which was followed by a 1,5-HAT process and a Minisci reaction of the distal C-centered radical to provide the final δ -C(sp³)–H heteroarylation product **159** (Scheme 43, Eq. 1). In the same year, Chen¹¹⁵ and co-workers reported a similar reaction using BI-OAc instead of PIFA to activate the amides N–H bond (Scheme 43, Eq. 2).



Scheme 43 Photoredox-mediated remote C(sp³)–H heteroarylation.

3.2 Results and discussion

Starting material **162** is readily prepared through the addition of a suitable thiol onto the corresponding nitro-olefin, followed by the reduction of the NO₂ function into the desired amine. The amine was finally protected by triflate (Figure 1). However, the substrate scope is also limited. If R is an electron-withdrawing group, such as a ketone or an ester, the desired product cannot be obtained. Because in the final step of the reaction, the amino group directly undergoes intramolecular attack on R, resulting in the formation of a lactam. If Ar is a heteroaromatic ring such as pyridine or indole, the desired product cannot be obtained as well. The pyridine tends to migrate from sulfur to nitrogen.

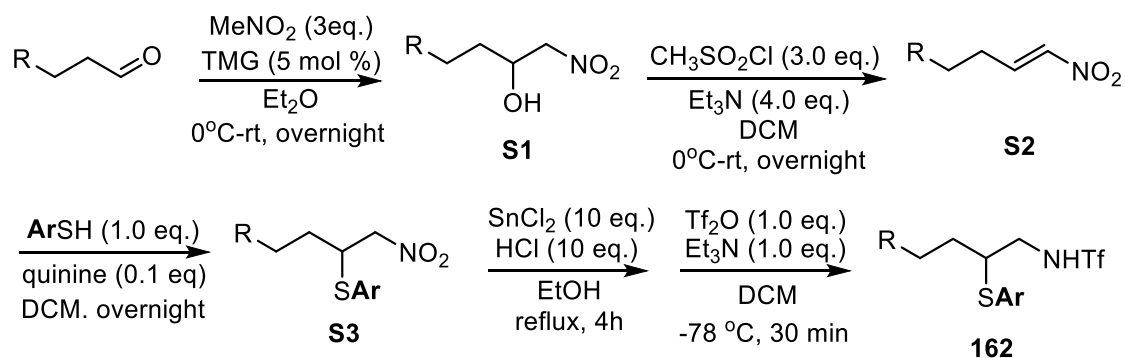
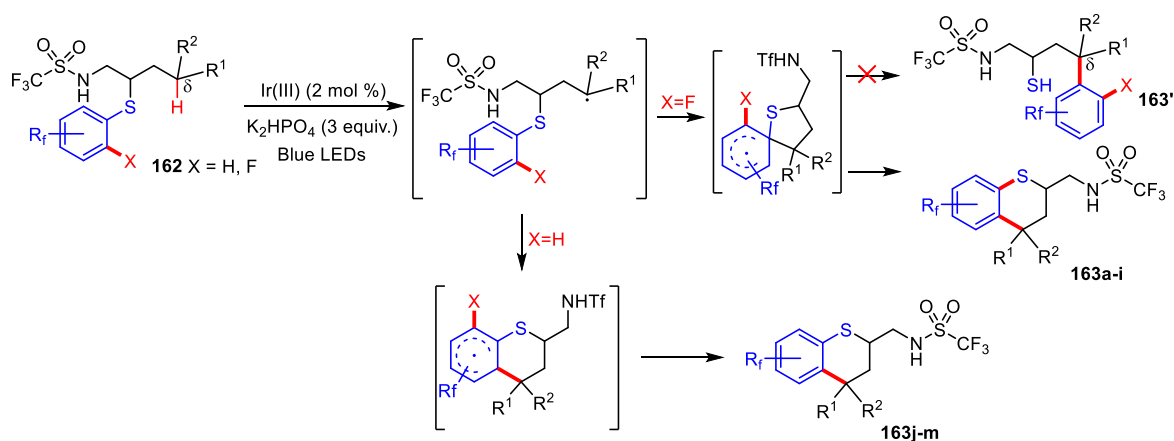


Figure 1 the synthesis of starting material **162**.

Inspired by the above works, we first planned to achieve remote migration of the aryl group using the sulfonamide **162** to construct product **163'**. Unfortunately, the desired product **163'** was not obtained under our conditions, but surprisingly, **163** was formed instead (Scheme 44). We thus present here an innovative approach involving photoredox mediation for the intramolecular δ -C(sp³)-H arylation of sulfonamides. This strategy relies on the utilization of an amidyl radical to facilitate 1,5-hydrogen atom transfer (HAT), followed by the cyclization of the resulting carbon-centered radical onto the phenyl ring of a polyfluorothioaryl fragment. This process is illustrated in Scheme 44. Under mild conditions, the synthesis of valuable thiochromanes of type **163** from amides **162** is achieved with high efficiency, resulting in satisfactory yields. Interestingly, product **163** may also be seen as the result of the cyclization of intermediate **163'**. The mechanism of the cyclization reaction has been investigated through Density Functional Theory (DFT) calculations. These calculations provide insights into the formation of thiochromanes **163** via two distinct processes depending on the nature of the substituents, which are located in *ortho* position relative to C-S bond of sulfonamide **162**.

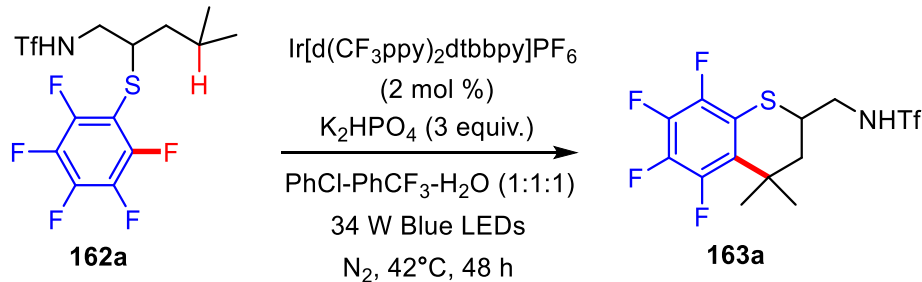


Scheme 44 Intramolecular δ -C(sp³)-H arylation of sulfonamides.

3.2.1 Optimization of intramolecular δ -C(sp³)-H arylation

The optimization of the process was carried out using sulfonamide **162a** as the model. The optimal reaction conditions of cyclized product **163a** were obtained by using 2 mol% Ir[d(CF₃ppy)₂dtbbpy]PF₆ photocatalyst and 3 equivalents of K₂HPO₄ in a ternary 1:1:1 PhCl-PhCF₃-H₂O solvent system (Table 1, entry 1). Under these conditions, the crude reaction mixture was clean, containing only the desired product **163a** along with starting **162a**, which was recovered in reasonable yields through a simple chromatography. Preliminary attempts and optimized conditions are summarized in Table 2. The catalyst (entry 2), light (entry 3) and base (entry 4) are essential for this reaction. When the reaction was performed in their absence, no reaction or traces of **163a** were observed, indicative of a photocatalyzed process involving the deprotonation of the sulfonamide. The photocatalyst was initially screened, first by varying the Ir ligand, the diverse ligand coordination resulting in significantly different redox potentials. Due to the low oxidation potentials of [Ir(ppy)₂(dtbbpy)]PF₆ (Ir-B) ($E_{1/2}^{*III/II} = +0.92\text{V}$)¹²⁶ (entry 5) and Ir(ppy)₃ (Ir-C) ($E_{1/2}^{*III/II} = +0.31\text{V}$)¹²⁶ (entry 6) in their excited-state, these were insufficient to oxidize the sulfonamide anion resulting from the deprotonation by K₂HPO₄, resulting in the absence of the final product **163a**. [Ir(dF(CF₃ppy)₂(5,5'-d(CF₃)bpy)]PF₆ (Ir-F) proved to be effective in producing **163a**, although the yield was relatively low (entry 8). The organophotocatalyst (Acr-Mes)(BF₄) (E) was not able to afford the desired product (entry 9). The base strength was finally investigated, and it was found that K₂HPO₄ exhibited higher efficiency. Stronger phosphate or carbonate bases consistently resulted in lower yields (entry 10-11).

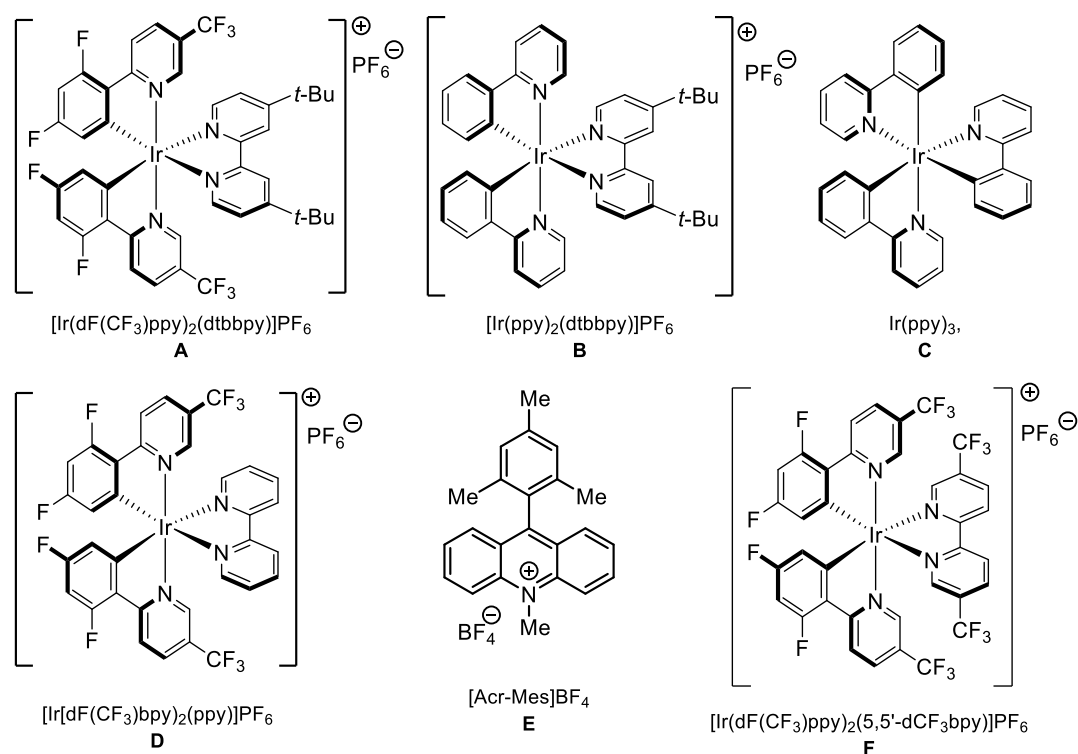
Table 2. Optimization of the photocatalyzed-(C_{sp³}-H) arylation of sulfonamide **163a**.



entry	Deviation from standard conditions ^a	Yield (%) ^b
1	None	54 (46)
2	no catalyst [Ir]	0
3	no light	0
4	no base	Trace
5	Ir-B	0

6	Ir-C	0
7	Ir-D	Trace
8	Ir-F	28
9	E	0
10	K ₃ PO ₄	34
11	K ₂ CO ₃	40
12	Cs ₂ CO ₃	15%

^a Standard conditions: Ir[d(CF₃ppy)₂dtbbpy]PF₆ (2 mol %), K₂HPO₄ (3 equiv.), PhCl-PhCF₃-H₂O (1:1:1) (1.5 mL), Kessil 34 W Blue LEDs, 42°C, 48 h. ^b ¹H NMR yield of **164a**, using mesitylene as an internal standard. Isolated yield under brackets.



3.2.2 Substrate scope

The scope and limitation of this $\delta\text{-C}(\text{sp}^3)\text{-H}$ sulfonamide arylation was then established as shown in Scheme 45. With pentafluorinated substrates **162a**, **162d-e** or **162g**, fluorine homolytic substitution led to the corresponding cyclization products **163a**, **163d-e** and **163g** in moderate yield, along with recovered starting material. When the transferred hydrogen is located on a prochiral center as in **162d**, the reaction occurred with some diastereocontrol, leading to the *cis*-isomer **163d**, as determined by ¹H 2D NMR (The hydrogen atom on the carbon adjacent to the sulfur atom and the hydrogen atom on the methyl group exhibit a cross peak) (Figure 2). Interestingly, when the reaction was extended to the symmetrical tetrafluorinated precursor **162b**, the cyclized product **163b** was obtained as shown unambiguously by X-ray diffraction studies (XRDS), suggesting a sulfur

migration through a radical Truce-Smiles type C-S rearrangement (*vide infra*),¹¹⁶ rather than a direct homolytic fluorine substitution (Figure 3).¹¹⁷ Examples of radical C-S Truce-Smiles rearrangements have flourished for sulfonyl and sulfoxidyl radicals,¹¹⁸ but those involving a thiyl radical are rare.¹¹⁹ A similar behavior was observed for **162c**, which led to thiochromane **163c**, the structure of which was also proven through XRDS. Accordingly, it was assumed that cyclopentyl- and cyclohexyl models **162e-h** provided the desired cyclized products **163e-h**. The reaction of **162b** and **162f** also produced a small amount of volatile **163b'** and **163f'** (GC-MS) lacking the aminomethyl fragment, which may explain the moderate yields in these reactions. A rationale is provided below to explain the presence of such by-products (Figure 6). Up-scaling to 1 mmol was carried out on **162b**, albeit with a slight loss in yield in **163b**. Finally, the reaction was extended to trifluoroacetamide **162i**, leading to the thiochromane **163i** in modest isolated yield.

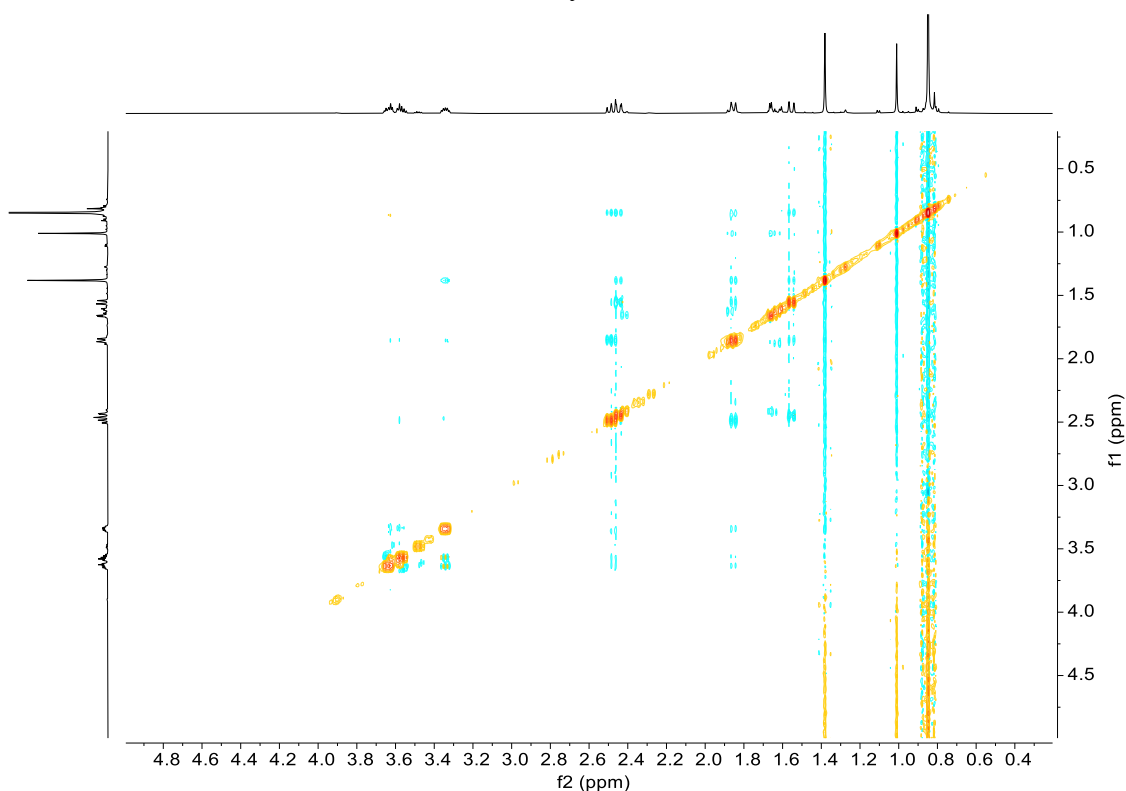


Figure 2 ¹H NOESY of compound **163d**.

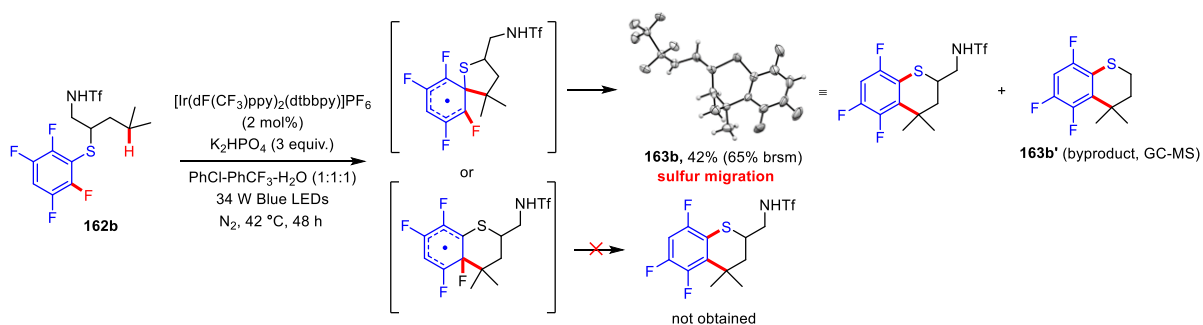
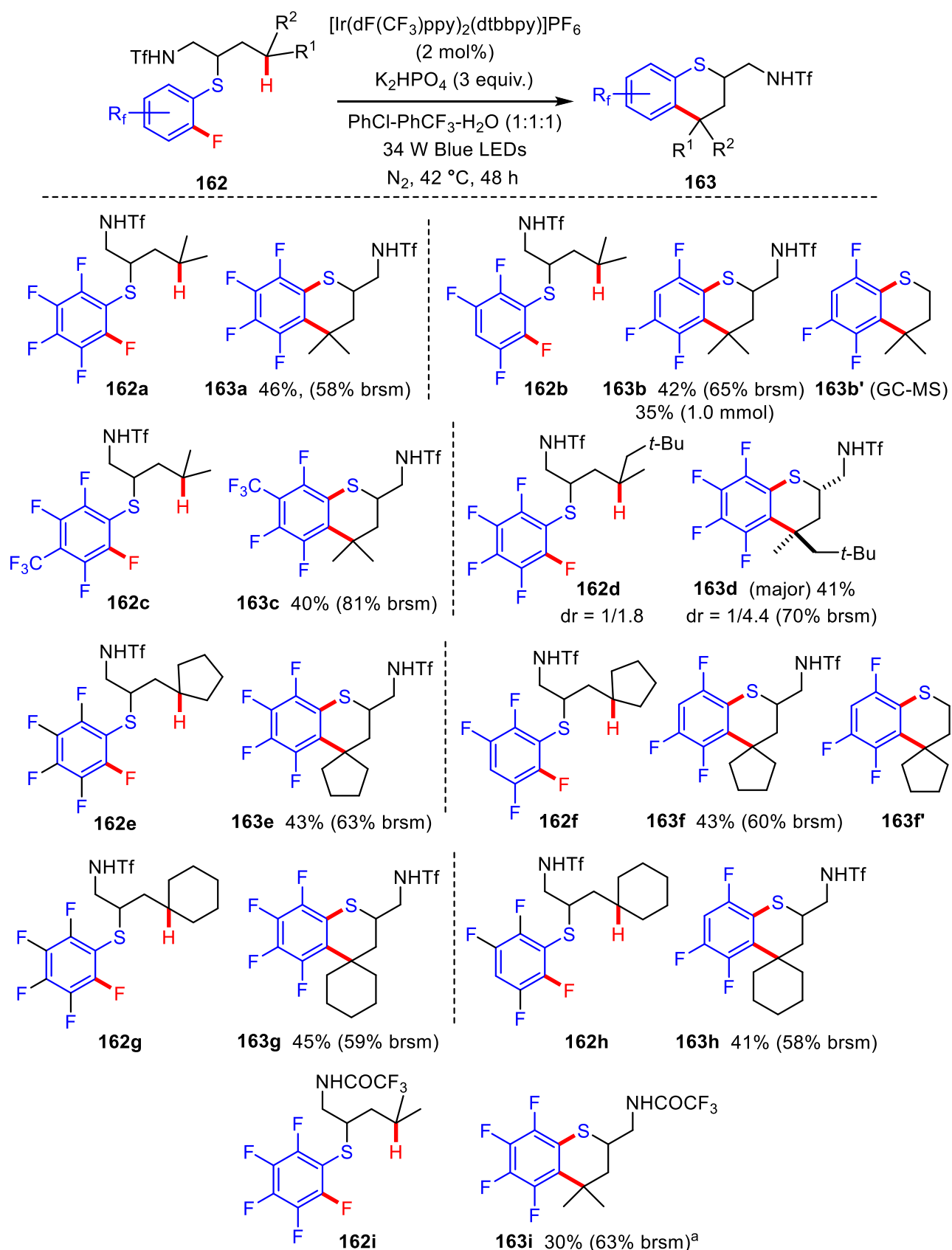


Figure 3 The product **163b** was isolated through Truce-Smiles rearrangement



Scheme 45 Photocatalyzed-(C_{sp3}-H) arylation of sulfonamide **162a-i**. Fluorine homolytic substitution.

For compounds having only hydrogens in *ortho* position relative to sulfur, as in **162j-k**, the hydrogen substitution took place with a relative efficiency as illustrated with the formation of **163j-k** (Scheme 46). The structure of **163j** was unambiguously assigned through XRDS, suggesting here a direct homolytic aromatic substitution (HAS).¹¹⁷ A similar observation was made for the synthesis of **163l** from **162l**, the structure of which was also assigned through XRDS (Figure 4). In this case, it was also possible to isolate small amount of **163l'** (similar to **163b'** and **163f'**), which became the major product after 72 h and may thus be formed from **163l** under the reaction conditions. Regioselectivity issues were noticed when both hydrogen and fluorine atoms were in competition as in **162n**, which led to the formation of a mixture of **163na** and **163nb**, in which hydrogen substitution was preferred. The structure of the monofluorinated **163nb** was determined through ¹H NMR and was clearly distinct from **163k** prepared above. Efforts to extend the scope of the process to electron-rich thioarenes substrates met with failures. As indicated in Scheme 46, electron-rich aryl substituents, as in **162o-p** effectively tends to migrate from sulfur to nitrogen as a result of a match polar effect between the electrophilic *N*-centered radical and the arene, the *ipso* attack superseding the [1,5]-HAT process.¹²⁰ Further oxidation of the resulting compound may then also take place as in the case of **162p**, where only NTf aniline **163p** was isolated. Computational studies were performed in the below, which clearly show that in **10-p**, the nitrogen radical attack at the *ipso* position is kinetically favored as compared to the [1,5]-HAT. In contrast, in **162a** or **162m**, [1,5]-HAT is slightly preferred, in line with experimental observations.

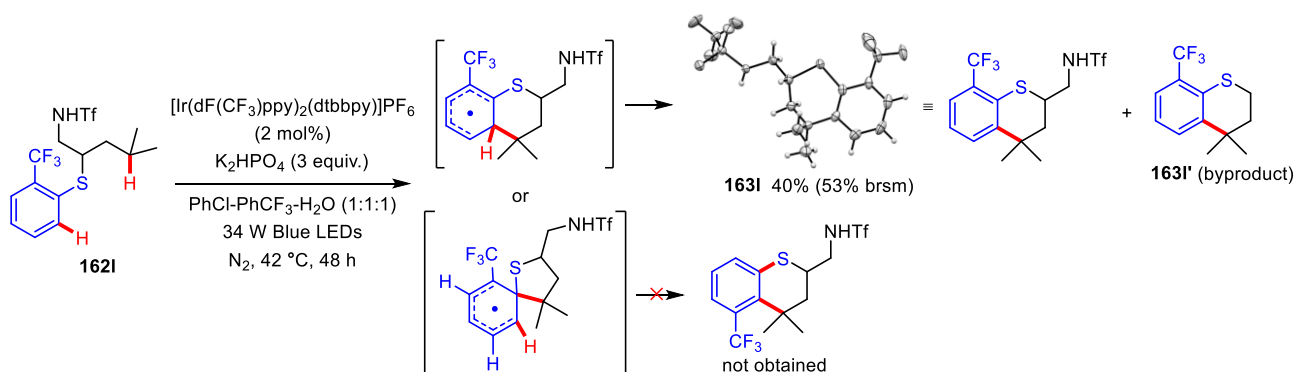
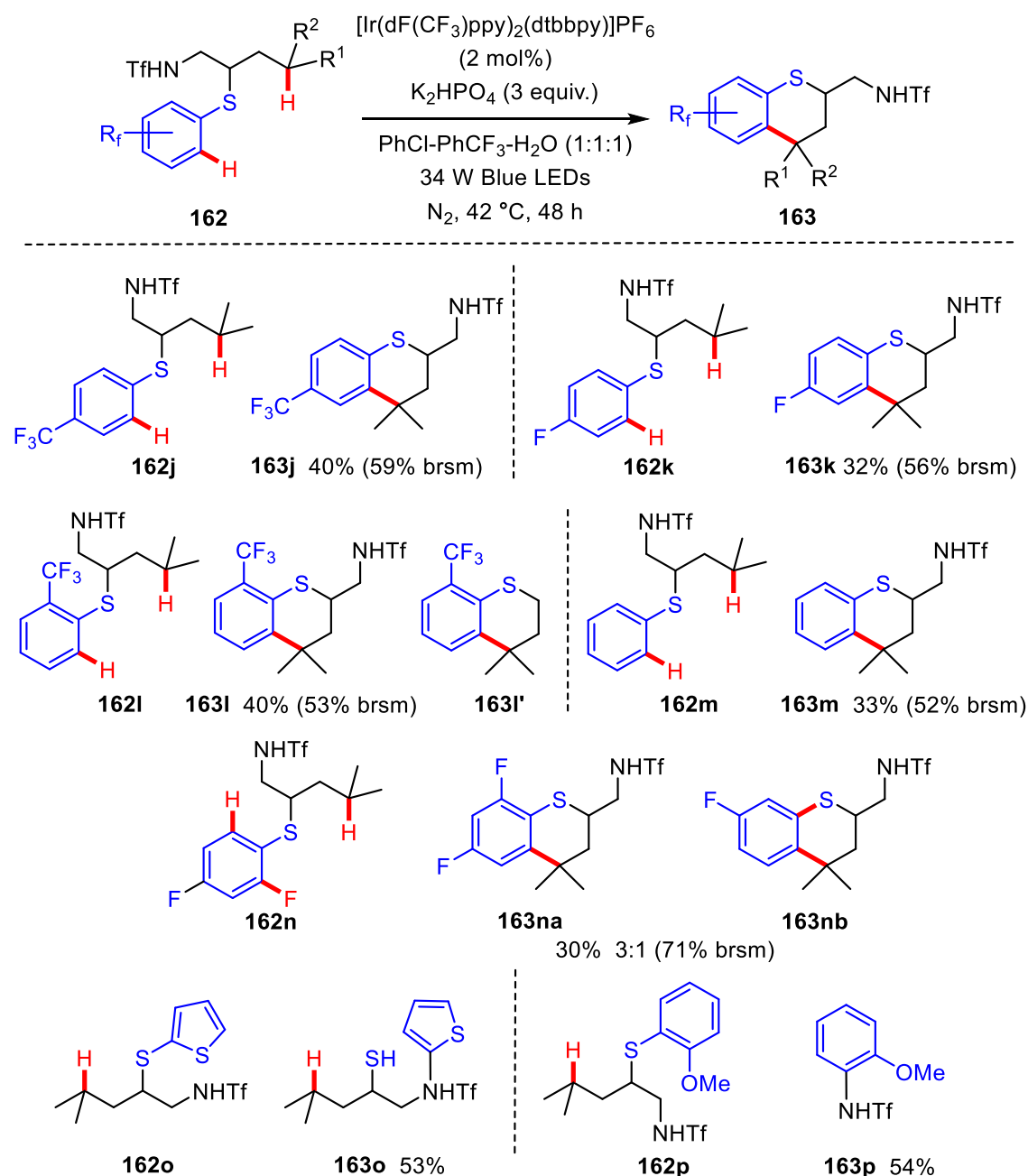


Figure 4 The product **163l** was isolated through hydrogen substitution.



Scheme 46 Photocatalyzed-(C_{sp3}-H) arylation of sulfonamide **162j-p**. Hydrogen homolytic substitution.

The examples of failure are shown in Figure 5, which illustrates the limitations of this strategy. First, the electrophilic N-centered radical tends to preferentially attack the electron-rich aryl group, resulting in the migration of the electron-rich aryl group from sulfur to nitrogen (Figure 5, 163o-163r). Second, sulfonamides possessing a secondary carbon center at the δ -position produce unstable C-centered radicals, resulting in the observation of only traces of the product (Figure 5, 163t). Furthermore, in cases where more stable C-centered radicals are present, such as the benzyl (Figure 5, 163aa), adjacent to oxygen (Figure 5, 163u), and adjacent to silicon (Figure 5, 163v) radical, the absence or trace amounts of the product were detected. Moreover, if the benzene ring bears strong electron-withdrawing groups, such as acyl (Figure 5, 163x) and cyanide (Figure 5, 163y) groups, the

substrate tends to undergo decomposition. Finally, sulfonamides that possess an electron-withdrawing group at the δ -position, such as trifluoromethyl (Figure 5, 163z), lead to the decomposition of the starting material.

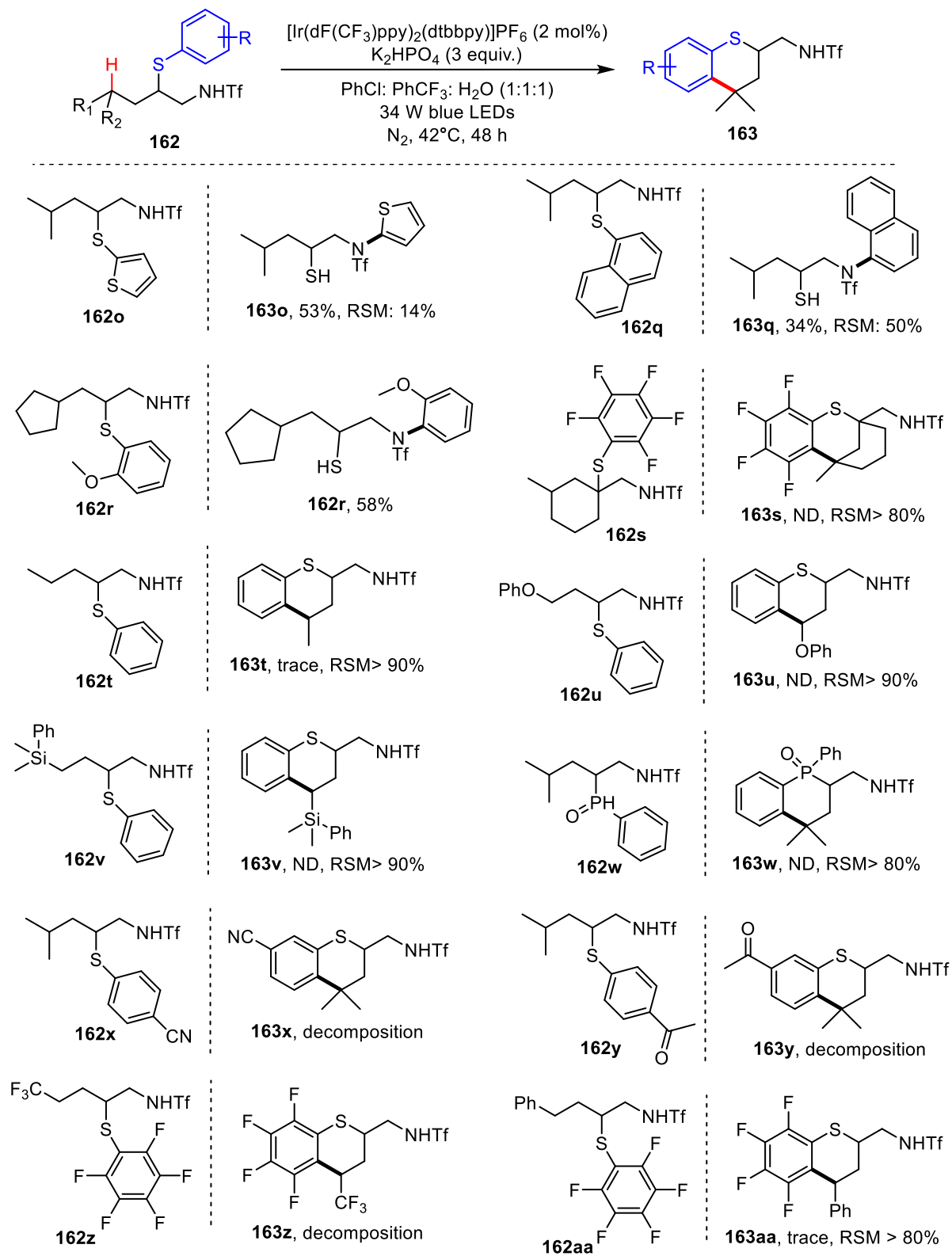
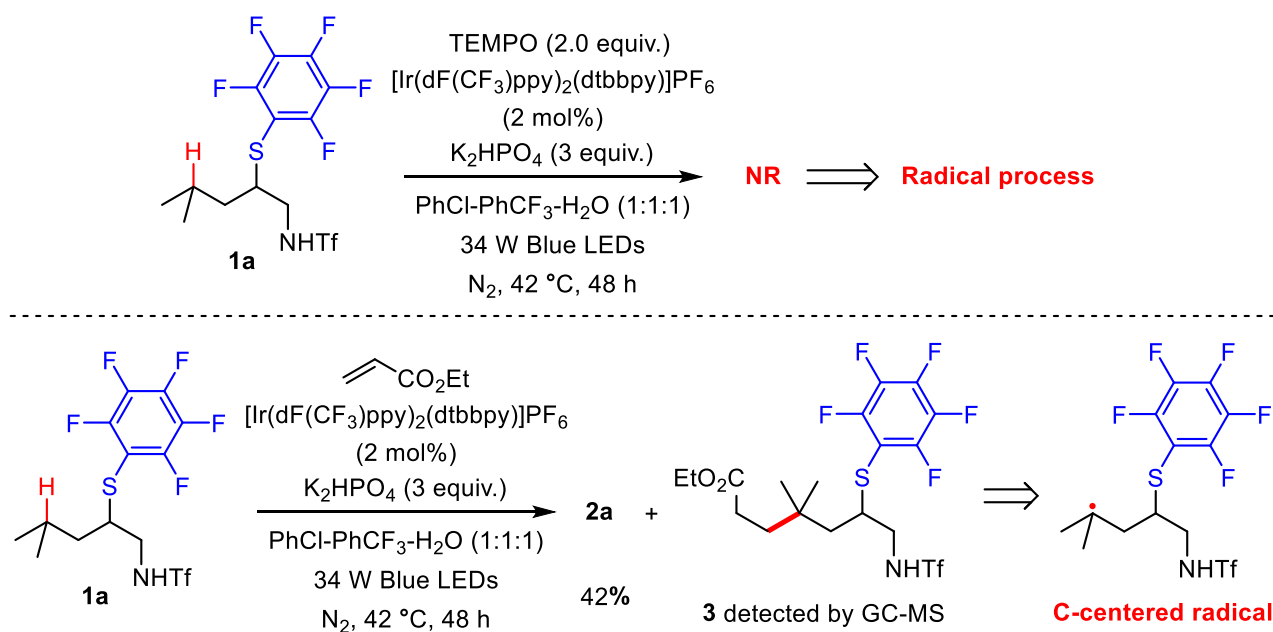


Figure 5 Unsuccessful examples.

3.2.3 Mechanistic studies

Additional experiments were finally carried out in order to get some mechanistic insights, through the trapping of potent radical intermediates (Scheme 47). For instance, when **162a** was treated as above, but in the presence of TEMPO, no reaction occurred, indicating the generation of radical species during the course of reaction process. The reaction of sulfonamide **162a** was also repeated under conditions above, but in the presence of ethyl acrylate. **163a** was isolated as a major compound, but addition product **164** could also be detected through GC-MS, indicating the formation at some stage of the C-centered radical at the δ -position (Scheme 47).



Scheme 47 Mechanistic experiments.

3.2.4 Side products formation

Two mechanisms may be proposed to rationalize the formation of **163b'**, **163f'**, and **163l'** as shown in Figure 6. The first one is a base-mediated cleavage of the C–C bond α - to sulfur, which would lead to a sulfur-stabilized carbanion, trapped in the medium by water. The second would involve the formation of a radical α - to sulfur, generated through a homolytic cleavage of the same C–C bond from a nitrogen-centered radical formed from **163b**, **163f** or **163l** under the oxidative and basic conditions. The formation of a highly basic sulfur-stabilized carbanion ($pK_a \sim 29$ -30) appears less favorable than the corresponding radical.

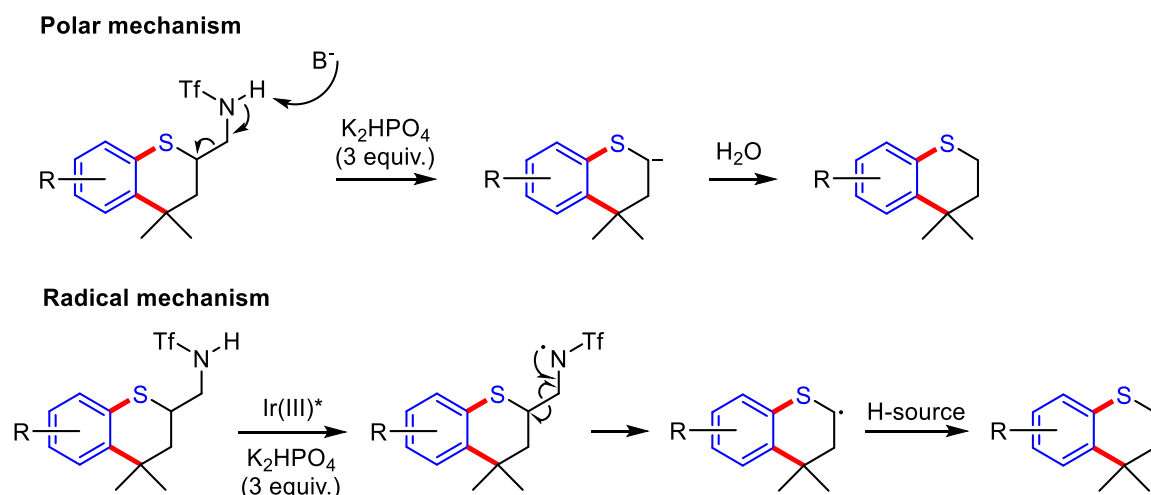


Figure 6 Possible mechanism for side products.

3.2.5 Computational studies

Above experiments indicate that a C-centered radical is generated during the process, which then cyclizes to produce heterocycles **163**. Computational studies were thus performed in order to study the fate of this C-centered radical species (Figure 7). Preliminary calculations were performed on a model C-centered radical **I** bearing a phenylsulfide substituent. This radical can lead to cyclohexadienyl radicals **IIa** or **IIb** through respectively 6- and 5-*exo* cyclization modes (noted *a* and *b*). The 6-*exo* mode is kinetically favored, leading also to the more stable **IIa**. In turn, **IIb** generated through a 5-*exo* process can easily lead to a thiyl radical **IIIb**,¹²¹ eventually cyclizing into the Truce-Smiles rearranged product **IVb**, through a more energetic pathway (Scheme 45). A second set of calculations was then performed starting from C-centered radical **V**, bearing a tetrafluorophenylsulfide substituent. With the fluorine substituents, the 5-*exo* process becomes the preferential pathway. But even if **VIb** is less stabilized than **VIa**, its rapid evolution towards the thiyl radical **VIIIb** still occurs. A 6-*exo* process can then take place with the displacement of a fluorine atom. A reduction of the thiyl radical **VIIIb** into the corresponding thiolate by the Ir(II) photocatalyst, followed by a nucleophilic aromatic substitution (S_NAr) on the C-F bond may also constitute a viable alternative (*vide infra*).¹²²

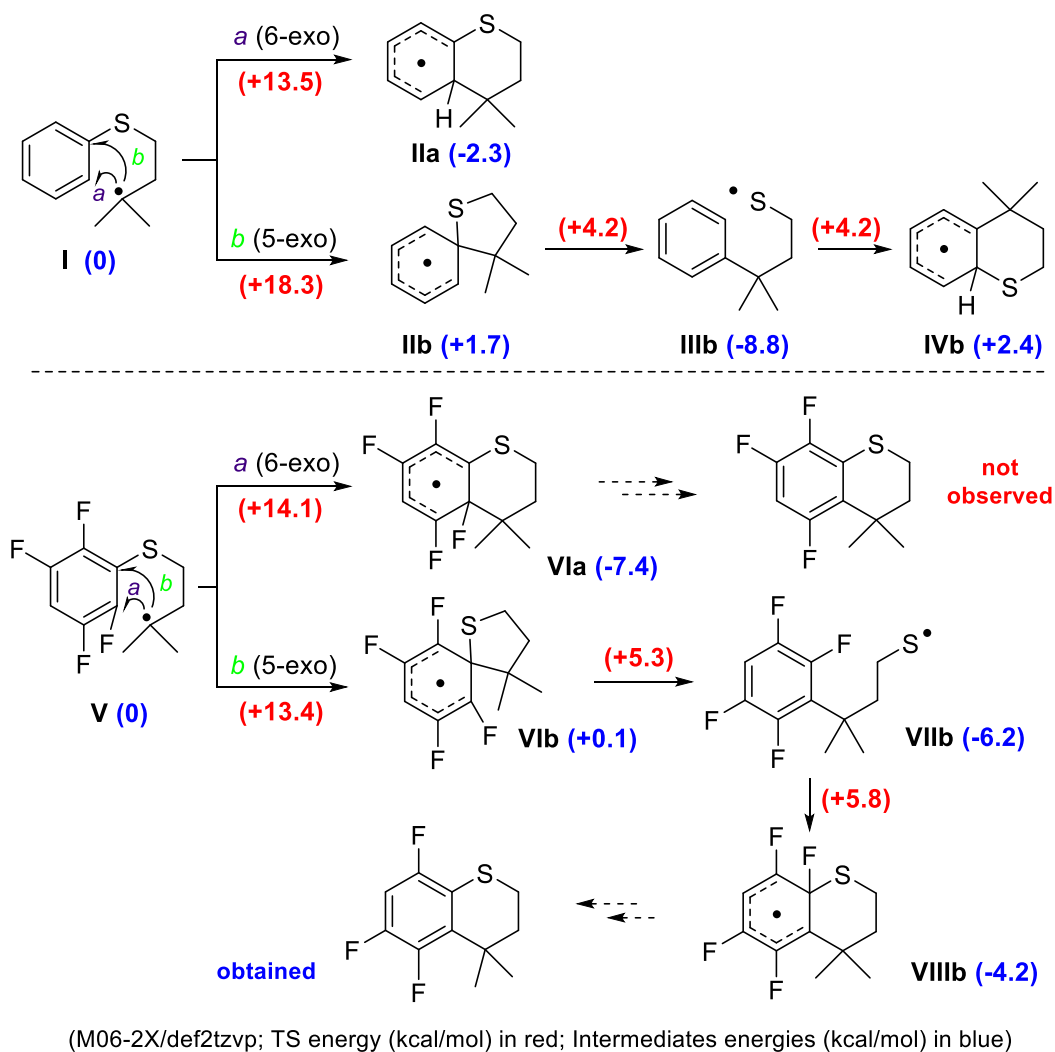
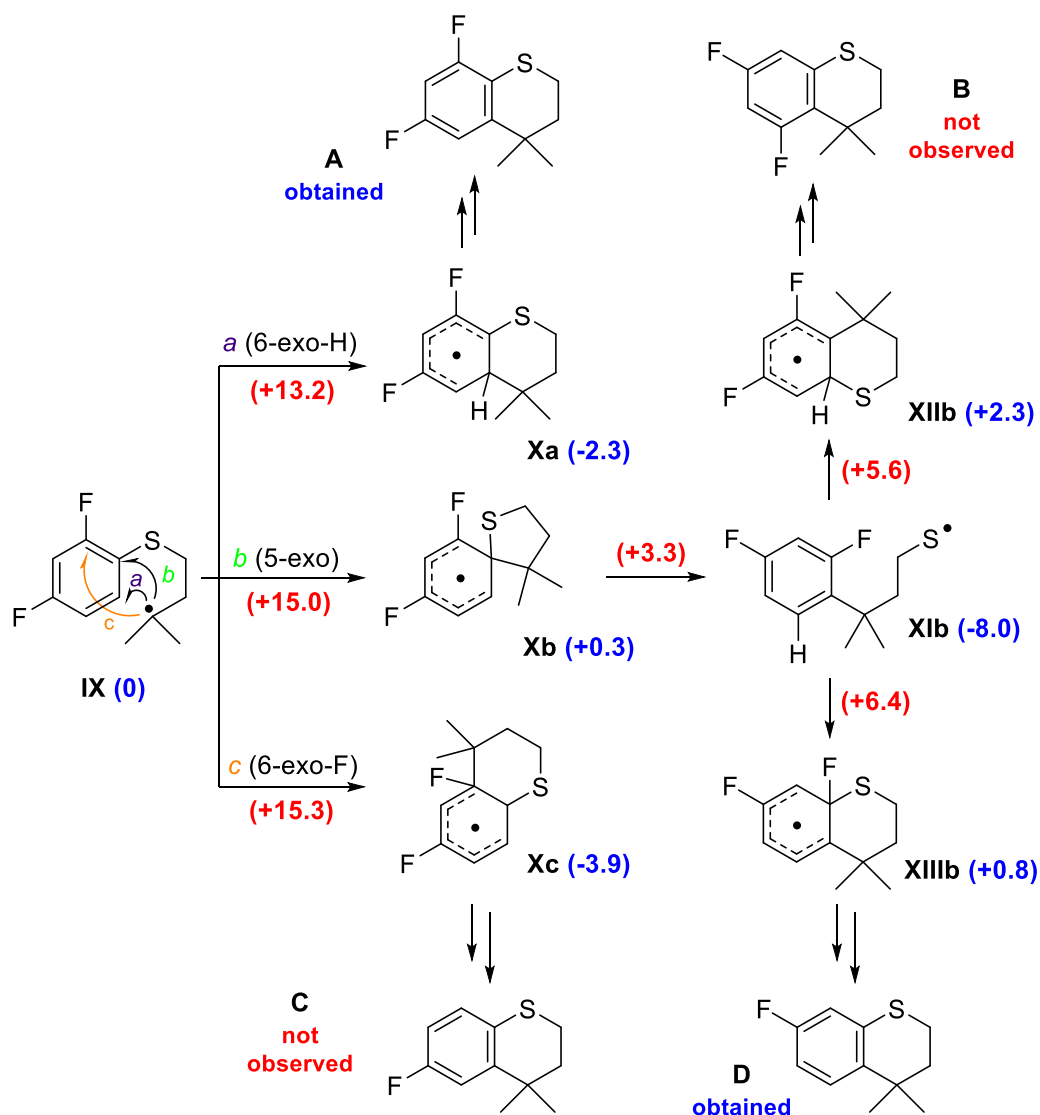


Figure 7 Computational studies on 5- versus 6-*exo* cyclization of the C-centered radical species.

An interesting case is that of cyclization of **162n** into the mixture of **163na** and **163nb** (Scheme 46). A computational study starting from model compound **IX** was undertaken to understand and rationalize the course of this transformation (Figure 8). In good agreement with experimental observations, these calculations indicate that the C-centered radical follows two pathways depending on the nature of the substituents *ortho* to C-S bond. The 6-*exo*-H cyclization was found to be slightly faster than the 5-*exo* mode, leading to the observed product **A** through a direct homolytic aromatic substitution (HAS). Although **Xc** is the more stable cyclohexadienyl intermediate, the absence of product **C** may be due to a higher TS barrier in this case. Again, the spiro[5,6] system **Xb** can evolve rapidly toward the formation of the thiyl radical **XIb**, the most stable species of all. The thiyl radical would then have the choice between a 6-*exo*-F or a 6-*exo*-H cyclization, the former being more favorable, leading to **XIIIb** the precursor of the observed product **D**. The cyclization of the thiyl radical leading to **XIb** or the more stable **XIIIb** being endergonic, a thermodynamically more

favored reduction of the thiyl radical **XIb** into the corresponding thiolate ($E^{\circ}_{RS/RS^-} = -0.22$ V, $E^{\circ}_{Ir(III)/Ir(II)} = -1.37$ V),¹²⁶ followed by S_NAr at the C-F center, as discussed above, would constitute a plausible alternative to the formation of **D** from **XIIIb**.¹²²



(M06-2X/def2tzvp; TS energy (kcal/mol) in red; Intermediates energies (kcal/mol) in blue)

Figure 8 Computational studies on 2,4-difluorophenyl sulfide model.

The above experimental results have also shown that there are two different reaction pathways, which depend on the electronic nature of the substituents on the thioaryl fragment. Two plausible pathways are shown in Figure 9. One approach involves a nitrogen radical-mediated 1,5-hydrogen atom transfer (HAT) followed by cyclization to yield the product. The other approach involves a direct attack of the nitrogen radical on the aromatic ring to form the S-N aryl migration product.

The migration of the aromatic from sulfur to nitrogen through a S-N radical Truce-Smiles

rearrangement has been computed by Dr. F. Robert at the same theory level for 4 different aromatic substituents, and compared with the expected 1,5-HAT. The substituents studied are Phenyl (**I** series), Pentafluorophenyl (**II** series), *ortho*-Methoxyphenyl (**III** series) and Thiophene (**IV** series) to be able to compare the pathways between non-migrating substituents (**I** and **II**) and migrating substituents (**III** and **IV**).

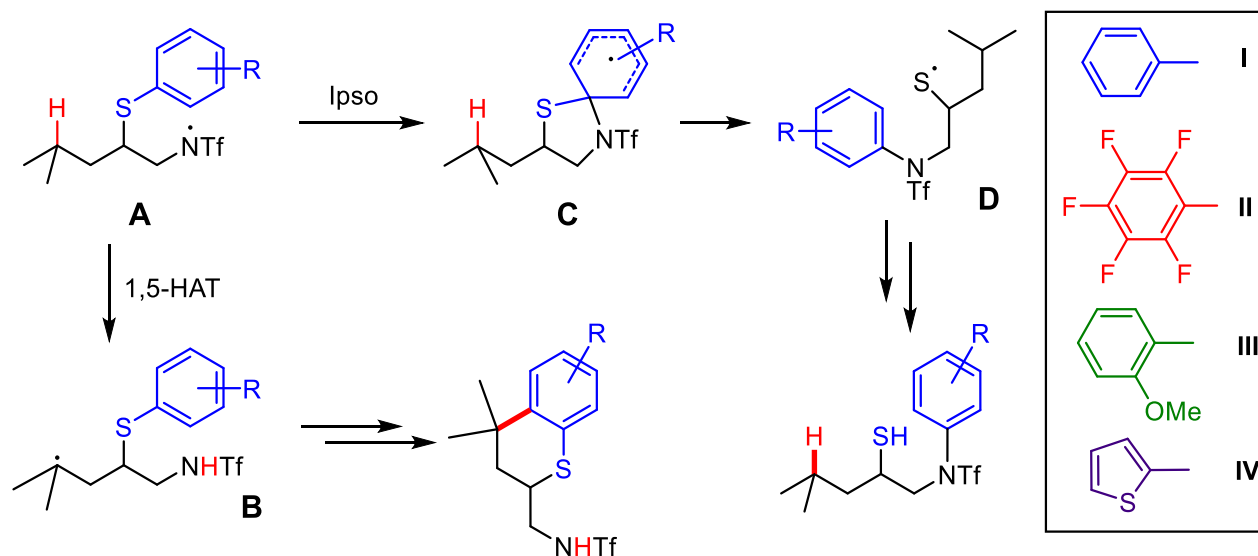


Figure 9 Two reaction pathways for different aromatic substituents.

Figure 10 displays the results of density functional theory (DFT) calculations for four distinct aromatic substituents. The 1,5-HAT from **A** to **B** is favored for phenyl (**I**) and pentafluorophenyl (**II**) substituents over the aryl migration pathway. For *o*-methoxy (**III**) or thiophene (**IV**) substituents, the aryl migration pathway through **C** and **D** is far more favored, explaining the observed products **163o** and **163p**. This can be rationalized based on match polarity effects between the electrophilic N-centered radical and electron-rich arenes (**III**) and (**IV**) illustrated with transition state **E**. The poorer polar complementarity between the electrophilic nitrogen radicals and arenes (**I**) and (**II**) disfavors the aryl migration. On the contrary the 1,5-HAT process becomes more favorable as illustrated by the transition state **F** below (Figure 5).

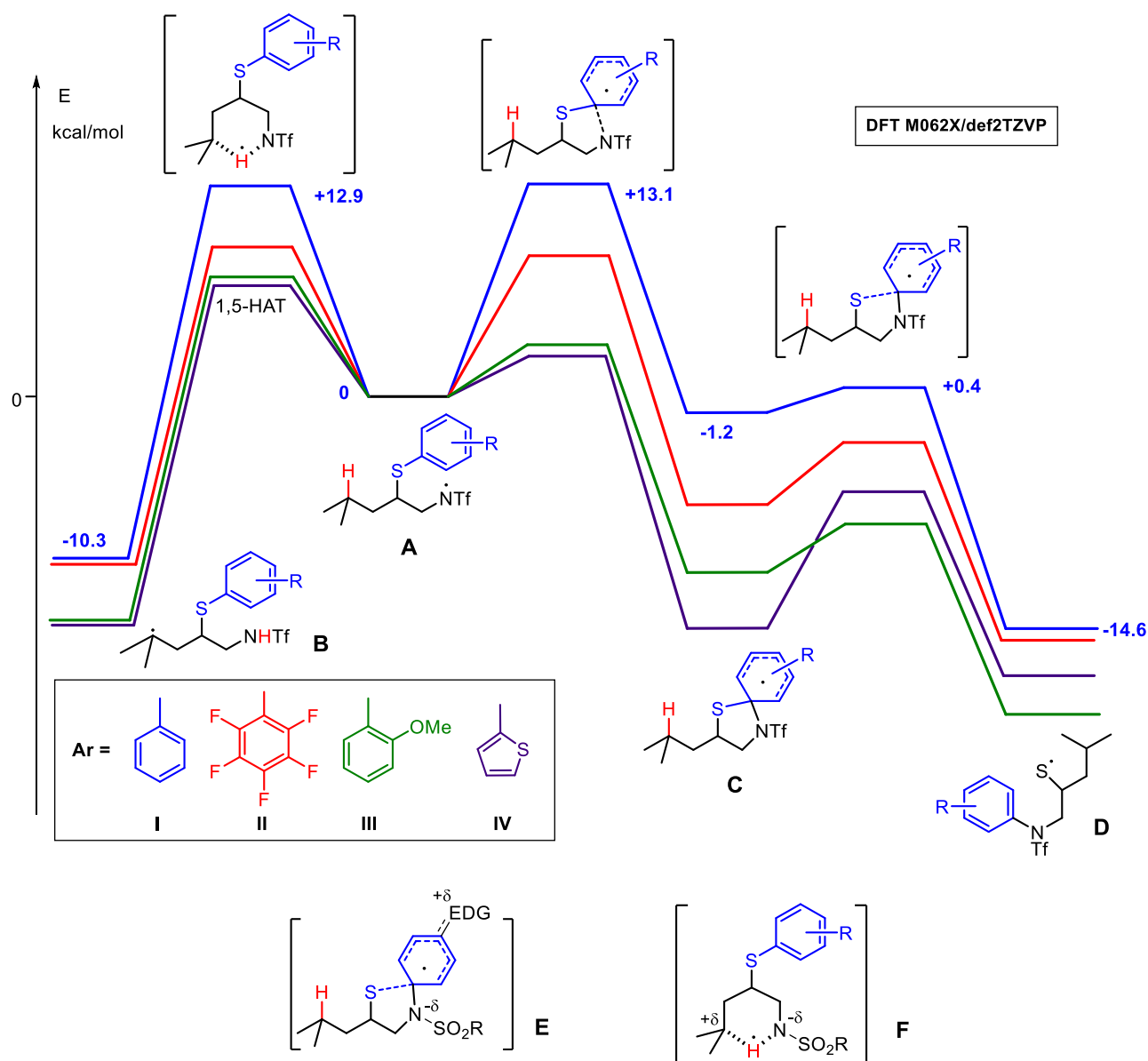
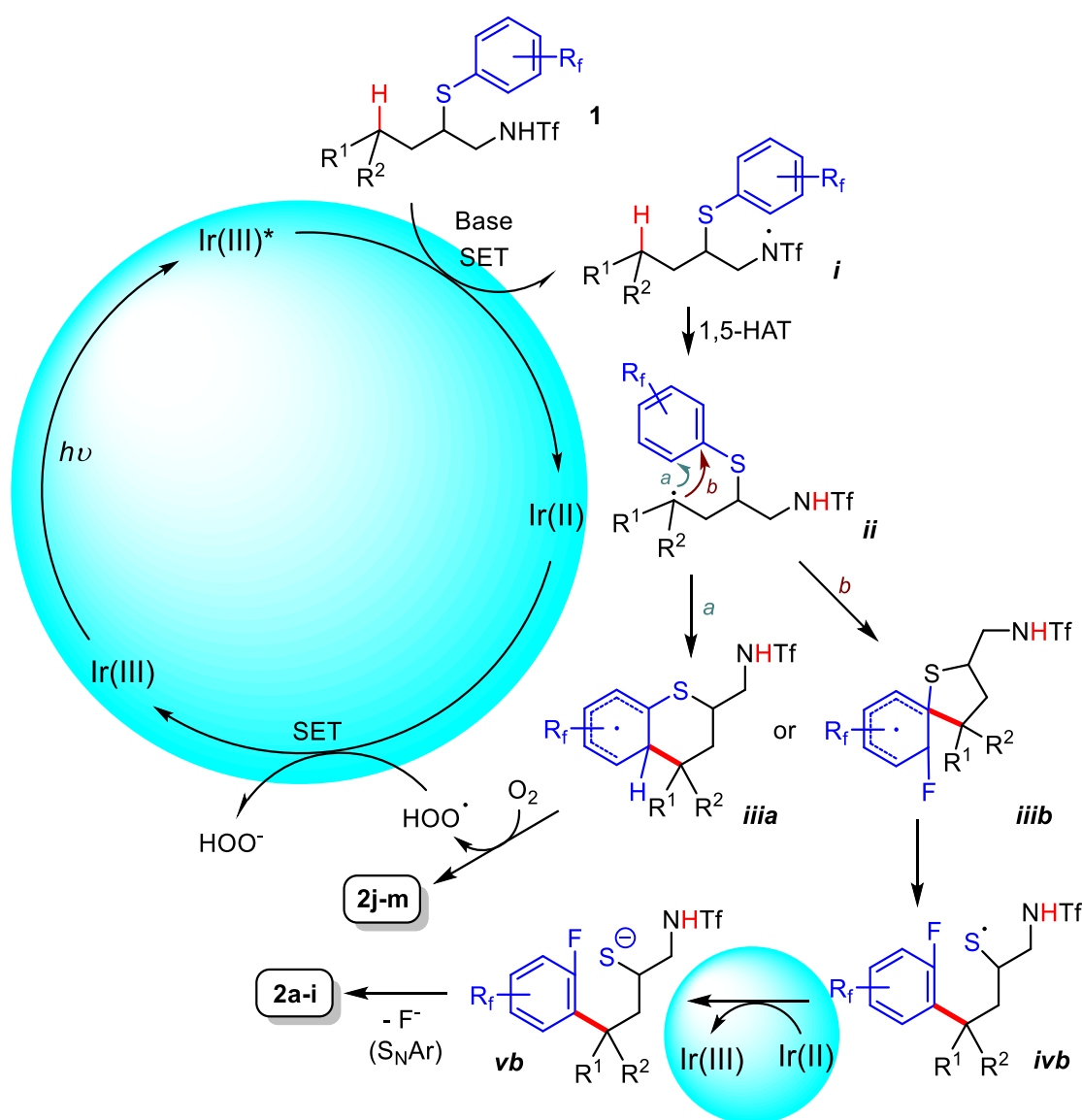


Figure 10 DFT calculations of 4 different aromatic substituents.

3.2.6 Proposed mechanism

Based on these premises and previous reports,¹²³ a plausible catalytic cycle may be proposed (Scheme 48). First a nitrogen-centered radical species *i* is generated through a deprotonation-oxidation process in the presence of the Ir(III) photocatalyst in its excited state. 1,5-HAT then follows to generate the C-centered radical *ii* that cyclizes onto the thioaryl moiety to form either a cyclohexadienyl radical *iii*_a or the spiro analogue *iii*_b. The latter can fragment to form the thiyl radical *iv*_b, which is known to be reduced by Ir(II) ($E^{\circ}_{\text{Ir(III)/Ir(II)}} = -1.37 \text{ V}$) into thiolate *vb* ($E^{\circ}_{\text{RS}/\text{RS}^-} = -0.22 \text{ V}$),¹²⁶ which finally displaces the fluorine atom through a $\text{S}_{\text{N}}\text{Ar}$ process affording **163a-i** (Scheme 45).^{122,123} The situation is not so clear-cut with cyclohexadienyl radical *iii*_a. The reduction of the latter by Ir(II) could restore the Ir(III) photocatalyst, leading to a cyclohexadienyl anion, the

protonation of which affording a cyclohexadiene. Although a precedent of such a pathway has been reported recently,¹²⁴ the formation of **163j-m** through aromatization of a cyclohexadiene appears unlikely here. Another route may then be suggested involving an autoxidation¹²⁵ of **iiia** by residual O₂ in the medium. Considering the experimental setup, a slow diffusion of O₂ may also occur on the time scale of the reaction (48 h), A slow oxidation of **iiia** would generate a hydroperoxyl radical finally reduced by Ir(II) into H₂O₂ (E^o_{HOO·/HOO-} = +1.51 V) and Ir(III). Although our efforts to detect H₂O₂ in the medium met with failure, this pathway would rationalize both moderate yields in **163j-m** and long reaction time to reach full conversion. Further investigations will however be required to shed light on this part of the mechanism.



Scheme 48 Photocatalyzed-(C_{sp3}-H) arylation of sulfonamide **162**. Photocatalytic cycle.

3.2.7 Conclusion

In summary, we disclosed here a new photocatalyzed distal arylation of alkylsulfonamides. The

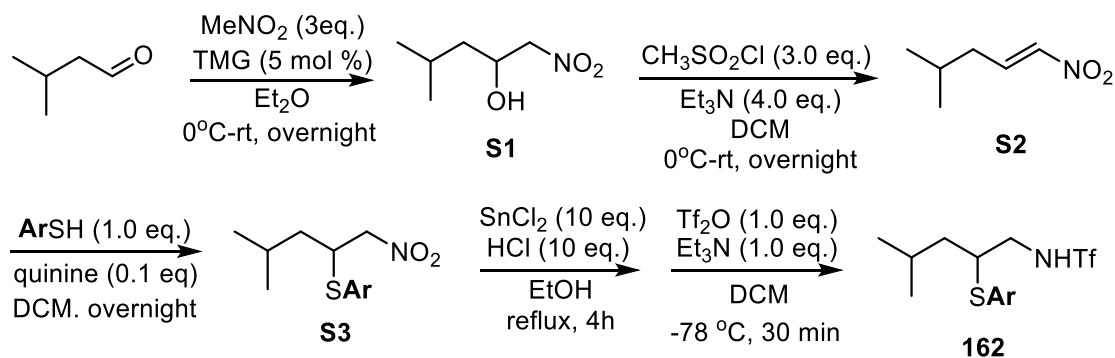
methodology opens an access to a range of polyfluorinated thiochromanes through a process including the generation of a sulfonamidyl radical from a simple sulfonamide, followed by a 1,5-HAT process. The δ C-centered radical thus generated then cyclizes onto the neighboring thioaryl moiety through two different pathways to afford the corresponding thiochromanes. The first route involves a 6-*exo* cyclization of the C-centered radical onto the arene and is favored for non-fluorinated substrates, while the latter proceeds through a radical Truce-Smiles-type rearrangement and occurs preferably with substrates having C_{sp2}-F *ortho* to the native C-S bond.

3.3 Experimental part

3.3.1 General information

All reactions were carried out under an argon atmosphere. Solvents were dried over activated alumina columns on a M-BRAUN Solvent Purification System (SPS-800) unless otherwise noted. The calculated experimental yields refer to chromatographically and spectroscopically (¹H-NMR) homogeneous materials unless otherwise stated. All reagent-grade chemicals were obtained from commercial suppliers and were used as received unless otherwise stated. ¹H NMR and ¹³C NMR were recorded at room temperature on various spectrometers: a Bruker Avance 300 (¹H: 300 MHz, ¹³C: 75 MHz, ¹⁹F: 282 MHz) and a Bruker Avance 600 (¹H: 600 MHz, ¹³C: 150 MHz) using CDCl₃ as internal reference unless otherwise indicated. The chemical shifts (δ) and coupling constants (J) are expressed in ppm and Hz respectively. The following abbreviations were used to explain the multiplicities: br = broad, s = singlet, d = doublet, t = triplet, q = quartet, dd = doublet of doublets, m = multiplet, dm = doublet of multiplet, quint = quintet, hex = hex(sex)tet, hept = hep(sep)tet. Structural assignments were made with additional information from gCOSY, gHSQC, and gHMBC experiments. FTIR spectra were recorded on a Perkin-Elmer Spectrum 100 using a KBr pellet. High-resolution mass spectra (HRMS) were recorded with a Waters Q-TOF 2 spectrometer in the electrospray ionization (ESI) or Field Ionization mode (FI). Melting points were not corrected and determined by using a Stuart Scientific SMP3 apparatus. Analytical thin layer chromatography was performed using silica gel 60 F254 pre-coated plates (Merck) with visualization by ultraviolet light. Flash chromatography was performed on silica gel (0.043-0.063 mm) with ethyl acetate (EA) and Petroleum ether (PE) as eluents unless otherwise indicated. Kessil lamp (LED Photoreaction Lighting) PR160L at 456 nm (34 W) were used for the photocatalyzed process. The lamp was generally located at a distance of 2-3 cm from the reaction vessel. No filter was used.

3.3.2 Synthesis of the starting Materials



To a solution of 3-methylbutanal (1.72 g, 20 mmol, 1.0 equiv.) and nitromethane (3.7 g, 60 mmol, 3.0 equiv.) in Et₂O (10 mL) at 0°C, tetramethylguanidine (115 mg, 1.0 mmol, 0.05 equiv.) was added. The reaction was gradually warmed to room temperature and stirred overnight. After being quenched with sat. NH₄Cl, the mixture was extracted with Et₂O. The organic phase was dried over MgSO₄. The solvent was removed under reduced pressure, and the crude residue **S1** was used for next step without further purification.¹²⁷

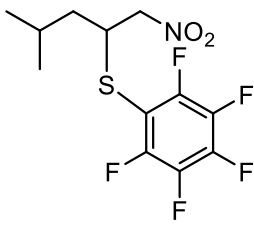
To a solution of 4-methyl-1-nitropent-2-ol **S1** in CH₂Cl₂ (80 mL) was added triethylamine (8.1 g, 80 mmol, 4.0 equiv.) and methanesulfonyl chloride (6.8 g, 60 mmol, 3.0 equiv.) at 0°C. Then, the resulting mixture was stirred at room temperature overnight. Sat. NH₄Cl was added to the reaction mixture, which was then extracted with DCM three times, dried over MgSO₄ and then concentrated to provide the crude product **S2**, which was used in the following step without any further purification.¹²⁸

General procedure A for the synthesis of nitrosulfanes:

To a 250 mL round-bottom flask equipped with a stir bar was added all of the crude **S2** from the previous step, quinine (648 mg, 2 mmol, 0.1 equiv.), and ArSH (20 mmol, 1.0 equiv.) in DCM (80 mL). The mixture was stirred at room temperature overnight. After that, the resulting mixture was concentrated in vacuo, and the residue was then purified by flash column chromatography to afford the product **S3**.¹²⁹

(4-Methyl-1-nitropent-2-yl)(perfluorophenyl)sulfane (S3a)

Based on general procedure **A**, starting from 2.0 g of pentafluorosulfane, product **S3a** has been obtained as an oil (2.21 g, 6.7 mmol, 67% yield).

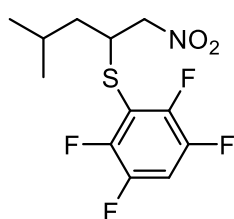
 R_f = 0.6 (PE: EA = 20:1)
¹H NMR (300 MHz, CDCl₃) δ 4.45 (d, *J* = 7.0 Hz, 2H), 3.82 – 3.72 (m, 1H), 2.11 – 1.94 (m, 1H), 1.58 – 1.37 (m, 2H), 0.99 (d, *J* = 1.1 Hz, 3H), 0.97 (d, *J* = 1.3 Hz, 3H). ¹³C{¹H} (76 MHz, CDCl₃) δ 148.2 (dm, C–F, ¹*J*_{C–F} = 246.9 Hz), 142.6 (dm, C–F, ¹*J*_{C–F} = 258.0 Hz), 138.0 (dm, C–F, ¹*J*_{C–F} = 257.0 Hz), 106.5 – 105.8 (m), 79.9, 44.6, 41.3, 25.5, 23.1, 21.3. ¹⁹F NMR (282 MHz, CDCl₃) δ -130.5 – -130.6 (m, 2F), -149.5 (t, *J* = 21.0 Hz, 1F), -159.5 – -159.8 (m, 2F).

FT-IR $\bar{\nu}_{\max}$ (cm⁻¹) = 2963, 2935, 2875, 1639, 1557, 1514, 1448, 1375, 1093.

HRMS (FI): Calcd. for C₁₂H₁₂F₅NO₂S: [M]⁺⁺ 329.0503, found 329.0503.

(4-Methyl-1-nitropentan-2-yl)(2,3,5,6-tetrafluorophenyl)sulfane (S3b)

Based on general procedure A, starting from 1.82 g of (2,3,5,6-tetrafluorophenyl)sulfane, product S3b has been obtained as an oil (2.33 g, 7.5 mmol, 75% yield).



R_f = 0.6 (PE: EA = 20:1)

¹H NMR (300 MHz, CDCl₃) δ 4.47 (dd, *J* = 6.8, 2.0 Hz, 2H), 4.02 – 3.92 (m, 1H), 2.08 – 1.93 (m, 1H), 1.54 (td, *J* = 8.8, 5.3 Hz, 2H), 1.00 (d, *J* = 1.1 Hz, 3H), 0.98 (d, *J* = 1.2 Hz, 3H). ¹³C {¹H} NMR (76 MHz, CDCl₃) δ 147.7 (dm, C–F, ¹*J*_{C–F} = 242.4 Hz), 144.2 (dm, C–F, ¹*J*_{C–F} = 258.0 Hz), 120.7 (q, *J* = 275.2 Hz), 117.4 (t,

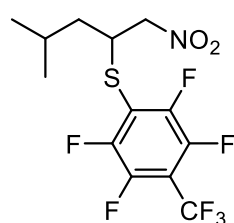
C–F, ²*J*_{C–F} = 20.2 Hz), 112.3 – 109.4 (m), 79.7, 44.3 (t, *J* = 2.4 Hz), 41.5, 25.6, 22.9, 21.3. ¹⁹F NMR (282 MHz, CDCl₃) δ -56.6 (t, *J* = 21.8 Hz, 3F), -130.1 – -130.3 (m, 2F), -139.0 – -139.4 (m, 2F).

FT-IR $\bar{\nu}_{\max}$ (cm⁻¹) = 3076, 2962, 2934, 2874, 1557, 1491, 1433, 1376, 1235.

HRMS (FI): Calcd. for C₁₂H₁₃F₄NO₂S: [M]⁺⁺ 311.0598, found 311.0608.

(4-Methyl-1-nitropentan-2-yl)(2,3,5,6-tetrafluoro-4-(trifluoromethyl)phenyl)sulfane (S3c)

Based on general procedure A, starting from 1.25 g of (2,3,5,6-tetrafluoro-4-(trifluoromethyl)phenyl)sulfane, product S3c has been obtained as an oil (1.56 g, 4.1 mmol, 82% yield).



R_f = 0.6 (PE: EA = 20:1)

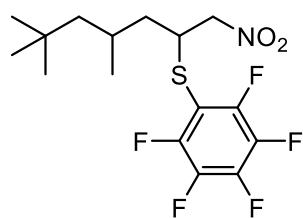
¹H NMR (300 MHz, CDCl₃) δ 4.47 (dd, *J* = 6.8, 2.0 Hz, 2H), 4.02 – 3.92 (m, 1H), 2.08 – 1.93 (m, 1H), 1.54 (td, *J* = 8.8, 5.3 Hz, 2H), 1.00 (d, *J* = 1.1 Hz, 3H), 0.98 (d, *J* = 1.2 Hz, 3H). ¹³C {¹H} NMR (76 MHz, CDCl₃) δ 147.7 (dm, C–F, ¹*J*_{C–F} = 242.4 Hz), 144.2 (dm, C–F, ¹*J*_{C–F} = 258.0 Hz), 120.7 (q, *J* = 275.2 Hz), 117.4 (t, C–F, ²*J*_{C–F} = 20.2 Hz), 112.3 – 109.4 (m), 79.7, 44.3 (t, *J* = 2.4 Hz), 41.5, 25.6, 22.9, 21.3. ¹⁹F NMR (282 MHz, CDCl₃) δ -56.6 (t, *J* = 21.8 Hz, 3F), -130.1 – -130.3 (m, 2F), -139.0 – -139.4 (m, 2F).

FT-IR $\bar{\nu}_{\max}$ (cm⁻¹) = 2964, 2936, 2876, 1645, 1559, 1481, 1375, 1328, 1184.

HRMS (FI): Calcd. for C₁₃H₁₂F₇NO₂S: [M]⁺⁺ 379.0472, found 379.0478.

(Perfluorophenyl)(4,6,6-trimethyl-1-nitroheptan-2-yl)sulfane (S3d)

Based on general procedure A, starting from 1.70 g of (perfluorophenyl)sulfane, product S3d has been obtained as an oil (2.73 g, 7.1 mmol, 83% yield) with a dr = 1/1.7.



R_f = 0.6 (PE: EA = 20:1)

¹H NMR (300 MHz, CDCl₃) δ 4.53 – 4.34 (m, 2H), 3.85 – 3.65 (m, 1H), 2.04 – 1.76 (m, 1H), 1.65 – 1.33 (m, 2H), 1.28 – 1.08 (m, 2H), 0.99 (d, *J* = 6.6 Hz, 3H), 0.92 (d, *J* = 1.7 Hz, 9H). ¹³C {¹H} NMR (76 MHz, CDCl₃) δ 148.1 (dm, C–F, ¹*J*_{C–F} = 246.9 Hz), 142.5 (dm, C–F, ¹*J*_{C–F} = 257.7 Hz), 138.0

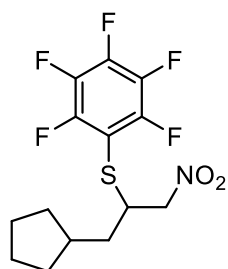
(dm, C–F, ¹*J*_{C–F} = 256.6 Hz), 107.0 – 105.5 (m), 80.0, 79.5, 51.6, 50.5, 44.9, 44.1, 42.0, 41.8, 31.3, 31.0, 30.1, 30.0, 27.1, 26.7, 22.9, 21.3. ¹⁹F NMR (282 MHz, CDCl₃) δ -130.3 – -130.4 (m, 0.76F), -130.9 – -131.0 (m, 1.28F), -149.9 (m, 0.37F), -150.1 – -150.2 (m, 0.63F), -159.9 – -160.1 (m, 2F).

FT-IR $\bar{\nu}_{\max}$ (cm⁻¹) = 2957, 2871, 1639, 1556, 1514, 1487, 1374, 1093, 981.

HRMS (FI): Calcd. for C₁₆H₂₀F₅NO₂S: [M]⁺⁺ 385.1129, found 385.1133.

(1-Cyclopentyl-3-nitropropan-2-yl)(perfluorophenyl)sulfane (S3e)

Based on general procedure A, starting from 1.0 g of (perfluorophenyl)sulfane, product S3e has been obtained as an oil (1.65 g, 4.6 mmol, 93% yield).



R_f = 0.6 (PE: EA = 20:1)

¹H NMR (300 MHz, CDCl₃) δ 4.52 – 4.39 (m, 2H), 3.77 – 3.67 (m, 1H), 2.26 – 2.15 (m, 1H), 1.96 – 1.77 (m, 2H), 1.72 – 1.52 (m, 6H), 1.20 – 1.03 (m, 2H).

¹³C{¹H} NMR (76 MHz, CDCl₃) δ 148.3 (dm, C–F, ¹J_{C–F} = 246.9 Hz), 142.5 (dm, C–F, ¹J_{C–F} = 258.4 Hz), 138.0 (dm, C–F, ¹J_{C–F} = 256.6 Hz), 106.7 – 106.0 (m), 79.8, 46.0 (d, C–F, ⁴J_{C–F} = 1.7 Hz), 38.7, 37.2, 33.0, 32.0, 25.2, 25.1. ¹⁹F NMR

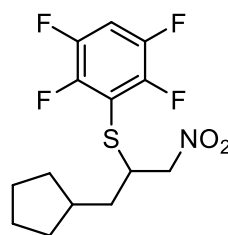
(282 MHz, CDCl₃) δ -130.6 – -130.7 (m, 2F), -149.7 (t, *J* = 20.9 Hz, 1F), -159.6 – -159.8 (m, 2F).

FT-IR $\bar{\nu}_{\max}$ (cm⁻¹) = 2953, 2870, 1639, 1557, 1514, 1489, 1376, 1093, 981.

HRMS (ESI): Calcd for C₁₄H₁₅F₅NO₂S [M+H]⁺: 356.0738, found 356.0750.

(1-Cyclopentyl-3-nitropropan-2-yl)(2,3,5,6-tetrafluorophenyl)sulfane (S3f)

Based on general procedure A, starting from 0.91 g of (2,3,5,6-tetrafluorophenyl)sulfane, product S3f has been obtained as an oil (1.6 g, 4.7 mmol, 94% yield).



R_f = 0.55 (PE: EA = 20:1)

¹H NMR (300 MHz, CDCl₃) δ 7.15 (tt, *J* = 9.4, 7.3 Hz, 1H), 4.47 (d, *J* = 7.0 Hz, 2H), 3.84 – 3.74 (m, 1H), 2.34 – 2.10 (m, 1H), 1.95 – 1.77 (m, 2H), 1.74 – 1.51

(m, 6H), 1.22 – 1.01 (m, 2H). ¹³C{¹H} NMR (76 MHz, CDCl₃) δ 147.5 (dm, C–F, ¹J_{C–F} = 246.6 Hz), 146.2 (dm, C–F, ¹J_{C–F} = 250.3 Hz), 112.3 (t, C–F, ²J_{C–F} =

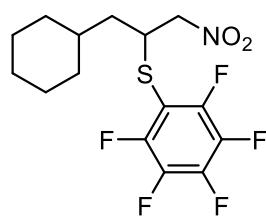
20.5 Hz), 107.9 (t, C–F, ²J_{C–F} = 22.8 Hz), 79.8, 45.7 (d, C–F, ⁴J_{C–F} = 2.0 Hz), 38.7, 37.2, 33.0, 31.9, 25.2, 25.1. ¹⁹F NMR (282 MHz, CDCl₃) δ -131.8 – -131.9 (m, 2F), -136.9 – -137.0 (m, 2F).

FT-IR $\bar{\nu}_{\max}$ (cm⁻¹) = 2952, 2869, 1557, 1490, 1433, 1376, 1235, 1176, 917.

HRMS (ESI): calcd for C₁₄H₁₆F₄NO₂S [M+H]⁺: 338.0832, found 338.0839.

(1-Cyclohexyl-3-nitropropan-2-yl)(perfluorophenyl)sulfane (S3g)

Based on general procedure A, starting from 1.20 g of (perfluorophenyl)sulfane, product S3g has been obtained as a solid (0.64 g, 1.7 mmol, 29% yield).



R_f = 0.6 (PE: EA = 20:1)

M.p. = 88–89°C

¹H NMR (300 MHz, CDCl₃) δ 4.45 (d, *J* = 7.0 Hz, 2H), 3.81 (p, *J* = 7.1 Hz, 1H), 1.88 – 1.61 (m, 6H), 1.48 (t, *J* = 7.0 Hz, 2H), 1.38 – 1.08 (m, 3H), 1.05 – 0.82 (m, 2H). ¹³C{¹H} (76 MHz, CDCl₃) δ 148.2 (dm, C–F, ¹J_{C–F} = 246.9

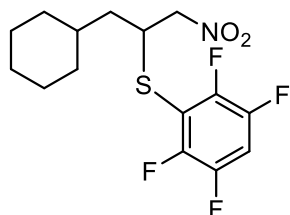
Hz), 142.5 (dm, C–F, ¹J_{C–F} = 258.0 Hz), 138.0 (dm, C–F, ¹J_{C–F} = 257.0 Hz) 106.7– 106.3 (m), 79.9, 44.0, 39.9, 34.8, 33.7, 32.3, 26.4, 26.2, 26.0.

FT-IR $\bar{\nu}_{\max}$ (cm⁻¹) = 2925, 2853, 1638, 1556, 1513, 1486, 1092, 980.

HRMS (FI): Calcd. for C₁₅H₁₆F₅NO₂S: [M]⁺⁺ 369.0816, found 369.0826.

(1-Cyclohexyl-3-nitropropan-2-yl)(2,3,5,6-tetrafluorophenyl)sulfane (S3h)

Based on general procedure A, starting from 1.20 g of (2,3,5,6-tetrafluorophenyl)sulfane, product **S3h** has been obtained as a solid (2.03 g, 5.8 mmol, 88% yield).



Rf = 0.6 (PE: EA = 20:1)

M.p. = 89-90°C

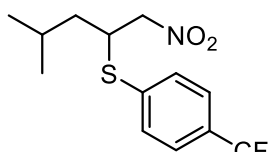
$^1\text{H NMR}$ (300 MHz, CDCl_3) δ 7.15 (tt, $J = 9.5, 7.4$ Hz, 1H), 4.45 (d, $J = 7.0$ Hz, 2H), 3.88 (p, $J = 7.1$ Hz, 1H), 1.89 – 1.62 (m, 6H), 1.47 – 1.51 (m, 2H), 1.37 – 1.07 (m, 3H), 1.05 – 0.80 (m, 2H). $^{13}\text{C}\{^1\text{H}\}$ NMR (75 MHz, CDCl_3) δ 147.6 (dm, C–F, $^1J_{\text{C-F}} = 246.3$ Hz), 146.2 (dm, C–F, $^1J_{\text{C-F}} = 250.4$ Hz), 112.30 (t, C–F, $^2J_{\text{C-F}} = 20.5$ Hz), 107.9 (t, C–F, $^2J_{\text{C-F}} = 22.8$ Hz), 79.9, 44.7 (t, C–F, $^4J_{\text{C-F}} = 1.9$ Hz), 40.0, 34.7, 33.8, 32.2, 26.4, 26.2, 26.0.

FT-IR $\bar{\nu}_{\text{max}}$ (cm^{-1}) = 2927, 2853, 1555, 1489, 1375, 1236, 1175, 915.

HRMS (FI): Calcd. for $\text{C}_{15}\text{H}_{17}\text{F}_4\text{NO}_2\text{S}$: $[\text{M}]^{+}$ 351.0911, found 351.0912.

(4-Methyl-1-nitropentan-2-yl)(4-(trifluoromethyl)phenyl)sulfane (S3i)

Based on general procedure A, starting from 0.89 g of (4-(trifluoromethyl)phenyl)sulfane, product **S3j** has been obtained as an oil (0.84 g, 2.7 mmol, 55% yield).



Rf = 0.5 (PE: EA = 20:1)

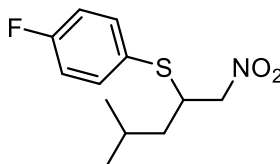
$^1\text{H NMR}$ (300 MHz, CDCl_3) δ 7.69 – 7.46 (m, 4H), 4.50 – 4.36 (m, 2H), 3.90 – 3.81 (m, 1H), 2.09 – 1.88 (m, 1H), 1.59 – 1.41 (m, 2H), 0.98 (d, $J = 4.3$ Hz, 3H), 0.96 (d, $J = 4.1$ Hz, 3H). $^{13}\text{C}\{^1\text{H}\}$ NMR (76 MHz, CDCl_3) δ 137.7 (d, C–F, $^4J_{\text{C-F}} = 1.5$ Hz), 132.0, 130.1 (q, C–F, $^2J_{\text{C-F}} = 32.9$ Hz), 126.3 (q, C–F, $^3J_{\text{C-F}} = 3.8$ Hz), 124.0 (q, C–F, $^1J_{\text{C-F}} = 272.1$ Hz), 79.3, 43.8, 41.0, 25.43, 2.10, 21.5. $^{19}\text{F NMR}$ (282 MHz, CDCl_3) δ -62.8 (s, 3F).

FT-IR $\bar{\nu}_{\text{max}}$ (cm^{-1}) = 2961, 2933, 2873, 1607, 1556, 1375, 1326, 1168.

HRMS (FI): Calcd. for $\text{C}_{13}\text{H}_{16}\text{F}_3\text{NO}_2\text{S}$: $[\text{M}]^{+}$ 307.0848, found 307.0855.

(4-Fluorophenyl)(4-methyl-1-nitropentan-2-yl)sulfane (S3k)

Based on general procedure A, starting from 2.50 g of (4-fluorophenyl)sulfane, product **S3k** has been obtained as an oil (2.55 g, 10.0 mmol, 50% yield).



Rf = 0.65 (PE: EA = 20:1)

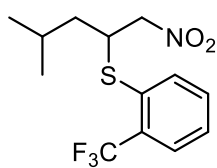
$^1\text{H NMR}$ (300 MHz, CDCl_3) δ 7.49 – 7.42 (m, 2H), 7.07 – 6.99 (m, 2H), 4.37 (dd, $J = 7.2, 4.8$ Hz, 1H), 3.64 – 3.55 (m, 1H), 2.09 – 1.92 (m, 1H), 1.44 (ddd, $J = 14.7, 9.9, 5.0$ Hz, 1H), 1.32 (ddd, $J = 14.1, 9.0, 4.9$ Hz, 1H), 0.95 (d, $J = 1.0$ Hz, 3H), 0.92 (d, $J = 0.8$ Hz, 3H). $^{13}\text{C}\{^1\text{H}\}$ NMR (76 MHz, CDCl_3) δ 163.2 (d, C–F, $^1J_{\text{C-F}} = 249.6$ Hz), 136.8 (d, C–F, $^3J_{\text{C-F}} = 8.4$ Hz), 126.4 (d, C–F, $^4J_{\text{C-F}} = 3.5$ Hz), 116.5 (d, C–F, $^2J_{\text{C-F}} = 21.9$ Hz), 79.2, 44.9 (d, C–F, $^4J_{\text{C-F}} = 1.3$ Hz), 40.6, 25.2, 23.0, 21.3. $^{19}\text{F NMR}$ (282 MHz, CDCl_3) δ -111.8 – -111.9 (m, 1F).

FT-IR $\bar{\nu}_{\text{max}}$ (cm^{-1}) = 2959, 2932, 2871, 1589, 1554, 1490, 1376, 1226.

HRMS (FI): Calcd. for $\text{C}_{12}\text{H}_{16}\text{FNO}_2\text{S}$: $[\text{M}]^{+}$ 257.0880, found 257.0896.

(4-Methyl-1-nitropentan-2-yl)(2-(trifluoromethyl)phenyl)sulfane (S3l)

Based on general procedure A, starting from 1.78 g of 2-(trifluoromethyl)benzenethiol, product **S3l** has been obtained as an oil (1.0 g, 3.3 mmol, 33% yield).



R_f = 0.5 (PE: EA = 20:1)

¹H NMR (300 MHz, CDCl₃) δ 7.76 – 7.65 (m, 2H), 7.56 (td, *J* = 7.6, 1.5 Hz, 1H), 7.41 (tt, *J* = 7.6, 1.1 Hz, 1H), 4.49 – 4.29 (m, 2H), 3.91 (tt, *J* = 9.5, 5.1 Hz, 1H), 2.03 – 1.92 (m, 1H), 1.68 – 1.43 (m, 2H), 0.98 (d, *J* = 4.3 Hz, 3H), 0.96 (d, *J* = 4.1

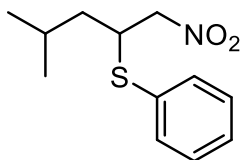
Hz, 3H). ¹³C{¹H} NMR (76 MHz, CDCl₃) δ 134.4, 132.6, 132.2 (q, C–F, ²*J*_{C–F} = 30.4 Hz), 128.0, 127.3 (q, C–F, ³*J*_{C–F} = 5.6 Hz), 123.5 (q, C–F, ¹*J*_{C–F} = 275.1 Hz), 79.3, 45.0, 41.1, 25.3, 23.1, 21.3.

FT-IR $\bar{\nu}_{\max}$ (cm⁻¹) = 3436, 2089, 1636, 1312, 1173, 1125, 1034, 689.

HRMS (FI): Calcd. for C₁₃H₁₆F₃NO₂S: [M]⁺ 307.0848, found 307.0857.

(Phenyl)(4-methyl-1-nitropentan-2-yl)sulfane (S3m)

Based on general procedure A, starting from 4.40 g of (phenyl)sulfane, product **S3m** has been obtained as a oil (5.74 g, 24.0 mmol, 60% yield).



R_f = 0.65 (PE: EA = 20:1)

¹H NMR (300 MHz, CDCl₃) δ 7.51 – 7.43 (m, 2H), 7.40 – 7.29 (m, 3H), 4.50 – 4.30 (m, 2H), 3.77 – 3.67 (m, 1H), 2.15 – 1.95 (m, 1H), 1.57 – 1.31 (m, 2H), 0.98 (s, 3H), 0.95 (s, 3H). ¹³C{¹H} NMR (75 MHz, CDCl₃) δ 133.9, 131.8,

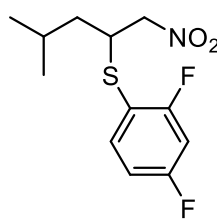
129.5, 128.6, 79.5, 44.4, 40.8, 25.3, 23.2, 21.4.

FT-IR $\bar{\nu}_{\max}$ (cm⁻¹) = 3074, 3060, 2931, 2958, 2870, 1582, 1553, 1375.

HRMS (EI): Calcd. for C₁₂H₁₇FNO₂S: [M]⁺ 239.0986, found 239.0987.

(2,4-Difluorophenyl)(4-methyl-1-nitropentan-2-yl)sulfane (S3n)

Based on general procedure A, starting from 1.46 g of (2,4-difluorophenyl)sulfane, product **S3n** has been obtained as an oil (2.28 g, 8.3 mmol, 83% yield).



R_f = 0.65 (PE: EA = 20:1)

¹H NMR (300 MHz, CDCl₃) δ 7.73 – 7.37 (m, 1H), 7.10 – 6.73 (m, 2H), 4.51 – 4.28 (m, 2H), 3.71 – 3.62 (m, 1H), 2.09 – 1.95 (m, 1H), 1.55 – 1.27 (m, 2H), 0.95 (d, *J* = 1.8 Hz, 3H), 0.93 (d, *J* = 1.9 Hz, 3H). ¹³C{¹H} NMR (76 MHz, CDCl₃) δ 165.5 (dd, C–F, ²*J*_{C–F} = 26.7 Hz, ³*J*_{C–F} = 12.0 Hz), 162.1 (dd, C–F, ²*J*_{C–F} = 23.5

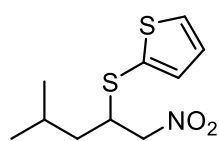
Hz, ³*J*_{C–F} = 12.0 Hz), 138.4 (dd, C–F, ³*J*_{C–F} = 9.6 Hz, ³*J*_{C–F} = 1.9 Hz), 114.1 (dd, C–F, ²*J*_{C–F} = 18.8 Hz, ⁴*J*_{C–F} = 4.1 Hz), 112.4 (dd, C–F, ²*J*_{C–F} = 21.4 Hz, ⁴*J*_{C–F} = 3.9 Hz), 105.1 (dd, C–F, ²*J*_{C–F} = 27.3 Hz, ²*J*_{C–F} = 25.8 Hz), 79.6, 44.3 (t, C–F, ⁴*J*_{C–F} = 1.6 Hz), 41.0, 25.3, 23.1, 21.3. ¹⁹F NMR (282 MHz, CDCl₃) δ -100.6 – -100.7 (m, 1F), -106.3 – -106.5 (m, 1F).

FT-IR $\bar{\nu}_{\max}$ (cm⁻¹) = 2960, 2933, 2872, 1596, 1555, 1485, 1419, 1376, 1264.

HRMS (FI): Calcd. for C₁₂H₁₅F₂NO₂S: [M]⁺ 275.0786, found 275.0791.

2-((4-Methyl-1-nitropentan-2-yl)thio)thiophene (S3o)

Based on general procedure **A**, starting from 1.8 g of thiophene-2-thiol, product **S3o** has been obtained as an oil (2.75 g, 11.2 mmol, 70% yield).



R_f = 0.5 (PE: EA = 20:1)

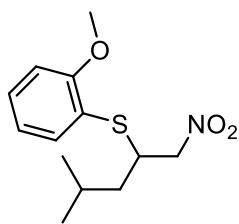
¹H NMR (300 MHz, CDCl₃) δ 7.46 (dd, *J* = 5.4, 1.3 Hz, 1H), 7.20 (dd, *J* = 3.6, 1.2 Hz, 1H), 7.05 (dd, *J* = 5.4, 3.6 Hz, 1H), 4.51 (dd, *J* = 12.8, 7.2 Hz, 1H), 4.34 (dd, *J* = 12.8, 7.4 Hz, 1H), 3.47 (dtd, *J* = 10.4, 7.3, 4.5 Hz, 1H), 2.20 – 1.94 (m, 1H), 1.45 (ddd, *J* = 14.2, 10.4, 4.6 Hz, 1H), 1.25 (ddd, *J* = 14.1, 9.3, 4.5 Hz, 1H), 0.97 (d, *J* = 1.1 Hz, 3H), 0.95 (d, *J* = 0.9 Hz, 3H). ¹³C{¹H} NMR (76 MHz, CDCl₃) δ 137.6, 131.9, 128.1, 128.0, 79.1, 45.6, 39.9, 25.2, 23.1, 21.3.

FT-IR $\bar{\nu}_{\max}$ (cm⁻¹) = 2958, 2931, 2870, 1554, 1376, 1218.

HRMS (FI): Calcd. for C₁₀H₁₅NO₂S₂: [M]⁺ 245.0539, found 245.0546.

(2-Methoxyphenyl)(4-methyl-1-nitropentan-2-yl)sulfane (S3p)

Based on general procedure **A**, starting from 2.8 g of 2-methoxybenzenethiol, product **S3p** has been obtained as an oil (3.7 g, 13.7 mmol, 68% yield).



R_f = 0.65 (PE: EA = 20:1)

¹H NMR (300 MHz, CDCl₃) δ 7.52 – 7.42 (m, 1H), 7.40 – 7.31 (m, 1H), 7.04 – 6.91 (m, 2H), 4.48 (dd, *J* = 12.7, 5.1 Hz, 1H), 4.37 (dd, *J* = 12.7, 9.1 Hz, 1H), 3.92 (s, 3H), 3.91 – 3.81 (m, 1H), 2.13 – 1.99 (m, 1H), 1.58 – 1.35 (m, 2H), 0.97 (d, *J* = 4.4 Hz, 3H), 0.95 (d, *J* = 4.6 Hz, 3H). ¹³C{¹H} NMR (76 MHz, CDCl₃) δ 159.6, 135.4, 130.4, 121.3, 119.9, 111.4, 80.0, 55.9, 42.5, 41.2, 25.4, 23.4, 21.3.

FT-IR $\bar{\nu}_{\max}$ (cm⁻¹) = 2958, 2970, 2888, 1552, 1476, 1245.

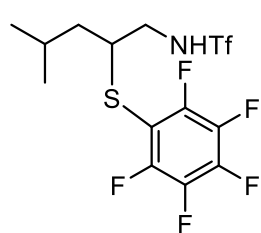
HRMS (FI): Calcd. for C₁₃H₁₉NO₃S: [M]⁺ 269.1080, found 269.1081.

General Procedure B for reduction of the amines:

In a 250 mL round-bottom flask with a stir bar was added (Aryl)sulfane **S3** (10 mmol, 1.0 equiv.) and anhydrous tin (II) chloride (19.0 g, 100 mmol, 10.0 equiv.) in EtOH (125 mL) containing 100 mmol HCl, prepared from 100 mmol of acetic chloride at 0°C in glove box. The mixture was heated to reflux for 4 h. After that, the resulting mixture was cooled to 0°C, quenched with sat. NH₄Cl and basified with NH₃·H₂O. DCM was added and vigorously stirred for 10 min. The white suspension was filtrated under suction. The aqueous phase was extracted with DCM and the combined organic phase was dried over Na₂SO₄. After suction and concentration, the residue was dissolved in DCM (68 mL) and cooled to -78°C. Et₃N (688 mg, 6.8 mmol, 1.0 equiv.) and Tf₂O (1.9 g, 6.8 mmol, 1.0 equiv.) were added. After stirring at -78°C for 30 min., the mixture was quenched with H₂O. The resulting mixture was extracted with DCM and the combined organic phase was dried over Na₂SO₄, concentrated under reduced pressure. The crude product was purified by silica gel chromatography to afford **162**.¹²⁷

1,1,1-Trifluoro-N-(4-methyl-2-((perfluorophenyl)thio)pentyl)methanesulfonamide (162a)

Based on general procedure **B**, starting from 2.21 g of sulfane, product **162a** has been obtained as a yellow solid (0.57 g, 1.3 mmol, 20% yield).



Rf = 0.4 (PE: EA = 10:1)

M.p.: 51 – 52°C

$^1\text{H NMR}$ (300 MHz, CDCl_3) δ 5.57 (t, $J = 5.7$ Hz, 1H), 3.42 – 3.17 (m, 3H), 2.03 – 1.90 (m, 1H), 1.59 – 1.35 (m, 2H), 0.98 (d, $J = 6.6$ Hz, 6H). $^{13}\text{C}\{^1\text{H}\}$ NMR (75 MHz, CDCl_3) δ 148.4 (dm, C–F, $^1J_{\text{C-F}} = 245.5$ Hz), 142.5 (dm, C–

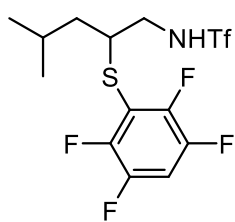
F, $^1J_{\text{C-F}} = 258.3$ Hz), 138.1 (dm, C–F, $^1J_{\text{C-F}} = 257.2$ Hz), 119.7 (q, C–F, $^1J_{\text{C-F}} = 321.0$ Hz), 106.1 – 105.5 (m), 48.8, 47.6, 41.0, 25.5, 22.6, 22.0. $^{19}\text{F NMR}$ (282 MHz, CDCl_3) δ -77.30 (s, 3F), -130.98 – -131.19 (m, 2F), -149.24 – -149.49 (m, 1F), -159.30 – -159.58 (m, 2F).

FT-IR $\bar{\nu}_{\text{max}}$ (cm^{-1}) = 3315, 2963, 2875, 1638, 1514, 1488, 1425, 1376, 1233.

HRMS (FI): Calcd. for $\text{C}_{13}\text{H}_{13}\text{F}_8\text{NO}_2\text{S}_2$: $[\text{M}]^{+}$ 431.0255, found 431.0260.

1,1,1-Trifluoro-N-(4-methyl-2-((2,3,5,6-tetrafluorophenyl)thio)pentyl)methanesulfonamide (162b)

Based on general procedure **B**, starting from 2.15 g of sulfane, product **162b** has been obtained as a yellow solid (1.14 g, 2.8 mmol, 40% yield).



Rf = 0.4 (PE: EA = 10:1)

M.p. = 88–90°C

$^1\text{H NMR}$ (300 MHz, CDCl_3) δ 7.17 (tt, $J = 9.5, 7.4$ Hz, 1H), 5.57 (t, $J = 5.9$ Hz, 1H), 3.40 – 3.16 (m, 3H), 2.01 – 1.88 (m, 1H), 1.59 – 1.35 (m, 2H), 0.96 (d, $J = 6.6$ Hz, 6H). $^{13}\text{C}\{^1\text{H}\}$ NMR (76 MHz, CDCl_3) δ 147.8 (dm, C–F, $^1J_{\text{C-F}} = 245.2$

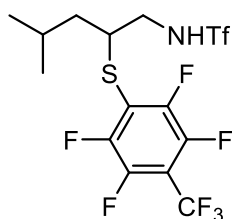
Hz), 146.3 (dm, C–F, $^1J_{\text{C-F}} = 250.4$ Hz), 119.7 (q, C–F, $^1J_{\text{C-F}} = 321.0$ Hz), 111.8 (t, C–F, $^2J_{\text{C-F}} = 20.6$ Hz), 108.1 (t, C–F, $^2J_{\text{C-F}} = 22.7$ Hz), 48.5, 47.6, 41.0, 25.5, 22.6, 21.9. $^{19}\text{F NMR}$ (282 MHz, CDCl_3) δ -77.3 (s, 3F), -132.2 – -132.3 (m, 2F), -136.6 – -136.8 (m, 2F).

FT-IR $\bar{\nu}_{\text{max}}$ (cm^{-1}) = 3309, 2962, 2874, 1631, 1491, 1470, 1431, 1375, 1233.

HRMS (FI): Calcd. for $\text{C}_{13}\text{H}_{14}\text{F}_7\text{NO}_2\text{S}_2$: $[\text{M}]^{+}$ 413.0349, found 413.0356.

1,1,1-Trifluoro-N-(4-methyl-2-((2,3,5,6-tetrafluoro-4-(trifluoromethyl)phenyl)thio)pentyl)methane sulfonamide (162c)

Based on general procedure **B**, starting from 1.35 g of sulfane, product **162c** has been obtained as a yellow solid (0.97 g, 2.0 mmol, 56% yield).



Rf = 0.4 (PE: EA = 10:1)

M.p. = 64–65°C

$^1\text{H NMR}$ (300 MHz, CDCl_3) δ 5.52 (t, $J = 6.1$ Hz, 1H), 3.53 – 3.23 (m, 3H), 2.01 – 1.87 (m, 1H), 1.59 – 1.44 (m, 2H), 0.98 (d, $J = 1.6$ Hz, 3H), 0.96 (d, $J = 1.5$ Hz, 3H). $^{13}\text{C}\{^1\text{H}\}$ NMR (76 MHz, CDCl_3) δ 146.9 (dm, C–F, $^1J_{\text{C-F}} = 247.6$ Hz), 143.3 (dm, C–F, $^1J_{\text{C-F}} = 266.0$ Hz), 119.7 (q, C–F, $^1J_{\text{C-F}} = 276.6$ Hz), 118.7 (q, C–F, $^1J_{\text{C-F}} = 320.9$ Hz), 116.4 (t, C–F, $^2J_{\text{C-F}} = 20.2$ Hz), 110.4 – 109.1 (m), 47.4, 47.1, 40.2, 24.6, 21.6, 20.8. $^{19}\text{F NMR}$ (282 MHz, CDCl_3) δ

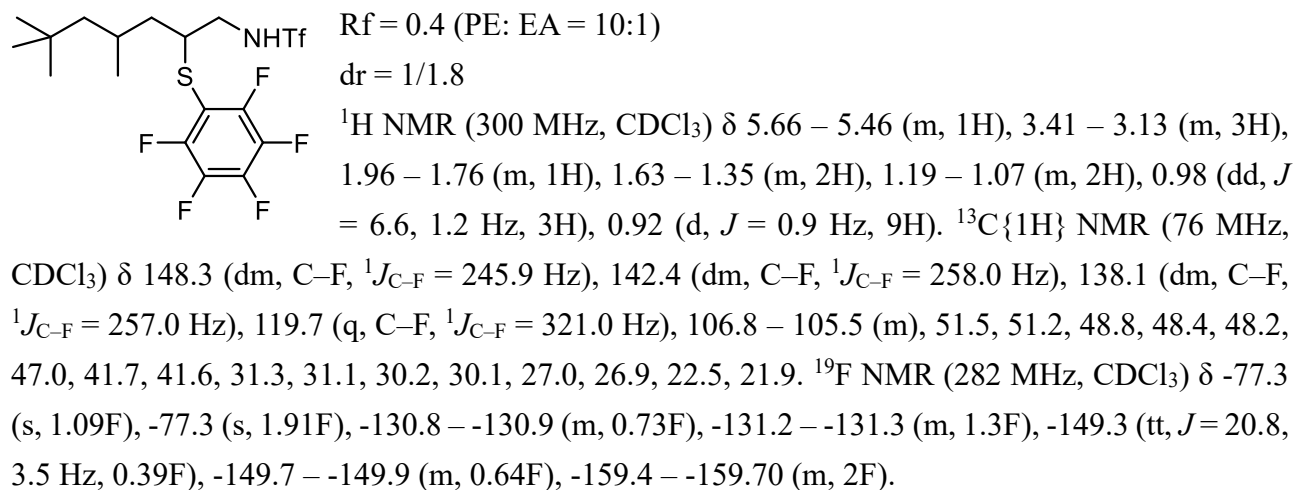
-56.54 (t, $J = 21.7$ Hz, 3F), -77.34 (s, 3F), -130.30 – -130.45 (m, 2F), -138.68 – -139.06 (m, 2F).

FT-IR $\bar{\nu}_{\max}$ (cm^{-1}) = 3313, 2964, 2877, 1644, 1592, 1478, 1426, 1376, 1328.

HRMS (FI): Calcd. for $\text{C}_{14}\text{H}_{13}\text{F}_{10}\text{NO}_2\text{S}_2$: $[\text{M}]^{+\bullet}$ 481.0223, found 481.0240.

1,1,1-Trifluoro-N-(4,6,6-trimethyl-2-((perfluorophenyl)thio)heptyl)methanesulfonamide (162d)

Based on general procedure **B**, starting from 2.48 g of sulfane, product **162d** has been obtained as a yellow oil (1.63 g, 3.3 mmol, 52% yield).

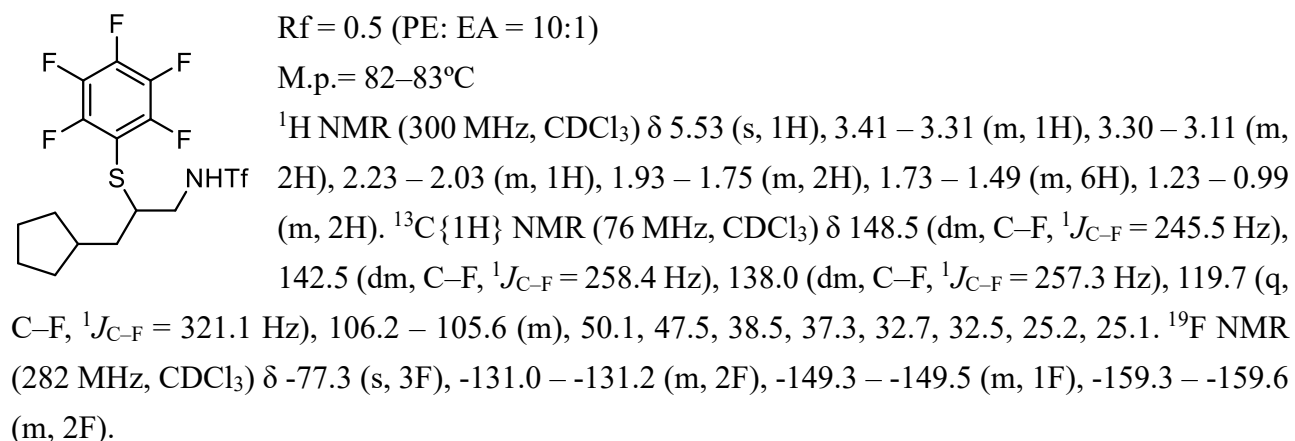


FT-IR $\bar{\nu}_{\max}$ (cm^{-1}) = 3313, 2958, 2871, 1638, 1514, 1488, 1426, 1377, 1233.

HRMS (FI): Calcd. for $\text{C}_{17}\text{H}_{21}\text{F}_8\text{NO}_2\text{S}_2$: $[\text{M}]^{+\bullet}$ 487.0881, found 487.0883.

N-(3-Cyclopentyl-2-((perfluorophenyl)thio)propyl)-1,1,1-trifluoromethanesulfonamide (162e)

Based on general procedure **B**, starting from 1.49 g of sulfane, product **162e** has been obtained as a yellow solid (0.65 g, 1.4 mmol, 34% yield).

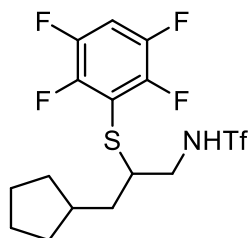


FT-IR $\bar{\nu}_{\max}$ (cm^{-1}) = 3316, 2953, 2871, 1638, 1486, 1426, 1377, 1233, 1198.

HRMS (ESI): calcd for $\text{C}_{15}\text{H}_{16}\text{F}_8\text{NO}_2\text{S}_2$ $[\text{M}+\text{H}]^{+}$: 458.0489, found 458.0486.

N-(3-Cyclopentyl-2-((2,3,5,6-tetrafluorophenyl)thio)propyl)-1,1,1-trifluoromethanesulfonamide (162f)

Based on general procedure **B**, starting from 1.44 g of sulfane, product **162f** has been obtained as a yellow solid (0.64 g, 1.5 mmol, 34% yield).



R_f = 0.4 (PE: EA = 10:1)

M.p. = 92–93°C

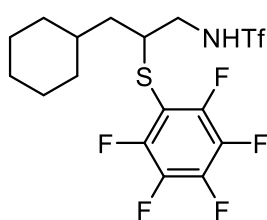
¹H NMR (300 MHz, CDCl₃) δ 7.16 (tt, *J* = 9.5, 7.4 Hz, 1H), 5.56 (s, 1H), 3.44 – 3.15 (m, 3H), 2.13 (hept, *J* = 7.9 Hz, 1H), 1.94 – 1.76 (m, 2H), 1.74 – 1.49 (m, 6H), 1.18 – 1.05 (m, 2H). ¹³C {1H} NMR (76 MHz, CDCl₃) δ 147.8 (dm, C–F, ¹*J*_{C–F} = 245.5 Hz), 146.2 (dm, C–F, ¹*J*_{C–F} = 250.5 Hz), 119.7 (q, C–F, ¹*J*_{C–F} = 321.0 Hz), 111.9 (t, C–F, ²*J*_{C–F} = 20.6 Hz), 108.0 (t, C–F, ²*J*_{C–F} = 22.7 Hz), 49.8, 47.6, 38.5, 37.3, 32.7, 32.5, 25.2, 25.1. ¹⁹F NMR (282 MHz, CDCl₃) δ -77.3 (s, 3F), -132.1 – -132.3 (m, 2F), -136.6 – -136.8 (m, 2F).

FT-IR $\bar{\nu}_{\max}$ (cm⁻¹) = 3316, 2952, 2870, 1631, 1491, 1428, 1377, 1233, 1196.

HRMS (ESI): calcd for C₁₅H₁₇F₇NO₂S₂ [M+H]⁺: 440.0583, found 440.0589.

N-(3-Cyclohexyl-2-((perfluorophenyl)thio)propyl)-1,1,1-trifluoromethanesulfonamide (162g)

Based on general procedure **B**, starting from 0.57 g of sulfane, product **162g** has been obtained as a yellow solid (0.23 g, 0.49 mmol, 32% yield).



R_f = 0.5 (PE: EA = 10:1)

M.p.: 83–84°C

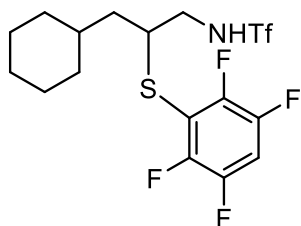
¹H NMR (300 MHz, CDCl₃) δ 5.49 (t, *J* = 5.7 Hz, 1H), 3.46 – 3.06 (m, 3H), 1.79 – 1.57 (m, 6H), 1.48 – 1.42 (m, 2H), 1.34 – 1.08 (m, 3H), 1.03 – 0.81 (m, 2H). ¹³C {1H} NMR (75 MHz, CDCl₃) δ 148.4 (dm, C–F, ¹*J*_{C–F} = 239.0 Hz), 142.7 (dm, C–F, ¹*J*_{C–F} = 231.8 Hz), 138.0 (dm, C–F, ¹*J*_{C–F} = 257.5 Hz), 119.7 (q, C–F, ¹*J*_{C–F} = 321.1 Hz), 106.0 – 105.8 (m), 48.2, 47.6, 39.7, 34.8, 33.5, 32.9, 26.5, 26.2, 26.1. ¹⁹F NMR (282 MHz, CDCl₃) δ -77.2 (s, 3F), -130.9 – -131.1 (m, 2F), -149.1 – -149.4 (m, 1F), -159.2 – -159.5 (m, 2F).

FT-IR $\bar{\nu}_{\max}$ (cm⁻¹) = 3314, 2928, 2854, 1638, 1514, 1487, 1450, 1425, 1377.

HRMS (FI): Calcd. for C₁₆H₁₇F₈NO₂S₂: [M]⁺ 471.0568, found 471.0578.

N-(3-Cyclohexyl-2-((2,3,5,6-tetrafluorophenyl)thio)propyl)-1,1,1-trifluoromethanesulfonamide (162h)

Based on general procedure **B**, starting from 1.89 g of sulfane, product **162h** has been obtained as a yellow solid (0.66 g, 1.5 mmol, 27% yield).



R_f = 0.4 (PE: EA = 10:1)

M.p. = 98–99°C

¹H NMR (300 MHz, CDCl₃) δ 7.16 (tt, *J* = 9.5, 7.4 Hz, 1H), 5.58 (s, 1H), 3.43 – 3.14 (m, 3H), 1.83 – 1.56 (m, 6H), 1.52 – 1.41 (m, 2H), 1.36 – 1.09 (m, 3H), 1.02 – 0.81 (m, 2H). ¹³C {1H} NMR (76 MHz, CDCl₃) δ 147.8 (dm, C–F, ¹*J*_{C–F} = 245.2 Hz), 146.2 (dm, C–F, ¹*J*_{C–F} = 250.5 Hz), 119.7 (q, C–F, ¹*J*_{C–F} = 321.0 Hz),

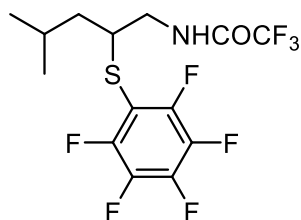
112.0 (t, C–F, $^2J_{C-F} = 20.6$ Hz), 108.0 (t, C–F, $^2J_{C-F} = 22.7$ Hz), 47.8 (d, C–F, $^4J_{C-F} = 5.3$ Hz), 39.7, 34.8, 33.5, 32.8, 26.5, 26.2 (d, C–F, $^4J_{C-F} = 5.8$ Hz). ^{19}F NMR (282 MHz, CDCl_3) δ -77.3 (s, 3F), -132.1 – -132.3 (m, 2F), -136.6 – -136.9 (m, 2F).

FT-IR $\bar{\nu}_{\text{max}}$ (cm^{-1}) = 3316, 2927, 2854, 1631, 1491, 1428, 1377, 1233, 1196.

HRMS (FI): Calcd. for $\text{C}_{16}\text{H}_{18}\text{F}_7\text{NO}_2\text{S}_2$: $[\text{M}]^+$ 453.0662, found 453.0668.

2,2,2-Trifluoro-N-(4-methyl-2-((perfluorophenyl)thio)pentyl)acetamide (162i)

In a 250 mL round-bottom flask with a stir bar was added (4-methyl-1-nitropentan-2-yl)(perfluorophenyl)sulfane (1.36 g, 4.13 mmol, 1 equiv.) and anhydrous tin (II) chloride (7.85 g, 41.3 mmol, 10 equiv.) in EtOH (52 mL) containing 41.3 mmol HCl, prepared from 41.3 mmol of acetic chloride at 0°C in glove box. The mixture was heated to reflux for 4h. After that, the resulting mixture was cooled to 0°C , quenched with sat. NH_4Cl and basified with $\text{NH}_3\cdot\text{H}_2\text{O}$. DCM was added and vigorously stirred for 10 minutes. The white suspension was filtrated under suction. The aqueous phase was extracted with DCM and the combined organic phase was dried over Na_2SO_4 . After suction and concentration, the residue was dissolved in DCM (14 mL) and cooled to 0°C . Et_3N (0.69 g, 6.8 mmol, 2.0 equiv.) and TFAA (0.71 mg, 3.4 mmol, 1.0 equiv.) were added. After stirring at room temperature overnight, quenched with sat. NH_4Cl . The resulting mixture was extracted with DCM and the combined organic phase was dried over Na_2SO_4 , concentrated under reduced pressure. The crude product was purified by silica gel chromatography to afford **162i** as a yellow solid (0.83 g, 2.1 mmol, 51%).



Rf = 0.3 (PE: EA = 10:1)

M.p. = 60–61 $^\circ\text{C}$

^1H NMR (300 MHz, CDCl_3) δ 6.94 (s, 1H), 3.53 – 3.40 (m, 1H), 3.39 – 3.19 (m, 2H), 2.02 – 1.88 (m, 1H), 1.52 – 1.32 (m, 2H), 0.95 (d, $J = 5.0$ Hz, 3H), 0.93 (d, $J = 4.9$ Hz, 3H). $^{13}\text{C}\{^1\text{H}\}$ NMR (76 MHz, CDCl_3) δ 157.5 (q,

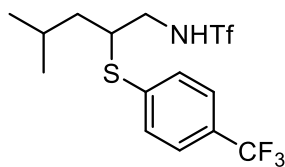
C–F, $^2J_{C-F} = 37.3$ Hz), 148.3 (dm, C–F, $^1J_{C-F} = 245.2$ Hz), 142.4 (dm, C–F, $^1J_{C-F} = 258.0$ Hz), 138.0 (dm, C–F, $^1J_{C-F} = 257.0$ Hz), 115.9 (q, C–F, $^1J_{C-F} = 287.7$ Hz), 106.8 – 106.2 (m), 48.0, 43.5, 41.7, 25.6, 22.7, 22.0. ^{19}F NMR (282 MHz, CDCl_3) δ -76.17 (s, 3F), -131.24 – -131.36 (m, 2F), -149.95 (tt, $J = 20.8, 3.4$ Hz, 1F), -159.60 – -159.81 (m, 2F).

FT-IR $\bar{\nu}_{\text{max}}$ (cm^{-1}) = 3311, 2962, 2875, 1711, 1638, 1552, 1513, 1487, 1211.

HRMS (FI): Calcd. for $\text{C}_{14}\text{H}_{13}\text{F}_8\text{NOS}$: $[\text{M}]^+$ 395.0585, found 395.0574.

1,1,1-Trifluoro-N-(4-methyl-2-((4-(trifluoromethyl)phenyl)thio)pentyl)methanesulfonamide (162j)

Based on general procedure **B**, starting from 0.78 g of sulfane, product **162j** has been obtained as a yellow solid (0.35 g, 0.86 mmol, 34% yield).



Rf = 0.4 (PE: EA = 10:1)

^1H NMR (300 MHz, CDCl_3) δ 7.61 – 7.57 (m, 2H), 7.51 – 7.47 (m, 2H), 5.42 (s, 1H), 3.45 – 3.28 (m, 3H), 1.99 – 1.86 (m, 1H), 1.52 – 1.47 (m, 2H), 0.96 (t, $J = 6.5$ Hz, 6H). $^{13}\text{C}\{^1\text{H}\}$ NMR (76 MHz, CDCl_3) δ 138.0, 131.7,

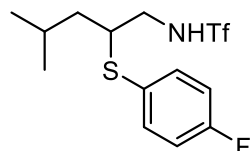
129.9 (q, C-F, $^2J_{C-F} = 32.9$ Hz), 126.3 (q, C-F, $^3J_{C-F} = 3.7$ Hz), 124.0 (q, C-F, $^1J_{C-F} = 274.4$ Hz), 119.7 (q, C-F, $^1J_{C-F} = 321.1$ Hz), 47.19, 47.15, 40.9, 25.5, 22.7, 22.1. ^{19}F NMR (282 MHz, CDCl_3) δ -62.8 (s, 3F), -77.2 (s, 3F).

FT-IR $\bar{\nu}_{\text{max}}$ (cm^{-1}) = 3309, 2961, 2874, 1608, 1424, 1374, 1327, 1233, 1197.

HRMS (FI): Calcd. for $\text{C}_{14}\text{H}_{17}\text{F}_6\text{NO}_2\text{S}_2$: $[\text{M}]^{+}$ 409.0599, found 409.0600.

1,1,1-Trifluoro-N-(2-((4-fluorophenyl)thio)-4-methylpentyl)methanesulfonamide (162k)

Based on general procedure **B**, starting from 2.06 g of sulfane, product **162k** has been obtained as a yellow oil (0.80 g, 2.2 mmol, 28% yield).



Rf = 0.4 (PE: EA = 10:1)

^1H NMR (400 MHz, CDCl_3) δ 7.52 – 7.33 (m, 2H), 7.13 – 6.99 (m, 2H), 5.49 (t, $J = 5.8$ Hz, 1H), 3.39 – 3.29 (m, 1H), 3.25 – 3.06 (m, 2H), 2.00 – 1.86 (m, 1H), 1.51 – 1.30 (m, 2H), 0.94 (d, $J = 2.1$ Hz, 3H), 0.93 (d, $J = 1.9$ Hz, 3H).

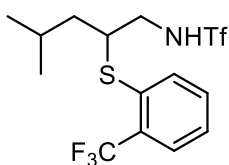
^{13}C {1H} NMR (101 MHz, CDCl_3) δ 163.2 (d, C-F, $^1J_{C-F} = 249.6$ Hz), 136.3 (d, C-F, $^3J_{C-F} J = 8.4$ Hz), 126.6, 119.8 (q, C-F, $^1J_{C-F} = 321.3$ Hz), 116.8 (d, C-F, $^2J_{C-F} = 22.0$ Hz), 48.4, 46.7, 40.8, 25.4, 22.7, 22.1. ^{19}F NMR (377 MHz, CDCl_3) δ -77.2 (s, 3F), -111.9 – -112.0 (m, 1F).

FT-IR $\bar{\nu}_{\text{max}}$ (cm^{-1}) = 3310, 2960, 2873, 1591, 1491, 1421, 1374, 1232, 1195, 1146.

HRMS (FI): Calcd. for $\text{C}_{13}\text{H}_{17}\text{F}_4\text{NO}_2\text{S}_2$: $[\text{M}]^{+}$ 359.0631, found 359.0638.

1,1,1-Trifluoro-N-(4-methyl-2-((2-(trifluoromethyl)phenyl)thio)pentyl)methanesulfonamide (162l)

Based on general procedure **B**, starting from 1.47 g of sulfane, product **162l** has been obtained as a yellow oil (0.73 g, 1.8 mmol, 37% yield).



Rf = 0.4 (PE: EA = 10:1)

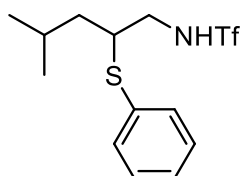
^1H NMR (300 MHz, CDCl_3) δ 7.77 – 7.67 (m, 1H), 7.65 – 7.49 (m, 2H), 7.44 – 7.38 (m, 1H), 5.34 (t, $J = 6.0$ Hz, 1H), 3.51 – 3.24 (m, 3H), 1.99 – 1.86 (m, 1H), 1.63 – 1.50 (m, 2H), 0.99 (d, $J = 5.0$ Hz, 3H), 0.97 (d, $J = 5.1$ Hz, 3H). ^{13}C {1H} NMR (75 MHz, CDCl_3) δ 134.7, 132.9, 132.5, 131.8 (t, C-F, $^2J_{C-F} = 29.7$ Hz), 127.9, 127.3 (q, C-F, $^3J_{C-F} = 5.6$ Hz), 123.6 (q, C-F, $^1J_{C-F} = 273.4$ Hz), 119.6 (q, C-F, $^1J_{C-F} = 321.1$ Hz), 48.8, 47.0, 40.5, 25.3, 22.5, 22.1. ^{19}F NMR (282 MHz, CDCl_3) δ -60.0 (s, 3F), -77.3 (s, 3F).

FT-IR $\bar{\nu}_{\text{max}}$ (cm^{-1}) = 3316, 2938, 1594, 1424, 1374, 1233.

HRMS (FI): Calcd. for $\text{C}_{14}\text{H}_{17}\text{F}_6\text{NO}_2\text{S}_2$: $[\text{M}]^{+}$ 409.0599, found 409.0595.

1,1,1-Trifluoro-N-(4-methyl-2-(phenylthio)pentyl)methanesulfonamide (162m)

Based on general procedure **B**, starting from 3.60 g of sulfane, product **162m** has been obtained as a yellow solid (1.60 g, 4.7 mmol, 31% yield).



Rf = 0.4 (PE: EA = 10:1)

M.p. = 52–53°C

^1H NMR (300 MHz, CDCl_3) δ 7.49 – 7.39 (m, 2H), 7.39 – 7.27 (m, 3H), 5.61 (t, $J = 5.5$ Hz, 1H), 3.38 – 3.31 (m, 1H), 3.29 – 3.16 (m, 2H), 2.02 – 1.89 (m, 1H), 1.54 – 1.35 (m, 2H), 0.96 (d, $J = 2.3$ Hz, 3H), 0.94 (d, $J = 2.1$ Hz, 3H). ^{13}C {1H} NMR (76 MHz,

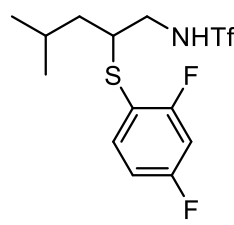
CDCl₃) δ 133.6, 131.8, 129.5, 128.5, 119.8 (q, C–F, $^1J_{C-F}$ = 321.2 Hz), 47.7, 46.9, 40.8, 25.3, 22.7, 22.0. ^{19}F NMR (282 MHz, CDCl₃) δ -77.2 (s, 3F).

FT-IR $\bar{\nu}_{\text{max}}$ (cm⁻¹) = 3205, 2960, 2915, 2872, 1585, 1469, 1448, 1374, 1287.

HRMS (FI): Calcd. for C₁₃H₁₈F₃NO₂S₂: [M]⁺ 341.0726, found 341.0735.

N-(2-((2,4-Difluorophenyl)thio)-4-methylpentyl)-1,1,1-trifluoromethanesulfonamide (162n)

Based on general procedure **B**, starting from 2.0 g of sulfane, product **162n** has been obtained as a yellow oil (0.83 g, 2.2 mmol, 30% yield).

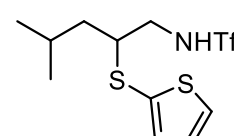
 R_f = 0.4 (PE: EA = 10:1)
 ^1H NMR (300 MHz, CDCl₃) δ 7.56 – 7.41 (m, 1H), 7.01 – 6.82 (m, 2H), 5.64 (s, 1H), 3.35 – 3.27 (m, 1H), 3.23 – 3.03 (m, 2H), 2.00 – 1.87 (m, 1H), 1.50 – 1.27 (m, 2H), 0.93 (d, J = 6.6 Hz, 6H). $^{13}\text{C}\{1\text{H}\}$ NMR (76 MHz, CDCl₃) δ 165.6 (dd, $^2J_{C-F}$ = 14.9 Hz, $^3J_{C-F}$ = 12.1 Hz), 162.3 (dd, $^2J_{C-F}$ = 12.1 Hz, $^3J_{C-F}$ = 9.4 Hz), 138.8 (dd, $^3J_{C-F}$ = 9.7, $^3J_{C-F}$ = 2.0 Hz), 119.7 (q, $^1J_{C-F}$ = 321.0 Hz), 113.5 (dd, $^2J_{C-F}$ = 19.0 Hz, $^4J_{C-F}$ = 4.0 Hz), 112.7 (dd, $^2J_{C-F}$ = 21.5 Hz, $^4J_{C-F}$ = 3.8 Hz), 105.1 (dd, C–F, $^2J_{C-F}$ = 27.9 Hz, $^2J_{C-F}$ = 25.8 Hz), 48.1, 47.0, 40.8, 25.3, 22.7, 22.0. ^{19}F NMR (282 MHz, CDCl₃) δ -77.3 (s, 3F), -101.7 (q, J = 9.1 Hz, 1F), -106.0 – -106.1 (m, 1F).

FT-IR $\bar{\nu}_{\text{max}}$ (cm⁻¹) = 3314, 2961, 2873, 1598, 1485, 1420, 1375, 1233, 1195.

HRMS (FI): Calcd. for C₁₃H₁₆F₅NO₂S₂: [M]⁺ 377.0537, found 377.0549.

1,1,1-Trifluoro-N-(4-methyl-2-(thiophen-2-ylthio)pentyl)methanesulfonamide (162o)

Based on general procedure **B**, starting from 2.45 g of sulfane, product **162o** has been obtained as a yellow oil (1.1 g, 3.2 mmol, 32% yield).

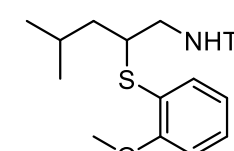
 R_f = 0.5 (PE: EA = 10:1)
 ^1H NMR (400 MHz, CDCl₃) δ 7.45 (dd, J = 5.4, 1.2 Hz, 1H), 7.16 (dd, J = 3.6, 1.2 Hz, 1H), 7.05 (dd, J = 5.4, 3.6 Hz, 1H), 5.55 (t, J = 5.8 Hz, 1H), 3.44 – 3.33 (m, 1H), 3.22 – 3.15 (m, 1H), 2.99 – 2.92 (m, 1H), 2.04 – 1.93 (m, 1H), 1.45 (ddd, J = 14.6, 9.1, 5.7 Hz, 1H), 1.34 – 1.25 (m, 1H), 0.96 (d, J = 2.7 Hz, 3H), 0.94 (d, J = 2.6 Hz, 3H). $^{13}\text{C}\{1\text{H}\}$ NMR (101 MHz, CDCl₃) δ 136.9, 131.6, 128.2, 119.8 (q, C–F, $^1J_{C-F}$ = 321.3 Hz), 49.4, 46.6, 40.3, 25.3, 22.8, 21.9. ^{19}F NMR (377 MHz, CDCl₃) δ -77.2 (s, 3F).

FT-IR $\bar{\nu}_{\text{max}}$ (cm⁻¹) = 3309, 2959, 2934, 2872, 1422, 1374, 1233, 1194, 1147.

HRMS (FI): Calcd. for C₁₁H₁₆F₃NO₂S₃: [M]⁺ 347.0290, found 347.0295.

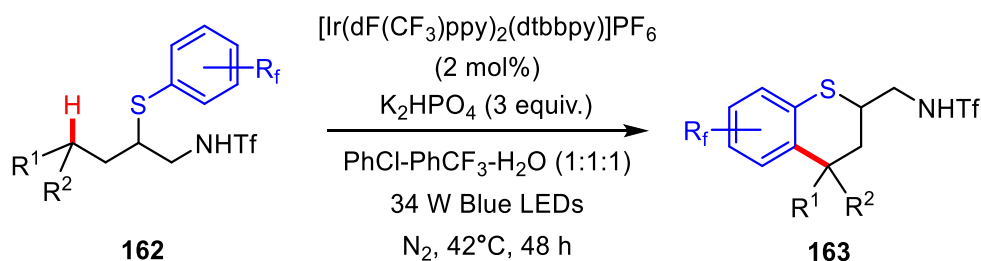
1,1,1-Trifluoro-N-(2-((2-methoxyphenyl)thio)-4-methylpentyl)methanesulfonamide (162p)

Based on general procedure **B**, starting from 3.7 g of sulfane, product **162p** has been obtained as a yellow oil (0.85 g, 2.3 mmol, 16% yield).

 R_f = 0.4 (PE: EA = 10:1)
 ^1H NMR (300 MHz, CDCl₃) δ 7.53 – 7.48 (m, 1H), 7.43 – 7.34 (m, 1H), 7.01 – 6.92 (m, 2H), 6.58 (t, J = 4.7 Hz, 1H), 3.91 (s, 3H), 3.39 – 3.22 (m, 1H), 3.16 – 2.96 (m, 2H), 2.06 – 1.93 (m, 1H), 1.50 (ddd, J = 14.3, 8.4, 6.0 Hz, 1H), 1.32 (ddd, J = 14.1, 8.2, 5.7 Hz, 1H), 0.94 (d, J = 6.6 Hz, 3H), 0.92 (d, J = 6.5 Hz, 3H). $^{13}\text{C}\{1\text{H}\}$ NMR

(76 MHz, CDCl₃) δ 160.01, 138.46, 131.36, 121.78, 119.88 (q, C–F, $^1J_{C-F}$ = 321.2 Hz) 119.05, 111.57, 55.97, 48.80, 47.37, 41.48, 25.28, 22.75, 22.03. ^{19}F NMR (282 MHz, CDCl₃) δ -77.50, (s, 3F). FT-IR $\bar{\nu}_{\text{max}}$ (cm⁻¹) = 3305, 2958, 1583, 1476, 1375, 1232, 1191, 1148. HRMS (ESI): calcd for C₁₄H₂₀F₃NO₃S₂Na [M+Na]⁺: C₁₄H₂₀F₃NO₃S₂Na: 394.0729, found 394.0718.

3.3.3 General Procedure C for photoredox reactions

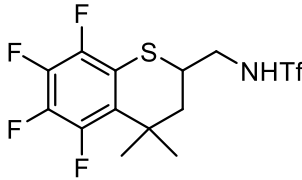


To a Schlenk tube with a screw-cap was added [Ir(dF(CF₃)ppy)₂(dtbbpy)]PF₆ (2.3 mg, 0.002 mmol, 2 mol%), sulfonamide (0.1 mmol, 1.0 equiv.) and K₂HPO₄ (52.0 mg, 0.3 mmol, 3.0 equiv.). The tube was evacuated and back-filled with nitrogen (this process was repeated three times), PhCF₃ (0.5 mL), PhCl (0.5 mL), and water (0.5 mL) (1:1:1 ratio) were added consecutively via syringe. The resulting mixture was bubbled with nitrogen to degas for 5 min and stirred at 42°C with 34 W blue LED irradiation for 48 h (the temperature without fan is about 42°C and the distance between the tube and the LED is 2-3cm). The mixture was diluted with ethyl acetate. The organic phase was washed with saturated NH₄Cl solution and brine, dried over anhydrous magnesium sulfate, filtered and concentrated under reduced pressure. The crude product was purified by silica gel chromatography to afford **163**.

3.3.4 Characterization Data

1,1,1-Trifluoro-N-((5,6,7,8-tetrafluoro-4,4-dimethylthiochroman-2-yl)methyl)methanesulfonamide (163a)

Based on general procedure C, starting from 43 mg of sulfane, product **163a** has been obtained as a yellow solid (19 mg, 46% yield).

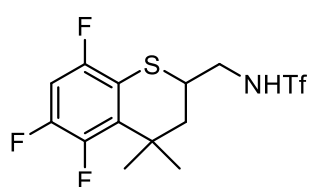


R_f = 0.25 (PE: EA = 10:1)
 M.p. = 81-83°C
 ^1H NMR (300 MHz, CDCl₃) δ 5.41 (t, J = 5.8 Hz, 1H), 3.70 – 3.30 (m, 3H), 2.03 – 1.79 (m, 2H), 1.53 (d, J = 3.3 Hz, 3H), 1.36 (s, 3H). $^{13}\text{C}\{^1\text{H}\}$ NMR (75 MHz, CDCl₃) δ 147.5 (dm, C–F, $^1J_{C-F}$ = 253.4 Hz), 142.8 (dm, C–F, $^1J_{C-F}$ = 239.2 Hz), 138.9 (dm, C–F, $^1J_{C-F}$ = 252.6 Hz), 138.4 (dm, C–F, $^1J_{C-F}$ = 254.0 Hz), 125.49 – 125.12 (m), 119.7 (q, C–F, $^1J_{C-F}$ = 321.0 Hz), 116.5 (dt, C–F, $^2J_{C-F}$ = 15.0 Hz, $^3J_{C-F}$ = 4.8 Hz), 48.2, 44.5, 36.8, 34.6, 29.4 (d, $^3J_{C-F}$ = 10.2 Hz), 28.3. ^{19}F NMR (282 MHz, CDCl₃) δ -77.0 (s, 3F), -134.4 – -134.6 (m, 1F), -137.5 (dd, J = 22.2, 9.1 Hz, 1F), -158.6 (td, J = 21.3, 4.3 Hz, 1F), -160.6 (t, J = 20.5 Hz, 1F). FT-IR $\bar{\nu}_{\text{max}}$ (cm⁻¹) = 3306, 2945, 1635, 1508, 1443, 1375, 1233, 1198, 1146.

HRMS (ESI): calcd for C₁₃H₁₃F₇NO₂S₂ [M+H]⁺: 412.0270, found 412.0277.

1,1,1-Trifluoro-N-((5,7,8-trifluoro-4,4-dimethylthiochroman-2-yl)methyl)methanesulfonamide (163b)

Based on general procedure C, starting from 41 mg of sulfane, product **163b** has been obtained as a yellow solid (16.3 mg, 42% yield).



R_f = 0.25 (PE: EA = 10:1)

M.p. = 105-106°C

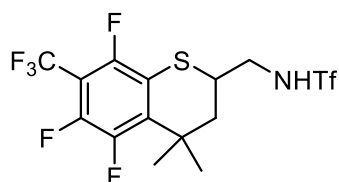
¹H NMR (300 MHz, CDCl₃) δ 6.81 (td, *J* = 9.3, 6.5 Hz, 1H), 5.63 (t, *J* = 6.2 Hz, 1H), 3.65 – 3.36 (m, 3H), 2.01 – 1.80 (m, 2H), 1.53 (d, *J* = 3.2 Hz, 3H), 1.37 (s, 3H). ¹³C {¹H} NMR (151 MHz, CDCl₃) δ 153.1 (dm, C–F, ¹*J*_{C–F} = 240.6 Hz), 148.1 (dm, C–F, ¹*J*_{C–F} = 247.7 Hz), 147.28 (dm, C–F, ¹*J*_{C–F} = 250.8 Hz), 131.7 (d, C–F, ²*J*_{C–F} = 12.1 Hz), 119.7 (q, C–F, ¹*J*_{C–F} = 320.9 Hz), 115.7 (dt, C–F, ²*J*_{C–F} = 18.1 Hz, ³*J*_{C–F} = 4.5 Hz), 103.1 (dd, C–F, ²*J*_{C–F} = 27.6 Hz, ²*J*_{C–F} = 21.9 Hz), 48.3, 44.6, 36.7, 35.0, 29.2 (d, C–F, ³*J*_{C–F} = 10.2 Hz), 28.2 (d, C–F, ⁴*J*_{C–F} = 2.1 Hz). ¹⁹F NMR (282 MHz, CDCl₃) δ -77.1 (s, 3F), -113.1 – -113.2 (m, 1F), -137.4 – -137.7 (m, 1F), -138.8 (dd, *J* = 20.2, 9.4 Hz, 1F).

FT-IR $\bar{\nu}_{\max}$ (cm⁻¹) = 3306, 2936, 1625, 1448, 1376, 1232, 1198, 1144.

HRMS (FI): Calcd. for C₁₃H₁₃F₆NO₂S₂ [M]⁺ 393.0286, Found 393.0287.

1,1,1-Trifluoro-N-((5,7,8-trifluoro-4,4-dimethyl-6-(trifluoromethyl)thiochroman-2-yl)methyl)methanesulfonamide (163c)

Based on general procedure C, starting from 48 mg of sulfane, product **163c** has been obtained as a yellow solid (18.3 mg, 40% yield).



R_f = 0.25 (PE: EA = 10:1)

M.p. = 114-116°C

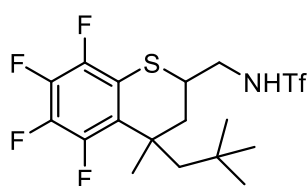
¹H NMR (300 MHz, CDCl₃) δ 5.41 (t, *J* = 6.1 Hz, 1H), 3.69 – 3.38 (m, 3H), 2.05 – 1.81 (m, 2H), 1.56 (d, *J* = 3.4 Hz, 3H), 1.40 (s, 3H). ¹³C {¹H} NMR (151 MHz, CDCl₃) δ 150.1 (dm, C–F, ¹*J*_{C–F} = 250.8 Hz), 147.5 (dm, C–F, ¹*J*_{C–F} = 250.2 Hz), 145.4 (dm, C–F, ¹*J*_{C–F} = 264.5 Hz), 135.4 (d, C–F, ²*J*_{C–F} = 12.0 Hz), 121.1 (q, C–F, ¹*J*_{C–F} = 273.8 Hz), 119.7 (C–F, ¹*J*_{C–F}, *J* = 320.9 Hz), 118.16 (d, C–F, ²*J*_{C–F} = 19.1 Hz), 107.63 – 106.92 (m), 48.14, 44.08, 36.85 (d, C–F, ⁴*J*_{C–F} = 2.3 Hz), 35.33, 28.99 (d, C–F, ³*J*_{C–F} = 10.2 Hz), 27.97. ¹⁹F NMR (282 MHz, CDCl₃) δ -56.6 (t, *J* = 21.7 Hz, 3F), -77.1 (s, 3F), -113.5 – -113.8 (m, 1F), -134.9 – -135.0 (m, 1F), -140.8 – -141.1 (m, 1F).

FT-IR $\bar{\nu}_{\max}$ (cm⁻¹) = 3306, 2932, 1636, 1447, 1434, 1376, 1341, 1308, 1233.

HRMS (FI): Calcd. for C₁₄H₁₂F₉NO₂S₂: [M]⁺ 461.0160, Found 461.0157.

1,1,1-Trifluoro-N-((5,6,7,8-tetrafluoro-4-methyl-4-neopentylthiochroman-2-yl)methyl)methanesulfonamide (163d)

Based on general procedure C, starting from 49 mg of sulfane, product **163d** has been obtained as a yellow solid (19 mg, 41% yield).



R_f = 0.25 (PE: EA = 10:1)

dr = 1/4.4

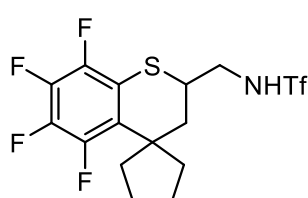
¹H NMR (300 MHz, CDCl₃) δ 5.62 (t, *J* = 6.0 Hz, 1H), 3.70 – 3.23 (m, 3H), 2.58 – 2.30 (m, 2H), 1.88 – 1.81 (m, 1H), 1.64 (d, *J* = 5.2 Hz, 1H), 1.59 – 1.49 (m, 1H), 1.36 (s, 2H), 0.99 (s, 1.64H), 0.82 (s, 7.35H). ¹³C {¹H} NMR (151 MHz, CDCl₃) δ 147.8 (dm, C–F, ¹*J*_{C–F} = 248.7 Hz), 143.3 (dm, C–F, ¹*J*_{C–F} = 241.1 Hz), 138.8 (dm, C–F, ¹*J*_{C–F} = 253.8 Hz), 138.4 (dm, C–F, ¹*J*_{C–F} = 249.7 Hz), 125.2 (d, C–F, ²*J*_{C–F} = 11.5 Hz), 119.7 (q, C–F, ¹*J*_{C–F} = 320.9 Hz), 117.2 (d, C–F, ²*J*_{C–F} = 15.7 Hz), 52.2 (d, C–F, ³*J*_{C–F} = 7.8 Hz), 49.1, 48.5, 48.2, 42.8, 41.6, 39.2, 37.7, 36.8, 32.9, 32.1, 31.9, 31.8, 31.6 (d, C–F, ⁴*J*_{C–F} = 2.8 Hz). ¹⁹F NMR (282 MHz, CDCl₃) δ -77.1 (s, 3F), -132.2 – -132.3 (m, 0.82F), -133.1 – -133.3 (m, 0.19F), -136.7 (dd, *J* = 22.7, 9.1 Hz, 0.81F), -137.3 (dd, *J* = 22.5, 9.2 Hz, 0.19F), -158.6 (td, *J* = 21.4, 4.5 Hz, 0.20F), -158.8 (td, *J* = 21.6, 4.3 Hz, 0.81F), -160.5 – -160.8 (m, 1F).

FT-IR $\bar{\nu}_{\max}$ (cm⁻¹) = 3306, 2957, 1634, 1507, 1439, 1376, 1232, 1198, 1146.

HRMS (FI): Calcd. for C₁₇H₂₀F₇NO₂S₂: [M]⁺ 467.0829, Found 467.0846.

1,1,1-Trifluoro-N-((5',6',7',8'-tetrafluorospiro[cyclopentane-1,4'-thiochroman]-2'-yl)methyl)methane sulfonamide (163e)

Based on general procedure C, starting from 46 mg of sulfane, product **163e** has been obtained as a yellow solid (18.8 mg, 43% yield).



R_f = 0.25 (PE: EA = 10:1)

M.p. = 104-105°C

¹H NMR (300 MHz, CDCl₃) δ 5.47 (s, 1H), 3.66 – 3.48 (m, 2H), 3.37 – 3.28 (m, 1H), 2.42 – 2.33 (m, 1H), 2.14 (dd, *J* = 14.0, 2.0 Hz, 1H), 2.04 – 1.81 (m, 4H), 1.79 – 1.55 (m, 4H). ¹³C {¹H} NMR (75 MHz, CDCl₃) δ

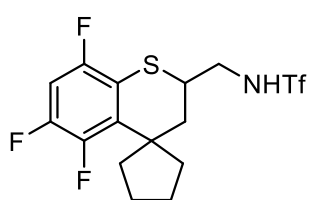
147.3 (dm, C–F, ¹*J*_{C–F} = 248.8 Hz), 142.9 (dm, C–F, ¹*J*_{C–F} = 236.8 Hz), 138.7 (dm, C–F, ¹*J*_{C–F} = 248.2 Hz), 138.3 (dm, C–F, ¹*J*_{C–F} = 249.6 Hz), 126.5 – 126.2 (m), 119.7 (q, C–F, ¹*J*_{C–F} = 321.0 Hz), 116.9 (dt, C–F, ²*J*_{C–F} = 15.4 Hz, ³*J*_{C–F} = 4.5 Hz), 48.1, 44.7 (dd, C–F, ³*J*_{C–F} = 3.2, ⁴*J*_{C–F} = 1.6 Hz), 42.4, 41.7, 41.6, 38.0 (d, C–F, ⁴*J*_{C–F} = 2.0 Hz), 26.2, 26.1. ¹⁹F NMR (282 MHz, CDCl₃) δ -77.1 (s, 3F), -134.1 – -134.3 (m, 1F), -138.5 (dd, *J* = 22.4, 8.9 Hz, 1F), -159.3 (td, *J* = 21.7, 4.3 Hz, 1F), -161.0 (t, *J* = 20.4 Hz, 1F).

FT-IR $\bar{\nu}_{\max}$ (cm⁻¹) = 3306, 2959, 2881, 1637, 1508, 1377, 1233, 1198, 1146.

HRMS (ESI): calcd for C₁₅H₁₃F₇NO₂S₂ [M-H]⁻: 436.0281, found 436.0272.

1,1,1-Trifluoro-N-((5',7',8'-trifluorospiro[cyclopentane-1,4'-thiochroman]-2'-yl)methyl)methanesulfonamide (163f)

Based on general procedure C, starting from 44 mg of sulfane, product **163f** has been obtained as a yellow solid (18 mg, 43% yield).



R_f = 0.25 (PE: EA = 10:1)

M.p. = 124-126°C

¹H NMR (300 MHz, CDCl₃) δ 6.81 (td, *J* = 9.2, 6.5 Hz, 1H), 5.37 (t, *J* = 6.1 Hz, 1H), 3.70 – 3.42 (m, 2H), 3.36 – 3.28 (m, 1H), 2.46 – 2.38 (m, 1H), 2.20 – 2.08 (m, 1H), 2.05 – 1.57 (m, 8H). ¹³C{¹H} NMR (76 MHz, CDCl₃)

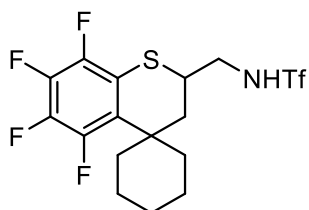
δ 153.1 (dm, C–F, ¹J_{C–F} = 240.3 Hz), 148.2 (dm, C–F, ¹J_{C–F} = 247.3 Hz), 146.9 (dm, C–F, ¹J_{C–F} = 246.6 Hz), 132.7 (dd, C–F, ²J_{C–F} = 10.7 Hz, ³J_{C–F} = 2.7 Hz), 119.7 (C–F, ¹J_{C–F} = 321.0 Hz), 116.1 (dt, C–F, ²J_{C–F} = 18.8 Hz, ³J_{C–F} = 3.7 Hz), 102.9 (dd, C–F, ²J_{C–F} = 27.5 Hz, C–F, ²J_{C–F} = 21.9 Hz), 48.2, 45.2 (d, C–F, ⁴J_{C–F} = 2.5 Hz), 42.5, 41.7, 41.6 (d, C–F, ⁴J_{C–F} = 2.0 Hz), 37.8 (d, C–F, ⁴J_{C–F} = 2.0 Hz), 26.3, 26.2. ¹⁹F NMR (282 MHz, CDCl₃) δ -77.1 (s, 3F), -113.8 – -114.0 (m, 1F), -137.2 (t, *J* = 14.1 Hz, 1F), -139.0 (dd, *J* = 19.9, 9.6 Hz, 1F).

FT-IR $\bar{\nu}_{\max}$ (cm⁻¹) = 3307, 2958, 2880, 1626, 1453, 1377, 1233, 1198, 1144.

HRMS (ESI): calcd for C₁₅H₁₆F₆NO₂S₂ [M+H]⁺: 420.0521, found 420.0523.

1,1,1-Trifluoro-N-((5',6',7',8'-tetrafluorospiro[cyclohexane-1,4'-thiochroman]-2'-yl)methyl)methane sulfonamide (163g)

Based on general procedure C, starting from 43 mg of sulfane, product **163g** has been obtained as a yellow solid (20 mg, 45% yield).



R_f = 0.25 (PE: EA = 10:1)

M.p. = 118-120°C

¹H NMR (300 MHz, CDCl₃) δ 5.31 (t, *J* = 5.7 Hz, 1H), 3.67 – 3.51 (m, 2H), 3.33 – 3.25 (m, 1H), 2.94 – 2.75 (m, 1H), 2.54 (td, *J* = 13.0, 4.5 Hz, 1H), 2.04 – 1.88 (m, 1H), 1.82 – 1.59 (m, 5H), 1.54 – 1.31 (m, 4H). ¹³C{¹H} NMR (76 MHz, CDCl₃)

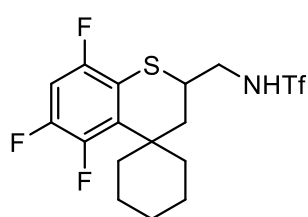
δ 147.8 (dm, C–F, ¹J_{C–F} = 247.6 Hz), 143.0 (dm, C–F, ¹J_{C–F} = 242.1 Hz), 138.8 (dm, C–F, ¹J_{C–F} = 253.5 Hz), 138.4 (dm, C–F, ¹J_{C–F} = 249.7 Hz), 126.8 – 126.3 (m), 119.7 (q, C–F, ¹J_{C–F} = 321.0 Hz), 117.3 (dt, C–F, ²J_{C–F} = 14.9 Hz, ³J_{C–F} = 4.5 Hz), 48.3, 38.5 (d, ⁴J_{C–F} = 4.9 Hz), 36.4 (d, ⁴J_{C–F} = 2.1 Hz), 36.1, 35.7 (d, ³J_{C–F} = 11.1 Hz), 32.8 (d, ⁴J_{C–F} = 3.8 Hz), 25.2, 21.9, 20.9. ¹⁹F NMR (282 MHz, CDCl₃) δ -77.01 (s, 3F), -133.2 – -133.3 (m, 1F), -137.1 (dd, *J* = 22.6, 8.8 Hz, 1F), -158.5 (td, *J* = 21.7, 4.7 Hz, 1F), -160.3 (t, *J* = 20.4 Hz, 1F).

FT-IR $\bar{\nu}_{\max}$ (cm⁻¹) = 3305, 2931, 2869, 1635, 1506, 1439, 1377, 1232, 1197.

HRMS (ESI): calcd for C₁₆H₁₇F₇NO₂S₂ [M+H]⁺: 452.0583, Found 452.0609.

1,1,1-Trifluoro-N-((5',7',8'-trifluorospiro[cyclohexane-1,4'-thiochroman]-2'-yl)methyl)methanesulfonamide (163h)

Based on general procedure C, starting from 45 mg of sulfane, product **163h** has been obtained as a yellow solid (17.7 mg, 41% yield).



R_f = 0.25 (PE: EA = 10:1)

M.p. = 93-94°C

¹H NMR (300 MHz, CDCl₃) δ 6.82 (td, *J* = 9.2, 6.5 Hz, 1H), 5.54 (s, 1H), 3.64 – 3.51 (m, 2H), 3.32 – 3.24 (m, 1H), 2.84 (dd, *J* = 14.2, 2.1 Hz, 1H), 2.58 (td, *J* = 13.1, 4.5 Hz, 1H), 2.06 – 1.95 (m, 1H), 1.92 – 1.21 (m, 10H).

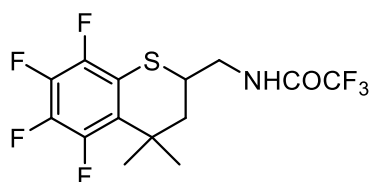
¹³C {¹H} NMR (75 MHz, CDCl₃) δ 153.2 (dm, C–F, ¹*J*_{C–F} = 240.3 Hz), 148.4 (dm, C–F, ¹*J*_{C–F} = 247.7 Hz), 147.5 (dm, C–F, ¹*J*_{C–F} = 247.7 Hz), 132.8 (dd, C–F, ²*J*_{C–F} = 9.2 Hz, ³*J*_{C–F} = 2.2 Hz), 119.7 (q, dm, C–F, ¹*J*_{C–F} = 321.1 Hz), 116.4 (dt, C–F, ²*J*_{C–F} = 18.4 Hz, ³*J*_{C–F} = 3.9 Hz), 103.1 (dd, C–F, ²*J*_{C–F} = 27.7 Hz, ²*J*_{C–F} = 22.0 Hz), 48.4, 38.9 (dt, C–F, ³*J*_{C–F} = 4.3 Hz, ⁴*J*_{C–F} = 1.9 Hz), 36.24, 36.17 (d, C–F, ⁴*J*_{C–F} = 2.2 Hz), 35.6 (d, C–F, ³*J*_{C–F} = 11.3 Hz), 32.6 (d, C–F, ⁴*J*_{C–F} = 3.8 Hz), 25.2, 21.9, 20.9. ¹⁹F NMR (282 MHz, CDCl₃) δ -77.1 (s, 3F), -112.7 (t, *J* = 10.4 Hz, 1F), -136.3 – -136.5 (m, 1F), -138.5 (dd, *J* = 19.4, 9.3 Hz, 1F).

FT-IR $\bar{\nu}_{\max}$ (cm⁻¹) = 3307, 2931, 2870, 1623, 1586, 1450, 1376, 1197, 1143.

HRMS (ESI): calcd for C₁₆H₁₈F₆NO₂S₂ [M+H]⁺: 434.0678, found 434.0683.

2,2,2-Trifluoro-N-((5,6,7,8-tetrafluoro-4,4-dimethylthiochroman-2-yl)methyl)acetamide (163i)

Based on general procedure C, starting from 43 mg of sulfane, product **163i** has been obtained as a yellow solid (11.2 mg, 30% yield).



R_f = 0.2 (PE: EA = 10:1)

¹H NMR (300 MHz, CDCl₃) δ 6.77 (s, 1H), 3.78 – 3.69 (m, 1H), 3.66 – 3.57 (m, 1H), 3.54 – 3.45 (m, 1H), 1.98 – 1.90 (m, 1H), 1.81 (dd, *J* = 13.9, 11.6 Hz, 1H), 1.50 (d, *J* = 3.2 Hz, 3H), 1.35 (s, 3H). ¹³C {¹H} NMR (151 MHz, CDCl₃) δ 158.0 (q, C–F, ²*J*_{C–F} = 37.6 Hz), 147.6 (dm,

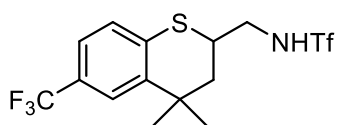
C–F, ¹*J*_{C–F} = 249.1 Hz), 142.9 (dm, C–F, ¹*J*_{C–F} = 241.6 Hz), 138.9 (dm, C–F, ¹*J*_{C–F} = 252.9 Hz), 138.32 (dm, C–F, ¹*J*_{C–F} = 249.1 Hz), 125.3 (d, C–F, ²*J*_{C–F} = 12.1 Hz), 116.9 (t, C–F, ³*J*_{C–F} = 6.0 Hz), 115.8 (q, C–F, ¹*J*_{C–F} = 287.6 Hz), 45.0, 44.1, 36.2, 34.7, 29.4 (d, C–F, ³*J*_{C–F} = 9.9 Hz), 28.4. ¹⁹F NMR (282 MHz, CDCl₃) δ -75.7 (s, 3F), -134.5 – -134.6 (m, 1F), -137.7 (dd, *J* = 22.3, 9.2 Hz, 1F), -159.0 (td, *J* = 21.6, 4.3 Hz, 1F), -161.0 (t, *J* = 20.5 Hz, 1F).

FT-IR $\bar{\nu}_{\max}$ (cm⁻¹) = 3307, 3106, 2967, 2940, 1710, 1557, 1508, 1440, 1212.

HRMS (ESI): calcd for C₁₄H₁₂F₇NO₂S₂ [M+H]⁺: 376.0601, found 376.0610.

N-((4,4-Dimethyl-6-(trifluoromethyl)thiochroman-2-yl)methyl)-1,1,1-trifluoromethanesulfonamide (163j)

Based on general procedure C, starting from 41 mg of sulfane, product **163j** has been obtained as a yellow solid (16 mg, 40% yield).



R_f = 0.25 (PE: EA = 10:1)

M.p. = 93-95°C

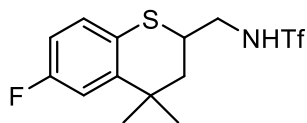
¹H NMR (300 MHz, CDCl₃) δ 7.61 (d, *J* = 2.0 Hz, 1H), 7.34 (dd, *J* = 8.3, 2.0 Hz, 1H), 7.22 (d, *J* = 8.3 Hz, 1H), 5.39 (d, *J* = 6.1 Hz, 1H), 3.83 – 3.45 (m, 3H), 2.00 (dd, *J* = 13.6, 4.1 Hz, 1H), 1.77 (d, *J* = 12.8 Hz, 1H), 1.52 (s, 3H), 1.30 (s, 3H). ¹³C{¹H} NMR (76 MHz, CDCl₃) δ 142.3, 135.6, 127.0, 126.2, 124.4 (q, C–F, ¹*J*_{C–F} = 271.9 Hz), 123.3 (q, C–F, ³*J*_{C–F} = 3.7 Hz), 122.7 (q, C–F, ³*J*_{C–F} = 4.0 Hz), 119.7 (q, C–F, ¹*J*_{C–F} = 321.0 Hz), 48.8, 40.7, 38.2, 34.7, 29.8, 28.5. ¹⁹F NMR (282 MHz, CDCl₃) δ -62.3 (s, 3F), -77.1 (s, 3F).

FT-IR $\bar{\nu}_{\max}$ (cm⁻¹) = 3308, 2950, 1609, 1432, 1374, 1333, 1197, 1122, 1081.

HRMS (FI): Calcd. for C₁₄H₁₅F₆NO₂S₂: [M]⁺ 407.0443, Found 407.0452.

1,1,1-Trifluoro-N-((6-fluoro-4,4-dimethylthiochroman-2-yl)methyl)methanesulfonamide (163k)

Based on general procedure C, starting from 36 mg of sulfane, product **163k** has been obtained as a yellow oil (11.4 mg, 32% yield).



R_f = 0.25 (PE: EA = 10:1)

¹H NMR (300 MHz, CDCl₃) δ 7.13 – 7.00 (m, 2H), 6.83 (ddd, *J* = 8.7, 7.8, 2.8 Hz, 1H), 5.36 (t, *J* = 6.1 Hz, 1H), 3.72 – 3.41 (m, 3H), 1.94 (dd, *J* =

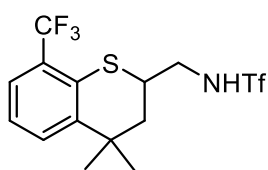
13.5, 4.2 Hz, 1H), 1.76 – 1.67 (m, 1H), 1.43 (s, 3H), 1.27 (s, 3H). ¹³C{¹H} NMR (76 MHz, CDCl₃) δ 160.9 (dm, C–F, ¹*J*_{C–F} = 243.4 Hz), 144.1 (d, C–F, ³*J*_{C–F} = 6.2 Hz), 128.0 (d, C–F, ³*J*_{C–F} = 7.7 Hz), 125.1 (d, C–F, ⁴*J*_{C–F} = 3.1 Hz), 119.7 (q, C–F, ¹*J*_{C–F} = 323.0 Hz), 114.1 (d, C–F, ²*J*_{C–F} = 22.2 Hz), 113.2 (d, C–F, ²*J*_{C–F} = 22.6 Hz), 48.9, 40.9, 38.0, 34.9 (d, C–F, ⁴*J*_{C–F} = 1.5 Hz), 30.0, 28.4. ¹⁹F NMR (282 MHz, CDCl₃) δ -77.1 (s, 3F), -117.2 – -117.3 (m, 1F).

FT-IR $\bar{\nu}_{\max}$ (cm⁻¹) = 3303, 2960, 2919, 1469, 1375, 1231.

HRMS (FI): Calcd. for C₁₃H₁₅F₄NO₂S₂: [M]⁺ 357.0475 Found 357.0476.

N-((4,4-Dimethyl-8-(trifluoromethyl)thiochroman-2-yl)methyl)-1,1,1-trifluoromethanesulfonamide (163l)

Based on general procedure C, starting from 41 mg of sulfane, product **163l** has been obtained as a yellow solid (16.1 mg, 40% yield).



R_f = 0.25 (PE: EA = 10:1)

¹H NMR (300 MHz, CDCl₃) δ 7.58 – 7.49 (m, 2H), 7.18 (td, *J* = 7.9, 0.9 Hz, 1H), 5.54 (s, 1H), 3.70 – 3.40 (m, 3H), 2.01 (dd, *J* = 13.5, 4.4 Hz, 1H), 1.77 – 1.66 (m, 1H), 1.48 (s, 3H), 1.33 (s, 3H). ¹³C{¹H} NMR (76 MHz, CDCl₃)

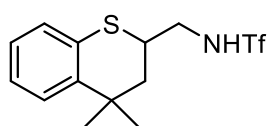
δ 144.5, 130.4, 129.3, 127.3 (q, C–F, ²*J*_{C–F} = 30.0 Hz), 125.4 (q, C–F, ³*J*_{C–F} = 6.1 Hz), 124.6, 124.1 (q, C–F, ¹*J*_{C–F} = 274.0 Hz), 119.7 (q, C–F, ¹*J*_{C–F} = 321.0 Hz), 48.9, 40.4, 38.3, 35.1, 30.8, 28.0. ¹⁹F NMR (282 MHz, CDCl₃) δ -61.6 (s, 3F), -77.1 (s, 3F).

FT-IR $\bar{\nu}_{\max}$ (cm⁻¹) = 3309, 2964, 1589, 1415, 1375, 1313, 1232, 1196, 1131.

HRMS (ESI): calcd for C₁₄H₁₄F₆NO₂S₂ [M-H]⁻: 406.0376, Found 406.0375.

N-((4,4-Dimethylthiochroman-2-yl)methyl)-1,1,1-trifluoromethanesulfonamide (163m)

Based on general procedure C, starting from 34 mg of sulfane, product **163m** has been obtained as a yellow solid (11 mg, 33% yield).



R_f = 0.25 (PE: EA = 10:1)

M.p. = 58-59°C

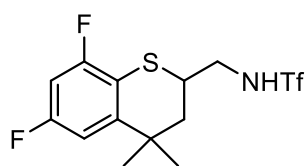
¹H NMR (300 MHz, CDCl₃) δ 7.40 – 7.35 (m, 1H), 7.17 – 7.00 (m, 3H), 5.31 (s, 1H), 3.74 – 3.42 (m, 3H), 1.93 (dd, *J* = 13.5, 4.1 Hz, 1H), 1.81 – 1.68 (m, 1H), 1.46 (s, 3H), 1.27 (s, 3H). ¹³C {¹H} NMR (76 MHz, CDCl₃) δ 141.9, 130.2, 126.8, 126.7, 126.0, 125.2, 119.7 (q, C-F, ¹*J*_{C-F} = 321.1 Hz), 49.0, 41.3, 38.0, 34.5, 30.1, 28.7. ¹⁹F NMR (282 MHz, CDCl₃) δ -77.1 (s, 3F).

FT-IR $\bar{\nu}_{\max}$ (cm⁻¹) = 3308, 2941, 1435, 1375, 1200, 1071

HRMS (FI): Calcd. for C₁₃H₁₆F₃NO₂S₂: [M]⁺ 339.0569, found 339.0571.

N-((6,8-Difluoro-4,4-dimethylthiochroman-2-yl)methyl)-1,1,1-trifluoromethanesulfonamide (163na)

Based on general procedure C, starting from 38 mg of sulfane, product **163na** has been obtained as a yellow oil (2na + 2nb = 11 mg, 30% yield). (2na and 2nb are mixtures.)



R_f = 0.25 (PE: EA = 10:1)

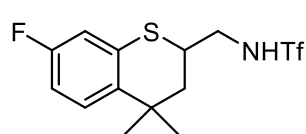
¹H NMR (300 MHz, CDCl₃) δ 6.94 (ddd, *J* = 10.2, 2.6, 1.5 Hz, 1H), 6.70 (ddd, *J* = 9.7, 8.2, 2.6 Hz, 1H), 5.38 (s, 1H), 3.63 – 3.50 (m, 3H), 1.95 (dd, *J* = 13.6, 3.7 Hz, 1H), 1.72 (dd, *J* = 13.7, 11.9 Hz, 1H), 1.44 (s, 3H), 1.27 (s, 3H). ¹³C {¹H} NMR (76 MHz, CDCl₃) δ 161.9 (d, C-F, ²*J*_{C-F} = 12.8 Hz), 161.0 (dm, C-F, ¹*J*_{C-F} = 246.3 Hz), 159.7 (d, C-F, ²*J*_{C-F} = 12.4 Hz), 158.6 (d, C-F, ²*J*_{C-F} = 12.8 Hz), 156.5 (d, C-F, ²*J*_{C-F} = 12.4 Hz), 145.3 (dd, C-F, ³*J*_{C-F} = 7.5 Hz, ³*J*_{C-F} = 2.9 Hz), 137.6 (d, C-F, ⁴*J*_{C-F} = 3.2 Hz), 132.3 (d, C-F, ³*J*_{C-F} = 8.3 Hz), 127.5 (d, C-F, ³*J*_{C-F} = 8.3 Hz), 119.7 (q, C-F, ¹*J*_{C-F} = 320.9 Hz), 114.0 (dd, C-F, ²*J*_{C-F} = 16.5 Hz, ⁴*J*_{C-F} = 3.9 Hz), 113.0 (d, C-F, ²*J*_{C-F} = 23.7 Hz), 112.1 (d, C-F, ²*J*_{C-F} = 21.2 Hz), 109.0 (dd, C-F, ²*J*_{C-F} = 22.5 Hz, ⁴*J*_{C-F} = 3.2 Hz), 102.0 (t, C-F, ²*J*_{C-F} = 25.8 Hz), 48.9, 48.8, 41.3, 40.7, 38.2, 37.0, 34.8 (t, C-F, ⁴*J*_{C-F} = 2.1 Hz), 34.2, 30.2, 30.1, 28.8, 28.7. ¹⁹F NMR (282 MHz, CDCl₃) δ -77.1 (s, 3F), -108.5 (dd, *J* = 9.7, 5.8 Hz, 1F), -115.2 – -115.3 (m, 1F).

FT-IR $\bar{\nu}_{\max}$ (cm⁻¹) = 3308, 2967, 1614, 1584, 1375, 1196, 1146, 857.

HRMS (ESI): calcd for C₁₃H₁₅F₅NO₂S₂ [M+H]⁺: 376.0459, found 376.0465.

1,1,1-Trifluoro-N-((7-fluoro-4,4-dimethylthiochroman-2-yl)methyl)methanesulfonamide (163nb)

Based on general procedure C, starting from 38 mg of sulfane, product **163nb** has been obtained as a yellow oil (2na + 2nb = 11 mg, 30% yield). (2na and 2nb are mixtures.)



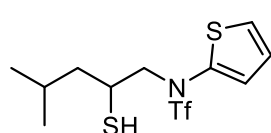
R_f = 0.25 (PE: EA = 10:1)

¹H NMR (300 MHz, CDCl₃) δ 7.31 (dd, *J* = 8.7, 5.8 Hz, 1H), 6.85 – 6.72 (m, 2H), 5.32 (s, 1H), 3.70 – 3.62 (m, 1H), 3.53 (dd, *J* = 5.8, 3.9 Hz, 2H), 1.93 (dd, *J* = 13.5, 4.1 Hz, 1H), 1.74 (dd, *J* = 12.1, 2.3 Hz, 1H), 1.44 (s, 3H), 1.24 (s, 3H). ¹³C {¹H} NMR (76 MHz, CDCl₃) δ 161.9 (d, C–F, ²*J*_{C–F} = 12.8 Hz), 161.0 (dm, C–F, ¹*J*_{C–F} = 246.3 Hz), 159.7 (d, C–F, ²*J*_{C–F} = 12.4 Hz), 158.6 (d, C–F, ²*J*_{C–F} = 12.8 Hz), 156.5 (d, C–F, ²*J*_{C–F} = 12.4 Hz), 145.3 (dd, C–F, ³*J*_{C–F} = 7.5 Hz, ³*J*_{C–F} = 2.9 Hz), 137.6 (d, C–F, ⁴*J*_{C–F} = 3.2 Hz), 132.3 (d, C–F, ³*J*_{C–F} = 8.3 Hz), 127.5 (d, C–F, ³*J*_{C–F} = 8.3 Hz), 119.7 (q, C–F, ¹*J*_{C–F} = 320.9 Hz), 114.0 (dd, C–F, ²*J*_{C–F} = 16.5 Hz, ⁴*J*_{C–F} = 3.9 Hz), 113.0 (d, C–F, ²*J*_{C–F} = 23.7 Hz), 112.1 (d, C–F, ²*J*_{C–F} = 21.2 Hz), 109.0 (dd, C–F, ²*J*_{C–F} = 22.5 Hz, ⁴*J*_{C–F} = 3.2 Hz), 102.0 (t, C–F, ²*J*_{C–F} = 25.8 Hz), 48.9, 48.8, 41.3, 40.7, 38.2, 37.0, 34.8 (t, C–F, ⁴*J*_{C–F} = 2.1 Hz), 34.2, 30.2, 30.1, 28.8, 28.7. ¹⁹F NMR (282 MHz, CDCl₃) δ -77.1 (s, 3F), -116.4 – -116.6 (m, 1F).

HRMS (ESI): calcd for C₁₃H₁₆F₄NO₂S₂ [M+H]⁺: 358.0553 Found 358.0556.

1,1,1-Trifluoro-N-(2-mercapto-4-methylpentyl)-N-(thiophen-2-yl)methanesulfonamide (163o)

Based on general procedure C, starting from 139 mg of sulfane, product **163o** has been obtained as a colorless oil (74 mg, 53% yield).



R_f = 0.6 (PE: EA = 10:1)

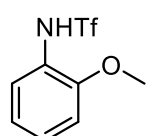
¹H NMR (300 MHz, CDCl₃) δ 7.29 (dd, *J* = 5.6, 1.4 Hz, 1H), 7.08 (dd, *J* = 3.8, 1.4 Hz, 1H), 6.96 (dd, *J* = 5.6, 3.8 Hz, 1H), 3.92 – 3.77 (m, 2H), 2.90 – 2.77 (m, 1H), 1.98 – 1.83 (m, 1H), 1.56 (dt, *J* = 9.4, 4.4 Hz, 1H), 1.41 – 1.30 (m, 2H), 0.92 (d, *J* = 6.7 Hz, 3H), 0.80 (d, *J* = 6.5 Hz, 3H). ¹³C {¹H} NMR (75 MHz, CDCl₃) δ 137.9, 127.7, 126.4, 126.0, 120.4 (q, C–F, ¹*J*_{C–F} = 324.8 Hz), 61.9, 44.3, 36.2, 25.6, 23.4, 21.2. ¹⁹F NMR (282 MHz, CDCl₃) δ -72.3 (s, 3F).

FT-IR $\bar{\nu}_{\max}$ (cm⁻¹) = 2959, 1534, 1401, 1228, 1194, 1131, 1082.

HRMS (FI): Calcd. for C₁₁H₁₆F₃NO₂S₃: [M]⁺ 347.0290, found 347.0299.

1,1,1-Trifluoro-N-(2-methoxyphenyl)methanesulfonamide (163p)

Based on general procedure C, starting from 37 mg of sulfane **162p**, product **163p** has been obtained as a solid (13.8 mg, 54% yield).⁵



R_f = 0.3 (PE: EA = 10:1)

¹H NMR (300 MHz, CDCl₃) δ 7.51 (dd, *J* = 8.0, 1.6 Hz, 1H), 7.22 (ddd, *J* = 8.2, 7.6, 1.6 Hz, 1H), 7.11 (s, 1H), 7.01 – 6.91 (m, 2H), 3.91 (s, 3H). ¹⁹F NMR (282 MHz, CDCl₃) δ -75.9 (s, 3F).

3.3.5 Crystallographic data

Instrumentation for the crystal measurement

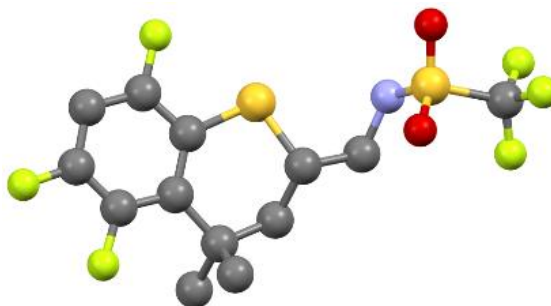
Crystallographic data were acquired at CESAMO (UMR 5255) on a Bruker APEX 2 DUO. A single crystal was mounted and immersed in a stream of nitrogen gas [$T = 150(2)$ K]. Data were collected, using a microfocus sealed tube of Mo $K\alpha$ radiation ($k = 0.71073$ Å) on a KappaCCD diffractometer. Data collection and cell refinement were performed using APEX2 2013.10-0 (Bruker AXS Inc.), and SAINT v8.34A (Bruker AXS Inc.). Data reduction was performed using SAINT v8.34A (Bruker AXS Inc.). Correction for absorption was performed using multi-scan integration as included in SADABS V2012/1 (Bruker AXS). Structure solutions were found by charge flipping methods (SUPERFLIP a computer program for the solution of crystal structures by charge flipping in arbitrary dimensions (Palatinus & Chapuis, *J. Appl. Cryst.* (2007). 40, 786-790) EDMA: a computer program for topological analysis of discrete electron densities (Palatinus et al., *J. Appl. Cryst.* (2012). 45, 575-580)) and refined with (SHELXL) (G.M. Sheldrick, A short history of SHELX, *Acta Crystallographica Section A*, 64 (2008), pp. 112-122).

Single crystal preparation

Approximately 15 mg of the sample was placed in a small vial and dissolved in a small amount of DCM. Then put this vial into a bottle with n-pentane and seal it. After about 3-5 days, crystals can be precipitated.

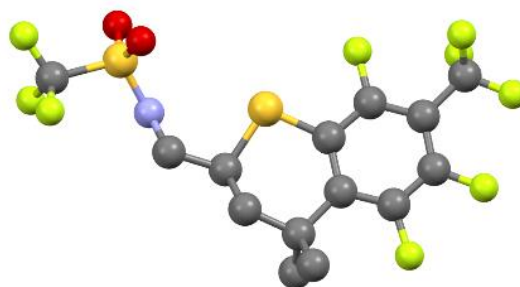
1,1,1-Trifluoro-N-((5,7,8-trifluoro-4,4-dimethylthiochroman-2-yl)methyl)methanesulfonamide

(163b)



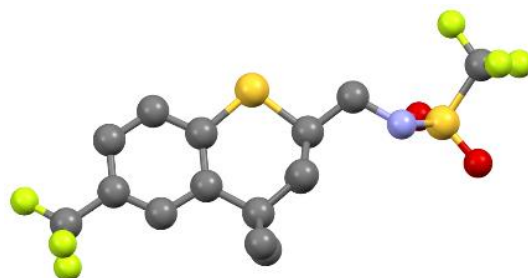
Empirical formula	C ₂₆ H ₂₆ F ₁₂ N ₂ O ₄ S ₄
Formula weight	786.73
Temperature	150(2) K
Wavelength	0.71073 Å
Crystal system, space group	Monoclinic, P 21/c
Unit cell dimensions	a = 8.4945(19) Å alpha = 90 deg. b = 35.341(8) Å beta = 90.971(6) deg. c = 10.719(2) Å gamma = 90 deg.
Volume	3217.5(12) Å ³
Z, Calculated density	4, 1.624 Mg/m ³
Absorption coefficient	0.402 mm ⁻¹
F(000)	1600
Crystal size	0.170 x 0.110 x 0.040 mm
Theta range for data collection	1.152 to 25.774 deg.
Limiting indices	-7<=h<=10, -43<=k<=41, -11<=l<=13
Reflections collected / unique	24705 / 6156 [R(int) = 0.0784]
Completeness to theta = 25.242	100.0 %
Absorption correction	Semi-empirical from equivalents
Max. and min. transmission	0.7453 and 0.6577
Refinement method	Full-matrix least-squares on F ²
Data / restraints / parameters	6156 / 0 / 437
Goodness-of-fit on F ²	1.015
Final R indices [I>2sigma(I)]	R1 = 0.0542, wR2 = 0.1158
R indices (all data)	R1 = 0.1005, wR2 = 0.1375
Extinction coefficient	n/a
Largest diff. peak and hole	0.538 and -0.404 e.Å ⁻³

1,1,1-Trifluoro-N-((5,6,8-trifluoro-4,4-dimethyl-7-(trifluoromethyl)thiochroman-2-yl)methyl)methanesulfonamide (163c)



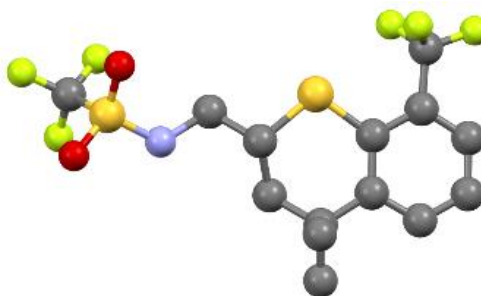
Empirical formula	C ₂₈ H ₂₄ F ₁₈ N ₂ O ₄ S ₄
Formula weight	922.73
Temperature	150(2) K
Wavelength	0.71073 Å
Crystal system, space group	Monoclinic, P 21/c
Unit cell dimensions	a = 16.408(4) Å alpha = 90 deg. b = 14.987(4) Å beta = 118.543(5) deg. c = 16.861(4) Å gamma = 90 deg.
Volume	3642.5(15) Å ³
Z, Calculated density	4, 1.683 Mg/m ³
Absorption coefficient	0.391 mm ⁻¹
F(000)	1856
Crystal size	0.300 x 0.100 x 0.070 mm
Theta range for data collection	1.413 to 26.991 deg.
Limiting indices	-20 ≤ h ≤ 20, -19 ≤ k ≤ 18, -21 ≤ l ≤ 21
Reflections collected / unique	59422 / 7927 [R(int) = 0.0533]
Completeness to theta = 25.242	99.9 %
Absorption correction	Semi-empirical from equivalents
Max. and min. transmission	0.7457 and 0.6869
Refinement method	Full-matrix least-squares on F ²
Data / restraints / parameters	7927 / 0 / 509
Goodness-of-fit on F ²	1.034
Final R indices [I > 2σ(I)]	R1 = 0.0581, wR2 = 0.1424
R indices (all data)	R1 = 0.0889, wR2 = 0.1646
Extinction coefficient	n/a
Largest diff. peak and hole	1.127 and -0.538 e.Å ⁻³

N-((4,4-Dimethyl-6-(trifluoromethyl)thiochroman-2-yl)methyl)-1,1,1-Trifluoromethanesulfonamide (163j)



Empirical formula	C ₁₄ H ₁₄ F ₆ N O ₂ S ₂
Formula weight	406.38
Temperature	150(2) K
Wavelength	0.71073 Å
Crystal system, space group	Orthorhombic, P c a 21
Unit cell dimensions	a = 11.3419(9) Å alpha = 90 deg. b = 18.3107(14) Å beta = 90 deg. c = 8.3648(7) Å gamma = 90 deg.
Volume	1737.2(2) Å ³
Z, Calculated density	4, 1.554 Mg/m ³
Absorption coefficient	0.375 mm ⁻¹
F(000)	828
Crystal size	0.360 x 0.360 x 0.010 mm
Theta range for data collection	2.112 to 26.623 deg.
Limiting indices	-14<=h<=14, -22<=k<=21, -10<=l<=10
Reflections collected / unique	17265 / 3244 [R(int) = 0.0305]
Completeness to theta = 25.242	99.6 %
Absorption correction	Semi-empirical from equivalents
Max. and min. transmission	0.7454 and 0.6809
Refinement method	Full-matrix least-squares on F ²
Data / restraints / parameters	3244 / 1 / 238
Goodness-of-fit on F ²	1.057
Final R indices [I>2sigma(I)]	R1 = 0.0576, wR2 = 0.1461
R indices (all data)	R1 = 0.0679, wR2 = 0.1560
Absolute structure parameter	0.12(4)
Extinction coefficient	n/a
Largest diff. peak and hole	0.774 and -0.410 e.Å ⁻³

N-((4,4-Dimethyl-8-(trifluoromethyl)thiochroman-2-yl)methyl)-1,1,1-trifluoromethanesulfonamide (163l)

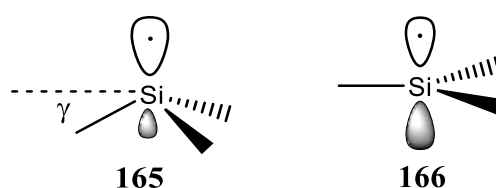


Empirical formula	C ₁₄ H ₁₅ F ₆ N O ₂ S ₂
Formula weight	407.39
Temperature	150(2) K
Wavelength	0.71073 Å
Crystal system, space group	Triclinic, P -1
Unit cell dimensions	a = 9.2122(14) Å alpha = 107.248(4) deg. b = 9.7955(15) Å beta = 111.373(3) deg. c = 10.6288(16) Å gamma = 94.241(3) deg.
Volume	834.9(2) Å ³
Z, Calculated density	2, 1.620 Mg/m ³
Absorption coefficient	0.390 mm ⁻¹
F(000)	416
Crystal size	0.130 x 0.090 x 0.040 mm
Theta range for data collection	2.195 to 28.336 deg.
Limiting indices	-9 ≤ h ≤ 12, -13 ≤ k ≤ 13, -14 ≤ l ≤ 13
Reflections collected / unique	16423 / 4148 [R(int) = 0.0680]
Completeness to theta = 25.242	100.0 %
Absorption correction	Semi-empirical from equivalents
Max. and min. transmission	0.7457 and 0.6873
Refinement method	Full-matrix least-squares on F ²
Data / restraints / parameters	4148 / 0 / 232
Goodness-of-fit on F ²	1.039
Final R indices [I > 2σ(I)]	R ₁ = 0.0501, wR ₂ = 0.1050
R indices (all data)	R ₁ = 0.0949, wR ₂ = 0.1264
Extinction coefficient	n/a
Largest diff. peak and hole	0.331 and -0.407 e.Å ⁻³

Chapter 4 Copper-Catalyzed Silylation of Alkenes by Photoinduced Ligand-to-Metal Charge Transfer

4.1 Structure and stability of silyl radicals

As we all know, silicon is the second most prevalent element on the earth, accounting for 26.4% of the total mass of the earth's crust, and it is found in a variety of rocks, gravels, and other substances. Organosilicon compounds featuring C–Si bonds have had unique applications in various areas over the last 100 years due to their distinctive physical and chemical properties, as well as biological activity.¹³⁰ In biologically active molecules, replacing carbon with silicon can improve lipophilicity and cell permeability, a strategy also known as "silicon switch".¹³¹ There were numerous publications on silyl radicals as early as the late 1940s due to the high functional group tolerance, atom economy, and chemical selectivity of radical chemistry. The hydrosilylation of alkenes was first thought to involve silicon-centered radicals as intermediates.¹³² Subsequent investigations into the structural features of silyl radicals found that they are primarily bent and best described as a σ -type structure **165**, albeit the geometry of these radicals is heavily influenced by the nature of the substituents attached to the silicon center. The simplest of all silyl radicals, $\text{H}_3\text{Si}\cdot$, is bent out of the plane by $16.0 \pm 2.0^\circ$ (angle γ in **165**) corresponding to an α angle of $112.5 \pm 2.0^\circ$.¹³³ The inversion barrier in $\text{H}_3\text{Si}\cdot$ is $5.4 \text{ kcal mol}^{-1}$. The degree of pyramidalization can be decreased by replacing the H in $\text{H}_3\text{Si}\cdot$ with trimethylsilyl on the silicon center.¹³⁴ The introduction of large substituents at silicon has a significant impact on the geometry of silyl radicals, as bulky species [e.g., $(\text{Et}_3\text{Si})_3\text{Si}\cdot$, $(i\text{Pr}_3\text{Si})_3\text{Si}\cdot$, $(t\text{-Bu}_2\text{MeSi})_3\text{Si}\cdot$] are almost planar due to steric repulsion between the bulky substituents, as shown in **166**.¹³⁵ Electron paramagnetic resonance (EPR) spectroscopy reveals that divergence from planarity rises in the sequence of tris(trialkylsilyl)silyl radicals ($\text{R}_3\text{Si}\cdot$) in the order $\text{R} = \text{SiMe}_3 < \text{SiEt}_2\text{Me} < \text{SiEt}_3 < \text{Si}(i\text{Pr})_3 < \text{Si}(t\text{-Bu})_2\text{Me}$.¹³⁶⁻¹³⁹ Silyl radicals with electronegative atoms as α -substituents are more pyramidal, which is attributed to an increase in the 3s character of the singly occupied molecular orbital (SOMO).¹⁴⁰

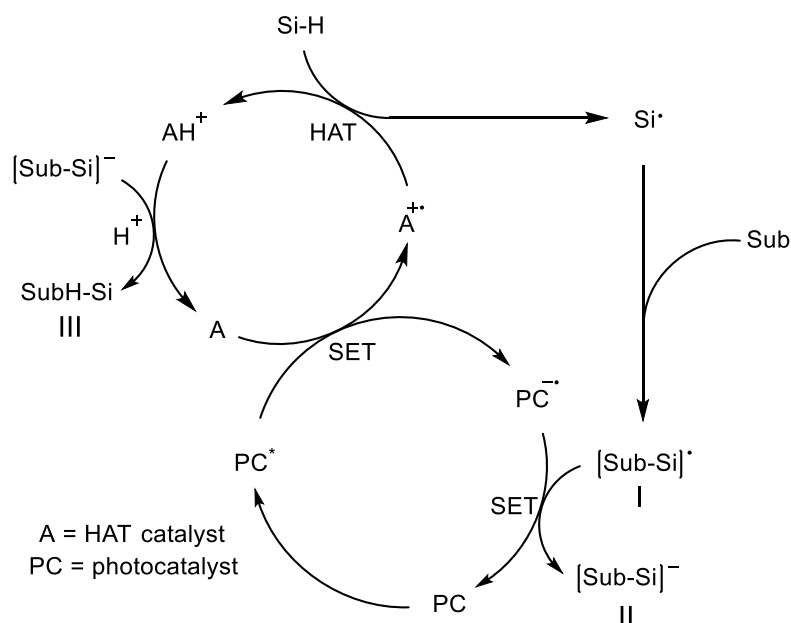


Scheme 49 Geometry of silyl radicals

As the size of the substituent rises, the silyl radical becomes more stable and may even turn persistent. For example, the crystalline tris[di-*tert*-butyl(methyl)silyl]silyl radical has been isolated. Its structure, as verified by X-ray diffraction analyses, exhibits a completely flat geometry around silicon atoms that remain in solution.¹³⁵ Other several long-lived silyl radicals have been reported and their half-lives calculated. For instance, half-lives for the silyl radicals tris(ethylmethylsilyl)silyl, tris[diethyl(methyl)silyl]silyl, tris(triethylsilyl)silyl, tris(triisopropylsilyl)silyl, and tris[di-*tert*-butyl(methyl)silyl]silyl are about 3 hours, 1 day, 1.5 months, 5 days, and 1 day, respectively, at 15 °C.¹³⁵⁻¹³⁸

4.2 General mechanism

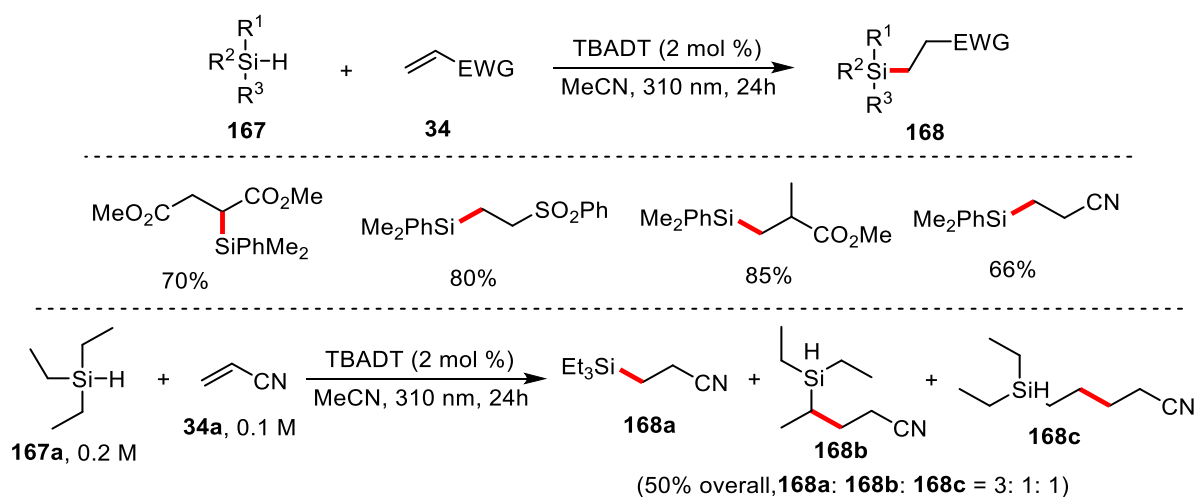
General mechanism for the visible-light-induced hydrosilylation is shown in Scheme 50. First, the HAT catalyst **A** was oxidized by the photoexcited state PC^* to form $PC^{\cdot-}$ and $A^{\cdot+}$. Subsequently, $A^{\cdot+}$ radical abstracts a hydrogen atom from the silane (HAT process), and the resulting silyl radical adds to the substrate to form a radical adduct **I** (radical addition process), which was then reduced by $PC^{\cdot-}$ leading to carbanion intermediate **II** and the regenerated photoactive PC. Eventually, the carbanion intermediate **II** undergoes a protonation process to obtain the final product **III**, while the deprotonated HAT catalyst re-enters the next catalytic cycle.



Scheme 50 General mechanism for the visible-light-induced hydrosilylation.

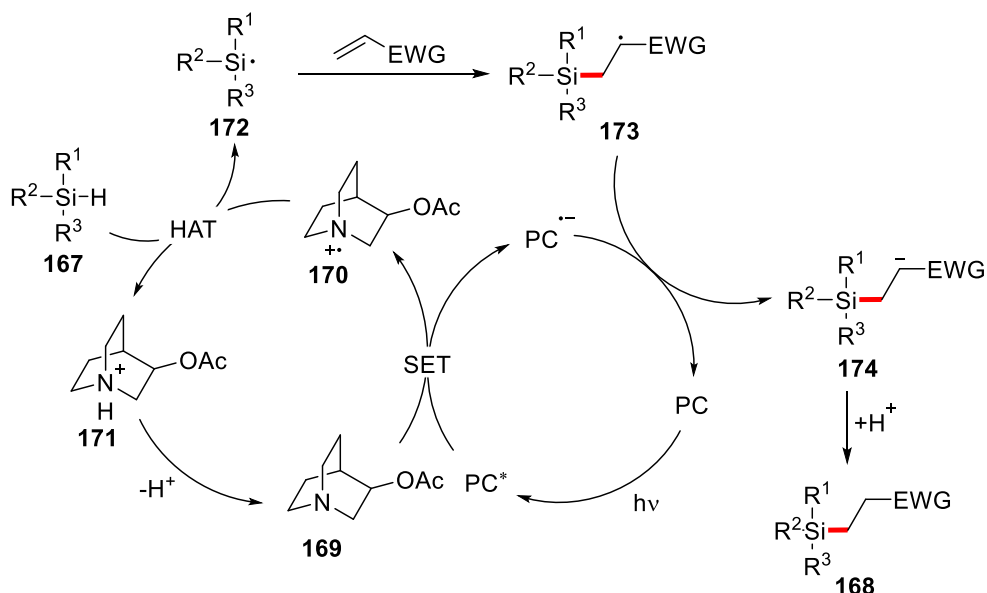
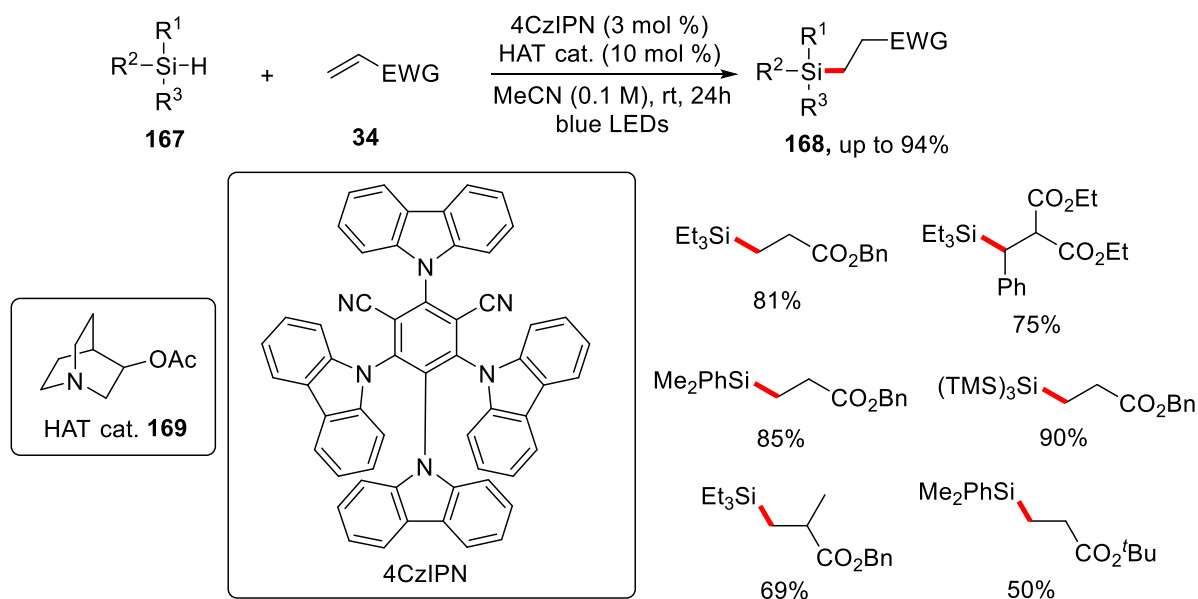
4.3 visible-light-mediated silylation of alkene

In 2015, Fagnoni¹⁴¹ *et al.* discovered a visible light-mediated hydrosilylation reaction of electron-deficient olefins, in which tetra-*n*-butylammonium decatungstate (TBADT) was used as a photocatalyst and HAT reagent in the reaction system (Scheme 51). Under UV or sunlight irradiation, dimethylphenylsilane and diphenylmethylsilane can react smoothly with a series of electron-deficient terminal alkenes or 1,2-disubstituted alkenes to afford the desired hydrosilylation products in moderate to excellent yields. When using more reactive triphenylsilane or ((Me₃Si)₃SiH) TTMSS participate to the reaction, a radical chain process occurs without the addition of a photocatalyst. When trialkyl substituted silanes (such as triethylsilane) are employed as substrates, the intramolecular C–H bond and Si–H bond trigger competing reactions in the HAT process, resulting in a mixed product of carbon radical addition and silyl radical addition.



Scheme 51 TBADT-catalyzed hydrosilylation of electron-poor alkenes.

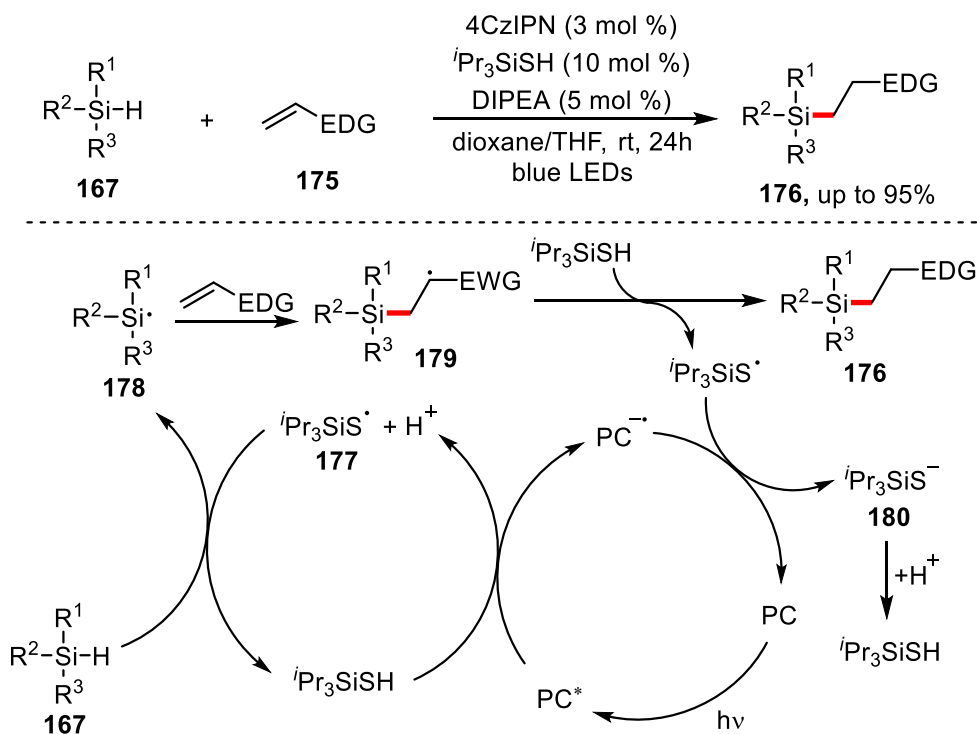
In 2017, Wu¹⁴² *et al.* reported visible-light-mediated hydrosilylation of both electron-rich and electron-deficient alkenes. When electron-deficient alkenes were used as substrates, 4CzIPN and quinuclidin-3-yl acetate were the optimal photocatalyst and HAT catalyst, respectively (Scheme 52). Based on the experimental results and known literature reports, the authors proposed a reasonable mechanism. First, the quinuclidin-3-yl acetate **169** was oxidized by 4CzIPN in its excited state to form cation-radical **170**, which would then abstract a hydrogen atom from silane **167** to generate silyl radical **172**. The latter then reacts with the electron-deficient alkene **34**, and the resulting carbon radical intermediate **173** is reduced to the carbanion **174** by the photocatalyst radical anion. Finally, the intermediate **174** is protonated to yield the target product **168**.



Scheme 52 Visible-light-mediated hydrosilylation of electron-deficient alkenes.

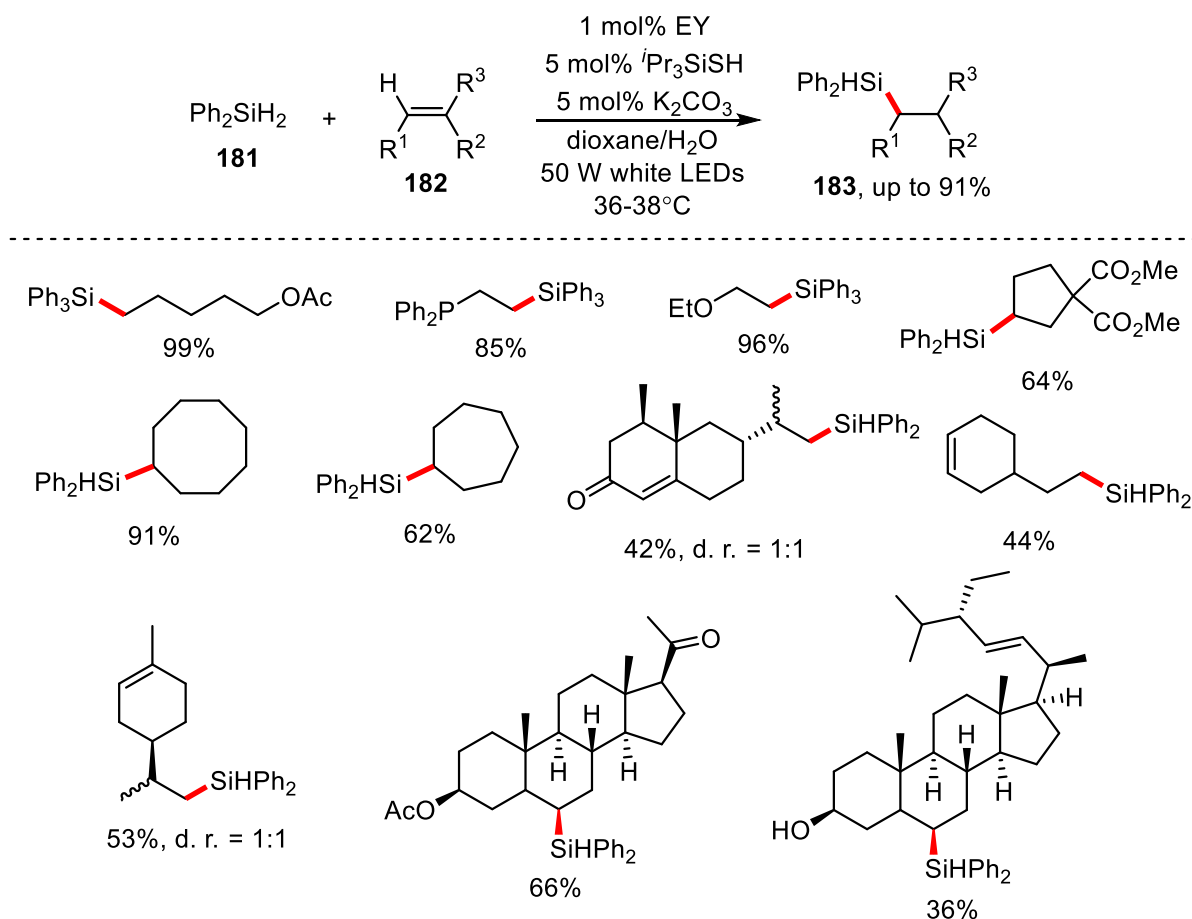
On the other hand, the hydrosilylation reaction of electron-rich alkenes can be achieved by using organic photocatalyst 4CzIPN, HAT catalyst triisopropylsilanethiol, and a catalytic amount of an organic base such as *N,N*-diisopropylethylamine (DIPEA) under blue-light conditions (Scheme 53). The authors also suggested a possible mechanistic cycle for the electron-rich alkenes. After being deprotonated by DIPEA, triisopropylsilanethiol is oxidized by the excited-state of 4CzIPN to generate a thiyl radical **177**. Next, a hydrogen atom transfer would take place from silane **167** to thiyl radical **177** forming silyl radical **178**, which is added to the electron-rich olefin to generate the nucleophilic carbon-centered radical **179**. Triisopropylsilanethiol can be utilized as a polarity reversal catalyst to achieve this HAT process and yield the desired product **176**, since the BDE of S–

H bond (369.0 kJ/mol) is somewhat lower than that of the C–H bond (389.9 kJ/mol) in intermediate **179**. Finally, the thiyl radical **177** undergoes single-electron reduction and protonation, regenerating triisopropylsilanethiol and the photocatalyst in its ground-state.



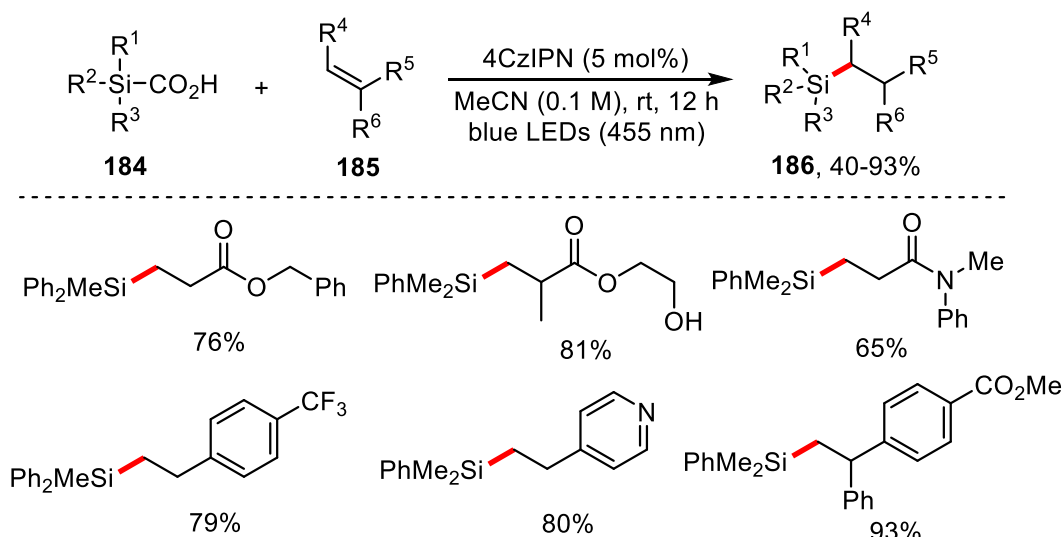
Scheme 53 Visible-light-mediated hydrosilylation of electron-rich alkenes.

Yao¹⁴³ *et al.* in 2018 developed a visible-light-mediated radical hydrosilylation approach for electron-neutral and electron-rich alkenes at room temperature in the presence of eosin Y, thiol, and base (Scheme 54). Under standard conditions, the hydrosilylation reaction of various acyclic and cyclic terminal olefins and internal olefins can occur smoothly, and the target products can be delivered in moderate to good yields (the highest yield reaches 99%). In addition, a variety of dienes and two steroid drug molecules could also be converted into hydrosilylation products with good regioselectivity in moderate yields.



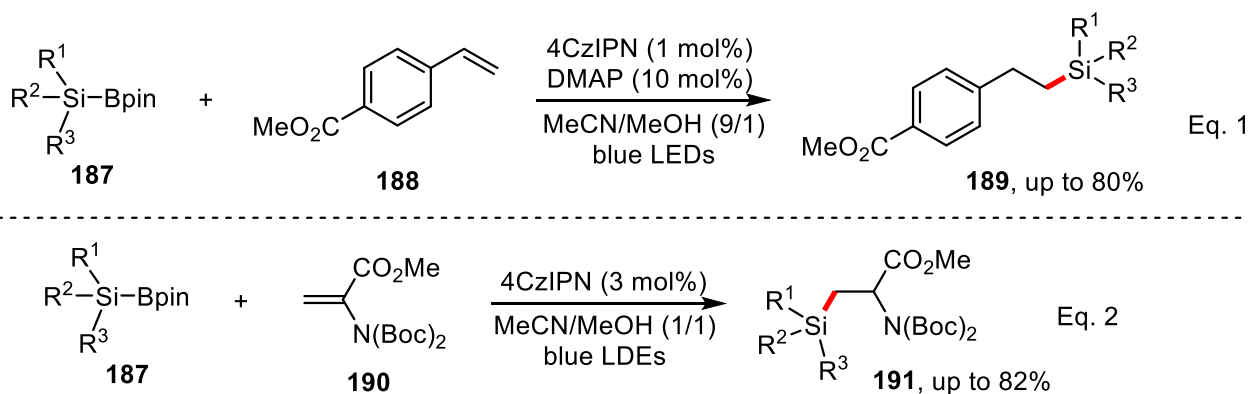
Scheme 54 Eosin-Y catalyzed silylation of alkenes.

Recently, Uchiyama¹⁴⁴ and colleagues published the first report on the production of silyl radicals using the photo-induced decarboxylation process of silacarboxylic acids (Scheme 55). The reaction was well tolerated by a wide range of alkenes including styrenes with different substituents at phenyl group and heteroaryl alkenes. The most plausible mechanism of the reaction was proposed by the authors. Single-electron transfer from silacarboxylic acids **184** to excited 4CzIPN, followed by decarboxylation yields silyl radical, which is added to alkenes **185** to furnish the carbon-centered radical. The corresponding product **186** would be formed after the reduction of carbon-centered radical by the *in situ* generated 4CzIPN⁻ and protonation.



Scheme 55 Visible-light-induced decarboxylative silylation of alkenes

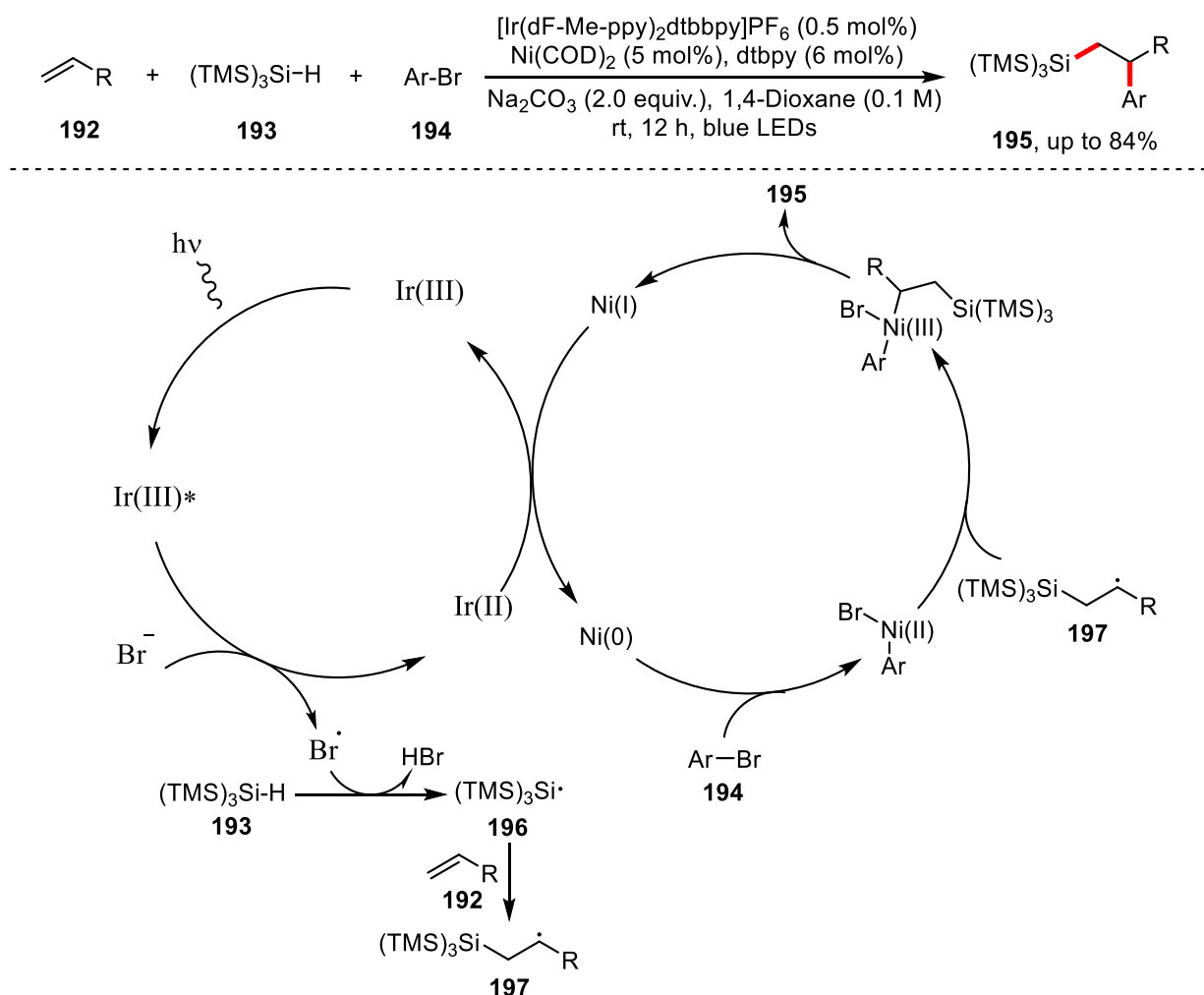
In 2022, Ohmiya¹⁴⁵ and co-workers developed a visible-light-driven silylation of alkenes **188** using Si-B reagents **187** as a silyl radical source (Scheme 56, Eq. 1). The activation of silylboronates with a catalytic amount of mild base facilitated the formation of silyl radicals via a single-electron oxidation process. In 2023, Zhang¹⁴⁶ *et al.* reported a similar reaction, using methanol to activate the silylboronates enabling the photocatalytic generation of silyl radicals (Scheme 56, Eq. 2).



Scheme 56 Visible-light-induced silylation of alkenes using silylboronates.

Recently, the Hu¹⁴⁷ group demonstrated an efficient approach for carbosilylation of electron-deficient terminal alkenes by combining photocatalysis and nickel catalysis (Scheme 57). With TTMSS as the source of silyl group, a variety of aryl and heteroaryl bromides containing electron-withdrawing, electron-donating, or electron-neutral groups can react efficiently with alkenes to deliver the target products in moderate to good yields. Mechanistic studies showed that the oxidative addition of aryl bromide **194** to Ni(0) catalyst provides Ni(II)(Ar)(Br) species. Meanwhile, the Ir(III)

photocatalyst is excited in the presence of blue light. The excited Ir(III) converts Br⁻ into Br[•] via a SET process. Next, the Br[•] abstracts a hydrogen atom from silane **193** to form silyl radical **196**, which is added to olefin **192**, leading to an alkyl radical **197**. The latter is trapped by the Ni(II) complex to generate Ni(III) species, which undergoes a reductive elimination, providing the arylsilylation product **195** and Ni(I) species. The latter is reduced by Ir(II) to regenerate both the Ir(III) photocatalyst and the Ni(0) catalyst.

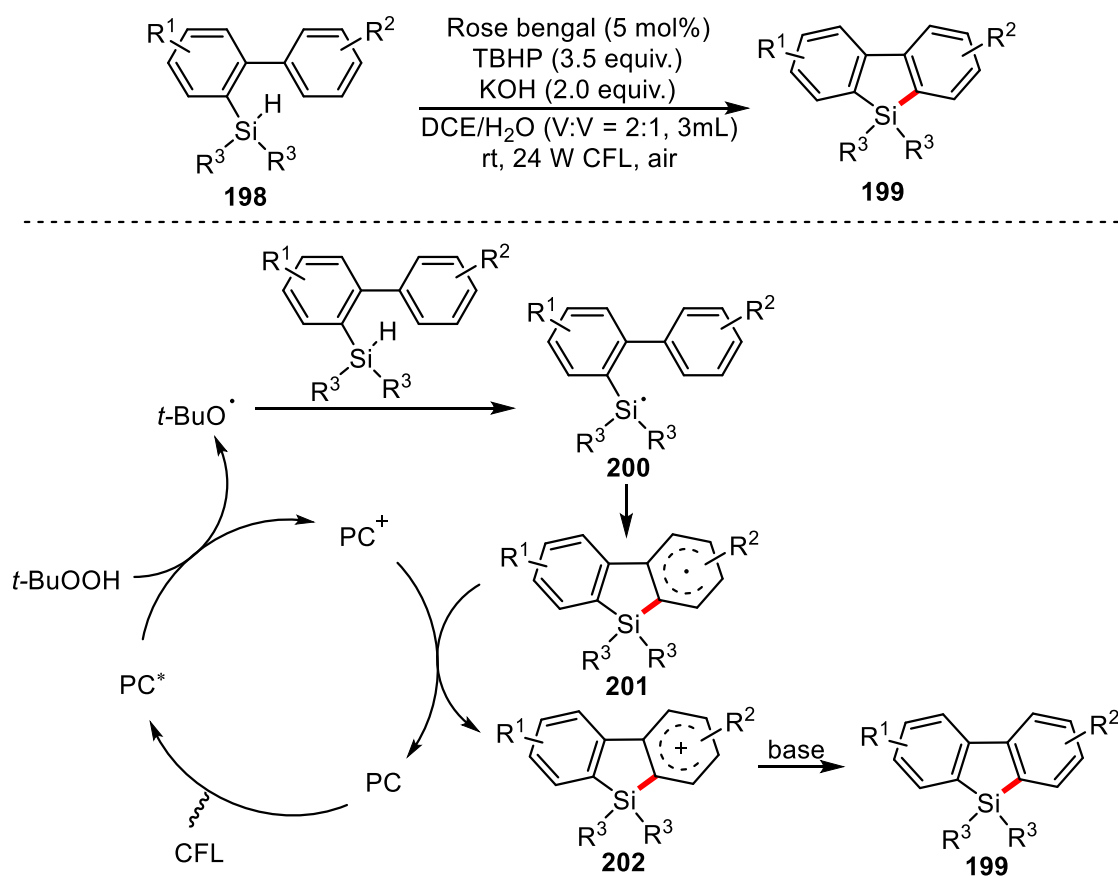


Scheme 57 Visible-light-induced arylsilylation of alkenes

4.4 visible-light-mediated silylation of arenes and heteroarenes

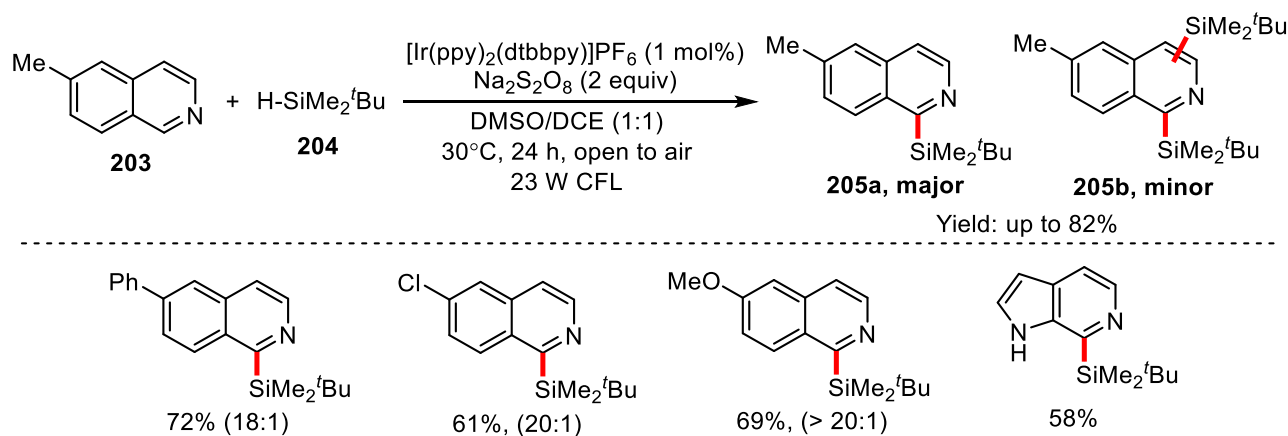
Jiang¹⁴⁸ *et al.* discovered in 2018 a visible light-induced radical silylation reaction of arenes, producing a variety of 9-silylfluorene compounds under mild conditions through dehydrogenative cyclization (Scheme 58). Based on several control experiments, the authors proposed a reasonable mechanism. First, the photocatalyst PC is excited by blue LED light. The excited-state is then oxidatively quenched by TBHP to give PC⁺ and *t*-BuO[•]. The latter abstracts a hydrogen atom from

silane **198** to form silyl radical **200**. Cyclization of the latter generates **201** which is further oxidized by PC^+ to provide carbocation intermediate **202**, finally deprotonated to afford the desired product **199**.



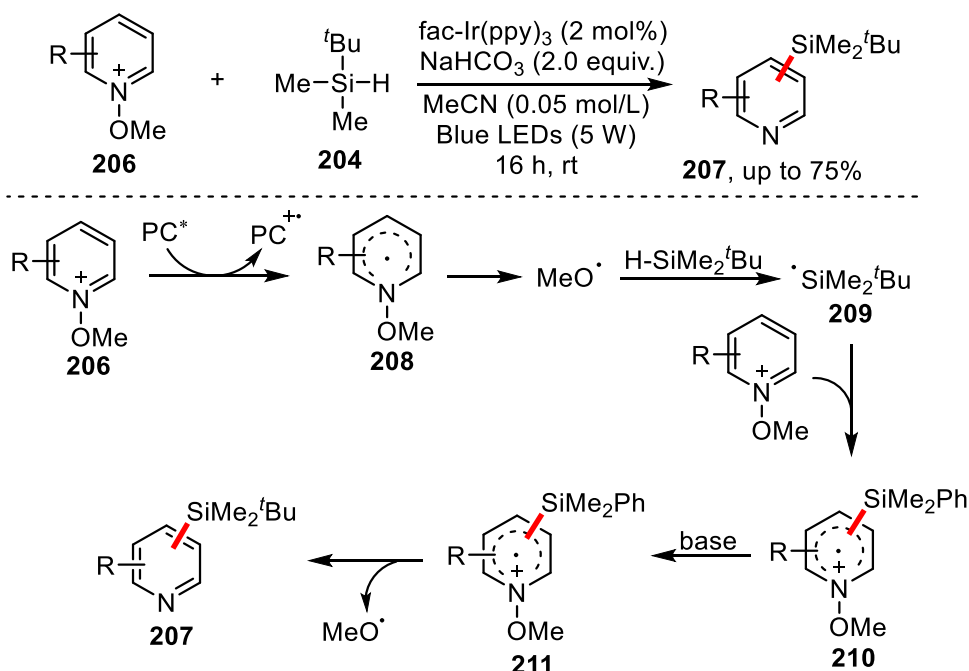
Scheme 58 Visible-light-induced silylation of biarylhydrosilanes.

In 2019, Zhang¹⁴⁹ *et al.* reported the photocatalytic Minisci-type C-H bond silylation reaction of nitrogen-containing aromatic heterocycles using $[\text{Ir}(\text{ppy})_2(\text{dtbbpy})]\text{PF}_6$ and $\text{Na}_2\text{S}_2\text{O}_8$ as photocatalyst and radical initiator, respectively (Scheme 59). Various isoquinoline substrates as well as different electron-rich and -deficient heteroarene derivatives are compatible with the reaction system to provide the corresponding silylated product in good yields.



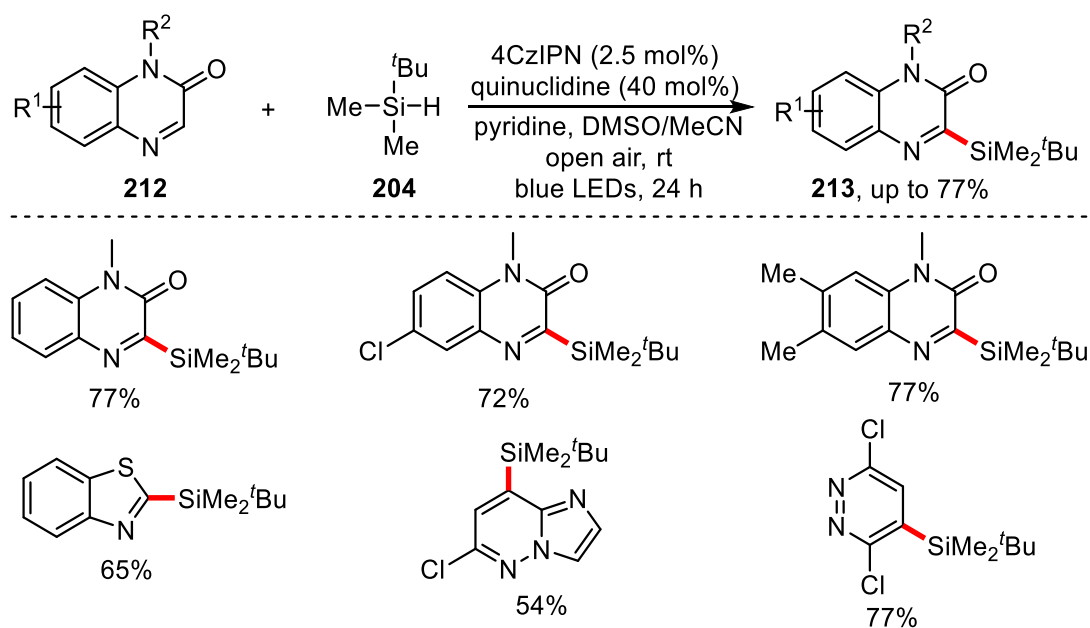
Scheme 59 Photocatalytic C-H silylation of heteroarenes.

Lakhdar¹⁵⁰ and co-workers also developed a visible light-induced synthesis of silicon-substituted pyridines in 2020 (Scheme 60). Unlike Zhang's report, this method begins with *N*-methoxy-pyridines **206**, which can provide a methoxy radical, a HAT reagent able to generate silyl radical intermediates without the addition of exogenous oxidants, through a photocatalytic single-electron oxidation process. A possible mechanism was proposed by the authors. The excited PC^* is oxidatively quenched by the starting material **206** to afford the radical intermediate **208**, which would rapidly release a methoxy radical, while producing substituted pyridine products. The methoxy radical interacts with the silane **204** to form silyl radical **209** and MeOH. The resulting radical **209** then reacts with substrates **206** providing radical intermediate **210**. The final products **207** could be obtained after deprotonation and loss of a methoxy radical.



Scheme 60 Photocatalytic silylation of pyridines

Liu¹⁵¹ *et al.* reported another metal-free photoredox catalyzed silylation of heterocycles in 2021 (Scheme 61). In this reaction system, 4CzIPN (2.5 mol%), quinuclidine (40 mol%) and pyridine were used as photocatalyst, hydrogen transfer reagent and base sources, respectively. A series of substituted quinolones could be converted into the corresponding silylated products with high yields. In addition, electron-deficient heteroaromatics such as benzothiazole, coumarin, pyridazine, benzoxazinone, imidazo[1,2-b]pyridazine, and ethyl isonicotinate can also react efficiently to deliver the target products.



Scheme 61 Visible-light-induced organophotocatalyzed silylation of quinolones

4.5 Results and discussion

In 1961, Kochi¹⁹⁵ made the pioneering discovery that copper chloride, when exposed to light, can produce chlorine radicals, thereby facilitating the chlorination of alkenes, allylic compounds, and alkanes, as well as the oxidation of alcohols to carbonyl compounds (Figure 11).

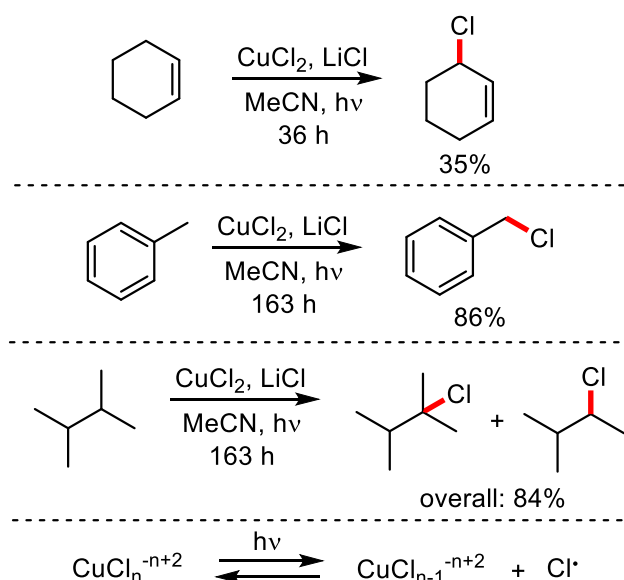


Figure 11 CuCl₂-catalyzed chlorination of alkane, allylic compound.

Recently, this strategy has regained attention from several research teams. For example, wang¹⁹⁶ and co-workers described a novel method for photoredox vicinal dichlorination of alkenes using inexpensive, low-molecular-weight CuCl₂ as chlorine source (Figure 12, Eq. 1). The catalytic process involves a ligand-to-metal charge transfer mechanism to generate chlorine atom radicals rapidly, offering a promising avenue for the synthesis of 1,2-dichloride compounds. This innovative process demonstrates a broad range of substrate compatibility, remarkable tolerance towards various functional groups, exceptionally mild reaction conditions, and does not necessitate the use of external ligands. Rovis³⁹ and his colleagues reported on the CuCl₂-catalyzed alkylation of C(sp³)-H bonds through the coupling of unactivated C(sp³)-H bonds with electron-deficient olefins (Figure 12, Eq. 2). The photoexcited CuCl₂ catalyst undergoes Ligand-to-Metal Charge Transfer (LMCT) to facilitate the generation of a chlorine radical. This chlorine radical serves as a potent hydrogen atom transfer reagent, capable of abstracting electron-rich C(sp³)-H bonds.

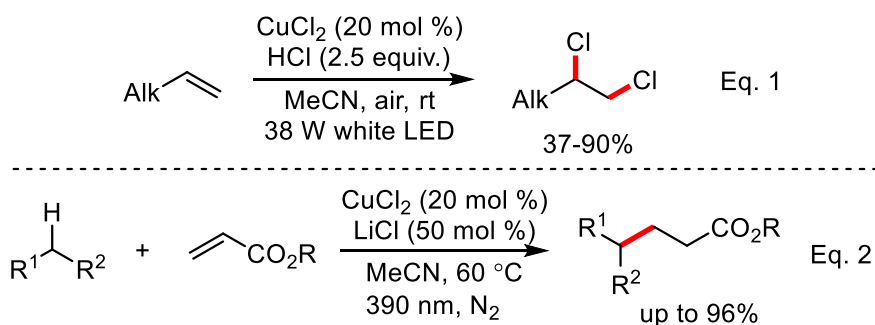
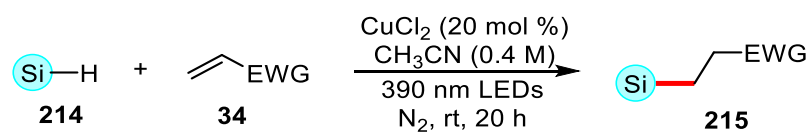


Figure 12 CuCl₂-catalyzed dichlorination of alkenes.

We are presenting here a straightforward and efficient procedure for silylating alkenes, which involves the use of catalytic CuCl₂ as a hydrogen atom transfer (HAT) reagent to abstract a hydrogen atom from hydrosilanes in an atom-economical manner (Scheme 62).

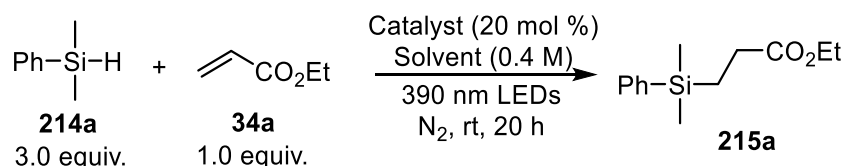


Scheme 62 CuCl₂-catalyzed silylation of alkenes.

4.5.1 Optimization of silylation of ethyl acrylate

Using CuCl₂ as catalyst, ethyl acrylate **34a** as the model substrate, and dimethyl(phenyl)silane **214a** as the silicon source, the reaction was initially conducted at room temperature in acetonitrile under 390 nm light. As a result, product **215a** was produced in 80% yield. After screening various catalysts, it was found that CuCl₂ exhibited the highest efficacy (entries 1-5). FeCl₃ is also an efficient catalyst, but gives only 51% yield (entry 2). A reduction in the amount of CuCl₂ resulted in a decrease in the yield of the product (entries 1, 6-7). The yield decreased to 53% when LiCl was used as an additive (entry 8). Lowering the amount of dimethyl(phenyl)silane **214a** to 2 equivalents resulted in a significant drop in yield (entry 9). A variety of other solvents, including DCM, THF or acetone, was tested, but no reaction occurred (entries 10-12). One possible explanation for this is that copper chloride readily dissolves in acetonitrile as copper can coordinate with this solvent acting as a ligand. The presence of catalyst and light is essential for this reaction to occur. Without them, the reaction does not take place (entries 13-14).

Table 3. Optimization of silylation of ethyl acrylate.



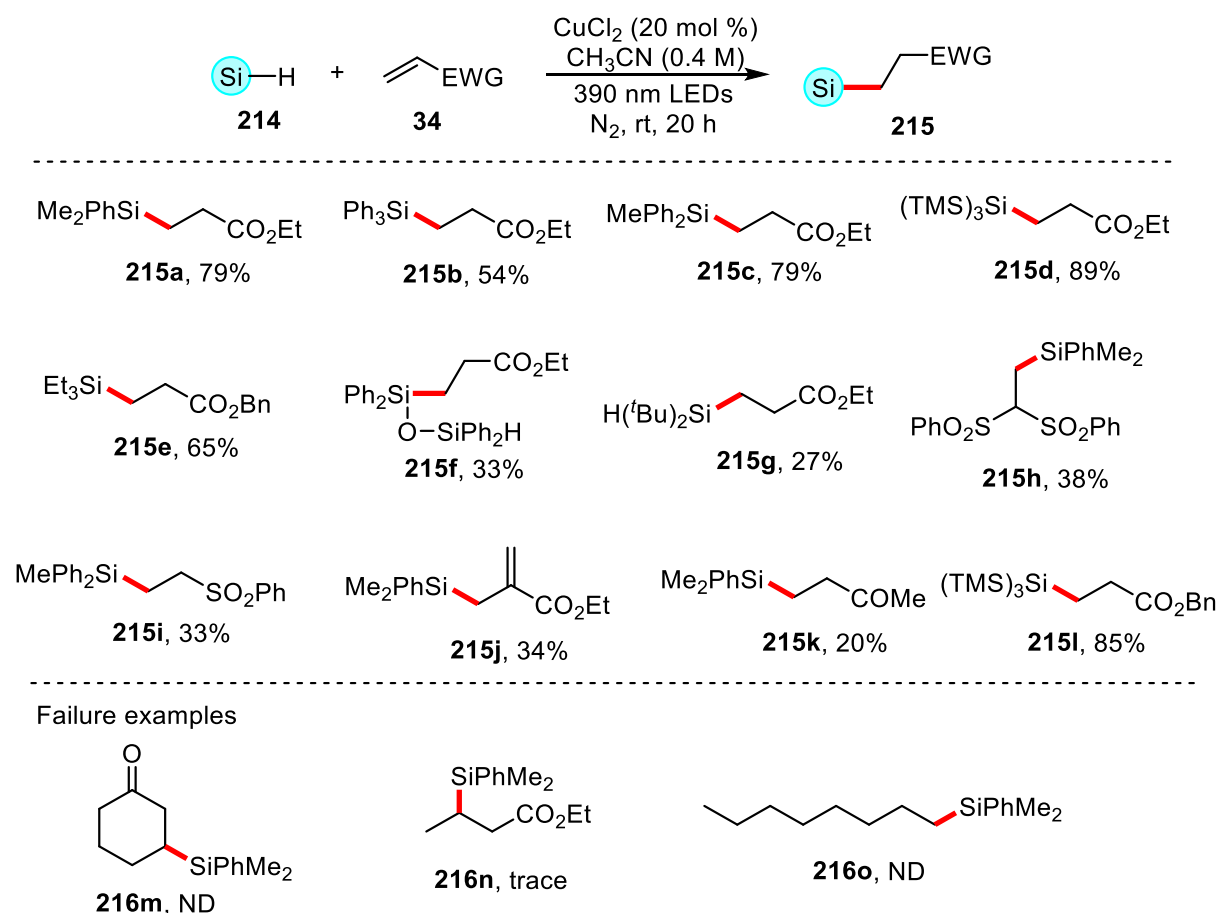
Entry ^a	Catalyst	Solvent	Additive	Yield(%)
1	CuCl ₂ (20 mol %)	CH ₃ CN	-	79
2	FeCl ₃ (20 mol %)	CH ₃ CN	-	51
3	NiCl ₂ (20 mol %)	CH ₃ CN	-	0
4	CeCl ₃ (20 mol %)	CH ₃ CN	-	0

5	[Co(NH ₃) ₆]Cl ₃ (20 mol %)	CH ₃ CN	-	0
6	CuCl ₂ (10 mol %)	CH ₃ CN	-	64
7	CuCl ₂ (5 mol %)	CH ₃ CN	-	44
8	CuCl ₂ (20 mol %)	CH ₃ CN	LiCl (50 mol %)	53
9 ^b	CuCl ₂ (20 mol %)	CH ₃ CN	-	57
10	CuCl ₂ (20 mol %)	DCM	-	0
11	CuCl ₂ (20 mol %)	THF	-	0
12	CuCl ₂ (20 mol %)	Acetone	-	0
13	-	Acetone	-	0
14 ^c	CuCl ₂ (20 mol %)	CH ₃ CN	-	0

^a Standard condition: CuCl₂ (20 mol %), **214a** (0.6 mmol, 3 equiv.), **34a** (0.2 mmol, 1 equiv.), CH₃CN (0.5 mL), Kessil 40 W 390 nm LEDs, rt, N₂, 20 h, isolated yields. ^b **214a** (0.4 mmol, 2 equiv.). ^c in the dark.

4.5.2 Substrate scope

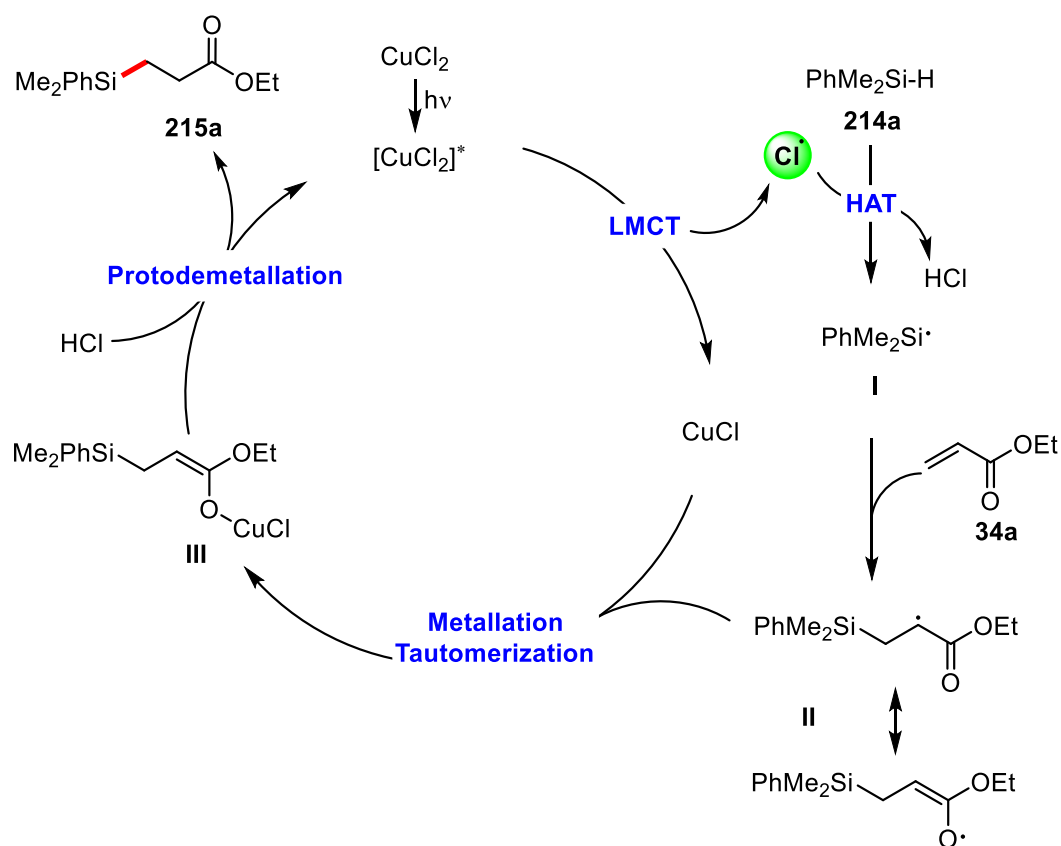
After having established the optimal conditions for the hydrosilylation of activated olefins, these were applied to a range of substrates. First, various arylsilanes (**215a-215c**) were tested and the corresponding products obtained in good yields. (TMS)₃Si-H (**215d**) reacts smoothly in this system to afford excellent yield. The alkylsilanes (**215e**) are also compatible with the reaction conditions. Interestingly, diphenylsilane **214f** can react efficiently to provide silicon ether **215f** in 33% yield. Dibutylsilane **214g** is also a suitable substrate, leading to the target product **215g** in moderate yield. Furthermore, this reaction has been tested with a wide range of electron deficient alkenes to determine the scope and limitation of the process. Alkyl acrylates, such as benzyl or ethyl acrylates, are viable alkene partners. Reaction with (ethene-1,1-diylldisulfonyl)dibenzene **34h** and (vinylsulfonyl)benzene **34i** gave moderate yields. In addition, ethyl 2-((phenylsulfonyl)methyl)acrylate **34j** and but-3-en-2-one **34k** are also compatible with the conditions, leading to desired product in useful yields. However, when cyclohex-2-en-1-one **34m** and ethyl (E)-but-2-enoate **34n** were used as substrates, either no product or only trace amounts of product were observed. This indicates that steric hindrance hinders the efficiency of the reaction in these particular cases. Electron-rich alkenes, such as 1-octene **34o**, are incompatible with this system and cannot yield the desired product.



Scheme 63 CuCl₂-catalyzed silylation of electron deficient alkenes

4.5.3 Proposed mechanism

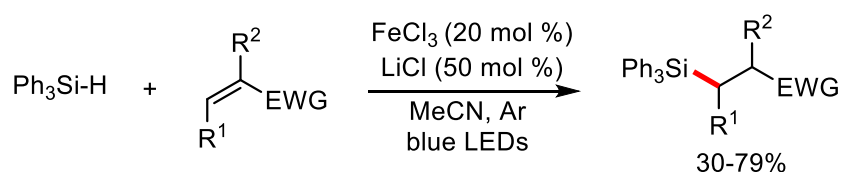
Based on previous literature reports and experimental data, a plausible mechanism was proposed (Scheme 64). First, upon irradiation with a 390 nm LED, CuCl₂ is excited to an excited state [CuCl₂*], which undergoes a Ligand-to-Metal Charge Transfer (LMCT) process, resulting in the generation of a chlorine atom radical. The chlorine atom radical would then react with dimethyl(phenyl)silane **214a** to provide HCl and silyl radical **I**. The addition reaction of the latter to ethyl acrylate **34a** would afford a more stable radical α to an ester **II** (which may also be written as an enoyl radical with spin density on the oxygen). A stable Cu(II)-enolate **III** is then formed by the recombination of CuCl with this electron-deficient radical **II**. The product **215a** is ultimately formed through protodemetalation with HCl, which leads to the regeneration of the photoactive CuCl₂.



4.6 Conclusion

In summary, we reported an efficient and practically simple strategy for the silylation of activated olefins using CuCl_2 as a HAT catalyst under 390 nm light. The interaction between copper(II) chloride and acetonitrile can produce a photoactive species, which generates an electrophilic chlorine radical through ligand-to-metal charge transfer under light irradiation. This radical can capture hydrogen atoms from silane to form a silicon-based radical, which can then undergo coupling reaction with an olefin to yield high-value-added products. This strategy is practical and easy to operate, with mild conditions and the use of inexpensive and readily available reagents. It is a meaningful alternative to the strategy of olefin silylation.

Unfortunately, a very similar work was recently published where FeCl_3 was used as a chlorine radical precursor instead of CuCl_2 (Figure 13),¹⁹⁷ so we will not pursue further study on this topic.



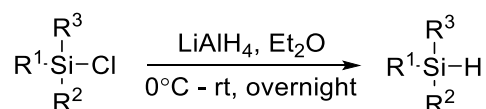
4.7 Experimental part

4.7.1 General information

General information is the same with chapter 3.

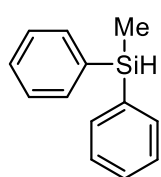
4.7.2 Synthesis of the starting Materials

General procedure A for the synthesis of silanes:



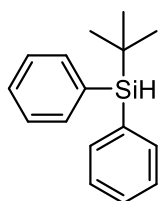
In a Schlenk tube under inert atmosphere chlorosilane (10 mmol, 1.0 equiv.) was dissolved in dry Et₂O (30 mL) and the mixture cooled to 0°C. The lithium aluminium hydride solution (4M, 10 mmol) was added dropwise. The reaction mixture was stirred at room temperature overnight. Then, H₂O (30 mL) was added dropwise to quench the reaction. Concentrated hydrochloric acid was added dropwise until two layers separated. The organic phases were washed with saturated NaHCO₃ until they gave basic PH, followed by washing with brine (30 mL). The organic phase was dried over Na₂SO₄, filtered and the residue was evaporated by reduced pressure to give product.

Methyldiphenylsilane (214c)¹⁵²

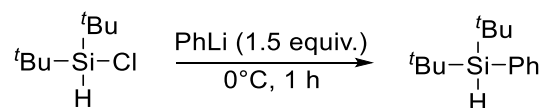


Based on general procedure A, starting from 2.3 g of chloro(methyl)diphenylsilane, product **215c** has been obtained as oil (1.75 g, 8.8 mmol, 88% yield). ¹H NMR (300 MHz, CDCl₃) δ 7.61 – 7.57 (m, 4H), 7.48 – 7.31 (m, 6H), 4.97 (qd, *J* = 3.8, 1.4 Hz, 1H), 0.66 (dd, *J* = 3.9, 1.1 Hz, 3H).

tert-Butyldiphenylsilane¹⁵³

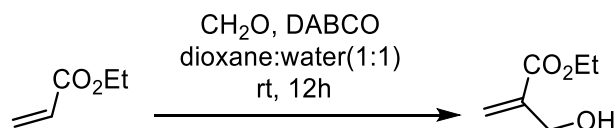


Based on general procedure A, starting from 1.65 g of tert-butylchlorodiphenylsilane, product has been obtained as oil (quantitative). ¹H NMR (300 MHz, CDCl₃) δ 7.73 – 7.63 (m, 4H), 7.45 – 7.33 (m, 6H), 4.65 (s, 1H), 1.08 (s, 9H).



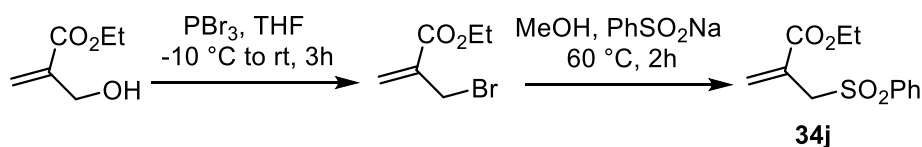
To a solution of di-*tert*-butyl(chloro)silane (1.43 g, 8.01 mmol, 1.0 equiv.) in THF (32 mL), phenyllithium (~ 1.9 M in n-Bu₂O, 6.3 mL, ~12 mmol, 1.5 equiv.) was added dropwise at 0°C. After stirring for 1 h, H₂O (~ 20 mL) was added. The phases were separated and the aqueous phase was extracted with *t*-Butylmethyl ether (~ 3 × 30 mL). The combined organic phase was dried over MgSO₄ and the solvents were removed under reduced pressure. Purification by flash column chromatography on silica gel using cyclohexane as eluent afford the desired product (1.32 g, 75%)¹⁵⁴

¹H NMR (300 MHz, CDCl₃) δ 7.63 – 7.54 (m, 2H), 7.43 – 7.27 (m, 3H), 3.87 (s, 1H), 1.06 (s, 18H).



To a solution of paraformaldehyde (3.98 g, 133.2 mmol) and ethylacrylate (10.8 mL, 100 mmol) in 80 mL of dioxane-water (1:1, v/v) was added DABCO (14.96 g, 133.2 mmol) and the reaction progress was monitored by TLC. Upon completion, the reaction mixture was partitioned with EtOAc (200 mL) and water (100 mL). The organic layer was separated and washed with brine (100 mL), dried over anhydrous Na_2SO_4 and concentrated under reduced pressure. The crude product was purified by column chromatography on silica gel to give the product as a colorless oil (6.10 g, 46% yield).¹⁵⁵

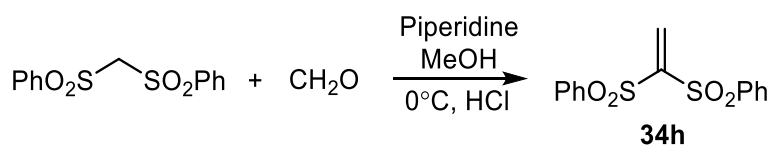
^1H NMR (300 MHz, CDCl_3) δ : 6.25 (q, $J = 0.9$ Hz, 1H), 5.82 (q, $J = 1.4$ Hz, 1H), 4.35-4.31 (m, 2H), 4.25 (qd, $J = 7.1, 1.2$ Hz, 2H), 2.27 (s, 1H), 1.32 (td, $J = 7.1, 1.0$ Hz, 3H).



First Step: Ethyl 2-(hydroxymethyl)acrylate (1.0 eq., 46.23 mmol, 6.10 g) was dissolved in dry THF (50 mL) at -10°C . To this mixture PBr_3 (0.34 eq., 16.18 mmol, 1.52 mL) was added. The temperature was allowed to rise to rt and stirring was continued for 3 h. Water (20 mL) was then added and the mixture was extracted with petroleum ether (3×100 mL). The organic phase was washed with brine (100 mL), dried over anhydrous Na_2SO_4 and concentrated under reduced pressure. The crude product was used in next step without purification.

Second Step: To the crude mixture of first step was taken in dry methanol (75 mL) and added sodium phenylsulfinate (1.2 eq., 47.43 mmol, 7.78g). After 2 h of reflux, the mixture was concentrated under reduced pressure. The obtained residue was dissolved in EtOAc and the mixture was washed with water, brine, dried with Na_2SO_4 , filtered and the filtrate was evaporated and purified by chromatography in silica gel with 8-10% EtOAc in PE as eluant to afford product as colorless oil (8.10 g, 69%).¹⁵⁵

^1H NMR (300 MHz, CDCl_3) δ : 7.91-7.80 (m, 2H), 7.70-7.58 (m, 1H), 7.60-7.47 (m, 2H), 6.50 (d, $J = 0.7$ Hz, 1H), 5.91 (q, $J = 0.8$ Hz, 1H), 4.16 (d, $J = 0.9$ Hz, 2H), 4.01 (q, $J = 7.1$ Hz, 2H), 1.16 (t, $J = 7.1$ Hz, 3H). ^{13}C NMR (100 MHz, CDCl_3) δ : 164.8, 138.4, 133.9, 133.3, 129.0, 128.8, 61.5, 57.5, 13.9.

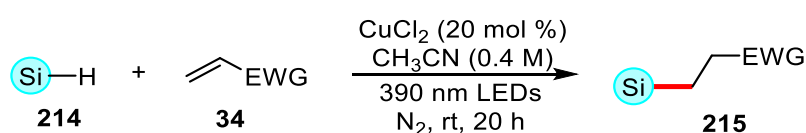


To a methanol (30 mL) solution of paraformaldehyde (40% in water), (2.3 g, 0.03 mol, 3 equiv.),

piperidine (4.9 mL, 0.15 mol; 5 equivalents) and bis(phenylsulfonyl)methane (3.05 g, 0.010 mol, 1 equiv.) were successively added slowly at 0°C. After 70 minutes at 0°C, a mixture of icy-water (70 mL) was added and stirred for 10 minutes. The white precipitate was filtered off and washed with additional 50 mL of cold water. The white solid thus obtained was re-dissolved in 30 mL of dichloromethane. 50 mL of HCl (1N) were added and the resulting biphasic mixture was stirred vigorously for 3 hours. Additional 25 mL of HCl (1N) were again added prior to separating the organic layer. The aqueous layer was further extracted 2 times with 50 mL of dichloromethane. The combined organic layers were dried on MgSO₄, filtered and the solvent evaporated to give the crude product (~95% pure). Recrystallization from CH₂Cl₂/cyclohexane (alternatively benzene can be used) yielded pure **34h** as a white solid (2.7 g; 8.7 mmol; 87% yield).¹⁵⁶

¹H NMR (300 MHz, CDCl₃) δ 7.99 – 7.93 (m, 4H), 7.73 – 7.63 (m, 2H), 7.60 – 7.52 (m, 4H), 7.22 (s, 2H).

4.7.3 General Procedure B for photoredox reactions



In a glovebox under an argon atmosphere, CuCl₂ (5.4 mg, 0.04 mmol, 20 mol%), silane **214** (0.6 mmol, 3 equiv.), and alkene **34** (0.2 mmol, 1 equiv.) in anhydrous MeCN (0.5 mL) were placed in a dried sealed tube. The tube was placed ~4 cm away from a 40 W 390nm LED and stirred for 20 h with cooling by fan. The mixture was concentrated in vacuo. The resulting residue was purified by silica gel chromatography using PE and EtOAc as eluent to afford **215**.

4.7.4 Characterization Data


Ethyl 3-(dimethyl(phenyl)silyl)propanoate (215a)¹⁵⁷

Based on general procedure **B**, starting from 20 mg of ethyl acrylate and 82 mg of dimethyl(phenyl)silane, product **215a** has been obtained as an oil (37.4 mg, 0.158 mmol, 79% yield). R_f = 0.5 (PE: EA = 10:1). ¹H NMR (300 MHz, CDCl₃) δ 7.57 – 7.50 (m, 2H), 7.41 – 7.37 (m, 3H), 4.12 (q, *J* = 7.1 Hz, 2H), 2.37 – 2.25 (m, 2H), 1.26 (t, *J* = 7.2 Hz, 3H), 1.20 – 1.06 (m, 2H), 0.33 (s, 6H).


Ethyl 3-(triphenylsilyl)propanoate (215b)¹⁵⁸

Based on general procedure **B**, starting from 20 mg of ethyl acrylate and 156 mg of triphenylsilane, product **215b** has been obtained as a white solid (39 mg, 0.108 mmol, 54% yield). R_f = 0.5 (PE: EA = 10:1). M.p. = 66 – 67°C. ¹H NMR (300 MHz, CDCl₃) δ 7.60 – 7.49 (m, 6H), 7.47 – 7.33 (m, 9H), 4.07 (q, *J* = 7.1 Hz, 2H), 2.51 – 2.37 (m, 2H), 1.81 – 1.68 (m, 2H), 1.22 (t, *J* = 7.1 Hz, 3H). ¹³C NMR (75 MHz, CDCl₃) δ 174.8, 135.7, 134.3, 129.8, 128.1, 60.6, 29.1, 14.3, 8.4. ²⁹Si NMR (60 MHz, CDCl₃) δ -10.64.

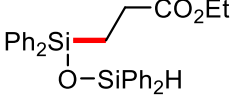
Ethyl 3-(methyldiphenylsilyl)propanoate (215c)¹⁵⁹

 Based on general procedure **B**, starting from 20 mg of ethyl acrylate and 119 mg of methyldiphenylsilane, product **215c** has been obtained as an oil (47 mg, 0.158 mmol, 79% yield). *R*_f = 0.5 (PE: EA = 10:1). ¹H NMR (300 MHz, CDCl₃) δ 7.60 – 7.47 (m, 4H), 7.45 – 7.30 (m, 6H), 4.08 (q, *J* = 7.1 Hz, 2H), 2.40 – 2.30 (m, 2H), 1.49 – 1.38 (m, 2H), 1.23 (t, *J* = 7.2 Hz, 3H), 0.59 (s, 3H). ¹³C NMR (76 MHz, CDCl₃) δ 174.8, 136.3, 134.6, 129.5, 128.1, 60.5, 29.0, 14.3, 9.5, -4.5. ²⁹Si NMR (60 MHz, CDCl₃) δ -6.77.

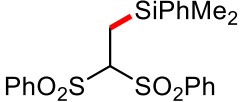
Ethyl 3-(1,1,1,3,3,3-hexamethyl-2-(trimethylsilyl)trisilan-2-yl)propanoate (215d)

 Based on general procedure **B**, starting from 20 mg of ethyl acrylate and 149 mg of 1,1,1,3,3,3-hexamethyl-2-(trimethylsilyl)trisilane, product **215d** has been obtained as an oil (62 mg, 0.178 mmol, 89% yield). *R*_f = 0.65 (PE: EA = 15:1). ¹H NMR (300 MHz, CDCl₃) δ 4.12 (q, *J* = 7.1 Hz, 2H), 2.41 – 2.25 (m, 2H), 1.25 (t, *J* = 7.1 Hz, 3H), 1.14 – 1.05 (m, 2H), 0.17 (s, 27H). ¹³C NMR (76 MHz, CDCl₃) δ 174.8, 60.5, 33.4, 14.4, 2.9, 1.2. ²⁹Si NMR (60 MHz, CDCl₃) δ -12.85, -80.79.


Ethyl 3-(1,1,3,3-tetraphenyldisiloxanyl)propanoate (215f)

 Based on general procedure **B**, starting from 20 mg of ethyl acrylate and 111 mg of diphenylsilane, product **215f** has been obtained as an oil (31 mg, 0.066 mmol, 33% yield). *R*_f = 0.5 (PE: EA = 10:1). ¹H NMR (300 MHz, CDCl₃) δ 7.60 – 7.48 (m, 8H), 7.47 – 7.28 (m, 12H), 5.63 (s, 1H), 4.02 (q, *J* = 7.1 Hz, 2H), 2.35 – 2.23 (m, 2H), 1.50 – 1.39 (m, 2H), 1.19 (t, *J* = 7.1 Hz, 3H). ¹³C NMR (76 MHz, CDCl₃) δ 174.6, 135.3, 134.5, 134.4, 130.4, 130.1, 128.1, 128.0, 60.5, 28.1, 14.3, 10.7. ²⁹Si NMR (60 MHz, CDCl₃) δ -9.14, -20.30.

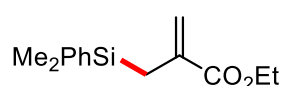
(2,2-Bis(phenylsulfonyl)ethyl)dimethyl(phenyl)silane (215h)

 Based on general procedure **B**, starting from 62 mg of (ethene-1,1-diyldisulfonyl)dibenzene and 82 mg of dimethyl(phenyl)silane, product **215h** has been obtained as an oil (34 mg, 0.076 mmol, 38% yield). *R*_f = 0.3 (PE: EA = 3:1). ¹H NMR (300 MHz, CDCl₃) δ 7.74 – 7.60 (m, 6H), 7.53 – 7.39 (m, 9H), 4.39 (t, *J* = 6.6 Hz, 1H), 1.61 (d, *J* = 6.6 Hz, 2H), 0.45 (s, 6H). ¹³C NMR (75 MHz, CDCl₃) δ 137.6, 136.6, 134.4, 134.3, 129.8, 129.7, 129.0, 128.3, 81.9, 11.4, -1.9. ²⁹Si NMR (60 MHz, CDCl₃) δ -0.14.

Methyldiphenyl(2-(phenylsulfonyl)ethyl)silane (215i)¹⁶⁰

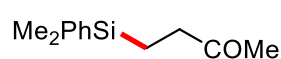
 Based on general procedure **B**, starting from 33.6 mg of (vinylsulfonyl)benzene and 119 mg of methyldiphenylsilane, product **215i** has been obtained as an oil (24 mg, 0.066 mmol, 33% yield). *R*_f = 0.3 (PE: EA = 5:1). ¹H NMR (300 MHz, CDCl₃) δ 7.91 – 7.84 (m, 2H), 7.70 – 7.61 (m, 1H), 7.59 – 7.53 (m, 2H), 7.46 – 7.29 (m, 10H), 3.08 – 2.97 (m, 2H), 1.54 – 1.43 (m, 2H), 0.55 (s, 3H). ¹³C NMR (75 MHz, CDCl₃) δ 138.7, 134.8, 134.4, 133.7, 130.0, 129.4, 128.4, 128.3, 52.4, 7.3, -4.5. ²⁹Si NMR (60 MHz, CDCl₃) δ -7.04.

Ethyl 2-((dimethyl(phenyl)silyl)methyl)acrylate (215j)



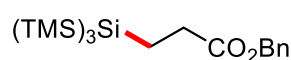
Based on general procedure **B**, starting from 51 mg of ethyl 2-((phenylsulfonyl)methyl)acrylate and 82 mg of dimethyl(phenyl)silane, product **215j** has been obtained as an oil (17 mg, 0.068 mmol, 34% yield). $R_f = 0.6$ (PE: EA = 10:1). $^1\text{H NMR}$ (300 MHz, CDCl_3) δ 7.54 – 7.49 (m, 2H), 7.37 – 7.34 (m, 3H), 5.98 (d, $J = 1.6$ Hz, 1H), 5.24 (q, $J = 1.3$ Hz, 1H), 4.10 (q, $J = 7.1$ Hz, 2H), 2.07 (d, $J = 1.1$ Hz, 2H), 1.24 (t, $J = 7.1$ Hz, 3H), 0.29 (s, 6H). $^{13}\text{C NMR}$ (76 MHz, CDCl_3) δ 167.7, 138.2, 133.8, 133.1, 129.2, 127.8, 122.3, 60.8, 21.5, 14.3, -3.2. $^{29}\text{Si NMR}$ (60 MHz, CDCl_3) δ -3.57.

4-(Dimethyl(phenyl)silyl)butan-2-one (215k)¹⁴²



Based on general procedure **B**, starting from 14 mg of but-3-en-2-one and 82 mg of dimethyl(phenyl)silane, product **215k** has been obtained as an oil (8 mg, 0.04 mmol, 20% yield). $R_f = 0.5$ (PE: EA = 10:1). $^1\text{H NMR}$ (300 MHz, CDCl_3) δ 7.56 – 7.45 (m, 2H), 7.42 – 7.31 (m, 3H), 2.42 – 2.32 (m, 2H), 2.09 (d, $J = 0.6$ Hz, 3H), 1.05 – 0.96 (m, 2H), 0.28 (s, 6H).

Benzyl 3-(1,1,1,3,3,3-hexamethyl-2-(trimethylsilyl)trisilan-2-yl)propanoate (215l)



Based on general procedure **B**, starting from 32.4 mg of benzyl acrylate and 149 mg of 1,1,1,3,3,3-hexamethyl-2-(trimethylsilyl)trisilane, product **215l** has been obtained as an oil (70 mg, 0.17 mmol, 85% yield). $R_f = 0.65$ (PE: EA = 20:1). $^1\text{H NMR}$ (300 MHz, CDCl_3) δ 7.42 – 7.31 (m, 5H), 5.13 (s, 2H), 2.45 – 2.34 (m, 2H), 1.20 – 1.10 (m, 2H), 0.19 (s, 27H). $^{13}\text{C NMR}$ (75 MHz, CDCl_3) δ 174.6, 136.3, 128.7, 128.4, 128.3, 66.4, 33.3, 3.0, 1.2. $^{29}\text{Si NMR}$ (60 MHz, CDCl_3) δ -12.83, -80.73.

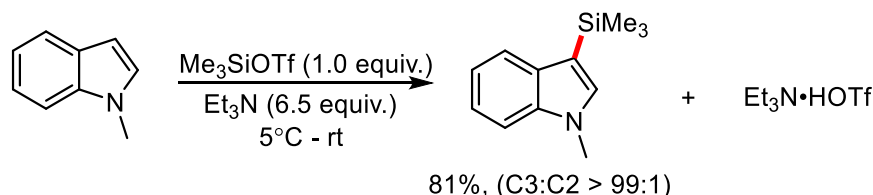
Chapter 5 Visible-light mediated silylation of aryl/ heteroaryl/alkyl bromide using hydrosilanes

5.1 Introduction

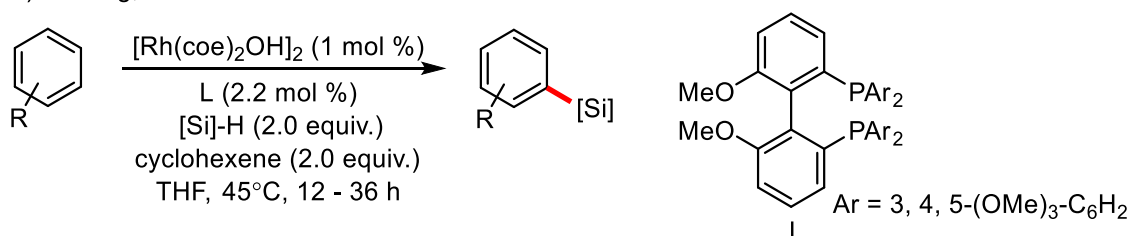
The traditional approach to build organosilicon compounds with C–Si bonds involves the nucleophilic coupling between organometallic reagents (such as Grignard reagents, organolithium reagents, organozinc reagents, etc.) and chlorosilanes and/or epoxysilanes.^{161, 162} This strategy, although very efficient has its drawbacks, including low functional group compatibility due to the high basicity of the reagents, often harsh reaction conditions, and poor atom economy. C–H silylation through electrophilic aromatic substitution (S_EAr, Friedel-Crafts) is a powerful technique. In 1984, Simchen¹⁶³ and co-workers achieved highly regioselective C–H silylation of indoles and pyrroles by using Me₃SiOTf as electrophile and Et₃N as solvent (Scheme 65a). Inspired by this, Kawashima¹⁶⁴, Oestreich¹⁶⁵⁻¹⁶⁸, Ingleson¹⁶⁹, Hou¹⁷⁰, and Zhang¹⁷¹ *et al.* developed a series of efficient S_EAr strategies to construct C–Si bonds. Typically, only aromatics with a high electron density could be smoothly silylated using this approach. Recently, transition metal-catalyzed cross-dehydrogenative coupling between arenes/heteroarenes and hydrosilanes to deliver arylsilanes has grown in popularity.¹⁷²⁻¹⁷⁵ For instance, Falck¹⁷⁶ reported an Iridium-catalyzed C–H silylation of heteroarenes in the presence of bipyridine and 2-norbornene. Oestreich¹⁶⁵ and co-workers later disclosed ruthenium(II) thiolate complex catalyzed indole C–H silylation with complete regioselectivity. In 2014, Hartwig¹⁷⁷ *et al.* developed an efficient method to access arylsilanes in high yields with excellent steric control using rhodium as catalyst, cyclohexene as a simple hydrogen acceptor, and a widely available hydrosilane as silicon source (Scheme 65b). The regioselectivity of arene silylation derives from a high level of steric control by *ortho* and *meta* substituents to the reacting C–H bond. The research group subsequently reported the iridium-catalyzed silylation of aryl C–H bonds.¹⁷⁸ Compared to the previously described rhodium-catalyzed silylation of aryl C–H bonds, this new catalytic system occurs with a much higher tolerance for functional groups and occurs with a variety of heteroarenes. The following challenges in arene C–H silylation nevertheless continue to exist, including: 1) low regioselectivity; 2) need of directing groups, noble metal catalysts, and hydrogen acceptors. More recently, Liu¹⁷⁹ and co-workers discovered a radical mediated site-selective aryl/heteroaryl C–H silylation in the presence of Cu₂O catalyst, DTBP, and hydrosilane (Scheme

65c). This strategy exhibits exceptional *para*-selectivity, possibly due to the resonance stability of the radical. However, large excess of peroxide and hydrosilane, and high temperatures are required. Hence, we reported a visible-light mediated synergistic catalytic strategy of iridium and nickel for the construction of arylsilanes, using inexpensive and readily available hydrosilanes as the silicon source and aryl bromides as the aryl source (Scheme 65d).

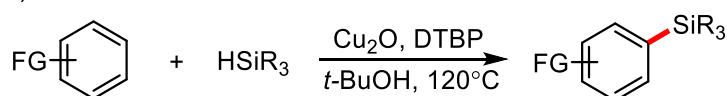
a) Simchen, 1984



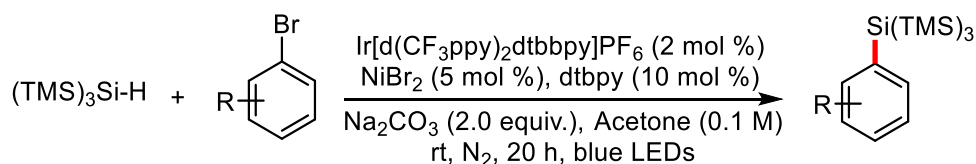
b) Hartwig, 2014



c) Liu, 2017



d) This work



Scheme 65 Cross-coupling reaction of aryl bromides or arenes with silylating reagents.

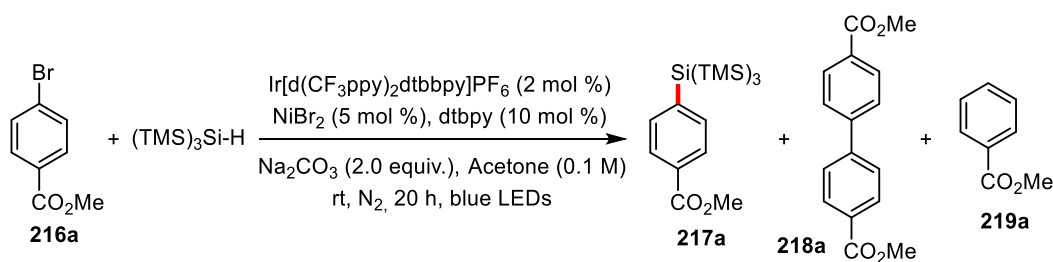
5.2 Results and discussion

5.2.1 Optimization of silylation of methyl 4-bromobenzoate

First, methyl 4-bromobenzoate **216a** was used as model substrate and TMS₃SiH as the silicon source to optimize the reaction conditions. Following extensive screening, we discovered that a combination of [Ir(dF(CF₃)ppy)₂(dtbbpy)]PF₆ as a photocatalyst with NiBr₂ as a synergistic catalyst, sodium carbonate (Na₂CO₃) as the base at room temperature in acetone, could deliver the product in optimum yield (entry 1). We also observed various amount of a biaryl compound **218a** as a result of a Ullmann-type coupling and the debrominated product **219a** which could not be separated from the

unreacted starting material. Absence or traces of **217a** was observed when the reaction was performed in the absence of a catalyst (entry 2), light (entry 3) or base (entry 4). The target product was then produced in 45% yield when the organic photocatalyst 4CzIPN was utilized in place of [Ir(dF(CF₃)ppy)₂(dtbbpy)]PF₆ (entry 5), indicating that 4CzIPN is also efficient photocatalyst. Stronger inorganic bases, as K₂CO₃ and K₃PO₄, led to decomposition of the starting material and a significantly lower yield (entry 6 and 7). The organic base 2,6-lutidine efficiently yielded the corresponding product, albeit in low yield (entry 8). The nature of the Ni(II) catalyst was also studied. NiCl₂·glyme, NiBr₂·glyme, and NiBr₂ all afforded comparable yields, however NiBr₂ is the cheapest available (entry 9-11). Next, several ligands were also screened, with dtbpy providing the best yields. Interestingly, when 5,5'-CF₃-bpy was employed as a ligand, the self-coupling product **218a** was the main product with a 47% yield (entry 14). Several solvents were also used to optimize the reaction conditions (entries 15-17). Acetone proved to be the best.

Table 4. Optimization for the silylation of methyl 4-bromobenzoate.



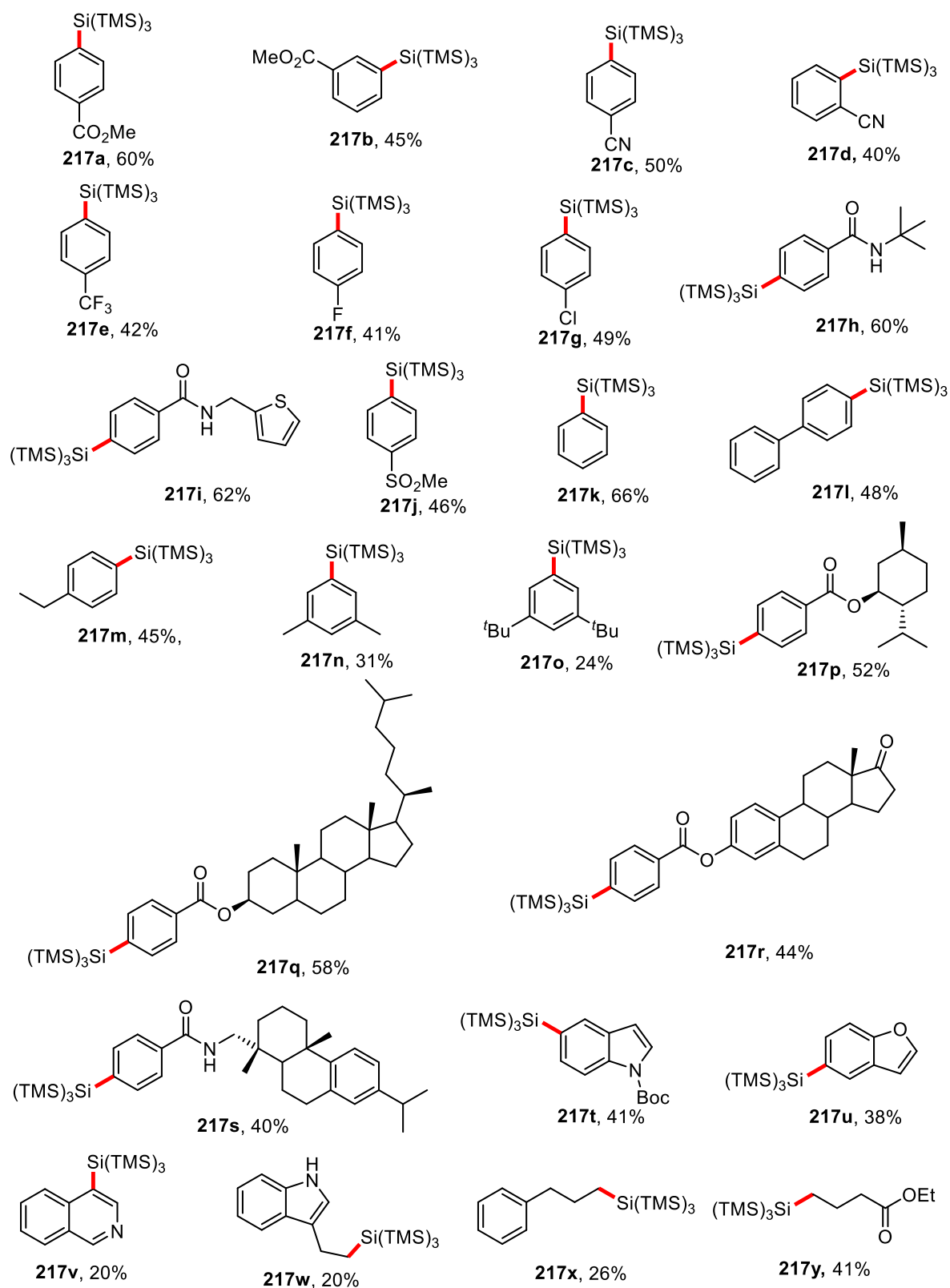
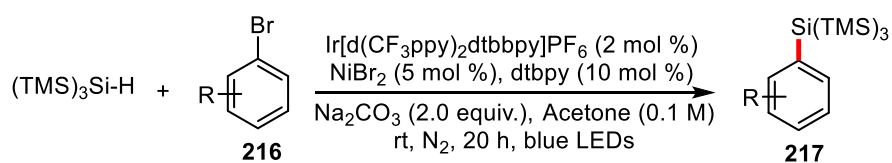
Entry	Deviation from standard conditions ^a	Yield (%) ^c (217a)	Yield (%) ^c (218a)	Yield (%) ^c (219a+216a)
1	none	62	11	14
2	no catalyst [Ir]	0	0	0
3	no light	0	0	0
4	no base	trace	trace	trace
5	4CzIPN instead of [Ir]	45	7	11
6 ^b	K ₂ CO ₃	< 10	-	-
7 ^b	K ₃ PO ₄	< 10	-	-
8 ^b	2,6-lutidine	37	4	36
9 ^b	NiCl ₂ ·glyme	42	16	30
10 ^b	NiBr ₂ ·glyme	44	17	20
11 ^b	NiBr ₂	44	5	12
12 ^b	bipy	38	24	25
13 ^b	4,4'-OMe-bpy	21	6	32
14 ^b	5,5'-CF ₃ -bpy	17	47	11
15 ^b	DCM	0	0	0
16 ^b	DME	39	30	19
17 ^b	MeCN	33	20	21

^a Standard conditions: Ir[d(CF₃ppy)₂dtbbpy]PF₆ (2 mol %), NiBr₂ (5 mol %), dtbpy (10 mol %), Na₂CO₃ (2 equiv.), **216a** (0.2 mmol, 1 equiv.), Tri(trimethylsilyl)silane (0.6 mmol, 3 equiv.), Acetone (2.0 mL), Kessil 40 W Blue LEDs, rt, 20 h. ^b Tri(trimethylsilyl)silane (0.4 mmol, 2 equiv.) ^c ¹H NMR yields of **217a**, **218a**, and **219a** using mesitylene as an internal standard.

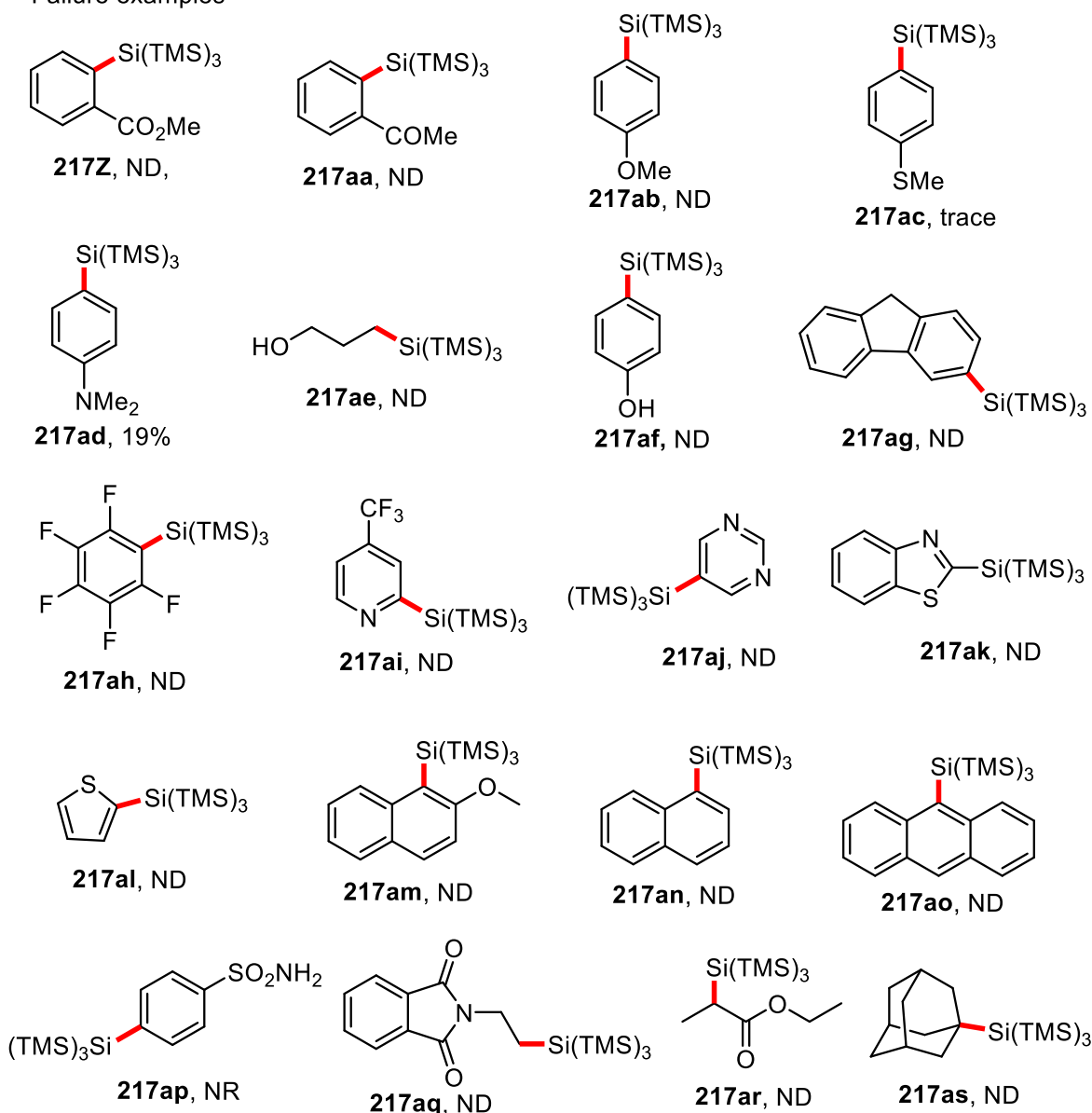
5.2.2 Substrate scope

After having established the optimal conditions, various bromides were investigated, and the corresponding products generated in moderate to good yields, as shown in Scheme 66. When the benzene ring bears electron-deficient groups, such as ester (**217a**, **217b**, **217p-r**), cyano (**217c**, **217d**), amide (**217h**, **217i**, **217s**), sulfone (**217j**), halogen (**217f**, **217g**), and trifluoromethyl (**217e**), it can react smoothly. Interestingly, the reaction is selective for bromine in the presence of chlorine as in **217g**. Steric hindrance around the reacting center appears as a limiting factor as shown with the formation of **217d** in moderate yield. When methyl 2-bromobenzoate **217z** was tried as a substrate, no reaction was observed. Certain electron-donating groups, such as methyl (**217n**), ethyl (**217m**), and *tert*-butyl (**217o**), are also compatible with this system, although the yield is lower, most likely due to the ease with which electron-rich aromatic rings are oxidized by excited-state photocatalyst. Interestingly, derivatives of some natural products (**217p-s**) also react efficiently, providing the desired product in moderate to good yields. To our satisfaction, although the yield was low, we found that heteroaromatics (**217t-v**) were also appropriate substrates for this reaction conditions. In addition, primary bromoalkanes can also react smoothly to afford the corresponding products (**217w-y**) in useful yields.

However, when strong electron-donating groups such as methoxy **217ab**, and methylthio **217ac** groups are present on the benzene ring, the silylated products were not detected. It appears that oxygen-containing functional groups, such as hydroxyl (**217ae** and **af**), and acyl (**217aa** and **217aq**) groups, are not compatible with this system. It is possible that Si-centered radicals and oxygen atoms have a strong affinity. Heteroaromatic rings **217ai-al** exhibit unsuitability as substrates and fail to produce the desired products. Substances with rigid structures such as naphthalene (**217am** and **217an**) and anthracene **217ao** tend to preferentially form self-coupling products. Free amino groups, such as **217 ap**, are also not tolerant under the reaction conditions.



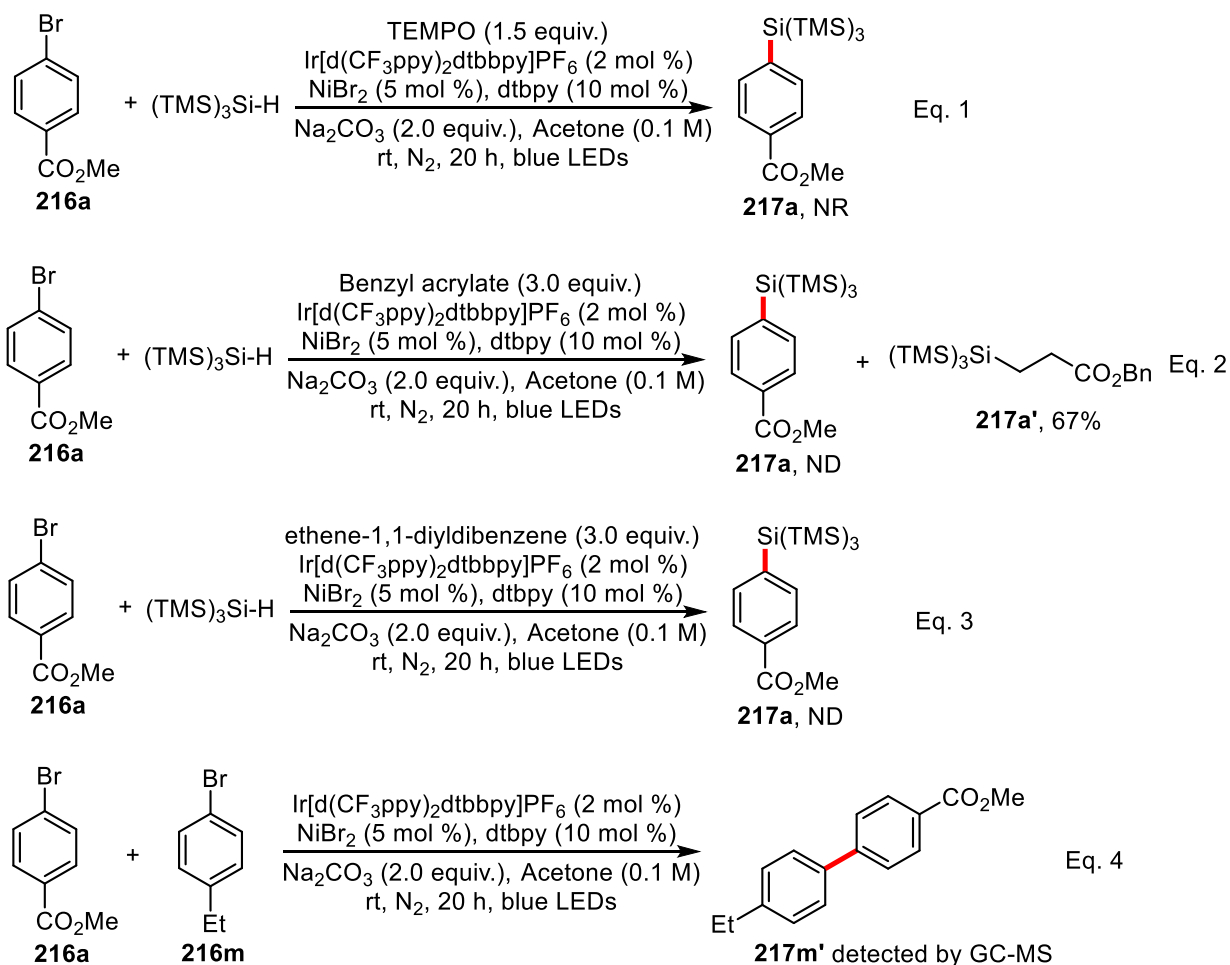
Failure examples



Scheme 66 Scope of bromide.

5.2.3 Mechanistic studies

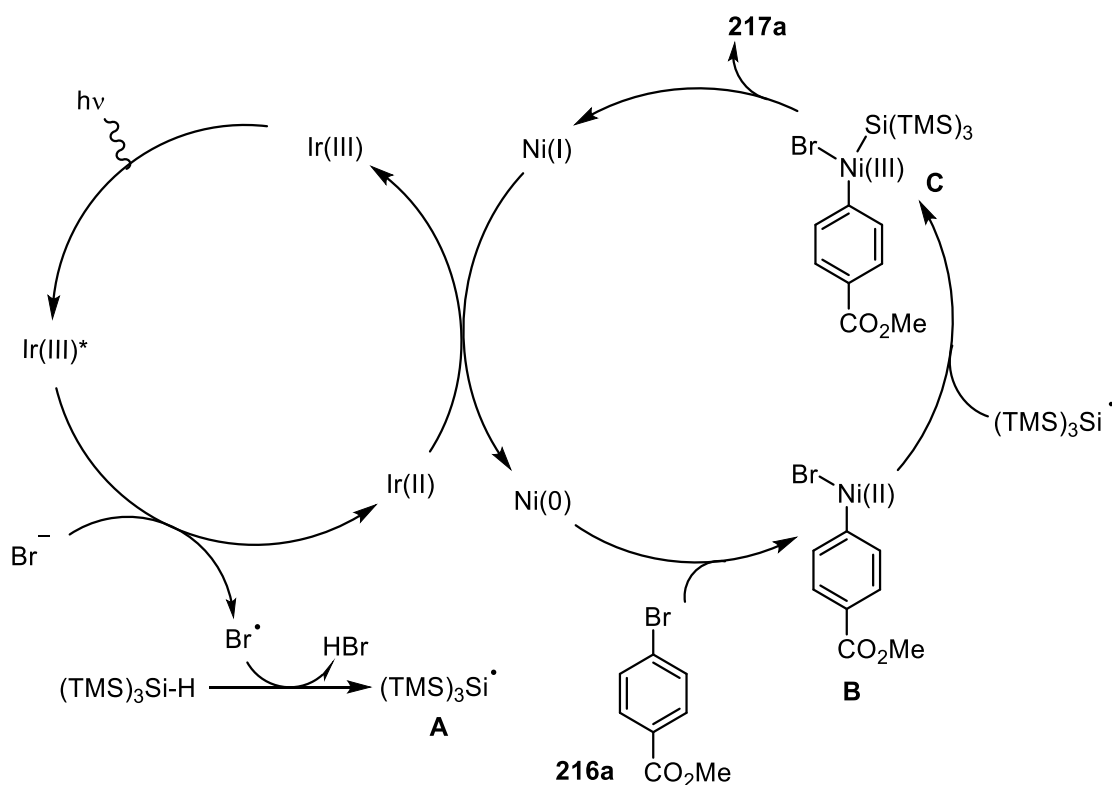
Preliminary mechanistic investigations were also performed. For instance, when the reaction between **216a** and $(\text{TMS})_3\text{Si-H}$ under the conditions described above is repeated in the presence of TEMPO, no reaction occurs, indicating the occurrence of a radical process (Scheme 67, Eq. 1). Next, benzyl acrylate was used as a radical trapper added to the reaction, the addition product **217a'** was isolated in 67% yield, indicating the generation of $(\text{TMS})_3\text{Si}\cdot$ radical. Finally, methyl 4-bromobenzoate **216a** reacts with 1-bromo-4-ethylbenzene **216m** under the standard conditions leading to the coupling product **217m'** which was detected by GC-MS. This observation suggests that an aryl radical is generated during the process.



Scheme 67 Mechanistic experiments.

5.2.4 Proposed mechanism

Based on previous literature reports and experimental data, a plausible mechanism was proposed (Scheme 68). The Br⁻ is oxidized by Ir(III)* in its excited-state, generated by blue LED light irradiation, to give Br[•] and Ir(II). The former abstracts a hydrogen from the silane to afford the silyl radical **A**. Meanwhile, the Ni(I) is reduced by the resulting Ir(II) to form the photoactivable Ir(III) and Ni(0). Oxidative addition of methyl 4-bromobenzoate **216a** to the Ni(0) provides the Ni(II) species **B**. The silyl radical **A** is trapped by Ni(II) species **B** leading to the Ni(III) complex **C**, which upon reductive elimination generates the final product **217a**.



Scheme 68 suggested mechanism.

5.3 Conclusion

In summary, we developed a powerful catalytic method for the synthesis of diverse arylsilanes from the corresponding aryl bromides without the recourse to strongly basic reagents including organo-lithiums. The use of the complex $[\text{Ir}(\text{dF}(\text{CF}_3)\text{ppy})_2(\text{dtbbpy})]\text{PF}_6$ in combination with NiBr_2 catalyst/dtbbpy system has been discovered to be a remarkably effective protocol for synthesizing aryl/heteroaryl/alkyl silanes using commercially available hydrosilanes as a silicon source. This approach exhibits extraordinary tolerance towards functional groups, regardless of whether they possess electron-deficient or electron-rich properties, leading to desired products with satisfactory yield. In addition, not only aryl bromides and heteroaryl bromides, but also primary alkyl bromides can serve as suitable substrates.

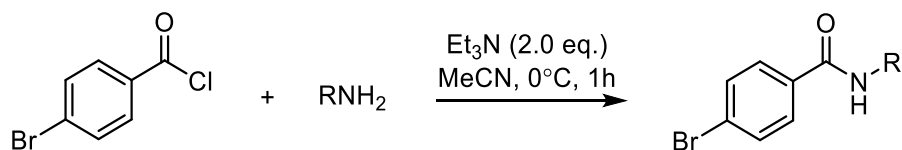
5.4 Experimental part

5.4.1 General information

General information is the same with chapter 3.

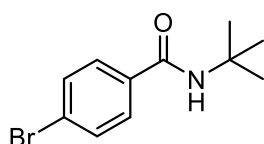
5.4.2 Synthesis of the starting Materials

General procedure A for the synthesis of amides:



To a solution of 4-bromobenzoyl chloride (1 equiv.) in acetonitrile (0.67 M) were added an appropriate amine (1.5 equiv.), triethylamine (2 equiv.), and then this reaction mixture was stirred at 0 °C for 1 h. The reaction mixture was washed with water, and then the aqueous layer was extracted with dichloromethane. The organic layer was dried and concentrated, and the resulting residue was purified by column chromatography on silica gel.

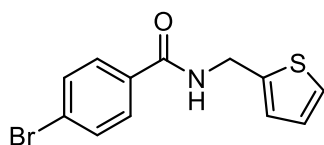
4-Bromo-N-(tert-butyl)benzamide (216h)¹⁸⁰



Based on general procedure A, starting from 1.1 g of 4-bromobenzoyl chloride, product **216h** has been obtained as white solid (0.78 g, 3.05 mmol, 61% yield).

¹H NMR (300 MHz, CDCl₃) δ 7.63 – 7.47 (m, 4H), 5.89 (s, 1H), 1.46 (s, 9H).

4-Bromo-N-(thiophen-2-ylmethyl)benzamide (216i)



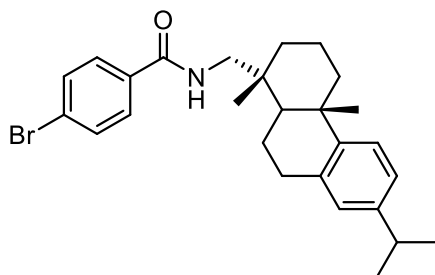
Based on general procedure A, starting from 1.1 g of 4-bromobenzoyl chloride, product **216i** has been obtained as white solid (0.79 g, 2.66 mmol, 53% yield). M.p. = 166 – 167 °C (DCM). ¹H NMR (300 MHz, CDCl₃) δ 7.68 – 7.60 (m, 2H), 7.58 – 7.51 (m, 2H), 7.24 (dd, *J* = 5.1, 1.3

Hz, 1H), 7.02 (dt, *J* = 3.1, 1.0 Hz, 1H), 6.96 (dd, *J* = 5.1, 3.5 Hz, 1H), 6.57 (s, 1H), 4.78 (dd, *J* = 5.6, 0.9 Hz, 2H). ¹³C NMR (76 MHz, CDCl₃) δ 166.3, 140.6, 133.1, 132.0, 128.8, 127.1, 126.5, 125.6, 39.0.

FT-IR $\bar{\nu}_{\max}$ (cm⁻¹) = 3318, 3081, 1641, 1546, 847, 696.

HRMS (ESI): calcd for C₁₂H₁₀NOSBrNa [M+Na]⁺: 317.95587, found 317.95471, delta = -3.64 ppm.

4-Bromo-N-(((1R,4aS)-7-isopropyl-1,4a-dimethyl-1,2,3,4,4a,9,10,10a-octahydrophenanthren-1-yl)methyl)benzamide (216s)



Based on general procedure A, starting from 1.1 g of 4-bromobenzoyl chloride, product **216s** has been obtained as white solid (1.22 g, 2.6 mmol, 52% yield). M.p. = 180 – 181 °C (DCM).

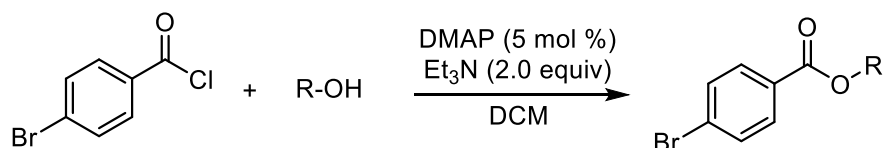
¹H NMR (300 MHz, CDCl₃) δ 7.67 – 7.47 (m, 4H), 7.18 (d, *J* = 8.2 Hz, 1H), 7.00 (dd, *J* = 8.1, 2.1 Hz, 1H), 6.89 (d, *J* = 2.0 Hz, 1H), 6.15 (t, *J* = 6.5 Hz, 1H), 3.49 – 3.26 (m, 2H), 3.01 – 2.73

(m, 3H), 2.40 – 2.25 (m, 1H), 1.97 (ddt, *J* = 13.2, 7.1, 2.1 Hz, 1H), 1.86 – 1.67 (m, 3H), 1.56 – 1.33 (m, 4H), 1.24 (d, *J* = 1.0 Hz, 6H), 1.22 (s, 3H), 1.01 (s, 3H). ¹³C NMR (76 MHz, CDCl₃) δ 166.9, 147.1, 145.8, 134.8, 133.8, 131.9, 128.6, 127.1, 126.1, 124.3, 124.1, 50.5, 46.0, 38.5, 37.8, 37.7, 36.6, 33.5, 30.5, 25.6, 24.09, 24.07, 19.2, 18.9, 18.8.

FT-IR $\bar{\nu}_{\max}$ (cm⁻¹) = 3315, 2957, 2925, 2854, 1640, 1545, 1482, 1305.

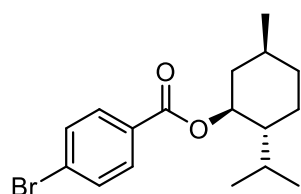
HRMS (ESI): calcd for C₂₇H₃₅BrNO [M+H]⁺: 468.18965, found 468.18799, delta = -3.56 ppm.

General procedure B for the synthesis of ester:



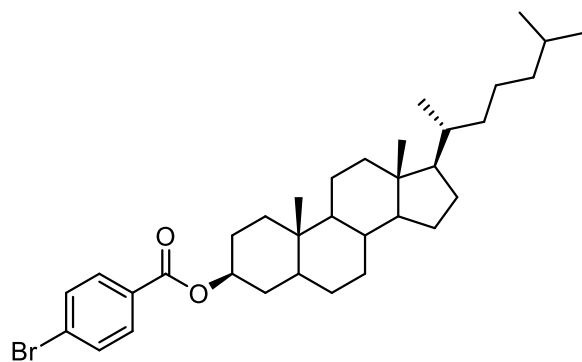
In a round bottom flask, 4-bromobenzoyl chloride (1.0 equiv.), the alcohol (1.2 equiv.) and 4-dimethylaminopyridine (5.0 mol%) are suspended in DCM (0.4 M). Next, triethylamine (2.0 equiv.) was added dropwise to the stirred solutions. The reaction was allowed to stir overnight at room temperature. Reaction was then quenched with saturated NH₄Cl and extracted with DCM. The crude material was purified by flash column chromatography to give the corresponding substituted aryl bromide.

(1S,2R,5S)-2-Isopropyl-5-methylcyclohexyl 4-bromobenzoate (216p)¹⁸¹



Based on general procedure **B**, starting from 1.75 g of 4-bromobenzoyl chloride, product **216p** has been obtained as oil (1.46 g, 4.3 mmol, 54% yield). ¹H NMR (300 MHz, CDCl₃) δ 7.92 – 7.88 (m, 2H), 7.59 – 7.56 (m, 2H), 4.92 (td, J = 10.9, 4.4 Hz, 1H), 2.14 – 2.08 (m, 1H), 1.97 – 1.87 (m, 1H), 1.80 – 1.66 (m, 2H), 1.62 – 1.50 (m, 2H), 1.23 – 1.00 (m, 2H), 0.99 – 0.88 (m, 7H), 0.78 (d, J = 6.9 Hz, 3H).

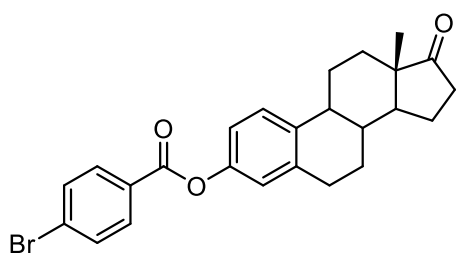
(3S,10S,13R,17R)-10,13-Dimethyl-17-((R)-6-methylheptan-2-yl)hexadecahydro-1H-cyclopenta[a]phenanthren-3-yl 4-bromobenzoate (216q)



Based on general procedure **B**, starting from 1.1 g of 4-bromobenzoyl chloride, product **216q** has been obtained as white solid (1.8 g, 3.14 mmol, 63% yield). M.p. = 181 – 182 °C (DCM). ¹H NMR (300 MHz, CDCl₃) δ 7.89 (d, J = 8.1 Hz, 2H), 7.55 (d, J = 8.1 Hz, 2H), 4.87 – 4.98 (m, 1H), 2.03 – 1.87 (m, 2H), 1.86 – 1.59 (m, 5H), 1.58 – 1.44 (m, 4H), 1.41 – 1.20 (m, 9H), 1.17 – 1.07 (m, 6H), 1.03 – 0.96 (m, 3H), 0.90 (d, J = 6.5 Hz, 3H), 0.89 – 0.80 (m, 10H), 0.75 – 0.66 (m, 1H), 0.65 (s, 3H). ¹³C NMR (76 MHz, CDCl₃) δ 165.5, 131.7, 131.2, 130.0, 127.9, 74.9, 56.6, 56.4, 54.4, 44.8, 42.7, 40.1, 39.7, 36.9, 36.3, 36.0, 35.6, 35.6, 34.2, 32.1, 28.8, 28.4, 28.2, 27.7, 24.4, 24.0, 23.0, 22.7, 21.4, 18.8, 12.4, 12.2. FT-IR $\bar{\nu}_{\max}$ (cm⁻¹) = 2950, 2932, 2849, 1715, 1287, 1270, 1115.

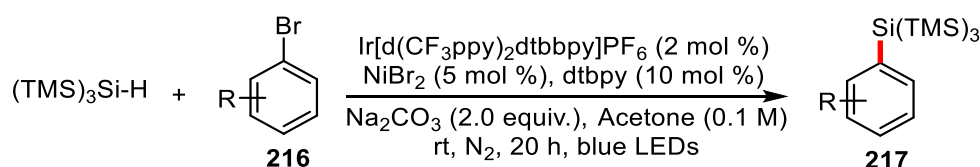
HRMS (ESI): calcd for C₃₄H₅₁O₂BrNa [M+Na]⁺: 593.2965, found 593.2966, delta = 0 ppm.

(13S)-13-Methyl-17-oxo-7,8,9,11,12,13,14,15,16,17-decahydro-6H-cyclopenta[a]phenanthren-3-yl 4-bromobenzoate (216r)¹⁸²



para-Bromobenzoic acid (1.01 g, 5.0 mmol), 1,3,5(10)-Estratrien-3-ol-17-one (1.38 g, 5.1 mmol), DMAP (122 mg, 1.0 mmol) and dry CH₂Cl₂ (50 mL) were added into a 250 mL round-bottom flask. Under a nitrogen atmosphere, DCC (1.15 g, 5.5 mmol) was added into the above flask in one portion at room temperature, then reaction mixture was stirred at room temperature for 12 hours. After filtering off the solids, the reaction solution was then concentrated by rotary evaporation and the resulting crude solid was purified by column chromatography (5% EtOAc in PE) to afford 70% yield (1.6 g) of **216r** as a white solid. ¹H NMR (300 MHz, CDCl₃) δ 8.10 – 8.00 (m, 2H), 7.70 – 7.60 (m, 2H), 7.34 (dd, *J* = 8.5, 1.1 Hz, 1H), 7.02 – 6.90 (m, 2H), 2.92 – 2.97 (m, 2H), 2.59 – 2.39 (m, 2H), 2.38 – 2.25 (m, 1H), 2.22 – 1.92 (m, 4H), 1.72 – 1.43 (m, 6H), 0.93 (s, 3H).

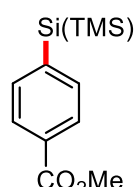
5.4.3 General Procedure C for photoredox reactions



To a Schlenk tube with a screw-cap was added [Ir[dF(CF₃)ppy]₂(dtbbpy)]PF₆ (4.5 mg, 0.004 mmol, 2 mol%), NiBr₂ (2.2 mg, 0.01 mmol, 5 mol %), dtbbpy (5.4 mg, 0.02 mmol, 10 mol %), aryl bromide **216** (0.2 mmol, 1.0 equiv.) (if solid) and Na₂CO₃ (42.4 mg, 0.4 mmol, 2.0 equiv.). The tube was evacuated and back-filled with nitrogen (this process was repeated three times). Aryl bromide **216** (0.2 mmol, 1.0 equiv.) (if liquid), (TMS)₃Si-H (149 mg, 0.6 mmol, 3.0 equiv.) and acetone (2 mL) were added consecutively via syringe. The resulting mixture degassed via three cycles of freeze-pump-backfill-thaw. The reaction was sealed and placed ~4 cm away from a 40 W blue LED and stirred for 20 h with cooling by fan. The mixture was concentrated in vacuo. The resulting residue was purified by silica gel chromatography to afford **217**.

5.4.4 Characterization Data

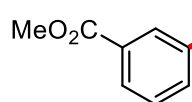
Methyl 4-(1,1,1,3,3,3-hexamethyl-2-(trimethylsilyl)trisilan-2-yl)benzoate (217a)

 Based on general procedure C, starting from 43 mg of methyl 4-bromobenzoate, product **217a** has been obtained as oil (46 mg, 0.12 mmol, 60% yield). ¹H NMR (300 MHz, CDCl₃) δ 7.93 – 7.86 (m, 2H), 7.55 – 7.50 (m, 2H), 3.90 (s, 3H), 0.22 (s, 27H). ¹³C NMR (76 MHz, CDCl₃) δ 167.6, 143.9, 136.5, 129.1, 128.4, 52.1, 1.3. ²⁹Si NMR (60 MHz, CDCl₃) δ -12.60, -75.72.

FT-IR $\bar{\nu}_{\max}$ (cm⁻¹) = 2953, 2895, 1727, 1280, 1246, 835.

HRMS (FI): calcd for C₁₇H₃₄BrO₂Si₄ [M]⁺: 382.16359, found 382.16472, delta = 2.98 ppm.

Methyl 3-(1,1,1,3,3,3-hexamethyl-2-(trimethylsilyl)trisilan-2-yl)benzoate (217b)

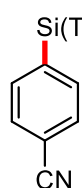


Based on general procedure **C**, starting from 43 mg of methyl 3-bromobenzoate, product **217b** has been obtained as oil (34 mg, 0.9 mmol, 45% yield). ¹H NMR (300 MHz, CDCl₃) δ 8.20 – 8.18 (m, 1H), 7.93 – 7.89 (m, 1H), 7.62 (dt, *J* = 7.4, 1.3 Hz, 1H), 7.30 – 7.35 (m, 1H), 3.91 (s, 3H), 0.23 (s, 27H). ¹³C NMR (75 MHz, CDCl₃) δ 167.6, 140.9, 137.7, 136.7, 129.4, 128.6, 127.8, 52.2, 1.2. ²⁹Si NMR (60 MHz, CDCl₃) δ -12.68, -75.94.

FT-IR $\bar{\nu}_{\max}$ (cm⁻¹) = 2952, 2895, 1728, 1280, 1260, 1119, 835.

HRMS (FI): calcd for C₁₇H₃₄BrO₂Si₄ [M]⁺: 382.16359, found 382.16455, delta = 2.52 ppm.

4-(1,1,1,3,3,3-Hexamethyl-2-(trimethylsilyl)trisilan-2-yl)benzotrile (217c)

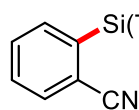


Based on general procedure **C**, starting from 36.4 mg of 4-bromobenzotrile, product **217c** has been obtained as oil (35 mg, 1.0 mmol, 50% yield). ¹H NMR (300 MHz, CDCl₃) δ 7.57 – 7.48 (m, 4H), 0.22 (s, 27H). ¹³C NMR (75 MHz, CDCl₃) δ 145.0, 136.9, 130.8, 119.4, 111.1, 1.2. ²⁹Si NMR (60 MHz, CDCl₃) δ -12.52, -74.47.

FT-IR $\bar{\nu}_{\max}$ (cm⁻¹) = 2958, 2896, 2228, 1248, 1055, 836.

HRMS (CI⁺): calcd for C₁₆H₃₂N₁Si₄ [M+H]⁺: 350.16118, found 350.16118, delta = 0 ppm

2-(1,1,1,3,3,3-Hexamethyl-2-(trimethylsilyl)trisilan-2-yl)benzotrile (217d)

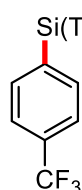


Based on general procedure **C**, starting from 36.4 mg of 2-bromobenzotrile, product **217d** has been obtained as oil (28 mg, 0.8 mmol, 40% yield). ¹H NMR (300 MHz, CDCl₃) δ 7.64 – 7.69 (m, 2H), 7.45 – 7.31 (m, 2H), 0.30 (s, 27H). ¹³C NMR (76 MHz, CDCl₃) δ 142.9, 138.2, 134.8, 131.2, 127.9, 121.6, 119.8, 2.1. ²⁹Si NMR (60 MHz, CDCl₃) δ -11.44, -71.48.

FT-IR $\bar{\nu}_{\max}$ (cm⁻¹) = 2955, 2897, 1247, 1053, 837.

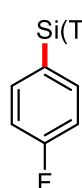
HRMS (CI⁺): calcd for C₁₆H₃₂N₁Si₄ [M+C₂H₅]⁺: 378.19248, found 378.19260, delta = 0.31 ppm.

1,1,1,3,3,3-Hexamethyl-2-(4-(trifluoromethyl)phenyl)-2-(trimethylsilyl)trisilane (217e)¹⁸³



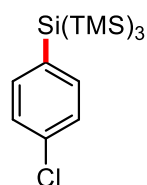
Based on general procedure **C**, starting from 45 mg of 1-bromo-4-(trifluoromethyl)benzene, product **217e** has been obtained as oil (33 mg, 0.84 mmol, 42% yield). ¹H NMR (300 MHz, CDCl₃) δ 7.56 (d, *J* = 7.4 Hz, 2H), 7.49 (d, *J* = 8.1 Hz, 2H), 0.23 (s, 27H). ¹⁹F NMR (282 MHz, CDCl₃) δ -62.8. ²⁹Si NMR (60 MHz, CDCl₃) δ -12.63, -75.75.

2-(4-Fluorophenyl)-1,1,1,3,3,3-hexamethyl-2-(trimethylsilyl)trisilane (217f)¹⁸³



Based on general procedure **C**, starting from 35 mg of 1-bromo-4-fluorobenzene, product **217f** has been obtained as oil (28 mg, 0.82 mmol, 41% yield). ¹H NMR (300 MHz, CDCl₃) δ 7.45 – 7.36 (m, 2H), 6.94 – 7.00 (m, 2H), 0.22 (s, 27H). ¹⁹F NMR (282 MHz, CDCl₃) δ -114.5 – -114.6 (m, 1F). ²⁹Si NMR (60 MHz, CDCl₃) δ -12.87, -76.79. ¹³C NMR (76 MHz, CDCl₃) δ 163.1 (d, *J* = 246.5 Hz), 138.1 (d, *J* = 7.0 Hz), 130.7 (d, *J* = 4.0 Hz), 115.1 (d, *J* = 19.5 Hz), 1.3.

2-(4-Chlorophenyl)-1,1,1,3,3,3-hexamethyl-2-(trimethylsilyl)trisilane (217g)

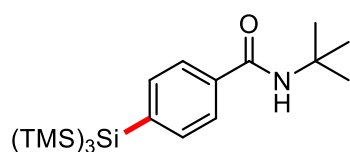


Based on general procedure C, starting from 38 mg of 1-bromo-4-chlorobenzene, product **217g** has been obtained as oil (35 mg, 0.98 mmol, 49% yield). ^1H NMR (300 MHz, CDCl_3) δ 7.42 – 7.31 (m, 2H), 7.28 – 7.19 (m, 3H), 0.22 (s, 31H). ^{13}C NMR (76 MHz, CDCl_3) δ 137.8, 134.2, 133.9, 128.1, 1.3. ^{29}Si NMR (60 MHz, CDCl_3) δ -12.82, -76.50.

FT-IR $\bar{\nu}_{\text{max}}$ (cm^{-1}) = 2957, 2897, 1580, 1481, 1254, 1064, 845.

HRMS (FI): calcd for $\text{C}_{15}\text{H}_{31}\text{ClSi}_4$ $[\text{M}]^+$: 358.11913, found 358.11830, delta = -2.32 ppm.

N-(tert-Butyl)-4-(1,1,1,3,3,3-hexamethyl-2-(trimethylsilyl)trisilan-2-yl)benzamide (217h)

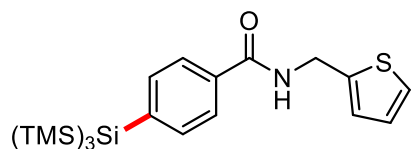


Based on general procedure C, starting from 51.2 mg of 4-bromo-N-(tert-butyl)benzamide, product **217h** has been obtained as white solid (51 mg, 1.2 mmol, 60% yield). M.p. = 217 – 218 °C (DCM). ^1H NMR (300 MHz, CDCl_3) δ 7.60 (d, J = 7.6 Hz, 2H), 7.49 (d, J = 7.6 Hz, 2H), 5.94 (s, 1H), 1.46 (s, 9H), 0.21 (s, 27H). ^{13}C NMR (75 MHz, CDCl_3) δ 167.2, 140.8, 136.7, 134.8, 125.9, 51.6, 29.0, 1.3. ^{29}Si NMR (60 MHz, CDCl_3) δ -12.68, -76.24.

FT-IR $\bar{\nu}_{\text{max}}$ (cm^{-1}) = 3240, 3059, 2955, 2894, 1629, 1243, 834.

HRMS (ESI): calcd for $\text{C}_{20}\text{H}_{42}\text{OSi}_4$ $[\text{M}+\text{H}]^+$: 424.23380, found 424.23224, delta = -3.67 ppm.

4-(1,1,1,3,3,3-Hexamethyl-2-(trimethylsilyl)trisilan-2-yl)-N-(thiophen-2-ylmethyl)benzamide (217i)

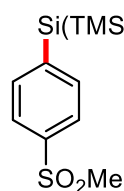


Based on general procedure C, starting from 59.2 mg of 4-bromo-N-(thiophen-2-ylmethyl)benzamide, product **217i** has been obtained as white solid (57 mg, 1.24 mmol, 62% yield). M.p. = 186 – 187 °C (DCM). ^1H NMR (300 MHz, CDCl_3) δ 7.71 – 7.62 (m, 2H), 7.56 – 7.47 (m, 2H), 7.23 (dd, J = 5.1, 1.3 Hz, 1H), 7.06 – 6.99 (m, 1H), 6.95 (dd, J = 5.1, 3.4 Hz, 1H), 6.53 (s, 1H), 4.80 (dd, J = 5.6, 0.9 Hz, 2H), 0.22 (s, 27H). ^{13}C NMR (76 MHz, CDCl_3) δ 167.5, 141.8, 141.0, 136.7, 133.1, 127.1, 126.3, 126.1, 125.4, 38.9, 1.3. ^{29}Si NMR (60 MHz, CDCl_3) δ -12.64, -76.01.

FT-IR $\bar{\nu}_{\text{max}}$ (cm^{-1}) = 3247, 3060, 2950, 2894, 1630, 1246, 835.

HRMS (ESI): calcd for $\text{C}_{21}\text{H}_{38}\text{ONSi}_4$ $[\text{M}+\text{H}]^+$: 464.17457, found 464.17337, delta = -2.58 ppm.

1,1,1,3,3,3-Hexamethyl-2-(4-(methylsulfonyl)phenyl)-2-(trimethylsilyl)trisilane (217j)

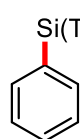


Based on general procedure C, starting from 47 mg of 1-bromo-4-(methylsulfonyl)benzene, product **217j** has been obtained as oil (37 mg, 0.92 mmol, 46% yield). M.p. = 94 – 95 °C (DCM). ^1H NMR (300 MHz, CDCl_3) δ 7.83 – 7.75 (m, 2H), 7.67 – 7.60 (m, 2H), 3.06 (s, 3H), 0.23 (s, 27H). ^{13}C NMR (76 MHz, CDCl_3) δ 146.0, 139.4, 137.1, 126.0, 44.6, 1.2. ^{29}Si NMR (60 MHz, CDCl_3) δ -12.47, -74.92.

FT-IR $\bar{\nu}_{\text{max}}$ (cm^{-1}) = 2953, 2895, 1577, 1315, 1247, 1155, 956, 836.

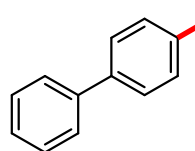
HRMS (FI): calcd for $\text{C}_{16}\text{H}_{34}\text{O}_2\text{S}_1\text{Si}_4$ $[\text{M}]^+$: 402.13566, found 402.13659, delta = 2.33 ppm.

1,1,1,3,3,3-Hexamethyl-2-phenyl-2-(trimethylsilyl)trisilane (217k)¹⁸⁴



Based on general procedure C, starting from 31.4 mg of bromobenzene, product **217k** has been obtained as oil (43 mg, 1.32 mmol, 66% yield). ¹H NMR (300 MHz, CDCl₃) δ 7.49 – 7.44 (m, 2H), 7.31 – 7.20 (m, 3H), 0.23 (s, 27H).

2-((1,1'-Biphenyl)-4-yl)-1,1,1,3,3,3-hexamethyl-2-(trimethylsilyl)trisilane (217l)

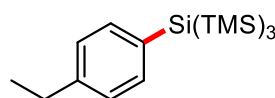


Based on general procedure C, starting from 47 mg of 4-bromo-1,1'-biphenyl, product **217l** has been obtained as oil (38 mg, 0.96 mmol, 48% yield). ¹H NMR (300 MHz, CDCl₃) δ 7.65 – 7.59 (m, 2H), 7.52 (d, *J* = 0.6 Hz, 4H), 7.48 – 7.40 (m, 2H), 7.38 – 7.30 (m, 1H), 0.26 (s, 27H). ¹³C NMR (75 MHz, CDCl₃) δ 141.2, 140.1, 137.1, 134.6, 128.9, 127.3, 127.1, 126.5, 1.4. ²⁹Si NMR (60 MHz, CDCl₃) δ -12.77, -77.10.

FT-IR $\bar{\nu}_{\max}$ (cm⁻¹) = 2950, 2893, 1482, 1245, 833.

HRMS (FI): calcd for C₂₁H₃₆Si₄ [M]⁺: 400.18941, found 400.18981, delta = 1.0 ppm.

2-(4-Ethylphenyl)-1,1,1,3,3,3-hexamethyl-2-(trimethylsilyl)trisilane (217m)

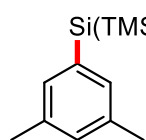


Based on general procedure C, starting from 37 mg of 1-bromo-4-ethylbenzene, product **217m** has been obtained as oil (31.9 mg, 0.9 mmol, 45% yield). ¹H NMR (300 MHz, CDCl₃) δ 7.40 – 7.32 (m, 2H), 7.14 – 7.06 (m, 2H), 2.62 (q, *J* = 7.6 Hz, 2H), 1.24 (t, *J* = 7.6 Hz, 3H), 0.22 (s, 27H). ¹³C NMR (76 MHz, CDCl₃) δ 143.4, 136.7, 131.6, 127.5, 28.8, 15.3, 1.4. ²⁹Si NMR (60 MHz, CDCl₃) δ -12.90, -77.56.

FT-IR $\bar{\nu}_{\max}$ (cm⁻¹) = 2958, 2896, 1246, 1055, 836.

HRMS (FI): calcd for C₁₇H₃₆Si₄ [M]⁺: 352.18941, found 352.18990, delta = 1.40 ppm.

2-(3,5-Dimethylphenyl)-1,1,1,3,3,3-hexamethyl-2-(trimethylsilyl)trisilane (217n)

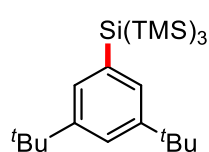


Based on general procedure C, starting from 37 mg of 1-bromo-3,5-dimethylbenzene, product **217n** has been obtained as oil (22 mg, 0.62 mmol, 31% yield). M.p.: 61 – 62 °C (DCM). ¹H NMR (300 MHz, CDCl₃) δ 7.06 – 7.05 (m, 2H), 6.88 – 6.90 (m, 1H), 2.28 (s, 6H), 0.22 (s, 27H). ¹³C NMR (76 MHz, CDCl₃) δ 136.8, 135.0, 134.6, 129.3, 21.6, 1.4. ²⁹Si NMR (60 MHz, CDCl₃) δ -12.93, -77.31.

FT-IR $\bar{\nu}_{\max}$ (cm⁻¹) = 2952, 2895, 1245, 1054, 836.

HRMS (FI): calcd for C₁₇H₃₆Si₄ [M]⁺: 352.18941, found 352.18940, delta = -0.02 ppm.

2-(3,5-Di-tert-butylphenyl)-1,1,1,3,3,3-hexamethyl-2-(trimethylsilyl)trisilane (217o)



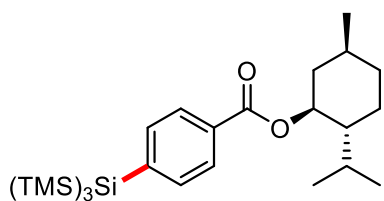
Based on general procedure C, starting from 54 mg of 1-bromo-3,5-di-tert-butylbenzene, product **217o** has been obtained as oil (21 mg, 0.48 mmol, 24% yield). ¹H NMR (300 MHz, CDCl₃) δ 7.31 (d, *J* = 1.9 Hz, 2H), 7.29 – 7.27 (m, 1H), 1.32 (s, 18H), 0.23 (s, 27H). ¹³C NMR (76 MHz, CDCl₃) δ 149.5, 133.8, 131.1, 121.2, 34.9, 31.7, 1.3. ²⁹Si NMR (60 MHz, CDCl₃) δ -12.86, -76.62.

FT-IR $\bar{\nu}_{\max}$ (cm⁻¹) = 2958, 2899, 1247, 1049, 836.

HRMS (FI): calcd for C₂₃H₄₈Si₄ [M]⁺: 436.28331, found 436.28410, delta = 1.82 ppm.

(1S,2R,5S)-2-isopropyl-5-methylcyclohexyl

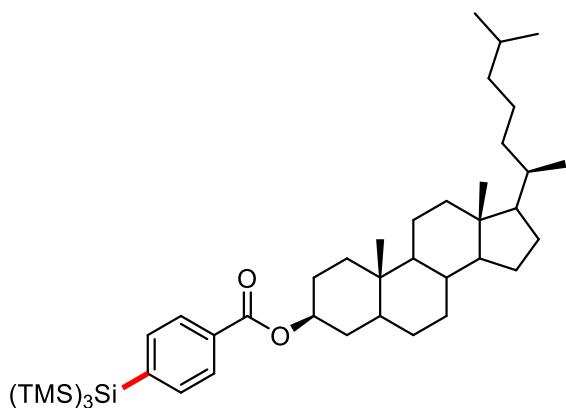
4-(1,1,1,3,3,3-hexamethyl-2-(trimethylsilyl)trisilan-2-yl)benzoate (217p)



Based on general procedure C, starting from 68 mg of (1S,2R,5S)-2-isopropyl-5-methylcyclohexyl 4-bromobenzoate, product **217p** has been obtained as oil (53 mg, 1.04 mmol, 52% yield). ¹H NMR (300 MHz, CDCl₃) δ 7.91 (d, *J* = 7.6 Hz, 2H), 7.53 (d, *J* = 7.6 Hz, 2H), 4.92 (td, *J* = 10.9, 4.2 Hz, 1H), 2.12 (d, *J* = 12.2 Hz, 1H), 2.05 – 1.95 (m, 1H), 1.73 (d, *J* = 12.1 Hz, 2H), 1.54 (t, *J* = 11.8 Hz, 2H), 1.23 – 0.95 (m, 3H), 0.92 (d, *J* = 7.0 Hz, 6H), 0.80 (d, *J* = 6.9 Hz, 3H), 0.23 (s, 27H). ¹³C NMR (75 MHz, CDCl₃) δ 166.6, 143.4, 136.5, 129.9, 128.5, 74.8, 47.5, 41.2, 34.5, 31.6, 26.5, 23.7, 22.2, 21.0, 16.6, 1.3. ²⁹Si NMR (60 MHz, CDCl₃) δ -12.60, -75.84.

HRMS (FI): calcd for C₂₆H₅₀O₂Si₄ [M]⁺: 506.28879, found 506.28928, delta = 0.98 ppm.

(3S,10S,13R)-10,13-Dimethyl-17-((R)-6-methylheptan-2-yl)hexadecahydro-1H-cyclopenta[a]phenanthren-3-yl 4-(1,1,1,3,3,3-hexamethyl-2-(trimethylsilyl)trisilan-2-yl)benzoate (217q)

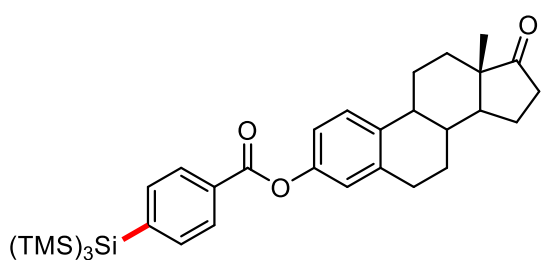


Based on general procedure C, starting from 114.3 mg of (3S,10S,13R,17R)-10,13-dimethyl-17-((R)-6-methylheptan-2-yl)hexadecahydro-1H-cyclopenta[a]phenanthren-3-yl 4-bromobenzoate, product **217q** has been obtained as white solid (86 mg, 1.16 mmol, 58% yield). M.p. = 172 – 174 °C (DCM). ¹H NMR (300 MHz, CDCl₃) δ 7.97 – 7.84 (m, 2H), 7.59 – 7.45 (m, 2H), 4.93 (tt, *J* = 10.8, 4.9 Hz, 1H), 2.02 – 1.88 (m, 2H), 1.82 – 1.45 (m, 9H), 1.42 – 1.25 (m, 8H), 1.20 – 0.93 (m, 10H), 0.93 – 0.84 (m, 13H), 0.72 – 0.68 (m, 1H), 0.66 (s, 3H), 0.22 (s, 27H). ¹³C NMR (76 MHz, CDCl₃) δ 166.6, 143.4, 136.5, 129.9, 128.4, 74.3, 56.6, 56.4, 54.41, 44.9, 42.8, 40.2, 39.7, 37.0, 36.3, 36.0, 35.7, 34.3, 32.2, 28.8, 28.4, 28.2, 27.8, 24.4, 24.0, 23.0, 22.7, 21.4, 18.8, 12.4, 12.2, 1.3. ²⁹Si NMR (60 MHz, CDCl₃) δ -12.61, -75.83.

FT-IR $\bar{\nu}_{\max}$ (cm⁻¹) = 2948, 2868, 1716, 1277, 1246, 1119, 836.

HRMS (FI): calcd for C₄₃H₇₈O₂Si₄ [M]⁺: 738.50789, found 738.50815, delta = 0.35 ppm.

(13S)-13-Methyl-17-oxo-7,8,9,11,12,13,14,15,16,17-decahydro-6H-cyclopenta[a]phenanthren-3-yl 4-(1,1,1,3,3,3-hexamethyl-2-(trimethylsilyl)trisilan-2-yl)benzoate (217r)



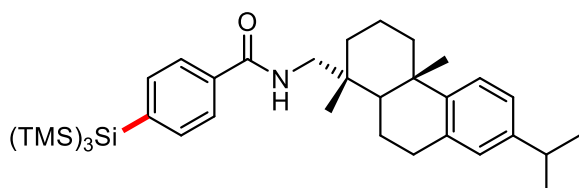
Based on general procedure C, starting from 91 mg of (13S)-13-methyl-17-oxo-7,8,9,11,12,13,14,15,16,17-decahydro-6H-cyclopenta[a]phenanthren-3-yl 4-bromobenzoate, product **217r** has been obtained as white solid (55 mg, 0.88 mmol, 44% yield). M.p. = 229 – 230 °C (DCM). ¹H NMR (300 MHz, CDCl₃) δ 8.14 –

8.00 (m, 2H), 7.67 – 7.54 (m, 2H), 7.34 (d, $J = 8.4$ Hz, 1H), 7.03 – 6.91 (m, 2H), 2.95 (dd, $J = 9.1$, 4.3 Hz, 2H), 2.59 – 2.39 (m, 2H), 2.38 – 2.26 (m, 1H), 2.22 – 1.94 (m, 4H), 1.69 – 1.43 (m, 6H), 0.93 (s, 3H), 0.25 (s, 27H). ^{13}C NMR (76 MHz, CDCl_3) δ 220.9, 165.9, 149.1, 145.0, 138.2, 137.5, 136.6, 129.0, 128.5, 126.6, 121.9, 119.0, 50.6, 48.1, 44.3, 38.2, 36.0, 31.7, 29.6, 26.5, 25.1, 21.7, 14.0, 1.3. ^{29}Si NMR (60 MHz, CDCl_3) δ -12.53, -75.44.

FT-IR $\bar{\nu}_{\text{max}}$ (cm^{-1}) = 2950, 2893, 1738, 1592, 1494, 1259, 1064, 837.

HRMS (ESI): calcd for $\text{C}_{34}\text{H}_{53}\text{O}_3\text{Si}_4$ $[\text{M}+\text{H}]^+$: 621.30663, found 621.30548, delta = -1.85 ppm.

4-(1,1,1,3,3,3-Hexamethyl-2-(trimethylsilyl)trisilan-2-yl)-N-(((1R,4aS)-7-isopropyl-1,4a-dimethyl-1,2,3,4,4a,9,10,10a-octahydrophenanthren-1-yl)methyl)benzamide (217s)



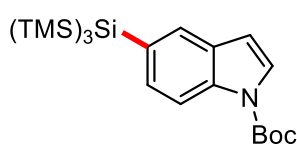
Based on general procedure C, starting from 94 mg of 4-bromo-N-(((1R,4aS)-7-isopropyl-1,4a-dimethyl-1,2,3,4,4a,9,10,10a-octahydrophenanthren-1-yl)methyl)benzamide, product **217s** has been obtained as oil (51 mg, 0.8 mmol, 40% yield). ^1H

NMR (300 MHz, CDCl_3) δ 7.63 – 7.57 (m, 2H), 7.54 – 7.48 (m, 2H), 7.18 (d, $J = 8.2$ Hz, 1H), 7.00 (dd, $J = 8.2$, 2.1 Hz, 1H), 6.90 (d, $J = 2.0$ Hz, 1H), 6.12 (t, $J = 6.3$ Hz, 1H), 3.51 – 3.26 (m, 2H), 2.99 – 2.76 (m, 3H), 2.31 (d, $J = 12.7$ Hz, 1H), 2.03 – 1.96 (m, 1H), 1.85 – 1.66 (m, 3H), 1.55 – 1.49 (m, 2H), 1.46 – 1.36 (m, 2H), 1.24 (d, $J = 1.8$ Hz, 6H), 1.21 (s, 3H), 1.02 (s, 3H), 0.22 (s, 27H). ^{13}C NMR (76 MHz, CDCl_3) δ 168.0, 147.2, 145.8, 141.4, 136.8, 135.0, 133.8, 127.1, 125.9, 124.4, 124.0, 50.3, 45.8, 38.5, 37.8, 37.7, 36.5, 33.6, 30.6, 25.6, 24.1, 19.2, 19.0, 18.8, 1.3. ^{29}Si NMR (60 MHz, CDCl_3) δ -12.64, -76.10.

FT-IR $\bar{\nu}_{\text{max}}$ (cm^{-1}) = 3329, 2955, 2895, 1643, 1538, 1246, 836.

HRMS (ESI): calcd for $\text{C}_{36}\text{H}_{62}\text{OSi}_4$ $[\text{M}+\text{H}]^+$: 636.39030, found 636.38861, delta = -2.65 ppm.

tert-Butyl 5-(1,1,1,3,3,3-hexamethyl-2-(trimethylsilyl)trisilan-2-yl)-1H-indole-1-carboxylate (217t)

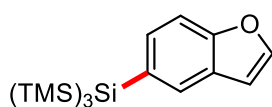


Based on general procedure C, starting from 94 mg of tert-butyl 5-bromo-1H-indole-1-carboxylate, product **217t** has been obtained as oil (51 mg, 0.8 mmol, 40% yield). ^1H NMR (300 MHz, CDCl_3) δ 8.02 (d, $J = 8.4$ Hz, 1H),

7.65 (t, $J = 1.1$ Hz, 1H), 7.56 (d, $J = 3.7$ Hz, 1H), 7.37 (dd, $J = 8.3$, 1.3 Hz, 1H), 6.52 (dd, $J = 3.8$, 0.8 Hz, 1H), 1.67 (s, 9H), 0.24 (s, 27H). ^{13}C NMR (75 MHz, CDCl_3) δ 150.0, 135.0, 132.6, 130.8, 129.3, 128.2, 125.6, 114.7, 107.3, 83.7, 28.4, 1.4. ^{29}Si NMR (60 MHz, CDCl_3) δ -12.88, -76.36.

FT-IR $\bar{\nu}_{\text{max}}$ (cm^{-1}) = 2956, 2927, 1738, 1370, 1250, 1160, 837.

2-(Benzofuran-5-yl)-1,1,1,3,3,3-hexamethyl-2-(trimethylsilyl)trisilane (217u)



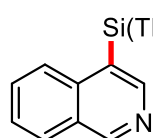
Based on general procedure C, starting from 39.4 mg of 5-bromobenzofuran, product **217u** has been obtained as oil (28 mg, 0.76 mmol, 38% yield). ^1H NMR (300 MHz, CDCl_3) δ 7.71 – 7.66 (m, 1H), 7.58 (d, $J = 2.2$ Hz, 1H),

7.43 (dt, $J = 8.3, 0.9$ Hz, 1H), 7.35 (dd, $J = 8.3, 1.3$ Hz, 1H), 6.73 (dd, $J = 2.2, 0.9$ Hz, 1H), 0.24 (s, 27H). ^{13}C NMR (76 MHz, CDCl_3) δ 155.1, 144.6, 132.5, 129.3, 128.3, 127.6, 111.1, 106.4, 1.4. ^{29}Si NMR (60 MHz, CDCl_3) δ -12.89, -75.90.

FT-IR $\bar{\nu}_{\text{max}}$ (cm^{-1}) = 2955, 2896, 1815, 1247, 1055, 835.

HRMS (FI): calcd for $\text{C}_{17}\text{H}_{32}\text{O}_1\text{Si}_4$ $[\text{M}]^+$: 364.15302, found 364.15320, delta = 0.48 ppm.

4-(1,1,1,3,3,3-Hexamethyl-2-(trimethylsilyl)trisilan-2-yl)isoquinoline (217v)

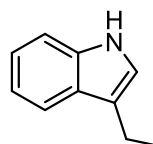


Based on general procedure C, starting from 41.6 mg of 4-bromoisoquinoline, product **217v** has been obtained as oil (15 mg, 0.4 mmol, 20% yield). ^1H NMR (300 MHz, CDCl_3) δ 9.15 (s, 1H), 8.69 (s, 1H), 8.03 – 7.92 (m, 2H), 7.70 – 7.56 (m, 2H), 0.26 (s, 27H). ^{13}C NMR (76 MHz, CDCl_3) δ 152.9, 150.8, 140.7, 129.5, 129.3, 128.7, 128.5, 128.3, 127.1, 2.2. ^{29}Si NMR (60 MHz, CDCl_3) δ -11.69, -81.08.

FT-IR $\bar{\nu}_{\text{max}}$ (cm^{-1}) = 2957, 2922, 1251, 1058, 842.

HRMS (Cl^+): calcd for $\text{C}_{18}\text{H}_{34}\text{N}_1\text{Si}_4$ $[\text{M}+\text{H}]^+$: 376.17683, found 376.17690, delta = 0.18 ppm.

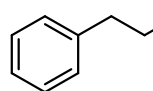
3-(2-(1,1,1,3,3,3-hexamethyl-2-(trimethylsilyl)trisilan-2-yl)ethyl)-1H-indole (217w)



Based on general procedure C, starting from 45 mg of 3-(2-bromoethyl)-1H-indole, product **217w** has been obtained as oil (16 mg, 0.4 mmol, 20% yield). ^1H NMR (300 MHz, CDCl_3) δ 7.89 (s, 1H), 7.63 – 7.57 (m, 1H), 7.36 (dt, $J = 8.1, 1.0$ Hz, 1H), 7.23 – 7.10 (m, 2H), 7.00 (dd, $J = 2.2, 1.1$ Hz, 1H), 2.91 – 2.78 (m, 2H), 1.28 – 1.21 (m, 2H), 0.23 (s, 27H). ^{13}C NMR (76 MHz, CDCl_3) δ 136.6, 127.2, 122.1, 120.6, 120.5, 119.3, 119.0, 111.3, 24.9, 9.1, 1.4. ^{29}Si NMR (60 MHz, CDCl_3) δ -12.71, -81.71. FT-IR $\bar{\nu}_{\text{max}}$ (cm^{-1}) = 3419, 3059, 2954, 2896, 1245, 1051, 835.

HRMS (ESI): calcd for $\text{C}_{19}\text{H}_{36}\text{N}_1\text{Si}_4$ $[\text{M}-\text{H}]^-$: 390.19303, found 390.19330, delta = 0.69.

1,1,1,3,3,3-hexamethyl-2-(3-phenylpropyl)-2-(trimethylsilyl)trisilane (217x)

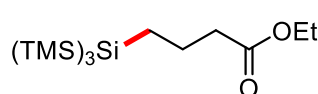


Based on general procedure C, starting from 40 mg of (3-bromopropyl)benzene, product **217x** has been obtained as oil (19 mg, 0.52 mmol, 26% yield). ^1H NMR (300 MHz, CDCl_3) δ 7.32 – 7.26 (m, 2H), 7.22 – 7.12 (m, 3H), 2.64 (t, $J = 7.5$ Hz, 2H), 1.77 – 1.65 (m, 2H), 0.86 – 0.78 (m, 2H), 0.15 (s, 27H). ^{13}C NMR (75 MHz, CDCl_3) δ 142.5, 128.6, 128.4, 125.8, 40.7, 31.1, 7.6, 1.3. ^{29}Si NMR (60 MHz, CDCl_3) δ -12.81, -81.99.

FT-IR $\bar{\nu}_{\text{max}}$ (cm^{-1}) = 2953, 2895, 1245, 1056, 835.

HRMS (Cl^+): calcd for $\text{C}_{18}\text{H}_{38}\text{Si}_4$ $[\text{M}]^+$: 366.20506, found 366.20510, delta = 0.11 ppm.

Ethyl 4-(1,1,1,3,3,3-hexamethyl-2-(trimethylsilyl)trisilan-2-yl)butanoate (217y)



Based on general procedure C, starting from 39 mg of ethyl 4-bromobutanoate, product **217y** has been obtained as oil (36 mg, 0.82 mmol, 41% yield). ^1H NMR (300 MHz, CDCl_3) δ 4.13 (q, $J = 7.1$ Hz, 2H), 2.33 (t, $J = 7.0$ Hz, 2H), 1.77 – 1.64 (m, 2H), 1.25 (t, $J = 7.1$ Hz, 3H), 0.84 – 0.72 (m, 2H), 0.16 (s, 27H). ^{13}C NMR (76 MHz, CDCl_3) δ 173.5, 60.3, 38.7, 24.9, 14.4, 7.7, 1.3. ^{29}Si NMR (60 MHz, CDCl_3)

δ -12.79, -81.93.

FT-IR $\bar{\nu}_{\max}$ (cm^{-1}) = 2955, 2896, 1739, 1245, 1049, 838.

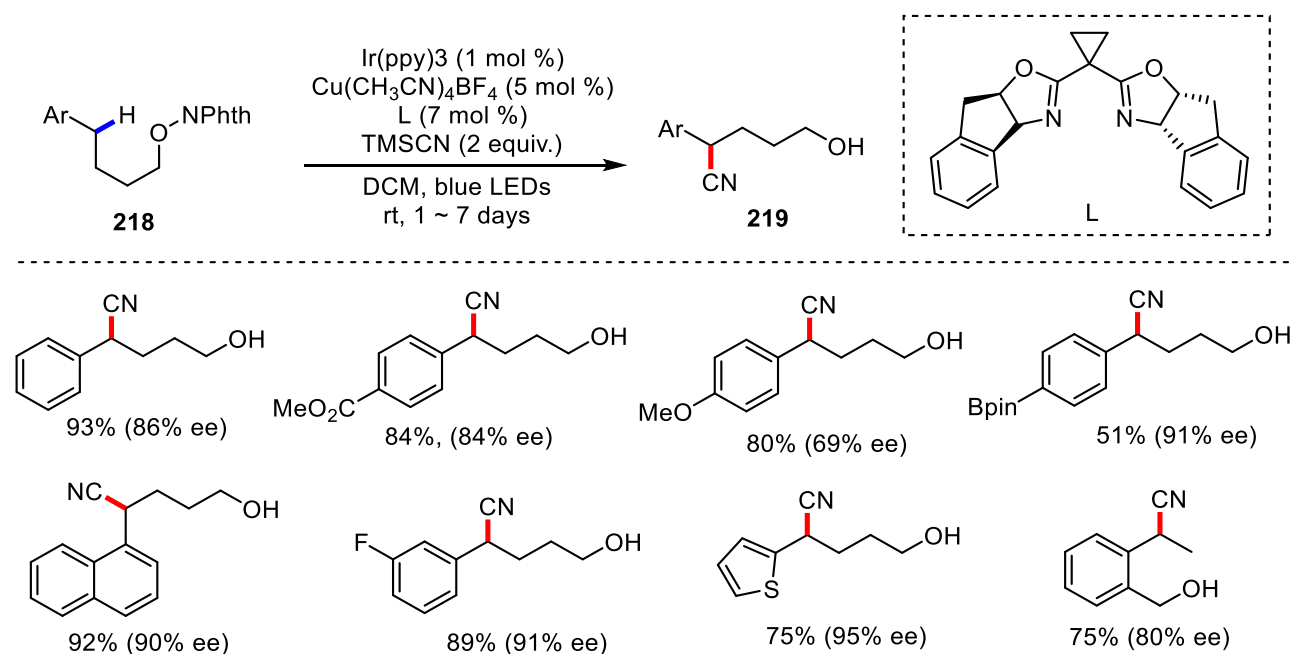
HRMS (ESI): calcd for $\text{C}_{15}\text{H}_{38}\text{O}_2\text{Si}_4$ $[\text{M}+\text{Na}]^+$: 385.18411, found 385.18362, $\delta = -1.25$ ppm.

Chapter 6 Cu-Catalyzed Remote C(sp³)-H silylation of Alcohol

6.1 Introduction

Oxygen-centered radical-mediated remote C(sp³)-H functionalization has long been a powerful strategy for modifying steroids and hydrocarbons. The Barton¹⁶ nitrite-ester reaction is a classic illustration of this methodology, enabling a simple means of achieving functionalization of δ -C(sp³)-H bonds in alcohols. Recently, this strategy, combined with Cu catalysis, has achieved a series of very interesting transformations that enable site-selective C-H functionalization and can be used for late-stage modification of complex molecules.¹⁰³

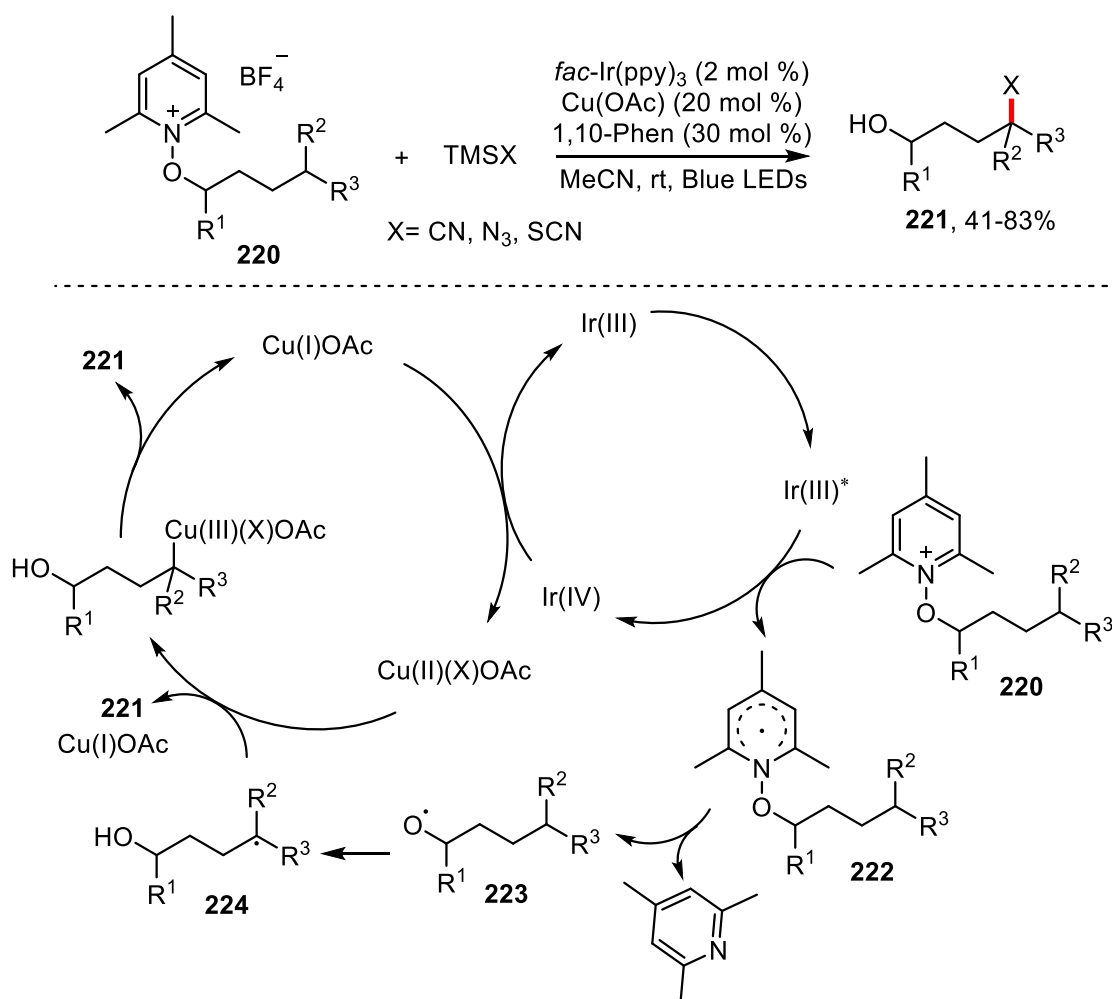
For instance, Liu¹⁸⁵ and co-workers reported a remote C-H asymmetric cyanation reaction using *N*-alkoxyphthalimide as the substrate, Ir(ppy)₃ as photocatalyst, and copper as the co-catalyst under blue light irradiation. The reaction involves an oxygen radical-mediated 1,5-hydrogen transfer process and employs a copper-catalyzed radical relay strategy to achieve excellent enantioselectivity and δ -site selectivity for aryl-substituted alkyl alcohols. The method is mild and exhibits good functional group compatibility and substrate generality, providing an efficient approach for the synthesis of optically active δ -cyanohydrins (Scheme 69).



Scheme 69 Cu-catalyzed enantioselective cyanation of remote C-H bonds.

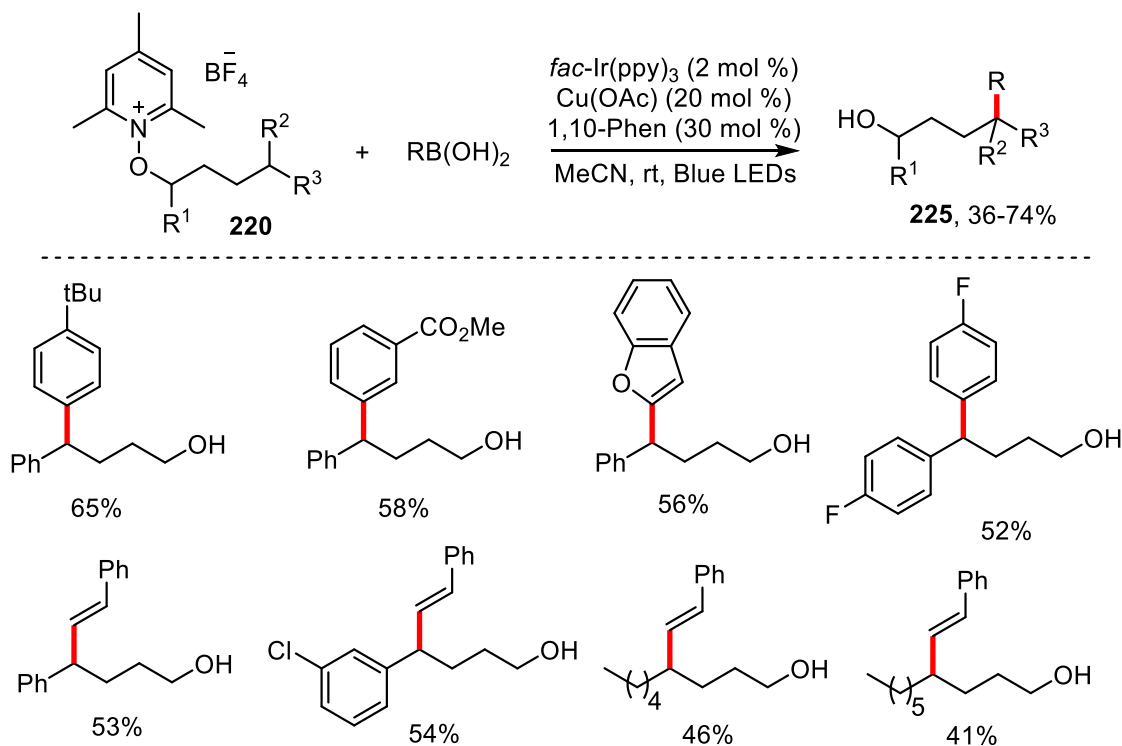
In 2019, Zhu¹⁸⁶ *et al.* developed a highly efficient reaction between *N*-alkoxyphthalimide salts and readily available silyl reagents (such as TMSN₃, TMSCN, and TMSNCS) to access δ -azido, δ -

cyano, and δ -thiocyanato alcohols with excellent yields, utilizing a mild dual catalysis system involving photoredox and copper (Scheme 70). The article provides a detailed mechanism for the reaction. First, excitation of Ir(III)* species could lead to the reduction of **220**, resulting in the generation of the radical **222** and Ir(IV) species. Cu(I) would be oxidized by the latter in the presence of TMSX to give Cu(II)(X)OAc. The radical **222** would release a 2,4,6-trimethylpyridine leading to the oxygen-centered radical **223**, which undergoes 1,5-HAT to afford the carbon-centered radical **224**. The Cu(III) species would be formed upon radical rebound of **224** with Cu(II)(X)OAc. Finally, reductive elimination would result in the formation of δ -C(sp³)-H functionalized products, while releasing Cu(I)OAc salt. Alternatively, the product could also be formed from radical **B** through a Cu-centered redox ligand transfer process.



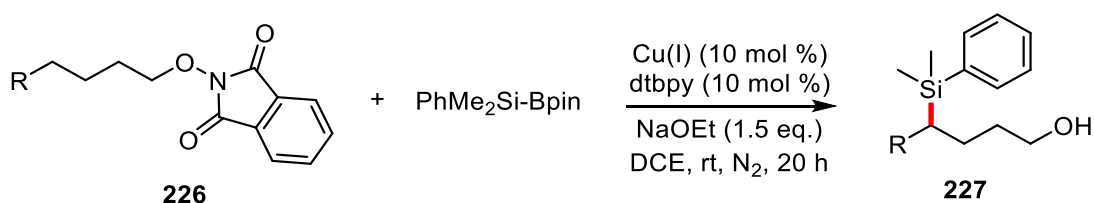
Subsequently, the same team carried out the synthesis of δ -aryl and δ -vinyl alkanols under similar conditions, via the reaction of alkoxy-pyridinium salts with aryl or vinylboronic acids (Scheme 71).¹⁸⁷ The process followed a domino sequence, starting with the reductive generation of alkoxy-

radicals, then a 1,5-hydrogen atom transfer, and finally a Cu-mediated cross-coupling reaction between the resulting translocated carbon radicals and aryl/vinyl boronic acids. This method complements the Minisci-type reaction and enables the introduction of both electron-rich and electron-poor arenes in the δ -position of alcohols.



Scheme 71 Remote $\text{C(sp}^3\text{)-H}$ arylation and alkenylation

To our knowledge, the silylation of distal C-H bonds has not been reported so far. According to previous literature reports,¹⁸⁸ Cu can react with Si-B reagents under strongly alkaline conditions to form Cu-Si species, which can undergo radical rebound with carbon-centered radical to construct C-Si bond. Therefore, we describe here a novel method for the synthesis of δ -silyl alcohols by utilizing Cu(I) as a catalyst to facilitate the reaction between *N*-alkoxyphthalimide and Si-B reagent (Scheme 72).

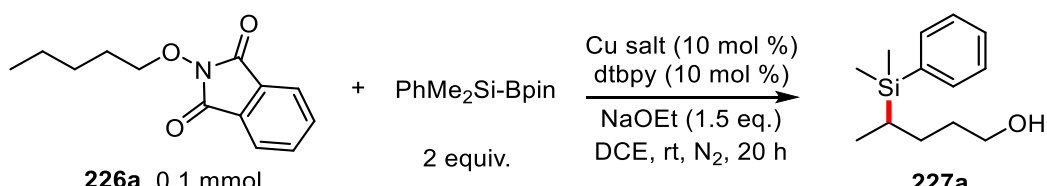


Scheme 72 Cu-catalyzed remote $\text{C(sp}^3\text{-H}$ silylation.

6.2 Optimization of the reaction conditions

Firstly, a large number of copper catalysts were screened, and the results are shown in Table 5. All monovalent copper species gave similar yields (entries-1, 2-7), but when $\text{Cu}(\text{MeCN})_4\text{PF}_6$ was used as the catalyst, the reaction mixture was the cleanest. $\text{Cu}(\text{OAc})_2$ is an ineffective catalyst and cannot provide the desired product (entry 8). In an attempt to increase the yield, 1 equivalent of catalyst and 1 equivalent of ligand were used, but unfortunately, the desired product was not detected (entry 2).

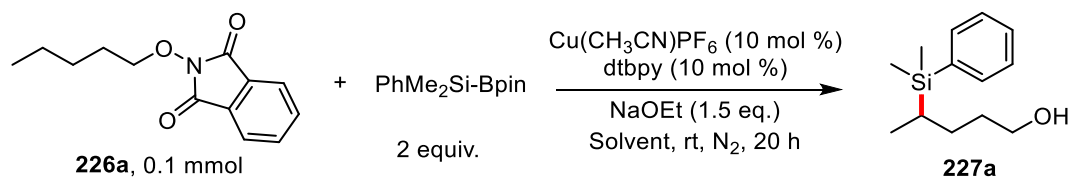
Table 5 Optimization of catalysts.



Entry	Cu salt	Yield	RSM
1	$\text{Cu}(\text{CH}_3\text{CN})_4\text{PF}_6$	5%	75%
2 ^a	$\text{Cu}(\text{CH}_3\text{CN})_4\text{PF}_6$	Trace	-
3	No	0	-
4	$\text{Cu}(\text{Tc})$	5%	22%
5	CuSCN	7%	44%
6	CuCl	6%	31%
7	CuCN	7%	69%
8	$\text{Cu}(\text{OAc})_2$	trace	71%
9	$\text{Cu}(\text{OTf})_2$	5%	62%

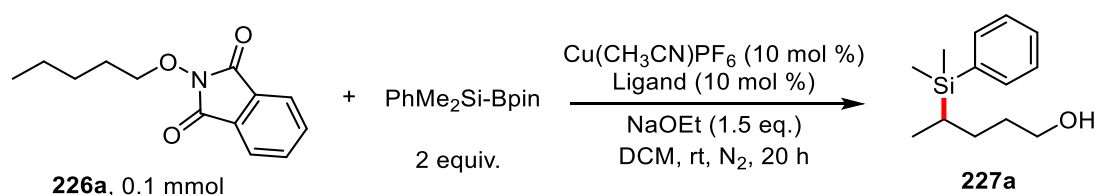
^a $\text{Cu}(\text{CH}_3\text{CN})_4\text{PF}_6$ (1 equiv.) and dtbpy (1equiv.)

Next, various solvents were also tested (Table 6). DCM (entry 8) provided the best yield. Highly polar solvents such as DMF (entry 1), DMA (entry 2), and NMP (entry 3) are incompatible with the reaction system. Ether solvents are also incompatible with the system due to the presence of labile hydrogen atoms that can undergo competing reactions (entry 4). Some alcohol solvents are not suitable as they can interact with the Si-B reagent (entry 5).

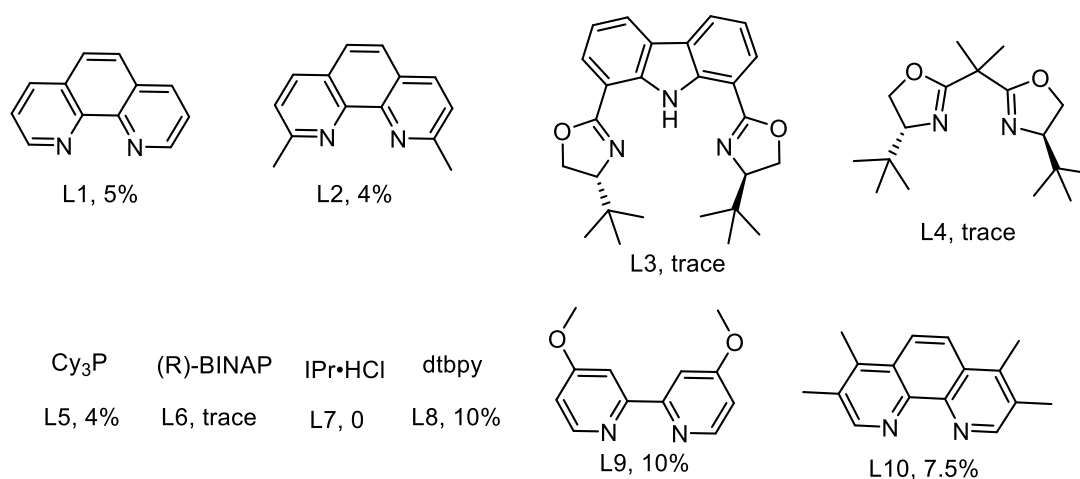
Table 6 Optimization of solvents.

Entry	Solvent	Yield	RSM
1	DMF	0	
2	DMA	0	
3	NMP	0	
4	THF	0	
5	HFIP	0	
6	CH ₃ CN	6%	29%
7	PhCF ₃	8%	46%
8	DCM	10%	66%
9	PhCl	7%	35%
10	Benzene	6%	28%
11	Acetone	Trace	71%

Afterward, a series of commonly used copper ligands were screened, as shown in Table 7. Unfortunately, none of the ligands provided good yields. L8 is the best to deliver product in 10% yield.

Table 7 Optimization of ligands.

Entry	Ligand	Yield	RSM
1	L1	5%	31%
2	L2	4%	71%
3	L3	Trace	-
4	L4	Trace	-
5	L5	4%	32%
6	L6	Trace	-
7	L7	0	-
8	L8	10%	66%
9	L9	10%	63%
10	L10	8%	65%

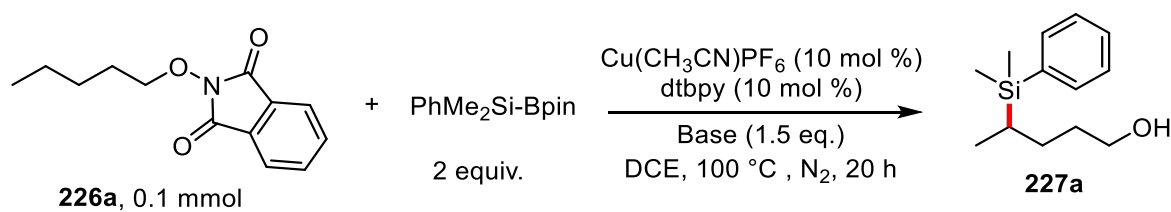


To improve the yield of the product, we increased the temperature from room temperature up to 120°C (Table 8). Due to the more stable generated benzyl radical, I have replaced substrate **226a** with **226b**. With increasing temperature, the yield of the product also gradually increased. The highest conversion was attained at 100°C, resulting in a product yield of 22% (entry 5).

Table 8 Optimization of temperature.

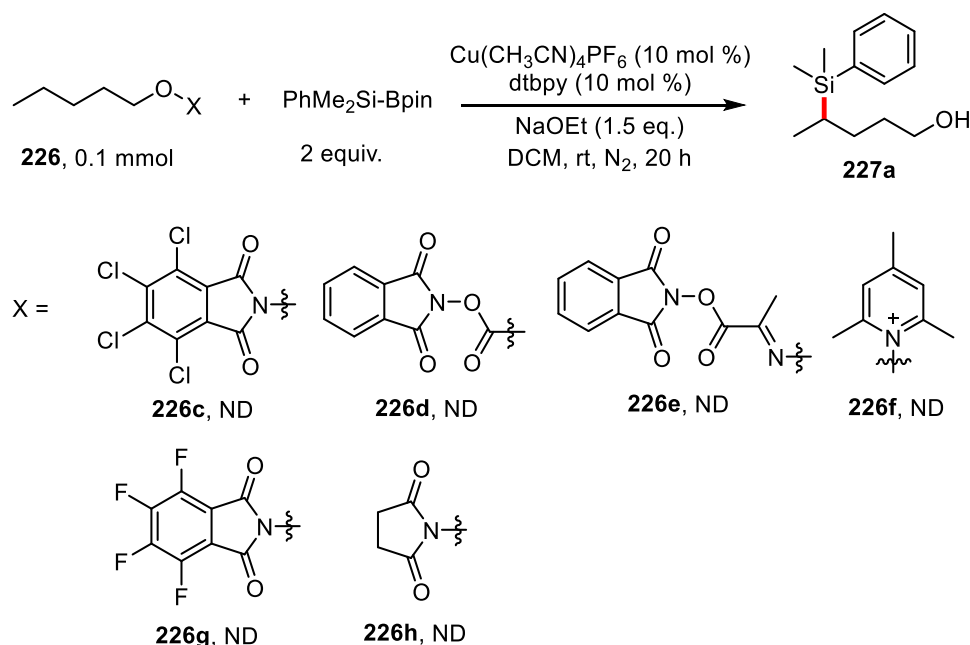
Entry	T (°C)	Yield	RSM
1	rt	10.0%	45%
2	40	9.0%	50%
3	60	9.0%	46%
4	80	20%	40%
5	100	22%	26%
6	120	15%	36%

Next, various types of inorganic and organic bases were also tested, and the results are shown in Table 9. Firstly, a series of strong bases including NaO*t*-Bu, LiO*t*-Bu, and KO*t*-Bu, are incompatible with the reaction conditions. The organic base DMAP cannot afford the desired product. Several fluoride salts were also screened (entries-7, 11-12) as they are known to efficiently activate the Si-B bond by reacting with the boron center, but no target product was observed. The base is crucial for the reaction as no reaction could be observed without it (entry 14). The best yield of the desired product, 20%, was obtained using NaOEt.

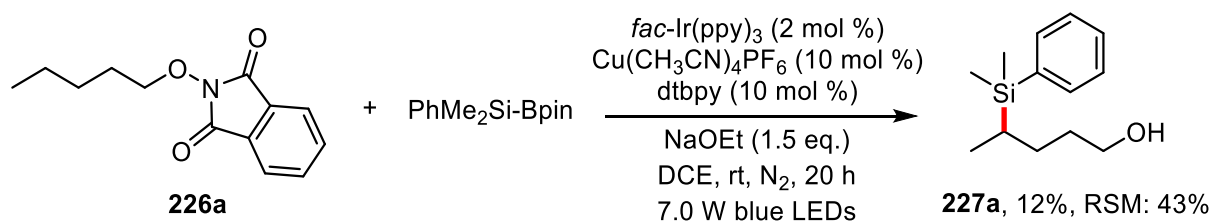
Table 9 Optimization of base.

Entry	Base	Yield	RSM
1	NaOEt	20%	42%
2	NaO ^t Bu	0	-
3	LiO ^t Bu	0	-
4	KO ^t Bu	0	-
5	DMAP	0	-
6	K ₃ PO ₄	trace	-
7	TBAT	trace	-
8	LiOMe	0	-
9	NaOPh	8.0%	50%
10	NaOSi(SiMe) ₃	0	-
11	KF	ND	-
12	CsF	ND	-
13	CS ₂ CO ₃	ND	-
14	Without	0	-

As reported by previous studies,¹⁸⁸ there is a significant difference in the oxidation-reduction potentials of various *N*-alkoxy derivatives. Therefore, we attempted to improve the yield using different *N*-alkoxy derivatives (Scheme 73), which unfortunately did not provide any improvement as compared to the phthalimidyl fragment used above.

**Scheme 73** Optimization of *N*-alkoxy derivatives.

Finally, we tried a dual photoredox/copper catalytic strategy to access δ -silylated alkanols from *N*-alkoxyphthalimide **226a** (Scheme 74). Reaction of **226a** with PhMe₂Si-Bpin in the presence of *fac*-Ir(ppy)₃ (2 mol %), Cu(MeCN)₄PF₆ (10 mol %), dtbpy (10 mol %), and NaOEt (1.5 equiv.) in DCE at room temperature under blue LED irradiation provided the target product in 12% yield, therefore offering no improvement as compared to the copper-catalysis described before.



Scheme 74 Dual Photoredox/Copper Catalyzed remote C(sp³)-H silylation.

6.3 Conclusion

The remote C-H silylation of alcohols is a particularly useful process as incorporation of silicon fragments on carbon skeleton often requires harsh conditions, basic reagents that are not compatible with functional groups and the use of costly catalysts. The preliminary results described above are encouraging although we failed to optimize the reaction conditions, varying numerous parameters. Competing reactions likely take place here, although we have been unable to isolate by-products which could provide useful information to improve the methodology. For instance, the oxygen-centered radical generated *in situ* might react with the Si-Bpin reagent, thus quenching the reaction. We have however not been able to isolate boron by-products supporting such an hypothesis. Based on these preliminary studies, we will continue our efforts towards the development of the C-H silylation of alcohols, which may also be extended to thiols and protected amines.

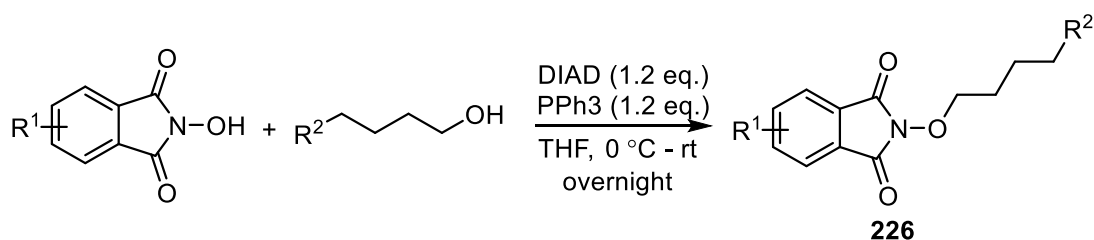
6.4 Experimental part

6.4.1 General information

General information is the same with chapter 3.

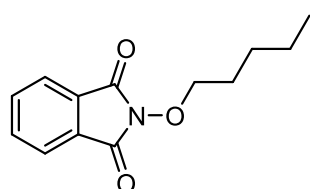
6.4.2 Synthesis of the starting Materials

General procedure A for the synthesis of *N*-alkoxyl derivatives:



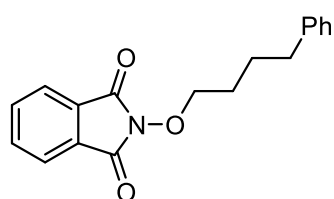
A solution of the alcohol (1.0 equiv.), NHPI derivatives (1.2 equiv.) and PPh₃ (1.2 equiv.) in THF under a nitrogen atmosphere was cooled in an ice bath. Neat diisopropylazodicarboxylate (1.2 equiv.) was added dropwise to the solution. The mixture was then stirred in the ice bath for 10 minutes before being allowed to come to room temperature. The mixture was stirred at room temperature for 12 hours or until the reaction was completed by TLC analysis. Then, the crude reaction mixture was evaporated and the residue was loaded directly onto a silica gel column chromatography using PE/EtOAc as the mobile phase to afford corresponding product.

2-(Pentyloxy)isoindoline-1,3-dione (226a)¹⁹⁰



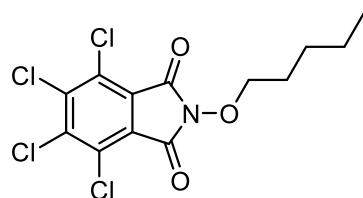
Based on general procedure A, starting from 2.2 g of pentan-1-ol, product **226a** has been obtained as white solid (5.36 g, 23 mmol, 92% yield). ¹H NMR (300 MHz, CDCl₃) δ 7.85 – 7.77 (m, 2H), 7.76 – 7.69 (m, 2H), 4.18 (t, *J* = 6.8 Hz, 2H), 1.83 – 1.71 (m, 2H), 1.51 – 1.29 (m, 4H), 0.91 (t, *J* = 7.1 Hz, 3H). ¹³C NMR (75 MHz, CDCl₃) δ 163.8, 134.5, 129.1, 123.6, 78.7, 27.9, 27.8, 22.5, 14.0.

2-(4-Phenylbutoxy)isoindoline-1,3-dione (226b)¹⁹¹



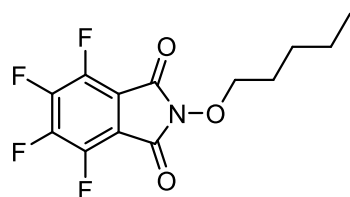
Based on general procedure A, starting from 1.5 g of 4-phenylbutan-1-ol, product **226b** has been obtained as white solid (2.64 g, 8.9 mmol, 89% yield). ¹H NMR (300 MHz, CDCl₃) δ 7.87 – 7.80 (m, 2H), 7.79 – 7.69 (m, 2H), 7.34 – 7.13 (m, 5H), 4.28 – 4.18 (m, 2H), 2.76 – 2.64 (m, 2H), 1.92 – 1.78 (m, 4H). ¹³C NMR (76 MHz, CDCl₃) δ 163.8, 142.1, 134.6, 129.1, 128.6, 128.5, 125.9, 123.6, 78.4, 35.6, 27.8, 27.5.

4,5,6,7-Tetrachloro-2-(pentyloxy)isoindoline-1,3-dione (226c)



Based on general procedure A, starting from 176 mg of pentan-1-ol, product **226c** has been obtained as white solid (180 mg, 0.48 mmol, 24% yield). ¹H NMR (300 MHz, CDCl₃) δ 4.20 (t, *J* = 6.7 Hz, 2H), 1.84 – 1.74 (m, 2H), 1.49 – 1.36 (m, 4H), 0.93 (t, *J* = 7.1 Hz, 3H).

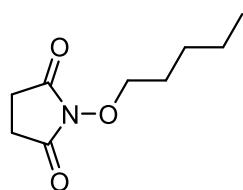
4,5,6,7-Tetrafluoro-2-(pentyloxy)isoindoline-1,3-dione (226g)



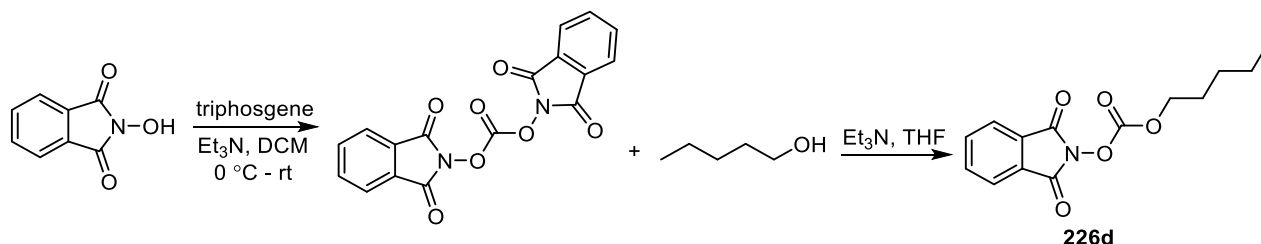
Based on general procedure A, starting from 1.05 g of 4,5,6,7-tetrafluoro-2-hydroxyisoindoline-1,3-dione, product **226g** has been obtained as white solid (270 mg, 0.88 mmol, 20% yield). ¹H NMR (300 MHz, CDCl₃) δ 4.19 (t, *J* = 6.7 Hz, 2H), 1.82 – 1.73 (m, 2H), 1.52 –

1.31 (m, 4H), 0.93 (t, $J = 7.1$ Hz, 3H). ^{19}F NMR (282 MHz, CDCl_3) δ -134.19 (q, $J = 9.7$ Hz), -141.23 (q, $J = 9.7$ Hz).

1-(Pentyloxy)pyrrolidine-2,5-dione (226h)

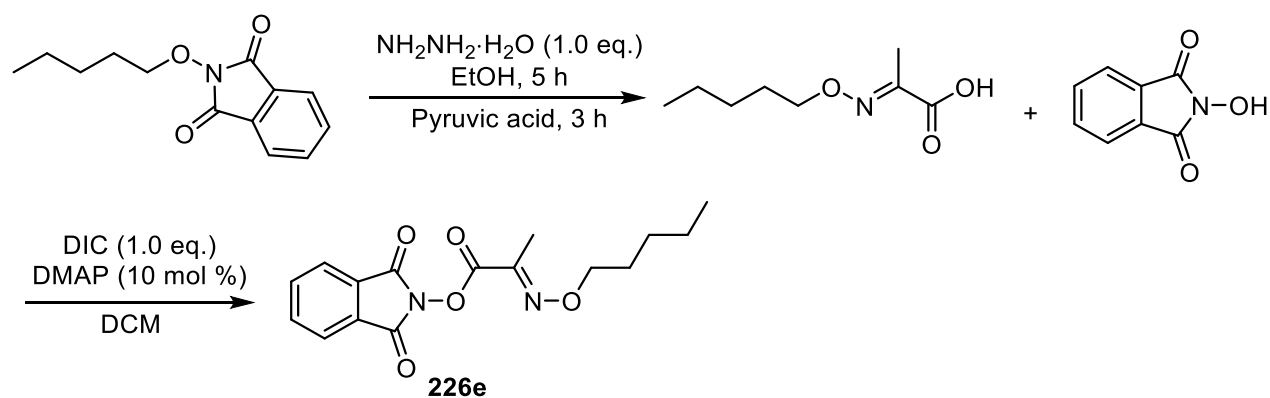


Based on general procedure **A**, starting from 881 mg of pentan-1-ol, product **226h** has been obtained as white solid (1.57 g, 8.5 mmol, 85% yield). ^1H NMR (300 MHz, CDCl_3) δ 4.08 (t, $J = 6.8$ Hz, 2H), 2.70 (s, 4H), 1.78 – 1.68 (m, 2H), 1.48 – 1.30 (m, 4H), 0.91 (t, $J = 7.1$ Hz, 3H).



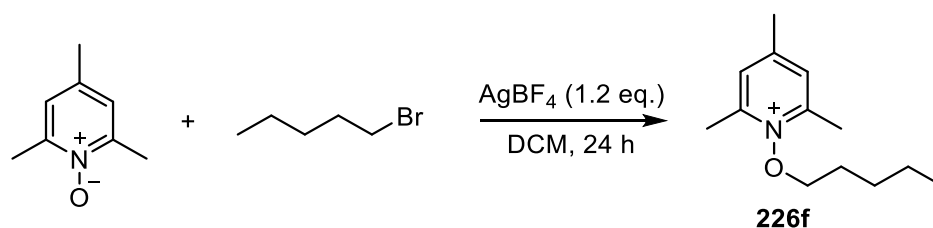
To a suspension of N-hydroxyphthalimide (8.40 g, 50 mmol) in CH_2Cl_2 (237 mL) was added triethylamine (7.11 mL, 50.2 mmol). The reaction mixture turned dark orange-brown while the hydroxyphthalimide went into solution. The mixture was cooled to 0 °C, and trichloromethyl chloroformate (1.44 mL, 11.85 mmol) was added slowly, during which time the reaction mixture became colorless and cloudy. The solution was stirred at 0 °C for 30 min, then at room temperature for 1 h, and then poured into a 0.1 M HCl solution. The aqueous layer was extracted with CH_2Cl_2 (3x). The combined organic layers were washed with 0.1 M HCl and water (2x), dried (MgSO_4), filtered and concentrated to provide bis(1,3-dioxoisindolin-2-yl) carbonate (3.8 g, 91%) as a white solid. ^1H NMR (300 MHz, CDCl_3) δ 8.37 – 8.30 (m, 1H), 7.97 – 7.90 (m, 2H), 7.89 – 7.80 (m, 5H).¹⁹²

To a suspension of bis(1,3-dioxoisindolin-2-yl) carbonate (1.05 g, 3 mmol) and 1-pentanol (0.31 mL, 2.9 mmol) in THF (30 mL) was added triethylamine (0.42 mL, 3 mmol). Upon addition of base, the suspension turned yellow, eventually progressing to a clear orange solution after 30 minutes. The reaction mixture was stirred for 4 h, and the solvent was evaporated. The residue was dissolved in EtOAc (25 mL) and washed with saturated aqueous NaHCO_3 (5×10 mL) until the organic layer became clear. The combined aqueous washings were extracted with EtOAc (30 mL). The combined organic layers were dried over MgSO_4 , filtered and concentrated. The residue was purified by flash column chromatography to afford the desired product **226d** (500 mg, 60% yield). ^1H NMR (300 MHz, CDCl_3) δ 7.95 – 7.86 (m, 2H), 7.84 – 7.76 (m, 2H), 4.35 (t, $J = 6.7$ Hz, 2H), 1.84 – 1.72 (m, 2H), 1.47 – 1.30 (m, 4H), 0.97 – 0.89 (m, 3H). ^{13}C NMR (76 MHz, CDCl_3) δ 161.7, 152.6, 135.0, 128.9, 124.2, 71.8, 28.2, 27.7, 22.3, 14.0.



2-(pentylthio)isoindolin-1,3-dione (2.33 g, 10 mmol, 1.0 equiv.) was then suspended in anhydrous ethanol (0.2 M) and hydrazine monohydrate (0.5 g, 10 mmol, 1.0 equiv.) was added in a single portion. The mixture was stirred at room temperature for 5 hours, resulting in the formation of a white precipitate. The mixture was filtered through a plug of Celite and the filter pad was washed with a minimal amount of ethanol. Then pyruvic acid (2.64 g, 30 mmol, 3.0 eq.) was added to the mixture. The mixture was stirred for 3 hours. The mixture was then concentrated by rotary evaporation and poured into dilute hydrochloric acid. The mixture was extracted with diethyl ether three times. The collected ether layers were then extracted with sodium hydroxide solution (2 M) four times. The collected basic aqueous phases were washed with ethyl ether twice. Then, the basic aqueous phases were carefully acidified to pH 1 using concentrated hydrochloric acid and extracted into diethyl ether three times. These collected ether layers were dried using sodium sulfate and then concentrated by rotary evaporation to yield the product (1.35 g, 78%). ^1H NMR (300 MHz, CDCl_3) δ 4.26 (t, $J = 6.7$ Hz, 2H), 2.06 (s, 3H), 1.80 – 1.64 (m, 2H), 1.39 – 1.32 (m, 4H), 1.00 – 0.83 (m, 3H).¹⁹³

To a solution of (E)-2-((pentylthio)imino)propanoic acid (1.35 g, 7.8 mmol, 1.0 equiv.), *N*-hydroxyphthalimide (1.27 g, 7.8 mmol, 1.0 equiv.) and DMAP (95 mg, 0.78 mmol, 0.1 equiv.) in DCM (23 mL), DIC (1.22 mL, 7.8 mmol, 1.0 equiv.) was added dropwise via syringe. The mixture was stirred at 25 °C for 3 hours. After completion, the mixture was filtered through a thin pad of celite and rinsed with additional DCM. The solvent was removed under reduced pressure, and purified by silica gel column chromatography to afford product **226e** (1.71 g, 69%). ^1H NMR (300 MHz, CDCl_3) δ 7.94 – 7.87 (m, 2H), 7.84 – 7.76 (m, 2H), 4.36 (t, $J = 6.7$ Hz, 2H), 2.14 (s, 3H), 1.81 – 1.69 (m, 2H), 1.43 – 1.32 (m, 4H), 0.96 – 0.88 (m, 3H). ^{13}C NMR (76 MHz, CDCl_3) δ 161.8, 160.5, 145.2, 135.0, 129.0, 124.2, 77.0, 28.8, 28.0, 22.5, 14.1, 11.8.



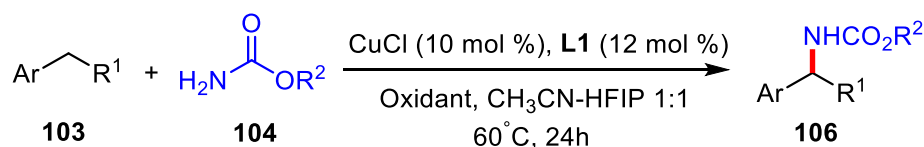
To a solution of 1-bromopentane (1.0 g, 6.6 mmol, 1.2 equiv.) and 2,4,6-trimethylpyridine 1-oxide (750 mg, 5.5 mmol, 1.0 equiv) in DCM (27 mL) was added AgBF_4 (1.28 g, 6.6 mmol, 1.2

equiv.) at room temperature. The reaction mixture was stirred at room temperature for 24 hours, then filtered through Celite, and the filter cake was washed with DCM (2×25 mL). The solvent was removed under reduced pressure. Purification by recrystallization from EtOAc and PE or by flash column chromatography on silica gel afforded 2,4,6-trimethyl-1-(pentyloxy)pyridin-1-ium **226f** (1.5 g, 92%). ¹H NMR (300 MHz, CDCl₃) δ 7.58 – 7.52 (m, 2H), 4.37 (t, *J* = 6.5 Hz, 2H), 2.77 (d, *J* = 0.6 Hz, 6H), 2.53 (d, *J* = 0.7 Hz, 3H), 1.94 – 1.80 (m, 2H), 1.55 – 1.29 (m, 4H), 0.92 (t, *J* = 7.1 Hz, 3H).¹⁹⁴

Conclusions and Perspectives

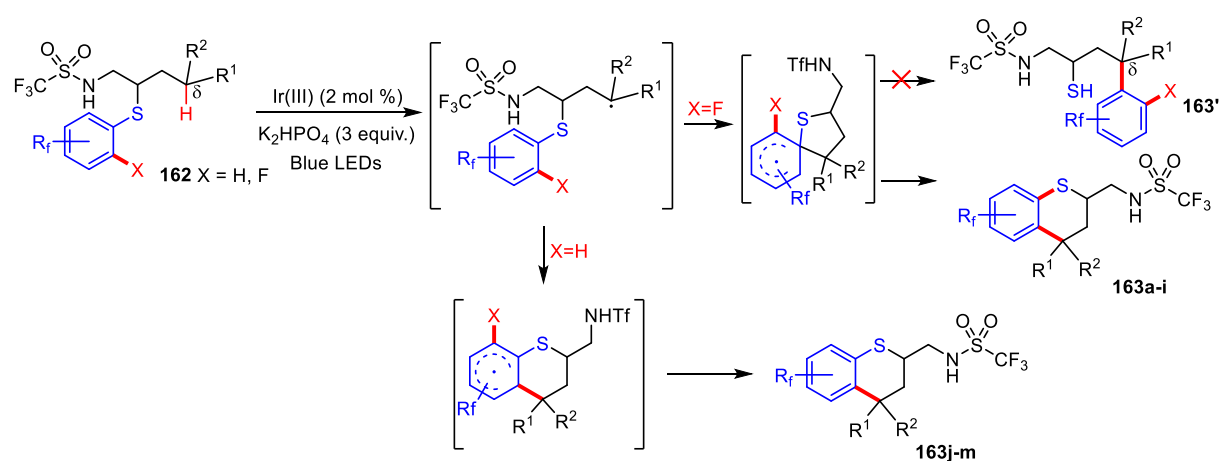
1. Conclusions

The first part of this thesis, an efficient protocol for the synthesis of benzylic carbamates through C–H activation was described, inspired by the Kharasch-Sosnovsky reaction (Scheme 26). The use of a catalytic amount of a Cu(I)/diimine ligand in combination with NFSI ((PhSO₂)₂NF) or F-TEDA-PF₆ as oxidants and H₂NCO₂R as an amine source directly leads to the C–N bond formation at the benzylic position. Compared with traditional methods, it has high atom economy and avoids the use of highly toxic phosgene, carcinogenic isocyanates, and unsafe peroxides. The mild reaction conditions and the broad substrate scope make this transformation a useful method for the late-stage incorporation of a ubiquitous carbamate fragment onto hydrocarbons.



Scheme 26 Copper-catalyzed oxidative benzylic C(sp³)-H amination

Next, Visible light-mediated intramolecular site-selective δ -C(sp³)-H bond arylation of aliphatic trifluoromethanesulfonamides in the presence of photocatalyst Ir[d(CF₃ppy)₂dtbbpy]PF₆ and a base K₂HPO₄ under visible-light irradiation was developed. The reaction proceeds through a radical cascade including the generation of a sulfonamidyl radical, which triggers a 1,5-hydrogen atom transfer, affording a δ -C-centered radical, which finally cyclized onto a neighboring thiopolyfluoroaryl moiety to deliver a range of synthetically useful thiochromanes. The cyclization process occurs through two distinct pathways depending on the nature of the substituent X, *ortho* to the native C-S bond (Scheme 44). Compounds with hydrogens only in the *ortho* position relative to sulfur tend to follow path a (*Homolytic Aromatic Substitution*, HAS), while compounds with fluorines only in the *ortho* position relative to sulfur tend to follow path b (*Truce-Smiles rearrangement*), as it is the more favorable route. The mechanism has been supported by experimental results and DFT calculations. At the same time, this strategy provides an alternative approach for the synthesis of thiochromanes.



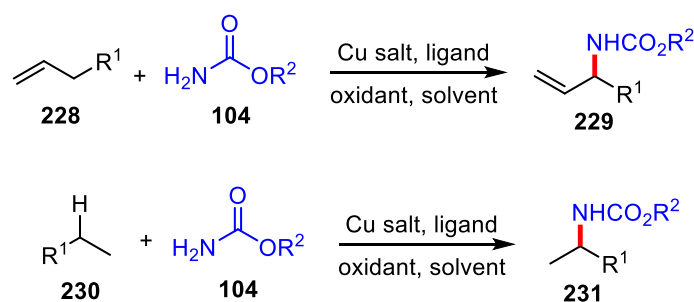
Scheme 44 Intramolecular δ -C(sp³)-H arylation of sulfonamides

Afterwards, our team has developed an effective method for silylating olefins by utilizing CuCl₂ as a catalyst for hydrogen atom transfer (HAT) in the presence of 390 nm light. By combining copper(II) chloride with acetonitrile, a photoactive species [Cu(MeCN)Cl₃]⁻ is generated that can produce a highly reactive chlorine radical through ligand-to-metal charge transfer when exposed to light. This radical can then react with silane to form a silicon-based radical, which can undergo a coupling reaction with an olefin to generate valuable products. This method is practical, straightforward, and employs mild conditions, as well as inexpensive and readily available reagents, making it a promising alternative to traditional olefin hydrosilylation techniques.

Finally, we reported a highly efficient catalytic method for synthesizing a broad range of organosilicon compounds. Our protocol is based on the use of the complex [Ir(dF(CF₃)ppy)₂(dtbbpy)]PF₆ in combination with NiBr₂ catalyst/dtbpy system, along with commercially available hydrosilanes as a source of silicon. This approach has demonstrated exceptional tolerance towards various functional groups, whether they possess electron-deficient or electron-rich properties, resulting in satisfactory yields of the desired products. Moreover, our method can utilize not only aryl bromides and heteroaryl bromides but also primary alkyl bromides as suitable substrates. Compared to traditional methods that avoid the use of highly reactive and sensitive organometallic reagents, this approach is applicable to a broader range of functionalized substrates.

2 Perspectives

For the first project, we have developed a method for benzylic C(sp³)-H carbamation using Kharasch-Sosnovsky type reactions as the key mechanism. However, this system is limited to only benzylic hydrocarbons. Therefore, the development of direct carbamoylation of allylic C(sp³)-H, aliphatic hydrocarbon C(sp³)-H, and even light hydrocarbon C(sp³)-H would be a significant breakthrough (Scheme 75).



Scheme 75 Copper-catalyzed oxidative C(sp³)-H amination

Site-selective C-H functionalization has always been a significant challenge, and 1,5-hydrogen atom transfer (HAT) initiated by nitrogen-centered radicals represents an efficient and powerful strategy. However, due to the high bond dissociation energy of the N-H bond, pre-activation of the amine is typically required. Recently, some highly efficient methods for *in-situ* activation of N-H bonds have also been developed, such as using stoichiometric amounts of high-valent iodine reagents or the synergistic effect of a photocatalyst Ir(III), and a base. Developing more practical and sustainable strategies to activate N-H bonds is crucial, such as the development of organic photocatalysts to replace expensive metal catalysts like iridium. Alternatively, this approach can be combined with metal-catalyzed coupling reactions to achieve diverse functionalization with site-selectivity.

The visible-light-induced hydrosilylation typically requires a photocatalyst and a hydrogen atom transfer catalyst. We described an efficient method for the hydrosilylation of olefins, utilizing CuCl₂ as a photocatalyst and HAT catalyst under 390 nm light irradiation. As is well known, some metal salts can generate reactive radicals through ligand-to-metal charge transfer under light excitation, and these radicals can abstract hydrogen efficiently. Therefore, by controlling the ligands through this strategy, different types of radicals can be generated, achieving selective activation of substrates.

Arylsilanes are widely used in material science, but the methods of access to these organosilanes

remains limited. Traditional methods are limited by highly reactive and moisture sensitive organometallic reagents, resulting with a relatively narrow substrate scope. Friedel-Crafts C–H silylation is limited to electron-rich aromatic compounds only. The transition metal-catalyzed cross-dehydrogenative coupling between arenes/heteroarenes and hydrosilanes is constrained by low regioselectivity, the requirement for directing groups, the use of noble metal catalysts, and the need for stoichiometric hydrogen acceptors. Therefore, developing a more general method for constructing C(sp²)–Si bonds is also a challenge. The coupling reaction between aryl halides and silanes catalyzed by nickel is a promising method, as the substrates are inexpensive and readily available, and the reaction has a broad substrate scope. However, the quest for a direct arene C(sp²)–H silylation still remains and will certainly deserves in depths studies to avoid costly iridium catalysts or prefunctionalization of the aromatic fragments.

References

- [1] Newhouse, T.; Baran, P. S. *Angew. Chem., Int. Ed.* **2011**, *50*, 3362-3374.
- [2] Ramirez, T. A.; Zhao, B. G.; Shi Y. *Chem. Soc. Rev.* **2012**, *41*, 931-942.
- [3] He, J.; Wasa, M.; Chan, K. S. L.; Shao, Q.; Yu, J.-Q. *Chem. Rev.* **2017**, *117*, 8754-8786.
- [4] Yi, H.; Zhang, G. T.; Lei, A. *Chem. Rev.* **2017**, *117*, 9016-9085.
- [5] Roudesly, F.; Oble, J.; Poli, G. *J. Mol. Catal. A Chemical* **2017**, *426*, 275-296.
- [6] Bergman, R. *Nature*, **2007**, *446*, 391-393.
- [7] Blanksby, S. J.; Ellison, G. B. *Acc. Chem. Res.* **2003**, *36*, 255-263.
- [8] Schmidt, V. A.; Quinn, R. K.; Brusoe, A. T.; Alexanian, E. J. *J. Am. Chem. Soc.* **2014**, *136*, 14389-14392.
- [9] Quinn, R. K.; Könst, Z. A.; Michalak, S. E.; Schmidt, Y.; Szklarski, A. R.; Flores, A. R.; Nam, S.; Horne, D. A.; Vanderwal, C. D.; Alexanian, E. J. *J. Am. Chem. Soc.* **2016**, *138*, 696-702.
- [10] Czaplyski, W. L.; Na, C. G.; Alexanian, E. J. *J. Am. Chem. Soc.* **2016**, *138*, 13854-13857.
- [11] Plummer C. M.; Zhou, H. B.; Zhu, W.; Huang, H.; Liu, L.; Chen, Y. *Polym. Chem.* **2018**, *9*, 1309-1317.
- [12] Mao, R.; Bera, S.; Turla, A. C.; Hu, X. *J. Am. Chem. Soc.* **2021**, *143*, 14667-14675.
- [13] Shen, Y.; Gu, Y.; Martin, R. *J. Am. Chem. Soc.* **2018**, *140*, 12200-12209.
- [14] Hofmann, A. W. *Ber. Dtsch. Chem. Ges.* **1883**, *16*, 558-560.
- [15] Fazekas, T. J., Alty, J. W., Neidhart, E. K., Miller, A. S., Leibfarth, F. A., Alexanian, E. J. *Science* **2022**, *375*, 545-550.
- [16] Barton, D. H. R.; Beaton, J. M.; Geller, L. E.; Pechet, M. M. *J. Am. Chem. Soc.* **1960**, *82*, 2640-2641.
- [17] Wu, X.; Zhu C. *CCS Chem.* **2020**, *2*, 813-828.
- [18] Wu, X.; Wang, M.; Huan, L.; Wang, D.; Wang J.; Zhu, C. *Angew. Chem., Int. Ed.* **2018**, *57*, 1640-1644.
- [19] Wu, X.; Zhang, H.; Tang, N.; Wu, Z.; Wang, D.; Ji, M.; Xu, Y.; Wang M.; Zhu, C. *Nat. Commun.* **2018**, *9*, 3343-3350.
- [20] Wang, M.; Huan, L.; Zhu, C. *Org. Lett.* **2019**, *21*, 821-825.
- [21] Zhang, J.; Li, Y.; Zhang, F.; Hu C.; Chen, Y. *Angew. Chem., Int. Ed.* **2016**, *55*, 1872-1875.
- [22] Hu, A.; Guo, J.; Pan, H.; Tang, H.; Gao Z.; Zuo, Z. *J. Am. Chem. Soc.* **2018**, *140*, 1612-1616.
- [23] Cheng, Z.; Chen P.; Liu, G. *Acta Chim. Sin.* **2019**, *77*, 856-860.
- [24] Lalevee, J.; Fouassier, J. P.; In *Overview of Radical Initiation*, John Wiley & Sons Ltd., **2012**, pp. 37-55.
- [25] Denisov, E. T.; Denisova, G. T.; Pokidova, T. S.; *Handbook of Free Radical Initiators*, John Wiley & Sons, Inc, Hoboken, NJ, **2003**.
- [26] Hu, A.; Guo, J.; Pan, H.; Zuo, Z. *Science* **2018**, *361*, 668-672.

- [27] Recupero, F.; Punta, C. *Chem. Rev.* **2007**, *107*, 3800-3842.
- [28] Kamijo, S.; Takao, G.; Kamijo, K.; Hirota, M.; Tao, K.; Murafuji, T. *Angew. Chem. Int. Ed.* **2016**, *128*, 9847-9851.
- [29] Vincent, J. M.; Abadie, B.; Jardel, D.; Pozzi, G.; Toullec, P.; *Chem. Eur. J.* **2019**, *25*, 16120-16127.
- [30] Thaler, W. A. *Methods Free Radic. Chem* **1969**, *2*, 121.
- [31] Nechvatal, A. *Adv. Free Radic.* **1972**, *4*, 175.
- [32] Russell, G. A. In *Free Radicals*; Kochi, J. K., Ed.; Wiley: New York, **1973**; Vol. 2, p. 289.
- [33] Russell, G. A. In *Free Radicals*; Kochi, J. K., Ed.; Wiley: New York, **1973**; Vol. 2, p. 311.
- [34] Ohkubo, K.; Fujimoto, A.; Fukuzumi, S. *Chem. Commun.* **2011**, *47*, 8515-8517.
- [35] Ohkubo, K.; Mizushima, K.; Fukuzumi, S. *Res. Chem. Intermed.* **2013**, *39*, 205-220.
- [36] Deng, H.-P.; Zhou, Q.; Wu, J. *Angew. Chem., Int. Ed.* **2018**, *57*, 12661-12665.
- [37] Rohe, S.; Morris, A. O.; McCallum, T.; Barriault, L. *Angew. Chem., Int. Ed.* **2018**, *57*, 15664-15669.
- [38] Shields, B. J.; Doyle, A. G. *J. Am. Chem. Soc.* **2016**, *138*, 12719-12722.
- [39] Treacy, S. M.; Rovis, T. *J. Am. Chem. Soc.* **2021**, *143*, 7, 2729-2735.
- [40] Afsina, C. M. A.; Aneeja, T.; Neetha, M.; Anilkumar, G. *Eur. J. Org. Chem.* **2021**, *12*, 1776-1808.
- [41] Yang, Y.; Gao, W.; Wang, Y.; Wang, X.; Cao, F.; Shi, T.; Wang, Z. *ACS Catal.* **2021**, *11*, 967-984.
- [42] Liu, S.; Achou, R.; Boulanger, C.; Pawar, G.; Kumar, N.; Lusseau, J.; Robert, F.; Landais, Y. *Chem. Commun.* **2020**, *56*, 13013-13016.
- [43] Suh, S.-E., Chen, S.-J., Mandal, M.; Guzei, I. A.; Cramer, C. J.; Stahl, S. S. *J. Am. Chem. Soc.* **2020**, *142*, 11388-11393.
- [44] Park, Y.; Kim, Y.; Chang, S. *Chem. Rev.* **2017**, *117*, 13, 9247-9301.
- [45] Trowbridge, A.; Walton, S. M.; Gaunt M. J. *Chem. Rev.* **2020**, *120*, 2613-2692.
- [46] Kharasch, M.S.; Fono, A. *J. Org. Chem.* **1958**, *23*, 325-326.
- [47] Kharasch, M. S.; Sosnovsky, G. *J. Am. Chem. Soc.* **1958**, *80*, 756.
- [48] Liu, X., Zhang, Y., Wang, L.; Fu, H.; Jiang, Y.; Zhao, Y. *J. Org. Chem.* **2008**, *73*, 6207-6212.
- [49] Clark, J.S., and Roche, C. *Chem. Commun.* **2005**, 5175-5177.
- [50] Smith, K., Hupp, C.D., Allen, K.L.; Slough, G.A. *Organometallics* **2005**, *24*, 1747-1755.
- [51] Gephart III, R. T.; Huang, D. L.; Aguila, M. J. B.; Schmidt, G., Shahu, A.; Warren, T. H. *Angew. Chem. Int. Ed.* **2012**, *51*, 6488-6492.
- [52] Zhang, Y., Fu, H., Jiang, Y.; Zhao, Y. *Org. Lett.* **2007**, *9*, 3813-3816.
- [53] Powell, D.A.; Fan, H. *J. Org. Chem.* **2010**, *75*, 2726-2729.
- [54] Ni, Z., Zhang, Q., Xiong, T. *et al.*, *Angew. Chem. Int. Ed.* **2012**, *51*, 1244-1247.
- [55] Zeng, H.-T., Huang, J.-M. *Org. Lett.* **2015**, *17*, 4276-4279.
- [56] Rabet, P. T. G., Fumagalli, G., Boyd, S.; Greaney, M. F. *Org. Lett.* **2016**, *18*, 1646-1649.

- [57] Suh, S.; Chen, S.; Mandal, M.; Guzei, I.; Cramer, C.; Stahl, S. *J. Am. Chem. Soc.* **2020**, *142*, 11388-11393.
- [58] Michaudel, Q.; Thevenet, D.; Baran, P.S. *J. Am. Chem. Soc.* **2012**, *134*, 2547-2550.
- [59] Tran, B.L.; Li, B.; Driess, M.; Hartwig, J.F. *J. Am. Chem. Soc.* **2014**, *136*, 2555-2563.
- [60] Fuentes, M.A.; Gava, R.; Saper, N. I.; Romero, E. A.; Caballero, A.; Hartwig, J. F.; Pérez, P. J. *Angew. Chem. Int. Ed.* **2021**, *60*, 18467-18471.
- [61] Teng, F.; Sun, S.; Jiang, Y.; Yu, J.; Cheng, J. *Chem. Commun.* **2015**, *51*, 5902-5905.
- [62] Wiese, S.; Badici, Y.M.; Gephart, R. T.; Mossin, S.; Varonka, M. S.; Melzer, M. M.; Meyer, K.; Cundari, T. R.; Warren, T. H. *Angew. Chem. Int. Ed.* **2010**, *49*, 8850-8855.
- [63] Gephart, R.T. III, Huang, D.L., Aguila, M.J.B.; Schmidt, G.; Shahu, A.; Warren, T. H. *Angew. Chem. Int. Ed.* **2012**, *51*, 6488-6492.
- [64] Wu, X.; Zhao, Y.; Zhang, G.; Ge, H. *Angew. Chem. Int. Ed.* **2014**, *53*, 3706-3710.
- [65] Wang, Z.; Ni, J.; Kuninobu, Y.; Kanai, M. *Angew. Chem. Int. Ed.* **2014**, *53*, 3496-3499.
- [66] Nozawa-Kumada, K.; Saga, S.; Matsuzawa, Y.; Hayashi, M.; Shigeno, M.; Kondo, Y. *Chem. Eur. J.* **2020**, *26*, 4496-4499.
- [67] Jin, R.-X.; Dai, J.-C.; Li, Y.; Wang, X.-S. *Org. Lett.* **2021**, *23*, 421-426.
- [68] Min, Q.-Q.; Yang, J. W.; Pang, M.-J. *Org. Lett.* **2020**, *22*, 2828-2832.
- [69] Adams, P.; Baron, F. A. *Chem. Rev.* **1965**, *65*, 567-602; (b) Ghosh, A. K.; Brindisi, M. *J. Med. Chem.* **2015**, *58*, 2895-2940.
- [70] Ghosh, A.K. *J. Org. Chem.* **2010**, *75*, 7967-7989; (b) Joshi, A.; Larhed, M. *J. Med. Chem.* **2013**, *56*, 8999-9007.
- [71] (a) Semetey, V.; Hemmerlin, C.; Didierjean, C.; Schaffner, A. P.; Giner, A. G.; Aubry, A.; Briand, J. P.; Marraud, M.; Guichard, G. *Org. Lett.* **2001**, *3*, 3843-3846; (b) Patil, B. S.; Vasanthakumar, G. R. and Suresh Babu, V. V. *J. Org. Chem.* **2003**, *68*, 7274-7280.
- [72] Badreshia, S.; Marks, J. G. *Am. J. Contact Dermatitis* **2002**, *13*, 77-79.
- [73] (a) Bayer, O. *Angew. Chem.* **1947**, *9*, 257-288; (b) Maisonneuve, L.; Lamarzelle, O.; Rix, E.; Grau, E.; Cramail, H. *Chem. Rev.* **2015**, *115*, 12407-12439.
- [74] Greene, T. W. and Wuts, P. G. M. *Protecting Groups in Organic Synthesis*, 3rd Ed. J. Wiley & Sons, New York, (1999), 503.
- [75] (a) Ozaki, S. *Chem. Rev.*, **1972**, *72*, 457-496; (b) Satchell, D. P. N.; Satchell, R. S. *Chem. Soc. Rev.* **1975**, *4*, 231-250; (c) Majer, P.; Randad, R. S. *J. Org. Chem.* **1994**, *59*, 1937-1938; (d) Migawa, M. T.; Swayze, E. E. *Org. Lett.* **2000**, *2*, 3309-3311; (e) Kim, J. G.; Jang, D. O. *Tetrahedron Lett.* **2009**, *50*, 2688-2692.
- [76] (a) Casedei, M. A.; Inesi, A.; Moracci, M. F.; Rossi, L. *Chem. Commun.* **1996**, 2575-2576; (b) Casadei, M. A.; Moracci, F. M.; Zappia, G.; Inesi, A.; Rossi, L. *J. Org. Chem.* **1997**, *62*, 6754-6759; (c) Yoshida, M. A.; Hara, N.; Okuyama, S. *Chem. Commun.* **2000**, *2*, 151-152; (d) Chaturvedi, D.; Kumar, A.; Ray, S. *Tetrahedron Lett.* **2003**, *44*, 7637-7639; (e) Peterson, S. L.; Stucka, S. M.; Dinsmore, C. J. *Org. Lett.* **2010**, *12*, 1340-1343.

- [77] Yoshida, Y.; Ishii, S.; Yamashita, T. *Chem. Lett.* **1984**, *13*, 1571-1572.
- [78] Zhang, Q.; Yuan, H. Y.; Fukaya, N.; Choi, J. C. *ACS Sustain. Chem. Eng.* **2018**, *6*, 6675-6681.
- [79] Ren, L.; Jiao, N. *Chem. Commun.* **2014**, *50*, 3706-3709.
- [80] Xiong, W. F.; Qi, C. R.; He, H. T.; Ouyang, L.; Zhang, M. and Jiang, H. F. *Angew. Chem. Int. Ed.* **2015**, *54*, 3084-3087.
- [81] Hong, J. Y.; Seo, U. R.; Chung, Y. K. *Org. Chem. Front.* **2016**, *3*, 764-767.
- [82] Chikkade, P. K.; Kuninobu, Y.; Kanai, M. *Chem. Sci.* **2015**, *6*, 3195-3200.
- [83] Ahn, J. M.; Peters, J. C.; Fu, G. C. *J. Am. Chem. Soc.* **2017**, *139*, 18101-18106.
- [84] (a) Fu, L.; Zhang, Z.; Chen, P.; Lin, Z.; Liu, G. *J. Am. Chem. Soc.*, **2020**, *142*, 12493-12500;
(b) Suh, S.-E.; Chen, S.-J.; Mandal, M.; Guzei, I. A.; Cramer, C. J. and Stahl, S. S. *J. Am. Chem. Soc.*, **2020**, *142*, 11388-11393.
- [85] Hartwig, J. F.; Larsen, M. A. *ACS Cent. Sci.* **2016**, *2*, 281-292.
- [86] Zhang, Y.; Yin, Z.; Wu, X.-F. *Org. Lett.* **2020**, *22*, 1889-1893.
- [87] Jianga, H.; Studer, A. *Chem. Soc. Rev.* **2020**, *49*, 1790-1811.
- [88] Jenkins, C. L.; Kochi, J. K. *J. Am. Chem. Soc.* **1972**, *94*, 856-865.
- [89] Min, Q.-Q.; Yang, J.-W.; Pang, M.-J.; Ao, G.-Z.; Liu, F. *Org. Lett.* **2020**, *22*, 2828-2832.
- [90] Li, S.-J.; Lan, Y. *Chem. Commun.*, **2020**, *56*, 6609-6619; (b) Yu, X.-Y.; Chen, J.; Chen, H.-W.; Xiao, W.-J.; Chen, J.-R. *Org. Lett.* **2020**, *22*, 2333-2338.
- [91] Furuya, T.; Strom, A. E.; Ritter, T. *J. Am. Chem. Soc.* **2009**, *131*, 1662-1663.
- [92] Sonawane, R. B.; Sonawane, S. R.; Rasala, N. K.; Jagtap, S. V. *Green Chem.* **2020**, *22*, 3186-3195.
- [93] Zhang, W.; Wang, F.; Mccann, S. D.; Wang, D.; Chen, P.; Stahl, S. S.; Liu, G. S. *Science* **2016**, *353*, 1014-1018.
- [94] Meng, Q.; Schirmer, T. E.; Berger, A. L.; Donabauer, K.; König, B. *J. Am. Chem. Soc.* **2019**, *141*, 11393-11397.
- [95] Flinker, M.; Yin, H.; Juhl, R. W.; Eikeland, E. Z.; Overgaard, J.; Nielsen, D. U.; Skrydstrup, T. *Angew. Chem. Int. Ed.* **2017**, *56*, 15910-15915.
- [96] Sang, R.; Korkis, S. E.; Su, W.; Ye, F.; Engl, P. S.; Berger, F.; Ritter, T. *Angew. Chem. Int. Ed.* **2019**, *58*, 16161-16166.
- [97] Niakan, M.; Asadi, Z.; Masteri-Farahani, M. *ChemistrySelect* **2019**, *4*, 1766-1775.
- [98] Fuse, H.; Kojima, M.; Mitsunuma, H.; Kanai, M. *Org. Lett.* **2018**, *20*, 2042-2045.
- [99] Cao, X.; Cheng, X.; Bai, Y.; Liu, S.; Deng, G.-J. *Green Chem.* **2014**, *16*, 4644-4648.
- [100] Zhang, J.; Zhao, X.; Liu, P.; Sun, P. P. *J. Org. Chem.* **2019**, *84*, 12596-12605.
- [101] Weix, D. J.; Marković, D.; Ueda, M.; Hartwig, J. F. *Org. Lett.* **2009**, *11*, 2944-2947.
- [102] Peña-López, M.; Neumann, H.; Beller, M. *ChemSusChem* **2016**, *9*, 2233-2238.
- [103] Guo, W.; Wang, Q.; Zhu, J. *Chem. Soc. Rev.* **2021**, *50*, 7359-7377.
- [104] Qin, Q. and Yu, S. *Org. Lett.* **2015**, *17*, 1894-1897.
- [105] Qin, Y.; Han, Y.; Tang, Y.; Wei, J.; Yang, M. *Chem. Sci.* **2020**, *11*, 1276-1282.

- [106] Chen, H.; Fan, W.; Yuan, X.; Yu, S. *Nat. Commun.* **2019**, *10*, 4743-4751.
- [107] Wu, K.; Wang, L.; Colón-Rodríguez, S.; Flechsig G.; Wang, T. *Angew. Chem., Int. Ed.* **2019**, *58*, 1774-1778.
- [108] Jiang, H.; Studer, A. *Angew. Chem., Int. Ed.* **2018**, *57*, 1692-1696.
- [109] Na, C.; Alexanian, E. J. *Angew. Chem., Int. Ed.* **2018**, *57*, 13106-13109.
- [110] Kim, N.; Lee, C.; Kim T.; Hong, S. *Org. Lett.* **2019**, *21*, 9719-9723.
- [111] (a) Choi, G. J.; Zhu, Q.; Miller, D. C.; Gu, C. J.; Knowles, R. R. *Nature* **2016**, *539*, 268-271. (b) Tyburski, R.; Liu, T.; Glover, S. D.; Hammarstrom, L. *J. Am. Chem. Soc.* **2021**, *143*, 560-576.
- [112] Chu, J. C. K.; Rovis, T. *Nature* **2016**, *539*, 272-275.
- [113] Xu, B.; Tambar, U. K. *ACS Catal.* **2019**, *9*, 4627-4631.
- [114] Tang, N.; Wu, X.; Zhu, C. *Chem. Sci.* **2019**, *10*, 6915-6919.
- [115] Deng, Z.; Li, G.-X.; He, G.; Chen, G. *J. Org. Chem.* **2019**, *84*, 15777-15787.
- [116] (a) Snape, T. J. *Chem. Soc. Rev.* **2008**, *37*, 2452-2458. (b) Kosowan, J. R.; W'Giorgis, Z.; Grewal, R.; Wood, T. E. *Org. Biomol. Chem.* **2015**, *13*, 6754-6765. For recent examples, see: (c) Hervieu, C.; Kirillova, M. S.; Suarez, T.; Muller, M.; Merino, E.; Nevado, C. *Nat. Chem.* **2021**, *13*, 327-334. (d) Whalley, D. M.; Duong, H. A.; Greaney, M. F. *Chem. Eur. J.* **2019**, *25*, 1927-1930. (e) Wang, Z.; Chen, Y.; Zhang, H.; Sun, Z.; Zhu, C.; Ye, L. *J. Am. Chem. Soc.* **2020**, *142*, 3636-3644.
- [117] (a) Bowman, W. R.; Storey, J. M. D. *Chem. Soc. Rev.* **2007**, *36*, 1803-1822. (b) Studer, A.; Curran, D. P. *Angew. Chem. Int. Ed.* **2011**, *50*, 5018-5022. (c) Gurry, M.; Aldabbagh, F. *Org. Biomol. Chem.* **2016**, *14*, 3849-3862.
- [118] (a) Chen, Z.-M.; Zhang, X.-M.; Tu, Y.-Q. *Chem. Soc. Rev.* **2015**, *44*, 5220-5245. (b) Whalley, D. M.; Seayad, J.; Greaney M. F. *Angew. Chem. Int. Ed.* **2021**, *60*, 22219-22223.
- [119] Montecvecchi, P. C.; Navacchia, M. L. *J. Org. Chem.* **1998**, *63*, 537-542.
- [120] Shu, W.; Genoux, A.; Li, Z.; Nevado, C. *Angew. Chem. Int. Ed.* **2017**, *56*, 10521-10524.
- [121] Dénès, F.; Pichowicz, M.; Povie, G.; Renaud, P. *Chem. Rev.* **2014**, *114*, 2587-2693.
- [122] Crowell, T. R.; Peach, M. E. *J. Fluorine Chem.* **1982**, *21*, 469-477.
- [123] (a) Arora, A.; Weaver, J. D. *Acc. Chem. Res.* **2016**, *49*, 2273-2283. (b) Sun, X.; Ritter, T. *Angew. Chem. Int. Ed.* **2021**, *60*, 10557-10562.
- [124] McAtee, R. C.; Noten, E. A.; Stephenson, C. R. J. *Nature Commun.* **2020**, *11*, 2528-2535.
- [125] Bhunia, A.; Studer, A. *Chem.* **2021**, *7*, 2060-2100.
- [126] (a) Zhao, K.; Yamashita, K.; Carpenter, J. E.; Sherwood, T. C.; Ewing, W. R.; Cheng, P. T. W.; Knowles, R. R. *J. Am. Chem. Soc.* **2019**, *141*, 8752-8757. (b) Chen, D.-F.; Chu, J. C. K.; Rovis, T. *J. Am. Chem. Soc.* **2017**, *139*, 14897-14900. (c) Connell, T. U.; Fraser, C. L.; Czyz, M. L.; Smith, Z. M.; Hayne, D. J.; Doeven, E. H.; Agugiaro, J.; Wilson, D. D.; Adcock, J. L.; Scully, A. D.; Gomez, D. E.; Barnett, N. W.; Polyzos, A.; Francis, P. S. *J. Am. Chem. Soc.* **2019**, *141*, 17646-17658.

- [127] Wei, Q.; Hou, W. D.; Liao, N.; Peng, Y. G. *Adv. Synth. Catal.* **2017**, *359*, 2364-2368.
- [128] Lu, H.-H.; Zhang, F. G.; Meng, X.-G.; Duan, S.-W.; Xiao, W.-J. *Org. Lett.* **2009**, *11*, 3946-3949.
- [129] Qiu, D.; He, J.; Yue.; Li, Y. *Org. Lett.* **2016**, *18*, 3130-3133.
- [130] Chatgililoglu, C., *Organosilanes in Radical Chemistry*, Wiley: Chichester, UK, (2004).
- [131] Ramesh, R.; Reddy, D. S. *J. Med. Chem.* **2018**, *61*, 3779-3798.
- [132] Sommer, L. H.; Pietrusza, E. W.; Whitmore, F. C. *J. Am. Chem. Soc.* **1947**, *69*, 188.
- [133] Nimlos, M. R.; Ellison, G. B. *J. Am. Chem. Soc.* **1986**, *108*, 6522-6529.
- [134] Chatgililoglu, C. *Chem. Rev.* **1995**, *95*, 1229-1251.
- [135] Sekiguchi, A.; Fukawa, T.; Nakamoto, M.; Lee, V. Ya.; Ichinohe, M. *J. Am. Chem. Soc.* **2002**, *124*, 9865-9869.
- [136] Kyushin, S.; Sakurai, H.; Betsuyaku, T.; Matsumoto, H. *Organometallics* **1997**, *16*, 5386-5388.
- [137] Kira, M.; Obata, T.; Kon, I.; Hashimoto, H.; Ichinohe, M.; Sakurai, H.; Kyushin, S.; Matsumoto, H. *Chem. Lett.* **1998**, 1097-1100.
- [138] Kyushin, S.; Sakurai, H.; Matsumoto, H. *Chem. Lett.* **1998**, 107-108.
- [139] Apeloig, Y.; Bravo-Zhivotovskii, D.; Yuzefovich, M.; Bendikov, M.; Shames, A. I. *Appl. Magn. Reson.* **2000**, *18*, 425-434.
- [140] Guerra, M. *J. Am. Chem. Soc.* **1993**, *115*, 11926-11929.
- [141] Qrareya, H.; Dondi, D.; Ravelli, D.; Fagnoni, M. *ChemCatChem* **2015**, *7*, 3350-3357.
- [142] Zhou, R.; Goh, Y. Y.; Liu, H.; Tao, H.; Li, L.; Wu, J. *Angew. Chem., Int. Ed.* **2017**, *56*, 16621-16625.
- [143] Zhu, J.; Cui, W.-C.; Wang, S.; Yao, Z.-J. *J. Org. Chem.* **2018**, *83*, 14600-14609.
- [144] Xu, N.; Li, B.; Wang, C. and Uchiyama, M. *Angew. Chem. Int. Ed.* **2020**, *59*, 10639-10644.
- [145] Takemura, N.; Sumida, Y.; Ohmiya, H. *ACS Catal.* **2022**, *12*, 7804-7810.
- [146] Wan, Y.; Zhao, Y.; Zhu, J.; Yuan, Q.; Wang, W.; Zhang, Y. *Green Chem.* **2023**, *25*, 256-263.
- [147] Zhang, Z.; Hu, X. *ACS Catal.* **2019**, *10*, 777-782.
- [148] Yang, C.; Wang, J.; Li, J.; Ma, W.; An, K.; He, W.; Jiang, C. *Adv. Synth. Catal.* **2018**, *360*, 3049-3054.
- [149] Liu, S.; Pan, P.; Fan, H.; Li, H.; Wang, W.; Zhang, Y. *Chem. Sci.* **2019**, *10*, 3817-3825.
- [150] Rammal, F.; Gao, D.; Boujnah, S.; Hussein, A. A.; Lalevée, J.; Gaumont, A.-C.; Morlet-Savary, F.; Lakhdar, S. *ACS Catal.* **2020**, *10*, 13710-13717.
- [151] Dai, C.; Zhan, Y.; Liu, P.; Sun, P. *Green Chem.* **2021**, *23*, 314-319.
- [152] Lesbani, A.; Kondo, H.; Yabusaki, Y.; Nakai, M.; Yamanoi, Y.; Nishihara, H. *Chem. Eur. J.* **2010**, *16*, 13519-13527.
- [153] Rodríguez, A. M.; Pérez-Ruiz, J.; Molina, F.; Poveda, A.; Pérez-Soto, R.; Maseras, F.; Díaz-Requejo, M. M.; Pérez, P. J. *J. Am. Chem. Soc.* **2022**, *144*, 10608-10614.
- [154] Omann, L.; Pudasaini, B.; Irran, E.; Klare, H. F. T.; Baik, M. H.; Oestreich, M. *Chem. Sci.* **2018**, *9*, 5600-5607.

- [155] Li, Y.; Zhang, J.; Liand D. F.; Chen, Y. Y. *Org. Lett.* **2018**, *20*, 3296-3299.
- [156] Quintard, A.; Alexakis, A.; Mazet, C. *Angew. Chem. Int. Ed.* **2011**, *50*, 2354-2358.
- [157] Ibrahim, A. D.; Entsminger, S. W.; Zhu, L.; Fout, A. R. *ACS Catal.* **2016**, *6*, 3589-3593.
- [158] Treacy, S. M.; Rovis, T. *J. Am. Chem. Soc.* **2021**, *143*, 2729-2735.
- [159] Takeuchi, R.; Ishii, N.; Sugiura, M.; Sato, N. *J. Org. Chem.* **1992**, *57*, 4189-4194.
- [160] Iannazzo, L.; Molander, G. A. *Eur. J. Org. Chem.* **2012**, 4923-4926.
- [161] Brook, M. A. *Silicon in Organic, Organometallic, and Polymer Chemistry*, Wiley, New York, **2000**.
- [162] Bähr, S.; Xue, W.; Oestreich, M. *ACS Catal.* **2018**, *9*, 16-24.
- [163] Frick, U.; Simchen, G. *Synthesis* **1984**, 929-933.
- [164] Furukawa, S.; Kobayashi, J.; Kawashima, T. *Dalton Trans.* **2010**, *39*, 9329-9336.
- [165] Klare, H. T.; Oestreich, M.; Ito, J.; Nishiyama, H.; Ohki, Y.; Tatsumi, K. *J. Am. Chem. Soc.* **2011**, *133*, 3312-3315.
- [166] Yin, Q.; Klare, H. F. T.; Oestreich, M. *Angew. Chem., Int. Ed.* **2016**, *55*, 3204-3207.
- [167] Chen, Q.; Klare, H. T.; Oestreich, M. *J. Am. Chem. Soc.* **2016**, *138*, 7868-7871.
- [168] Bähr, S.; Oestreich, M. *Angew. Chem., Int. Ed.* **2017**, *56*, 52-59.
- [169] Curless, L. D.; Clark, E. R.; Dunsford, J. J.; Ingleson, M. J. *Chem. Commun.* **2014**, *50*, 5270-5272.
- [170] Ma, Y.; Wang, B.; Zhang, L.; Hou, Z. *J. Am. Chem. Soc.* **2016**, *138*, 3663-3666.
- [171] Han, Y.; Zhang, S.; He, J.; Zhang, Y. *J. Am. Chem. Soc.* **2017**, *139*, 7399-7407.
- [172] Ihara, H.; Suginome, M. *J. Am. Chem. Soc.* **2009**, *131*, 7502-7503.
- [173] Simmons, E. M.; Hartwig, J. F. *J. Am. Chem. Soc.* **2010**, *132*, 17092-17095.
- [174] Oyamada, J.; Nishiura, M.; Hou, Z. *Angew. Chem., Int. Ed.* **2011**, *50*, 10720-10723.
- [175] Zarate, C.; Martin, R. *J. Am. Chem. Soc.* **2014**, *136*, 2236-2239.
- [176] Lu, B.; Falck, J. R. *Angew. Chem., Int. Ed.* **2008**, *47*, 7508-7510.
- [177] Cheng, C.; Hartwig, J. F. *Science* **2014**, *343*, 853-857.
- [178] Cheng, C.; Hartwig, J. F. *J. Am. Chem. Soc.* **2015**, *137*, 592-595.
- [179] Xu, Z. B.; Chai, L.; Liu, Z.-Q. *Org. Lett.* **2017**, *19*, 5573-5576.
- [180] Yu, J. H.; Ciancetta, A.; Dudas, S.; Duca, S.; Lottermoser, J.; Jacobson, K. A. *J. Med. Chem.* **2018**, *61*, 4860-4882.
- [181] Alandini, N.; Buzzetti, L.; Favi, G.; Schulte, T.; Candish, L.; Collins, K. D.; Melchiorre, P. *Angew. Chem. Int. Ed.* **2020**, *59*, 5248-5253.
- [182] Guo, T.; Ding, Y.; Zhou, L.; Xu, H.; Loh, T.-P.; Wu, X. *ACS Catal.* **2020**, *10*, 7262-7268.
- [183] Sanganee, M. J.; Steel, P. G.; Whelligan, D. K. *J. Org. Chem.* **2003**, *68*, 3337-3339.
- [184] Cheng, Z.; Chen, P.; Liu, G. *Acta Chim. Sin.* **2019**, *77*, 856-860.
- [185] Cheng, Z.; Chen, P.; Liu, G.; *Acta Chim. Sin.* **2019**, *77*, 856-860.
- [186] Bao, X.; Wang, Q.; Zhu, J.; *Angew. Chem., Int. Ed.* **2019**, *58*, 2139-2143.
- [187] Bao, X.; Wang, Q.; Zhu, J.; *Chem. – Eur. J.* **2019**, *25*, 11630-11634.

- [188] Feng, J.; Mao, W.; Zhang, L.; Oestreich, M. *Chem. Soc. Rev.* **2021**, *50*, 2010-2073.
- [189] Zhang, J.; Li, Y.; Xu, R.; Chen, Y. *Angew. Chem., Int. Ed.* **2017**, *129*, 12793-12797.
- [190] Fang, D.; Zhang, Y.; Chen, Y. *Org. Lett.* **2022**, *24*, 2050-2054.
- [191] Zhang, J.; Li, Y.; Zhang, F.; Hu, C.; Chen, Y. *Angew. Chem. Int. Ed.* **2016**, *55*, 1872-1875.
- [192] Krainz, T.; Gaschler, M.; Lim, C.; Sacher, J.; Stockwell, B.; Wipf, P. *ACS Cent. Sci.* **2016**, *2*, 653-659.
- [193] Herron, A. N.; Liu, D.; Xia, G.; Yu, J.-Q. *J. Am. Chem. Soc.* **2020**, *142*, 2766-2770.
- [194] Bao, X.; Wang, Q.; Zhu, J. *Angew. Chem. Int. Ed.* **2019**, *58*, 2139-2143.
- [195] Kochi, J. K. *J. Am. Chem. Soc.* **1962**, *84*, 2121-2127.
- [196] Lian, P.; Long, W.; Li, J.; Zheng, Y.; Wang, X. *Angew. Chem. Int. Ed.* **2020**, *59*, 23603-23608.
- [197] Ding, L.; Niu, K.; Liu, Y.; Wang, Q. *ChemSusChem* **2022**, *15*, e202200367.

